Pierre-Yves Lagrée

“Hydrodynamic and erosion models for flows over erodible beds 2/2”

Chalès 03/07/14

Institut Jean Le Rond ∂’Alembert

Erosion Model

link between the flow of water and the flow of grains

Problem :
What is the relationship between q and the flow?
hint: the larger u the larger the erosion, the larger q
q seems to be proportional to the skin friction

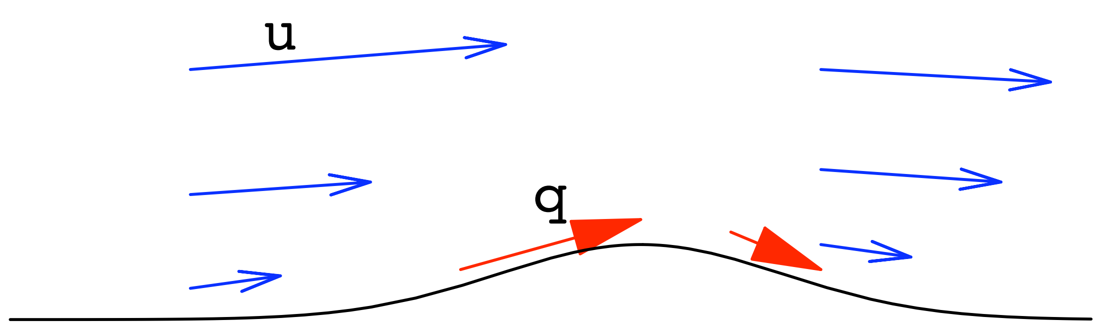

- look at the grain to obtain orders of magnitude
- experimental correlations
- conservation law

Erosion Model

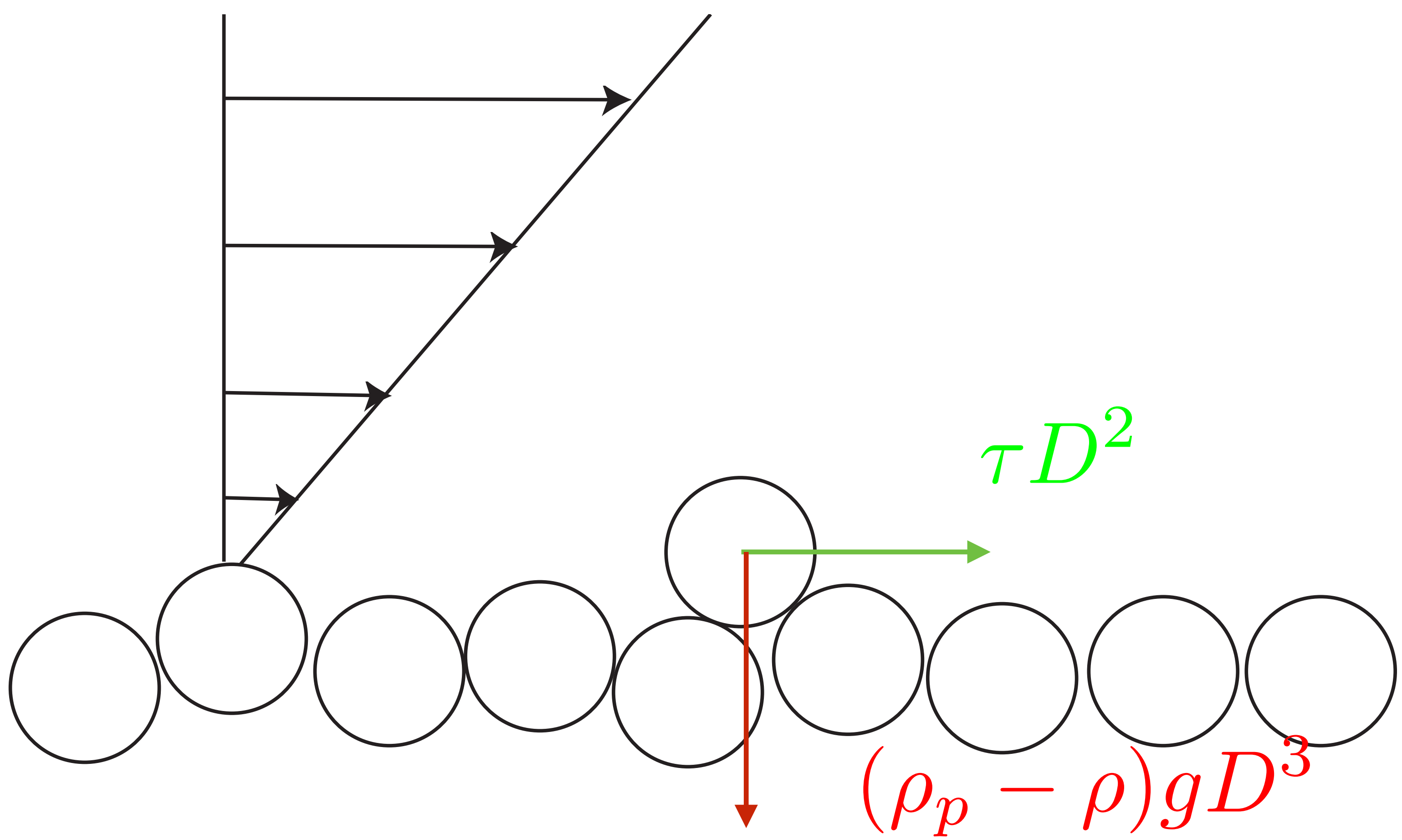

Stress larger than a threshold $\tau > \tau_s$

Shields number $$\frac{\tau}{(\rho_p - \rho) g D}$$

Albert F. Shields (1908–1974) no publication: phD Technischen Hochschule Berlin, 1936

Erosion Model

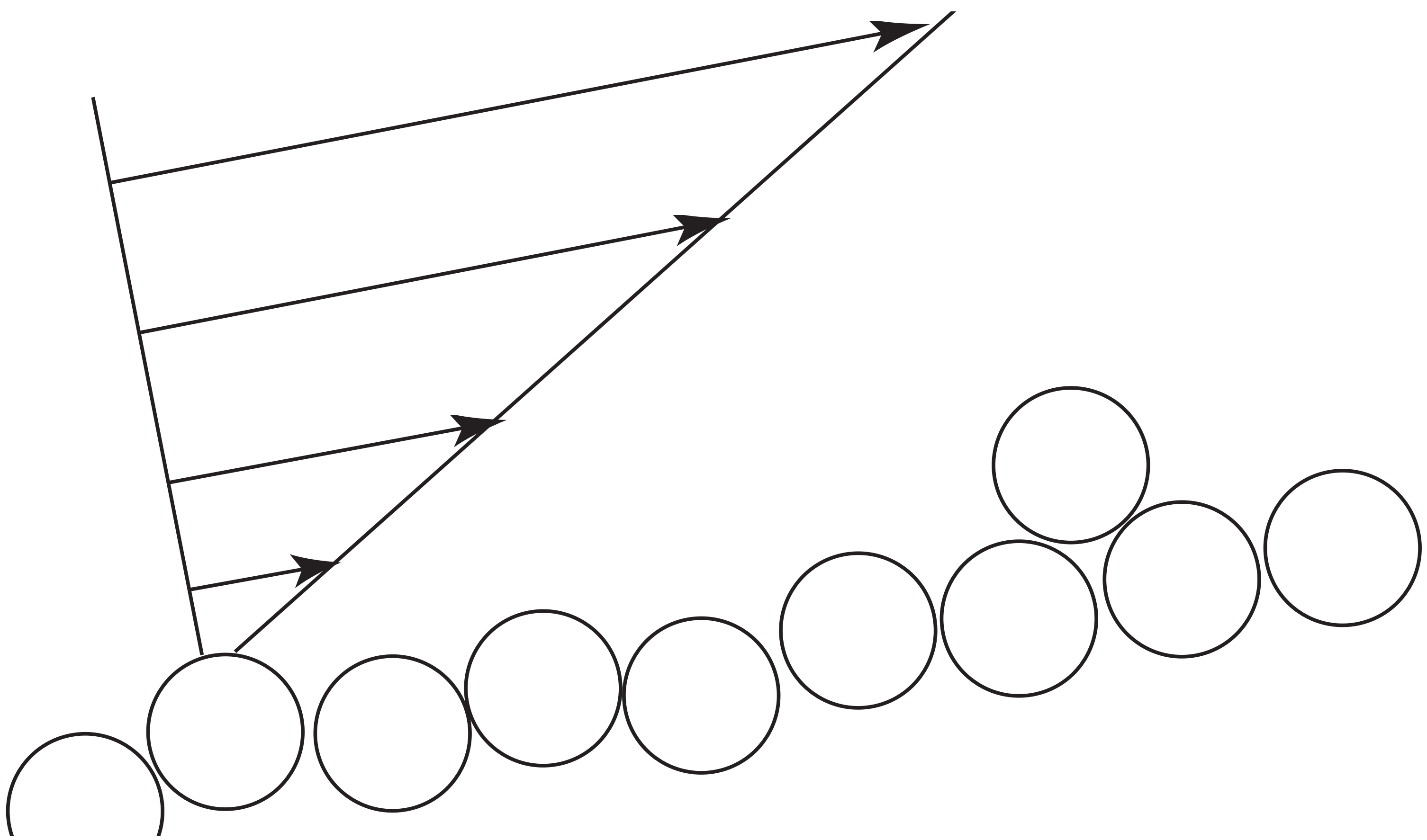

$$\tau_s + \Lambda \frac{\partial f}{\partial x}$$

Stress larger than a threshold $\tau > \tau_s$

Shields number $$\frac{\tau}{(\rho_p - \rho) g D}$$

Erosion Model

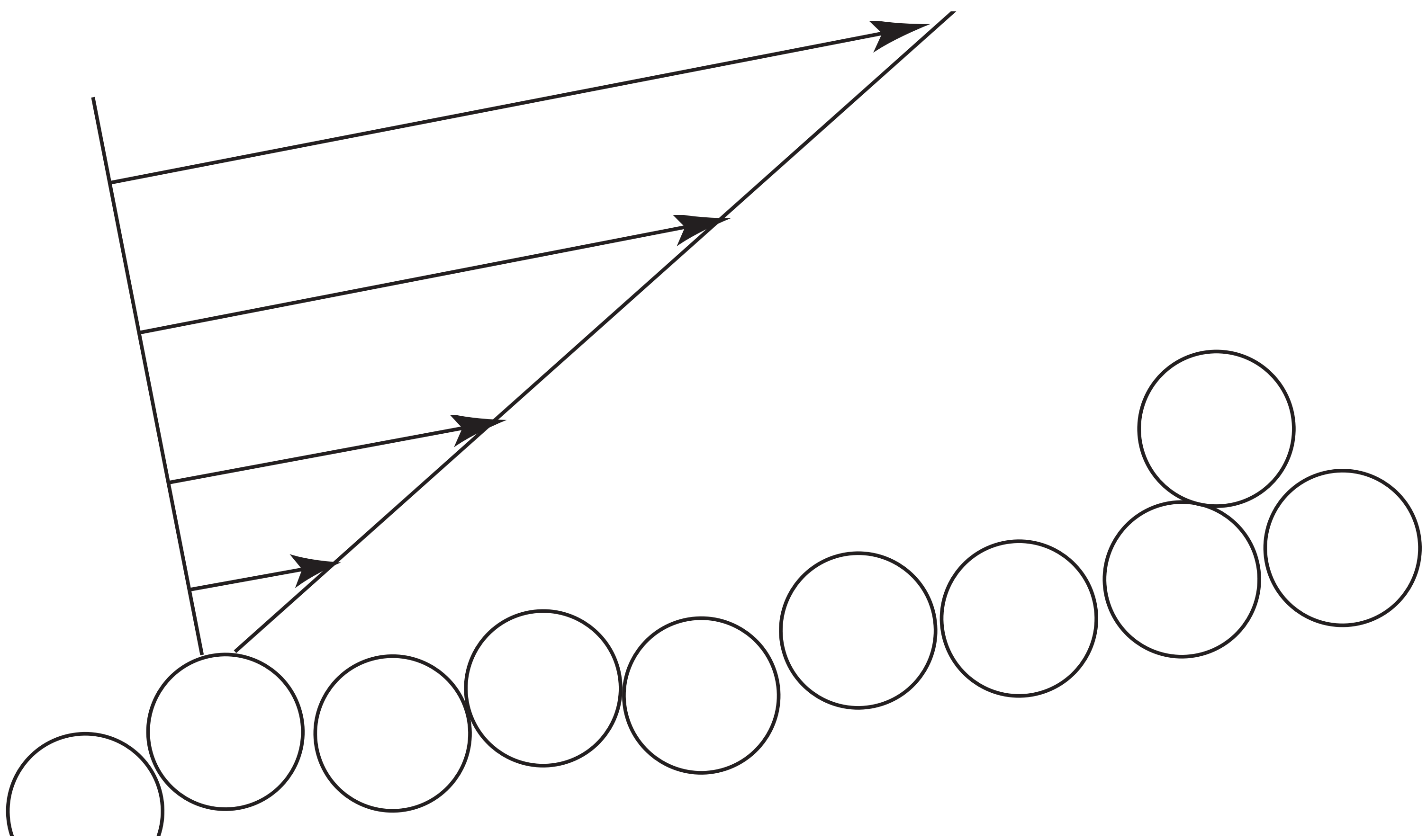

1806 Grenoble 1873

http://www.annales.org/archives/x/gras.html

Les lois d'entraînement de M. Scipion Gras
sur les torrents des Alpes (Annales des ponts et Chaussées, 1857, 2^e semestre) résumées par du Boys 1879 :

"*un caillou posé au fond d'un courant liquide, peut être déplacé par l'impulsion des filets qui le rencontrent : le mouvement aura lieu si la vitesse est supérieure à une certaine limite qu'il (S. Gras) nomme vitesse d'entraînement. Cette vitesse limite dépend de la densité, du volume et de la forme du caillou ; elle dépend aussi de la densité du liquide et de la profondeur du courant.*"

Erosion Model

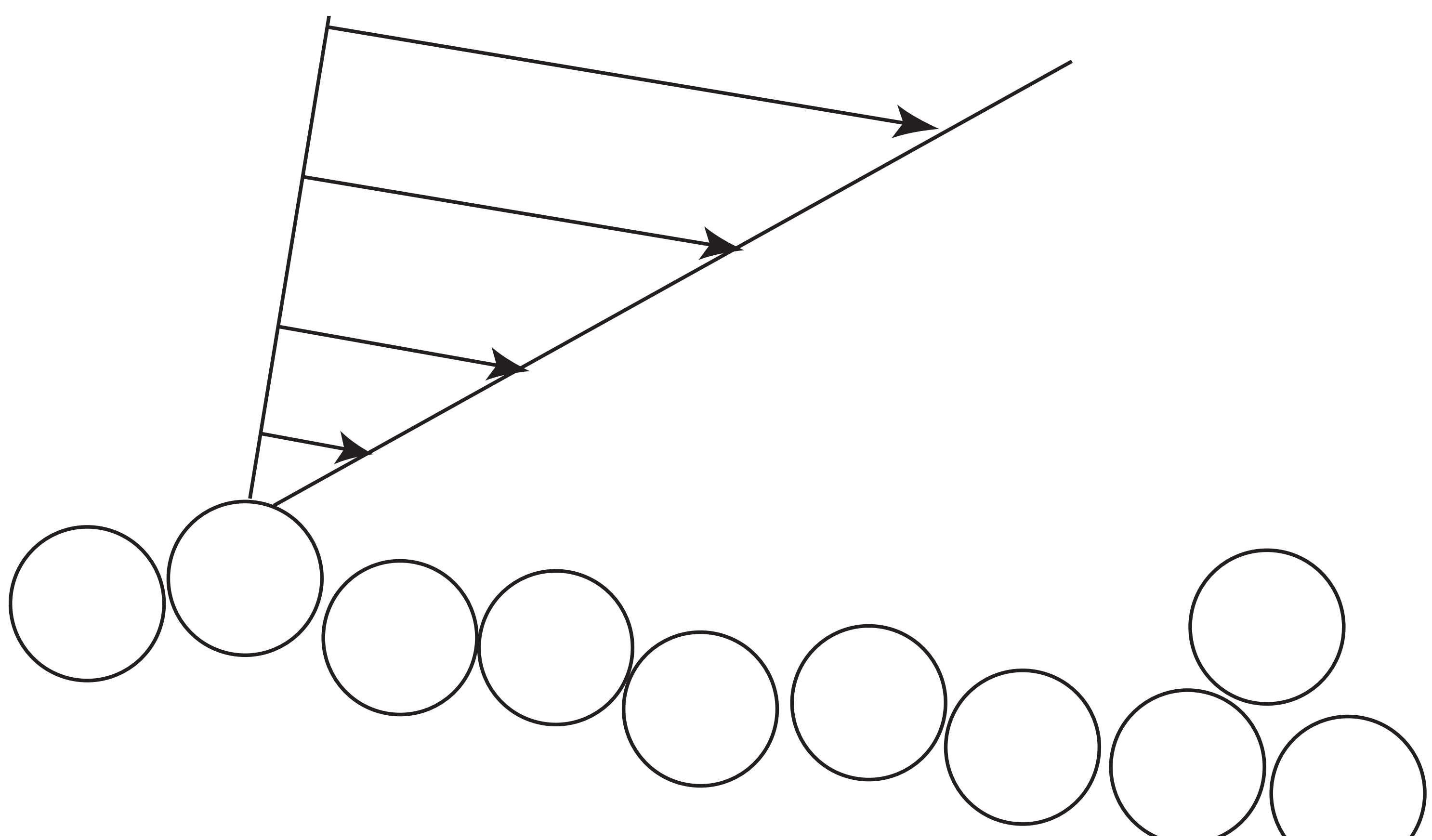

Slope effect

$$\tau_s + \Lambda \frac{\partial f}{\partial x}$$

Erosion Model

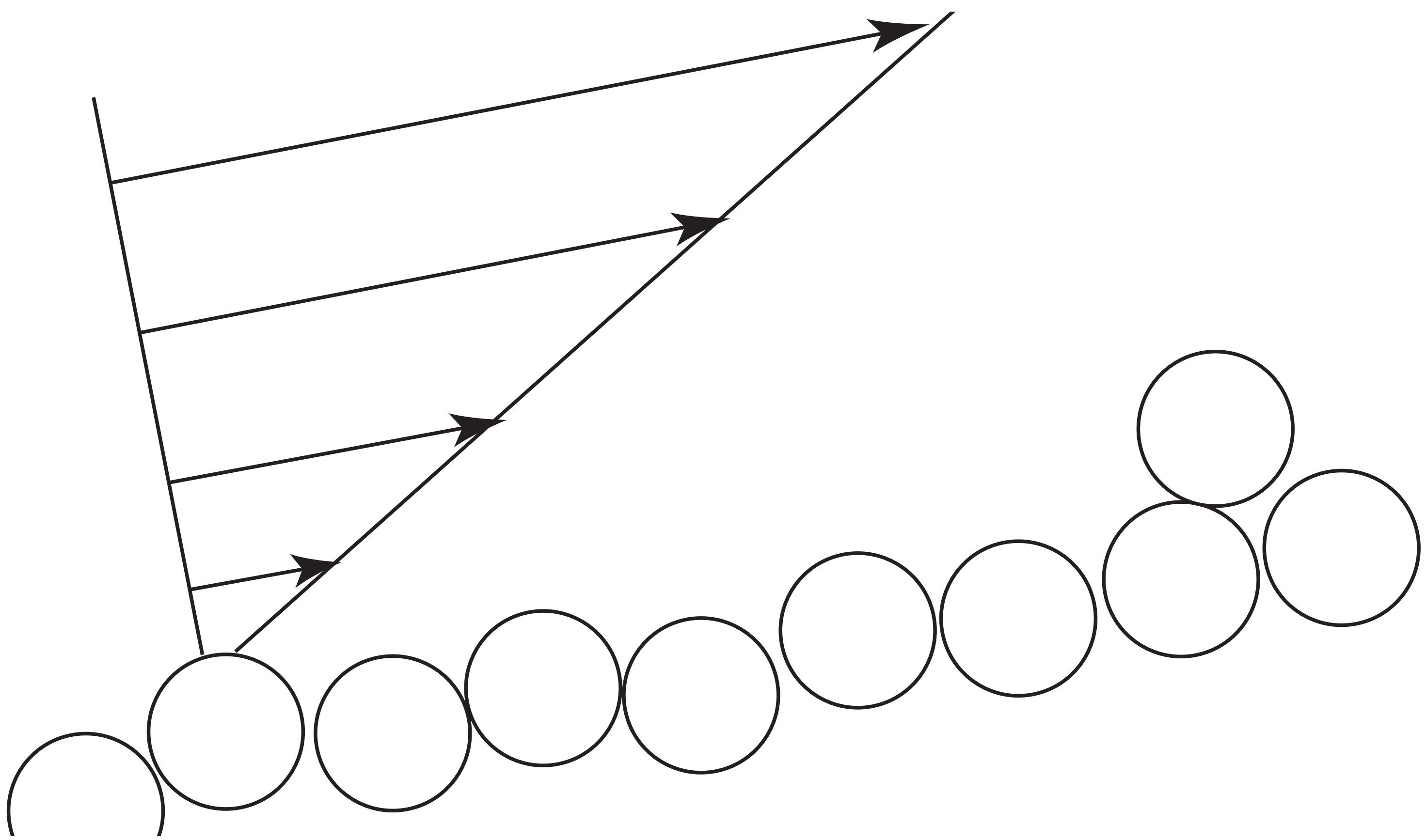

Reynolds

$$Re = \frac{Ud}{\nu}$$

Erosion Model

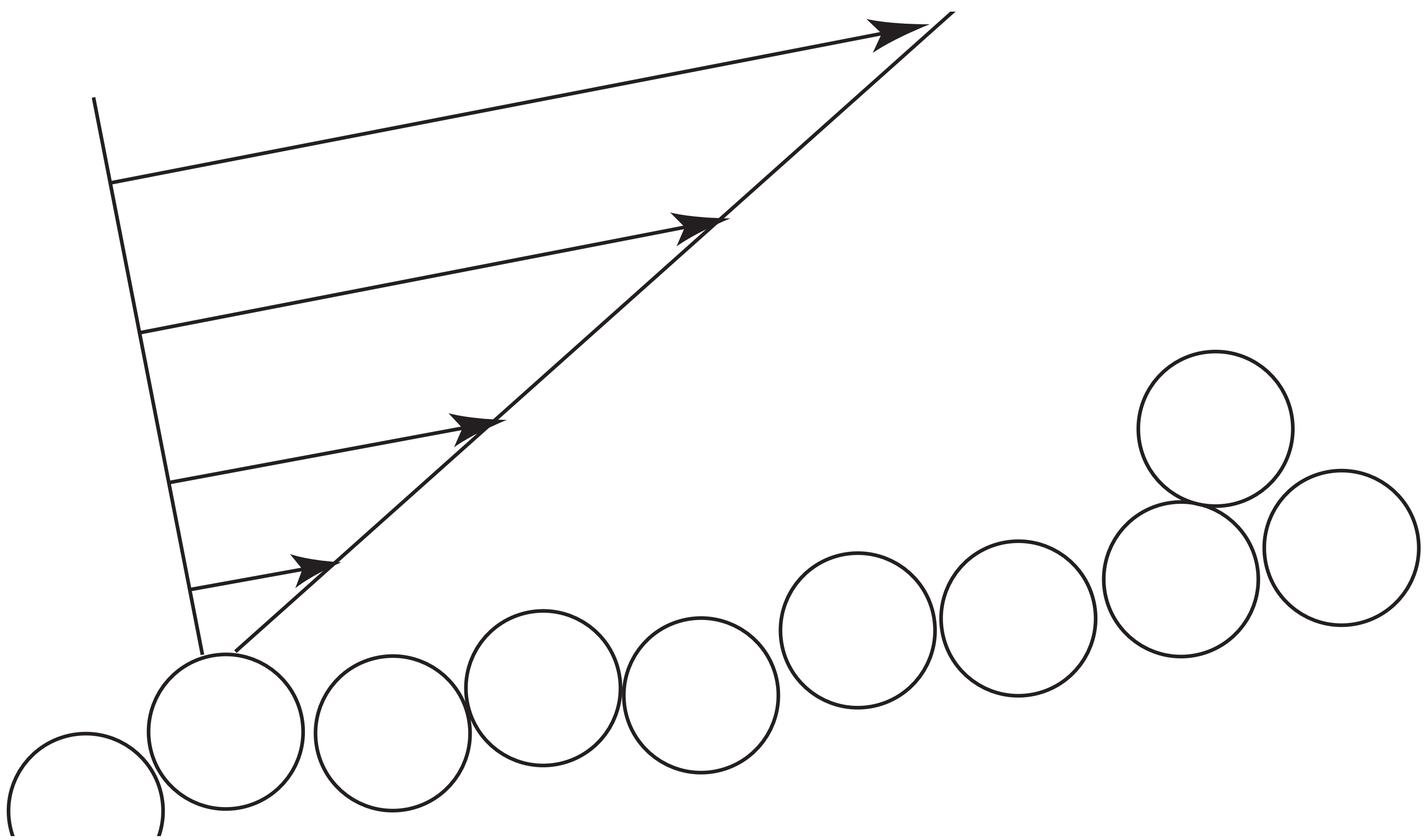

Reynolds

$$Re = \frac{d^2}{\nu}\frac{\partial u}{\partial y}$$

Erosion Model

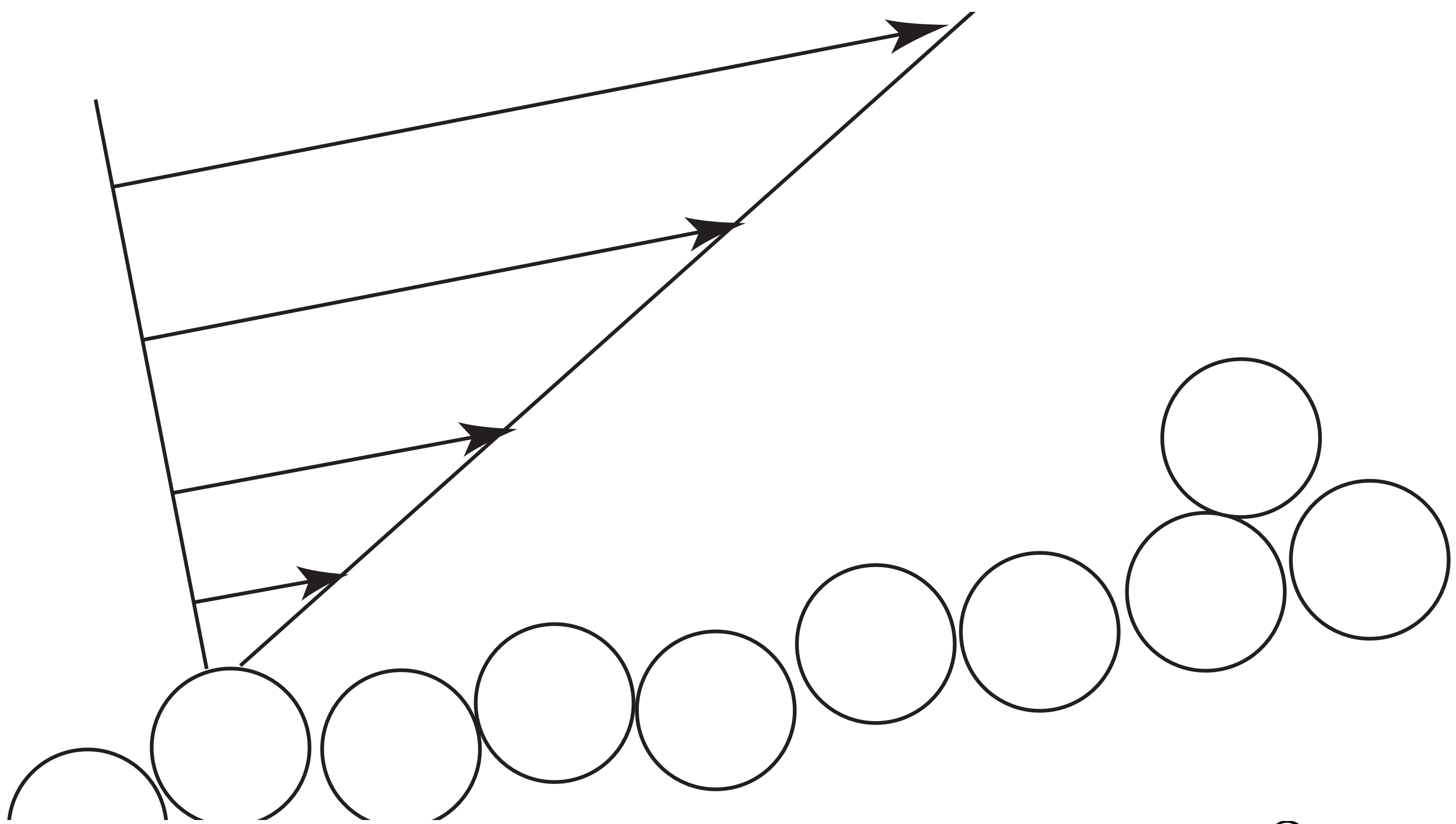

Reynolds

$$Re = u_* d/\nu$$

turbulent $$\mu \frac{\partial < u >}{\partial y} = \rho u_*^2$$

(friction velocity)

Albert F. Shields (1908–1974). all the citations are to a single publication: his doctoral thesis submitted to the Technischen Hochschule Berlin in 1936

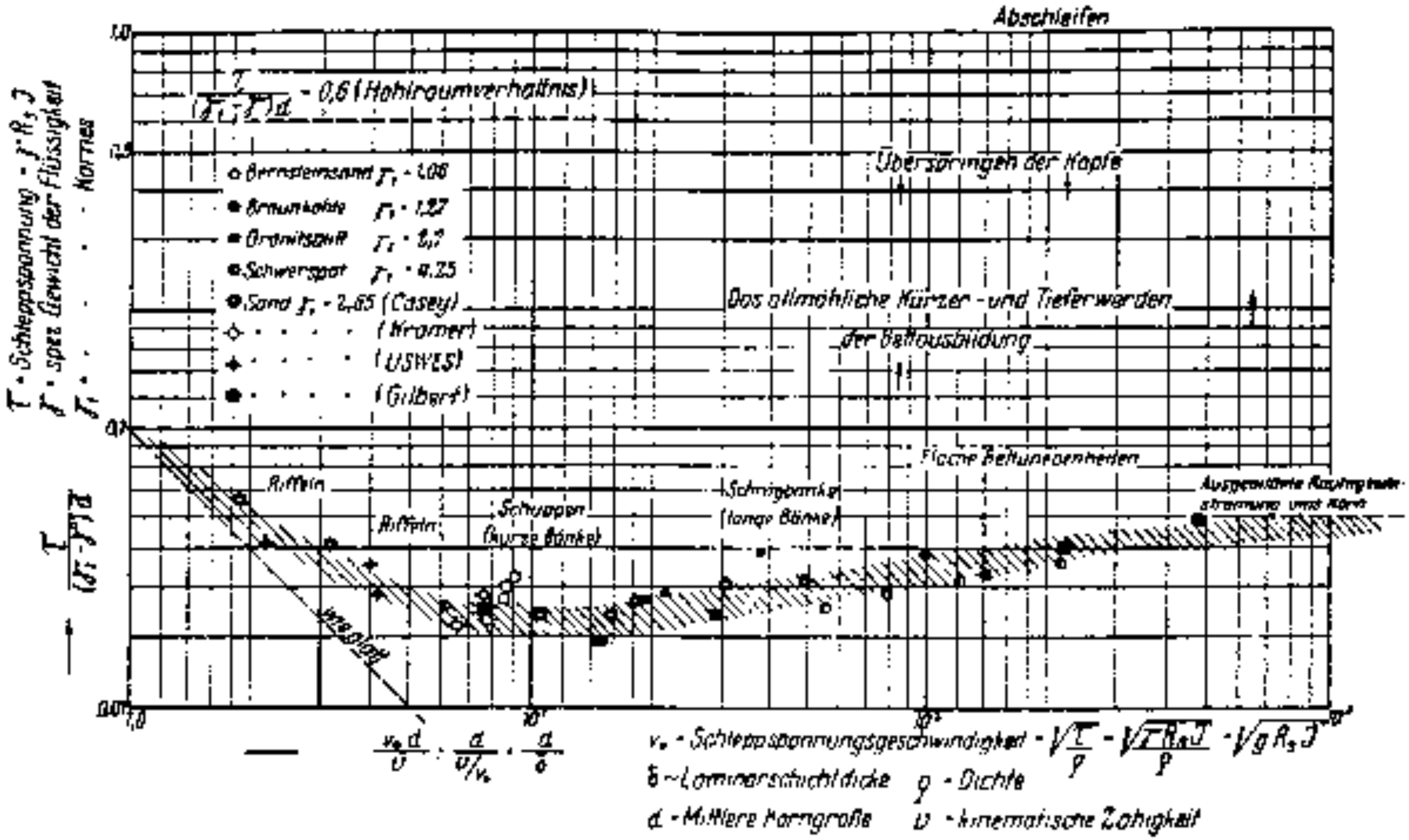

Abb. 6.

Schleppspannungsbeiwert $\frac{\tau}{(\gamma_1 - \gamma)\, d}$ gegen die Reynold'sche Zahl des Kornes $\frac{v_* d}{\nu}$.

*The original diagram by Shields: Shields, A. 1936. "**Anwendung der Aehnlichkeitsmechanik und der Turbulenzforschung auf die Geschiebebewegung.**" Mitteilungen der Preussiischen Versuchsanstalt f/r Wasserbau und Schiffhau, Heft 26, Berlin, Germany*

source Ask Doctor Hydro

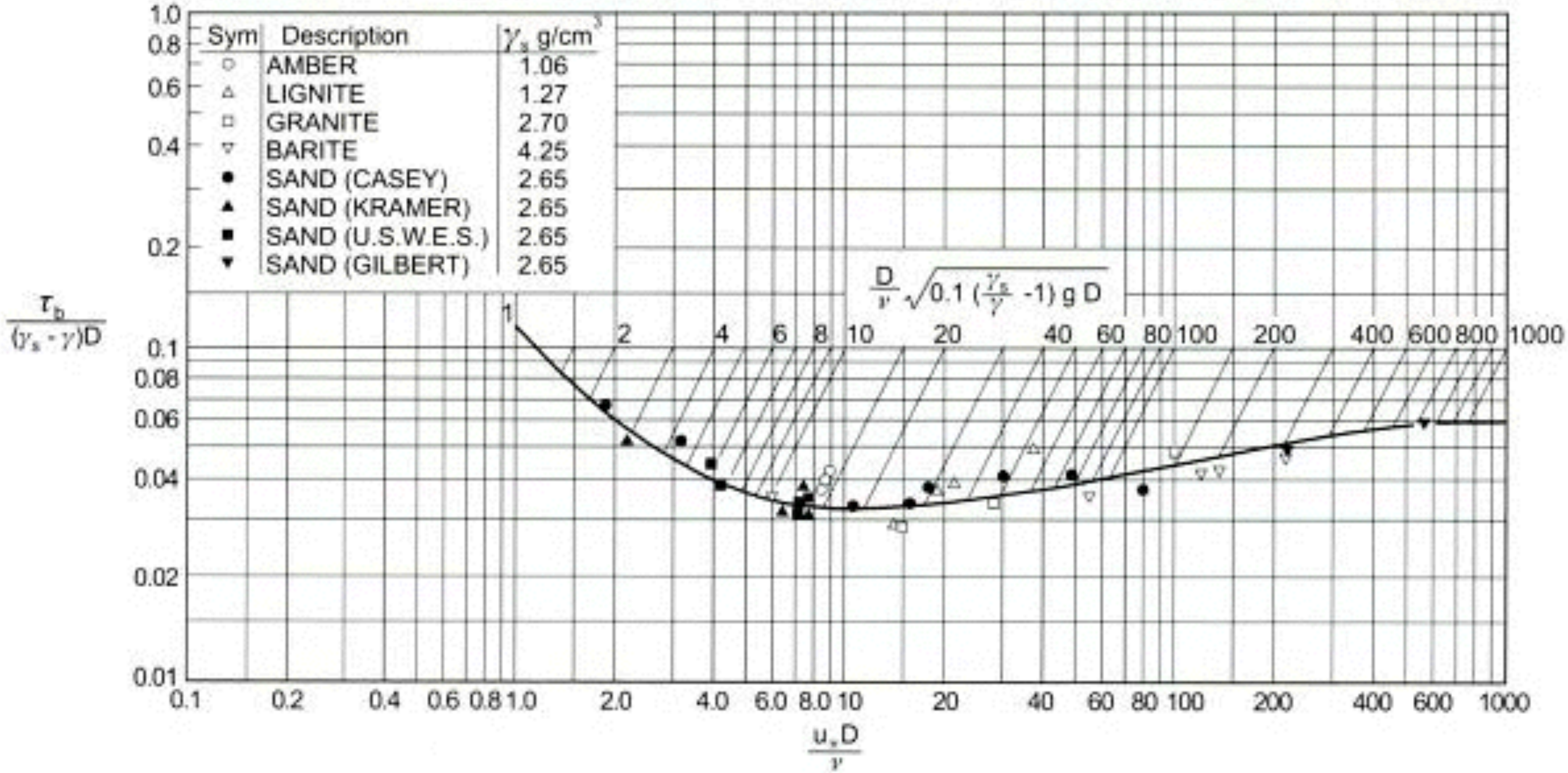

Fig. 2.18. Shields diagram for initiation of motion (source Vanoni, 1964).

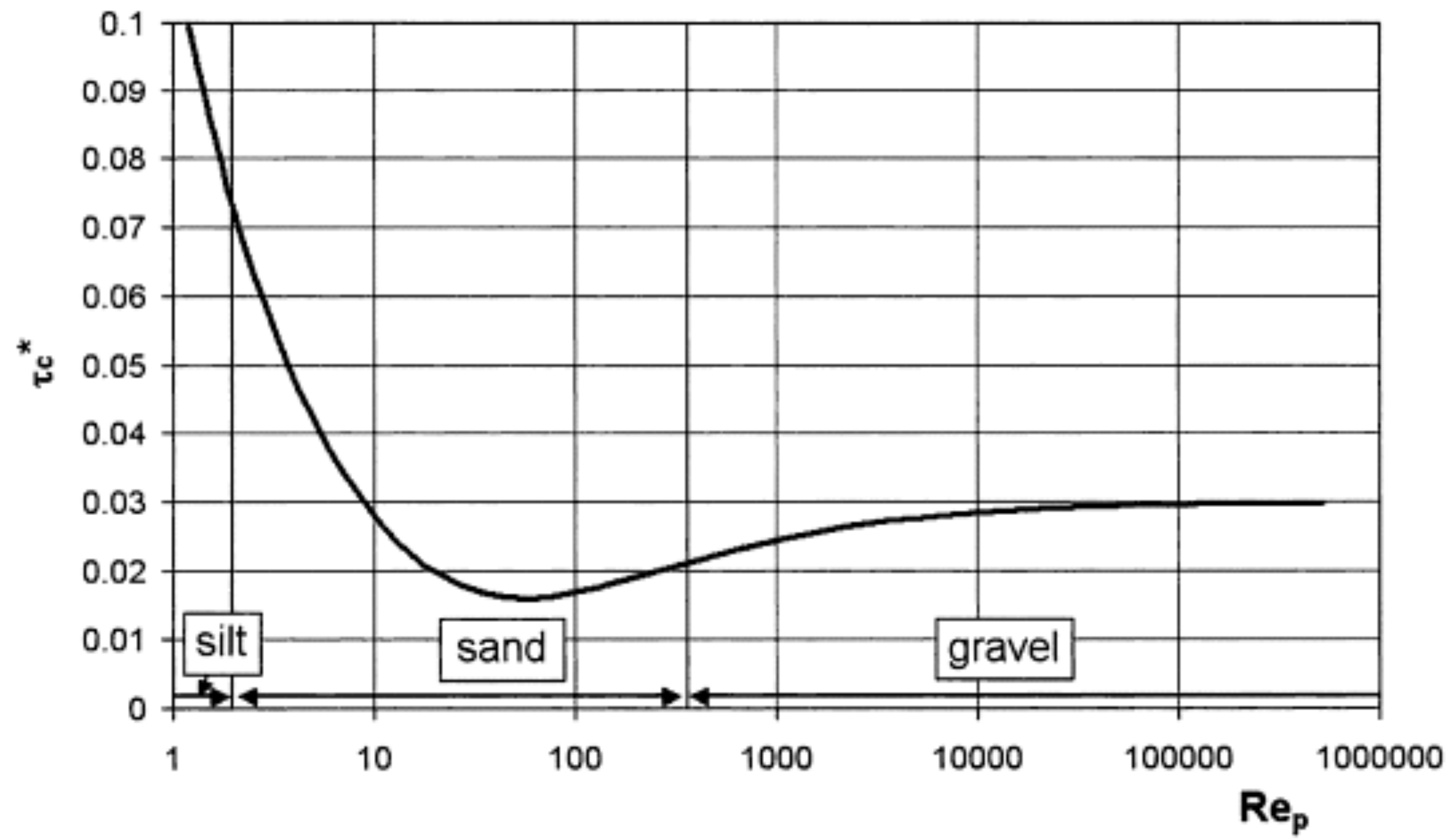

Fig. 2-19. Modified Shields diagram (after Parker 2005).

Bilan I

- A criteria for incipient displacement «Shields»
- now: flux of particules «q»

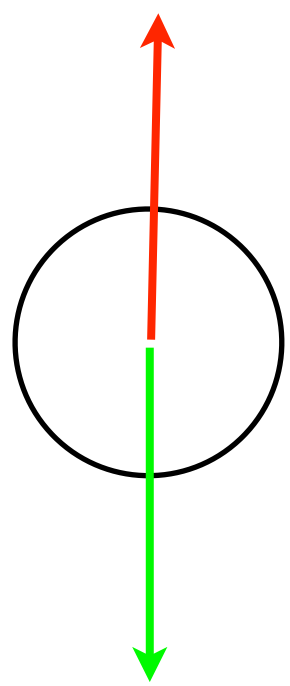

free fall equilibrium

$$\frac{4}{3}\pi(\Delta\rho)R^3 g = 6\pi\eta R V_s$$

terminal velocity

$$V_s = \frac{d^2}{18\eta}(\Delta\rho)g$$

Stokes velocity

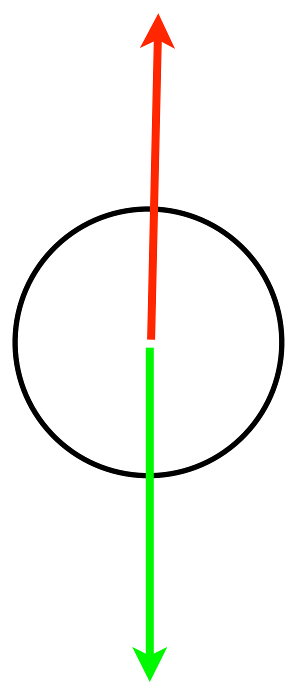

free fall equilibrium

$$\frac{4}{3}\pi(\Delta\rho)R^3 g = 6\pi\eta R V_s$$

terminal velocity

$$V_s = \frac{d^2}{18\eta}(\Delta\rho)g$$

characteristic flux

$$Q_s = \frac{d^3}{\eta}(\Delta\rho)g$$

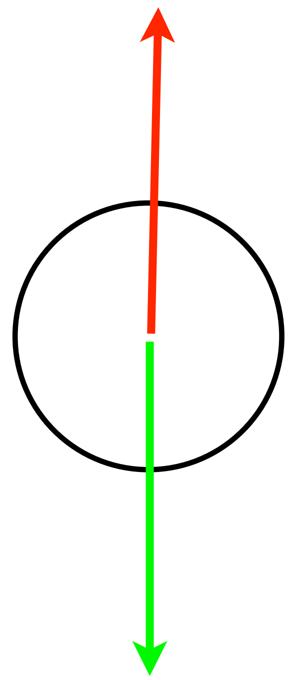

free fall equilibrium

$$\frac{4}{3}\pi(\Delta\rho)R^3 g = \frac{\rho C_D V_s^2}{2}$$

terminal velocity

$$V_s = \sqrt{\frac{(\Delta\rho) g d}{\rho C_D}}$$

flux

$$Q_s = \sqrt{\frac{(\Delta\rho) g d^3}{\rho}}$$

mesurements/ correlations

- with the previous orders of magnitude
- experimental flux of materials

$$\frac{q}{Q_s} = 8\left(\frac{(\tau - \tau_c)}{\Delta\rho g d}\right)^{3/2}$$

$$Q_s = \sqrt{\frac{(\Delta\rho) g d^3}{\rho}}$$

Sediment transport mechanisms: 1. Bed-load transport

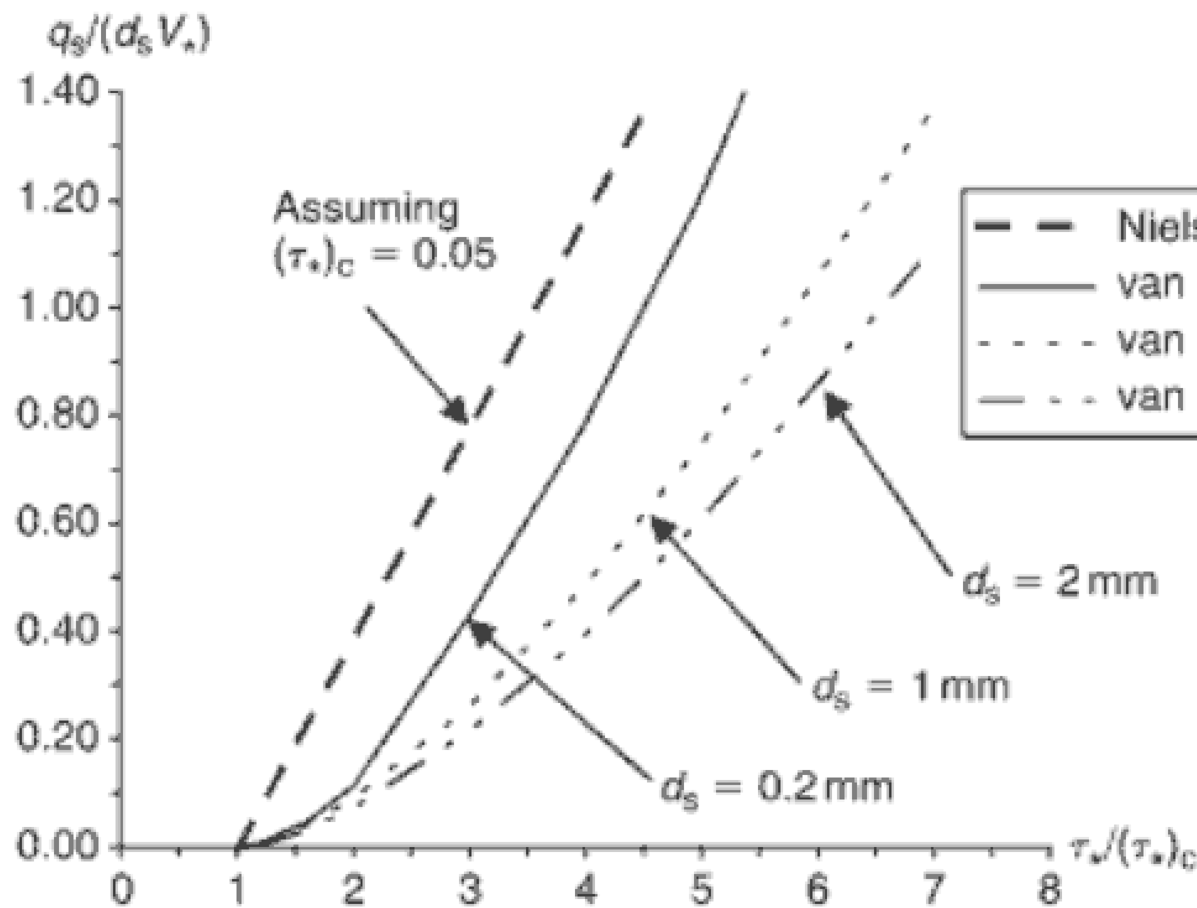

Fig. 10.5 Dimensionless bed-load transport rate $q_s/(d_s V_*)$ as a function of the dimensionless Shields parameter $\tau_*/(\tau_*)_c$ (Table 10.2).

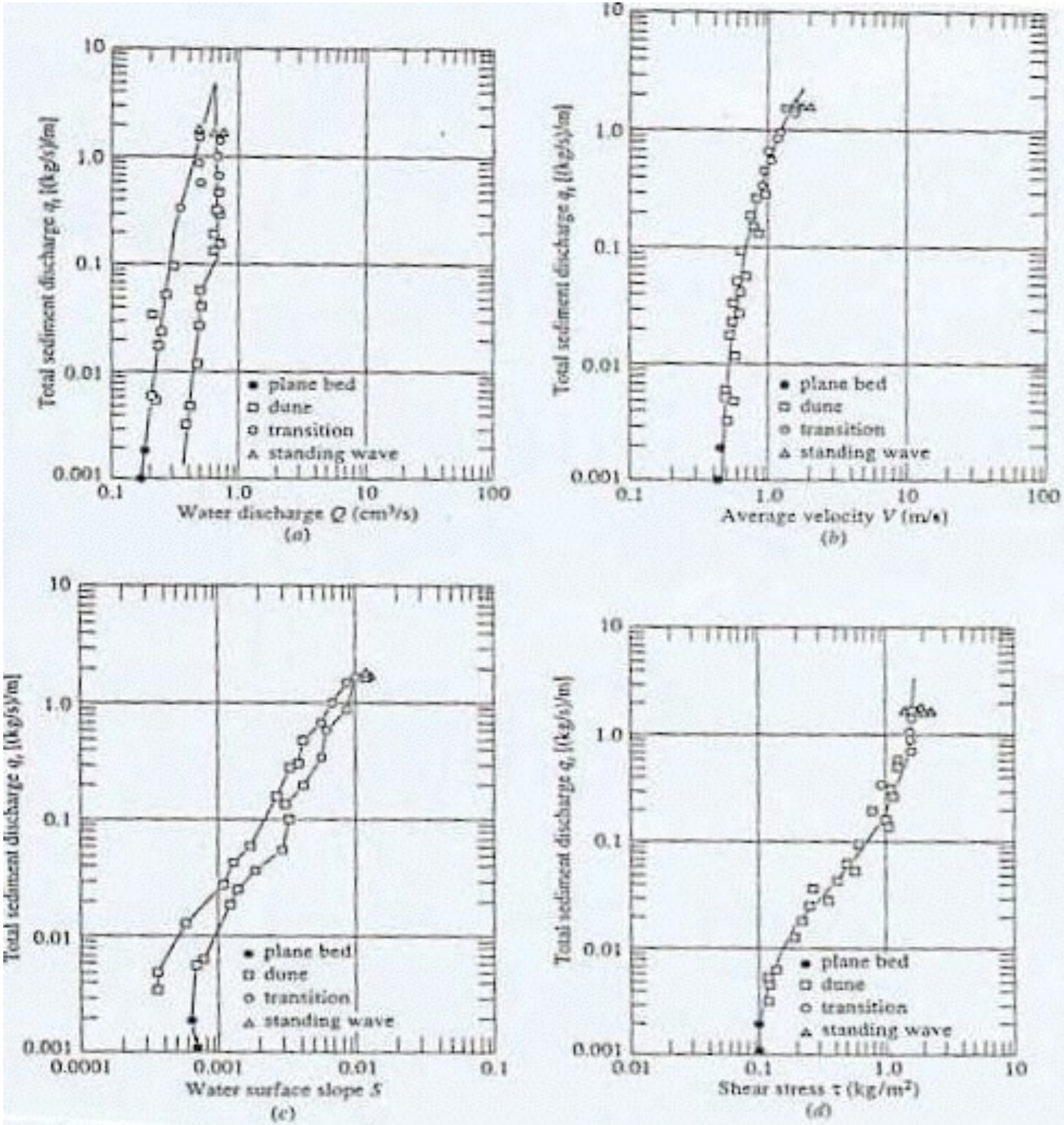
Total sediment discharge q_t [(kg/s)/m]
plane bed
dune
transition
standing wave
Water discharge Q (cm³/s)
(a)
Average velocity V (m/s)
(b)
Water surface slope S
(c)
Shear stress τ (kg/m²)
(d)

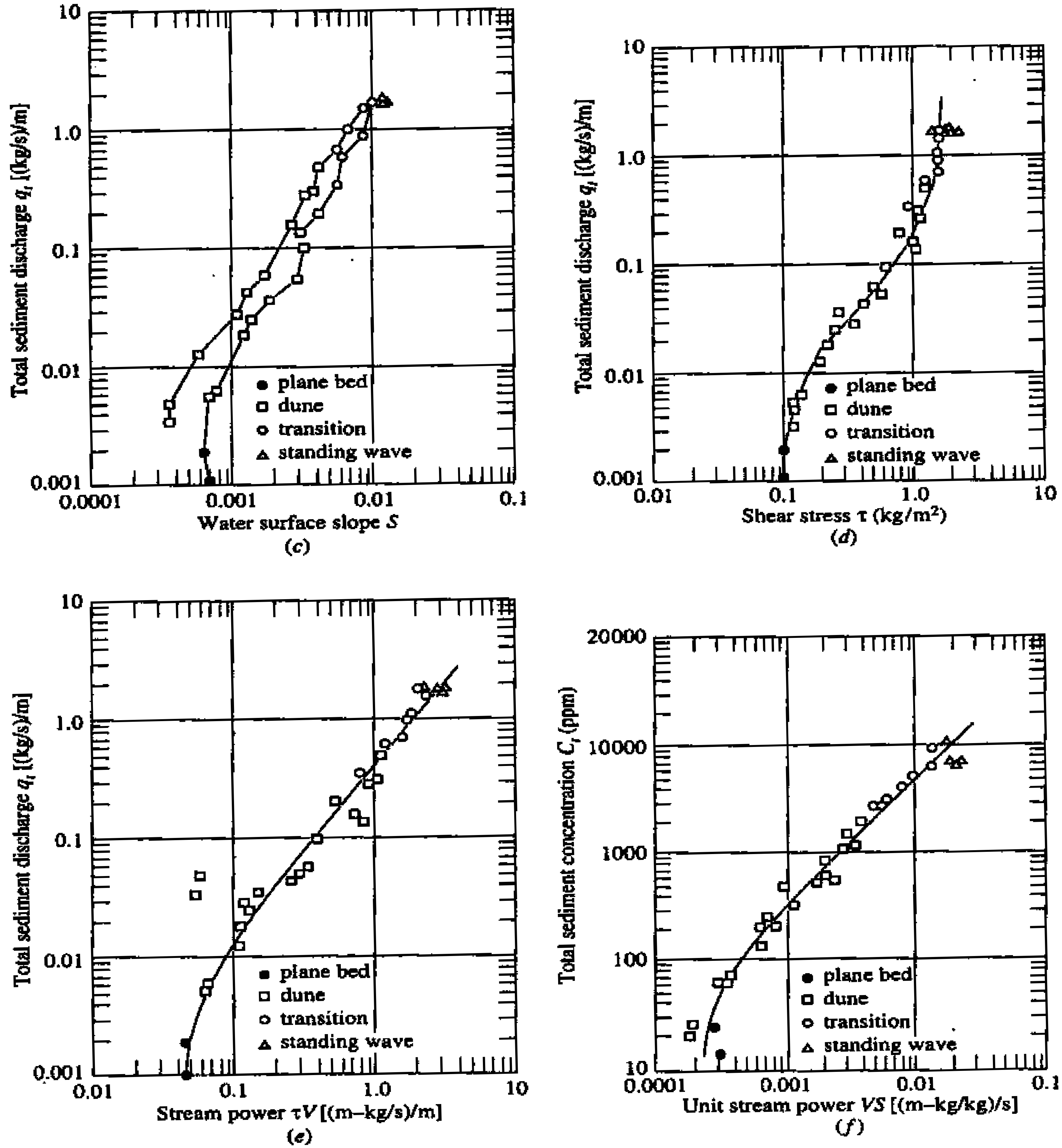

FIGURE 7.1
Relationships between total sediment discharge and (*a*) water discharge, (*b*) velocity, (*c*) slope, (*d*) shear stress, (*e*) stream power, and (*f*) unit stream power, for 0.93 mm sand in an 8 ft wide flume (Yang, 1983).

Meyer-Peter and Muller (1948):

$$q^* = 8\left(\tau^* - \tau_c^*\right)^{3/2} \tag{2-95a}$$

where $\tau_c^* = 0.047$. This formula is empirical in nature; it has been verified with data for uniform coarse sand and gravel. Even though it was developed for alpine streams in Switzerland, it enjoys wide use in coastal sediment transport (e.g. Soulsby, 1997). Recently, Wong and Parker (2006b) reanalysed the data used by Meyer-Peter and Muller and found that a better fit is provided by one of the two alternative forms;

$$q^* = 4.93\left(\tau^* - 0.047\right)^{1.6} \tag{2-95b}$$

$$q^* = 3.97\left(\tau^* - 0.0495\right)^{3/2} \tag{2-95c}$$

Garcia

Wilson (1966):

$$q^* = 12\left(\tau^* - \tau_c^*\right)^{3/2} \tag{2-98}$$

where τ_c^* is determined from the Shields diagram. This relation is empirical in nature; most of the data used to fit it pertain to very high rates of bed load transport. It has been used extensively to estimate transport of sand and industrial materials such as nylon in pressurized flows (e.g., Wilson 1987).

Paintal (1971):

$$q^* = 6.56 \times 10^{18}\, \tau^{*16} \tag{2-99}$$

was obtained though extensive measurements of very low bed load transport rates. It is valid for $0.007 < \tau^* < 0.06$ and sediment grain sizes between 1 mm (coarse sand) and 25 mm

Garcia

Engelund and Fredsøe (1976):

$$q^* = 18.74\left(\tau^* - \tau_c^*\right)\left[\left(\tau^*\right)^{1/2} - 0.7\left(\tau_c^*\right)^{1/2}\right] \qquad (2\text{-}100a)$$

where $\tau_c^* = 0.05$.

This formula resembles that of Ashida and Michiue because its derivation, albeit obtained independently, is almost identical. This relation was rederived by Fredsøe and Deigaard (1992, p. 214), resulting in a very similar relation,

$$q^* = \frac{30}{\pi\mu_d}\left(\tau^* - \tau_c^*\right)\left[\left(\tau^*\right)^{1/2} - 0.7\left(\tau_c^*\right)^{1/2}\right] \qquad (2\text{-}100b)$$

Garcia

Fernandez-Luque and van Beek (1976):

$$q^* = 5.7\left(\tau^* - \tau_c^*\right)^{3/2} \tag{2-101}$$

where τ_c^* varies from 0.05 for 0.9-mm material to 0.058 for 3.3-mm material. The relation is empirical in nature and was obtained through laboratory observations.

Parker (1979):

$$q^* = 11.2\frac{\left(\tau^* - 0.03\right)^{4.5}}{\tau^{*3}} \tag{2-102}$$

developed as a simplified fit to the relation of Einstein (1950) for the range of Shields numbers likely to be encountered in gravel-bed streams. This formula was used to analyze the hydraulic geometry of gravel-bed streams (Parker 1979).

Van Rijn (1984a):

$$q^* = 0.053\frac{T^{2.1}}{D_*^{0.3}} \tag{2-103a}$$

can be used to estimate bed load transport rates of particles with mean sizes in the range between 0.2 and 2.0 mm. This

Garcia

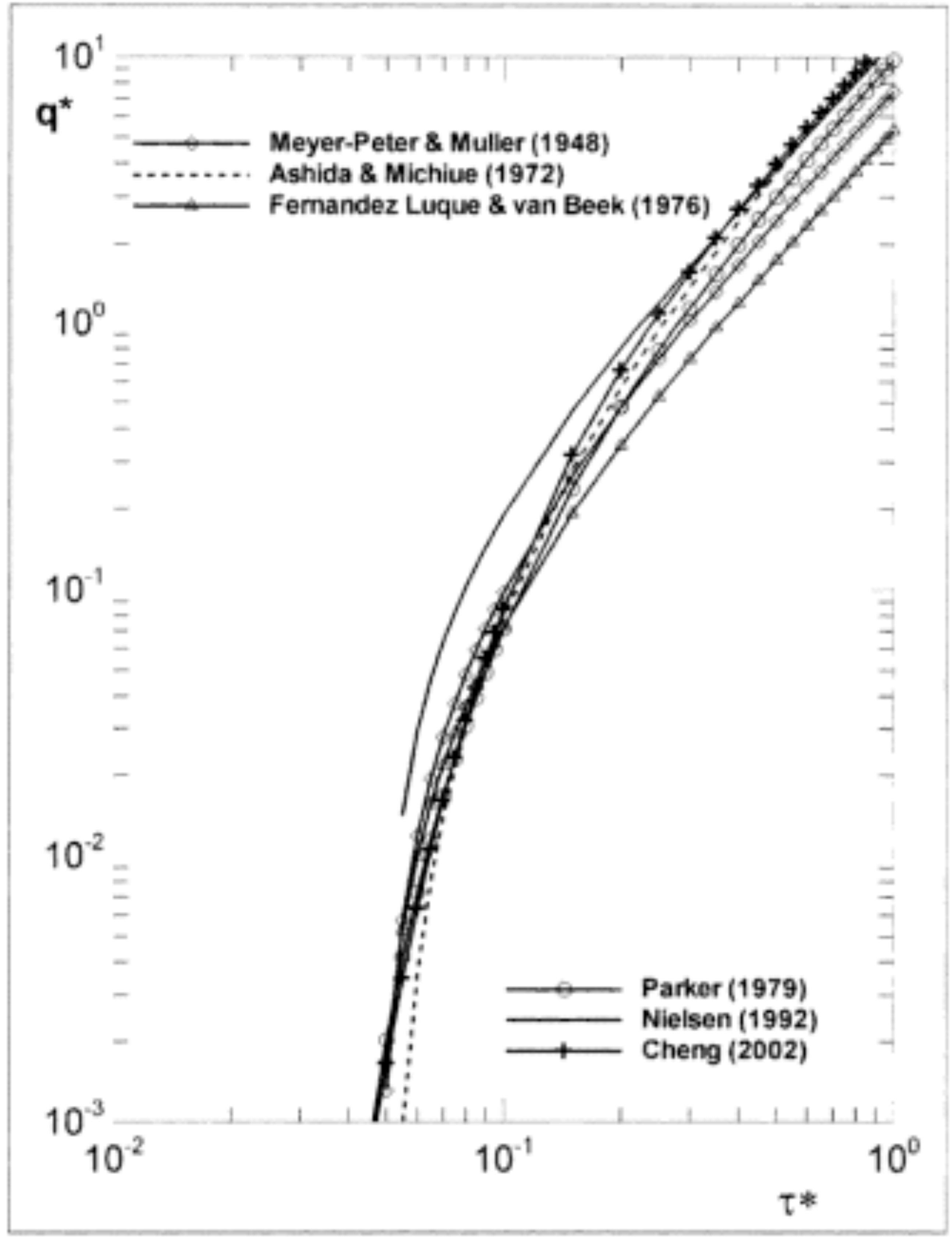

Fig. 2-33. Plot of several bed load functions found in the literature.

Garcia

Table 1. Most Commonly Used Formulas to Describe Bed Load Transport in a Turbulent Flow[a]

Authors	Transport Rate q^*	Comments
Meyer-Peter and Müller [1948]	$8\,(\tau^* - \tau_c^*)^{\frac{3}{2}}$	Derived from a fit of experimental data.
Wong [2003]	$3.97\,(\tau^* - \tau_c^*)^{\frac{3}{2}}$	Derived from a fit of experimental data.
Einstein [1950]	$12f\,(\tau^* - \tau_c^*)^{\frac{3}{2}}$	Theoretical derivation; f is a fitting parameter.
Bagnold [1973]	$\frac{V}{\mu\sqrt{Rgd}}\,(\tau^* - \tau_c^*)$	Theoretical derivation; μ is a friction coefficient and V is the average particle velocity.
Ashida and Michiue [1973]	$17\,(\tau^* - \tau_c^*)\left(\sqrt{\tau^*} - \sqrt{\tau_c^*}\right)$	Theoretical derivation and fit of experimental data.
Fernandez-Luque and Van Beek [1976]	$5.7\,(\tau^* - \tau_c^*)^{\frac{3}{2}}$	Derived from a fit of experimental data.
Engelund and Fredsoe [1976]	$18.74\,(\tau^* - \tau_c^*)\left(\sqrt{\tau^*} - 0.7\sqrt{\tau_c^*}\right)$	Theoretical derivation.
Bridge and Dominic [1984]	$\frac{\alpha}{\mu}\,(\tau^* - \tau_c^*)\left(\sqrt{\tau^*} - \sqrt{\tau_c^*}\right)$	Theoretical derivation and fit of experimental data; μ is a friction coefficient and α is a fitting parameter.

[a]This list is not exhaustive and other transport formulas can be found in the work by *García* [2006].

Authors	Method	$q_p\sqrt{\frac{\rho_f}{\Delta\rho g d^3}}$
Einstein (1942)	empirical	$e^{0.391\frac{1}{\theta}}\dfrac{\sqrt{\frac{2}{3}+\frac{36\eta^2}{gd^3\rho_f\Delta\rho}}-\sqrt{\frac{36\eta^2}{gd^3\rho_f\Delta\rho}}}{0.465}$
Meyer-Peter & Muller (1948)	empirical	$8\left(c_2c_3\theta-\theta^c\right)^{1.5}$
Einstein (1950)	semi-empirical	$\dfrac{1-\frac{1}{\sqrt{\pi}}\int_{-0.156f\frac{1}{\theta}-2}^{0.156f\frac{1}{\theta}-2}e^{-t^2}dt}{27f_c\left(2-\frac{1}{\sqrt{\pi}}\int_{-0.156f\frac{1}{\theta}-2}^{0.156f\frac{1}{\theta}-2}e^{-t^2}dt\right)}$
Bagnold (1956)	semi-empirical	$8.5\sqrt{2\tan\alpha/(3\psi)}(\theta-\theta^c)\theta^{0.5}$
Yalin (1963)	semi-empirical	$\left[1-\dfrac{\log(1+2.45\left(\frac{\rho_f}{\rho_p}\right)^{0.4}\theta^{c\,0.5}\left(\frac{\theta}{\theta^c}-1\right))}{2.45\left(\frac{\rho_f}{\rho_p}\right)^{0.4}\theta^{c\,0.5}\left(\frac{\theta}{\theta^c}-1\right)}\right]\times 0.635\left(\dfrac{\theta}{\theta^c}-1\right)$
Ribberink (1998)	empirical	$10.4\left(\theta-\theta^c\right)^{1.67}$
Camemen & Larson (2005)	empirical	$12\,\theta^{1.5}e^{-4.5\frac{\theta^c}{\theta}}$
Wong & Parker (2006)	empirical	$4.93\left(\theta-\theta^c\right)^{1.60}$

Table 1. Various expressions for turbulent flow, where c_2 is a side-wall correction, c_3 a bed-form correction, f_c the percentage of grains of a given size put into motion, f the correction function obtained experimentally for grain size dispersion, ψ the drag coefficient, ρ_p the density of the solid, ρ_f the density of the fluid ($\Delta\rho=\rho_p-\rho_f$), η the viscosity of the fluid, d the particle diameter, and $\tan\alpha$ the dynamic friction coefficient.

Authors	Method	$q_p \frac{\eta}{\Delta\rho g d^3}$
Charru & Mouilleron-Arnould (2002)	semi-empirical	$0.42\,(\theta - \theta^c)^3$
Cheng (2004)	semi-empirical	$\frac{\eta}{\sqrt{\Delta\rho g d^3 \rho_f}} 41\,\theta^{0.5}\,Re_*$ $\times[\sinh(0.139\,\theta^{1.181}\,Re_*^{0.39})]^2$
Charru *et al.* (2004)	empirical	$0.025\,\theta\,(\theta - \theta^c)$
Charru & Hinch (2006)	semi-empirical	$0.096 N \frac{\theta}{\theta^c}$

Table 2. Various expressions for laminar flow, where $Re_* = u_* d\rho_f/\eta$ is the shear Reynolds number, u_* the shear velocity, and N the number of particles in motion per area.

Erosion Model

In the literature one founds Charru /Izumi & Parker / Yang / Blondeau Du Boys

$$q_s = E\varpi(\tau^a(\tau - \tau_s)^b)$$

if $x > 0$ then $\varpi(x) = x$ else $\varpi(x) = 0$.

or with a slope correction for the threshold value:

a, E coefficients, $a = 0, b = 3$ or $a = b = 1$ or $a = 1/2, b = 1$ or ...

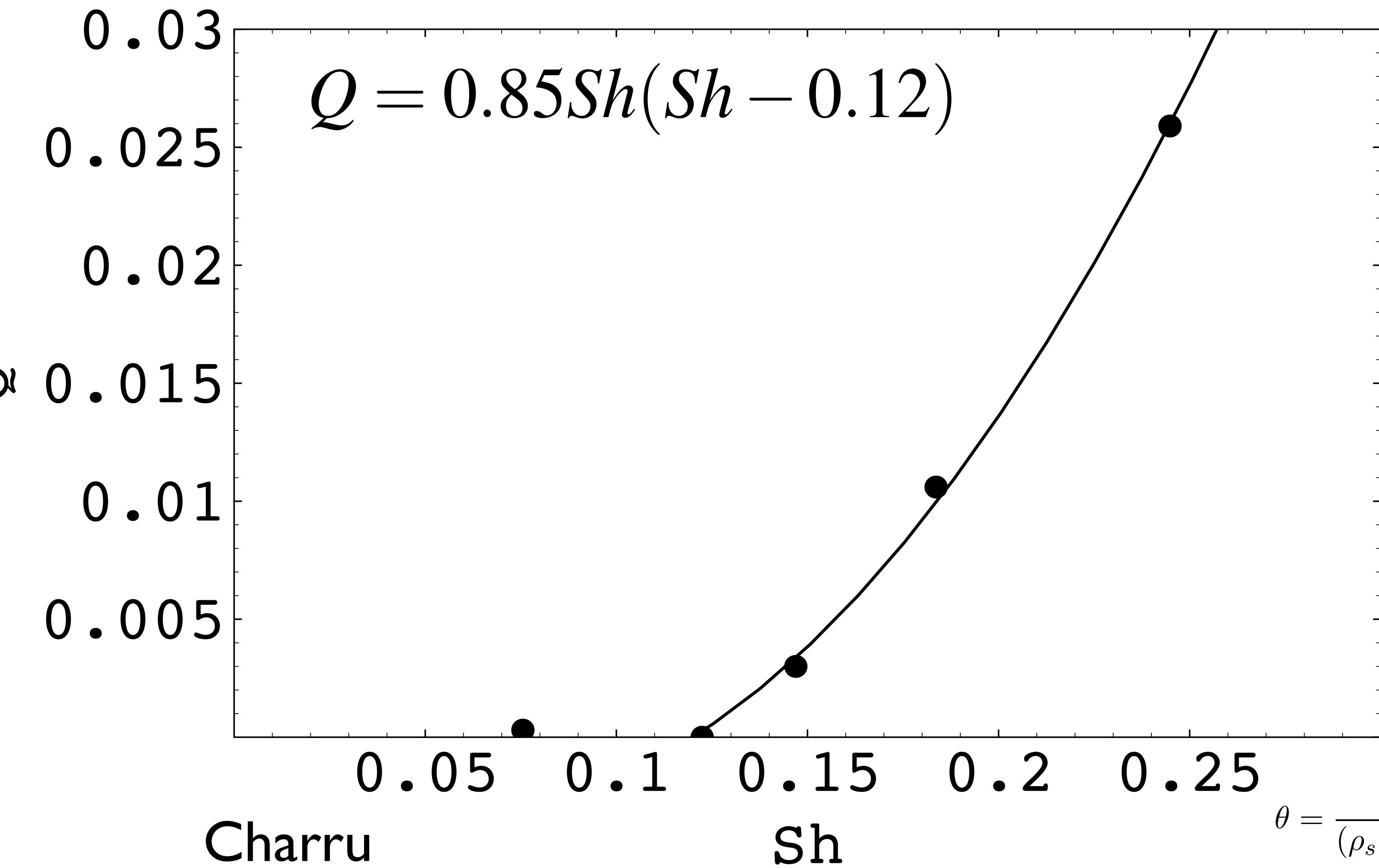

Charru

$\theta = \frac{\eta\gamma}{(\rho_s - \rho_f)gd}$

Erosion Model

In the literature one founds Charru /Izumi & Parker / Yang / Blondeau Du Boys

$$q_s = E\varpi(\tau^a(\tau - \tau_s)^b)$$

if $x > 0$ then $\varpi(x) = x$ else $\varpi(x) = 0$.

or with a slope correction for the threshold value:

a, E coefficients, $a = 0, b = 3$ or $a = b = 1$ or $a = 1/2, b = 1$ or ...

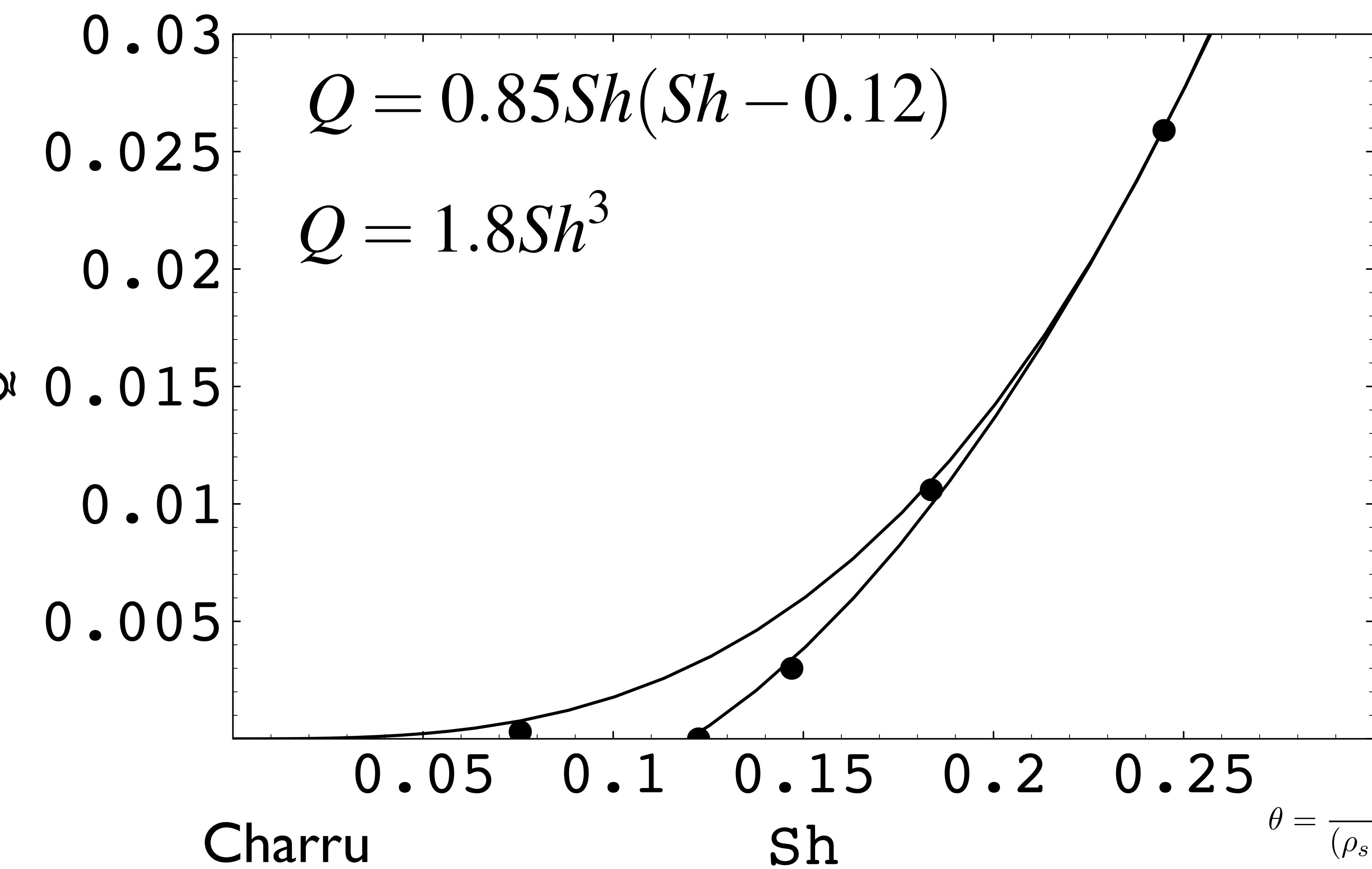

Charru

$\theta = \frac{\eta\gamma}{(\rho_s - \rho_f)gd}$

Erosion Model

In the literature one founds Charru /Izumi & Parker / Yang / Blondeau Du Boys

$$q_s = E\varpi(\tau^a(\tau - \tau_s)^b)$$

if $x > 0$ then $\varpi(x) = x$ else $\varpi(x) = 0$.

or with a slope correction for the threshold value:

a, E coefficients, $a = 0, b = 3$ or $a = b = 1$ or $a = 1/2, b = 1$ or ...

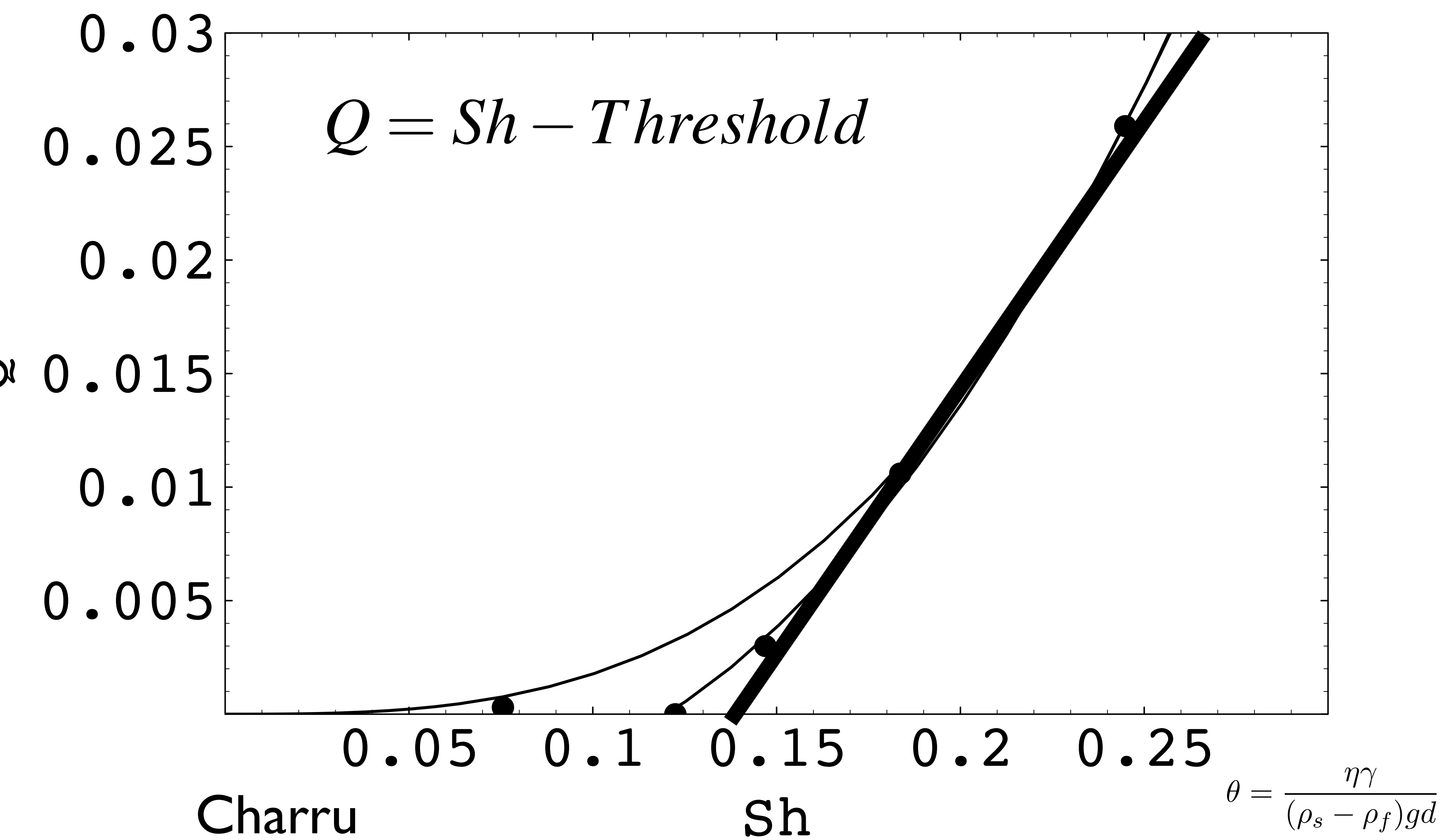

Erosion Model

In the literature one founds Charru /Izumi & Parker / Yang / Blondeau Du Boys

$$q_s = E\varpi(\tau^a(\tau - \tau_s)^b)$$

if $x > 0$ then $\varpi(x) = x$ else $\varpi(x) = 0$.

or with a slope correction for the threshold value:

a, E coefficients, $a = 0, b = 3$ or $a = b = 1$ or $a = 1/2, b = 1$ or ...

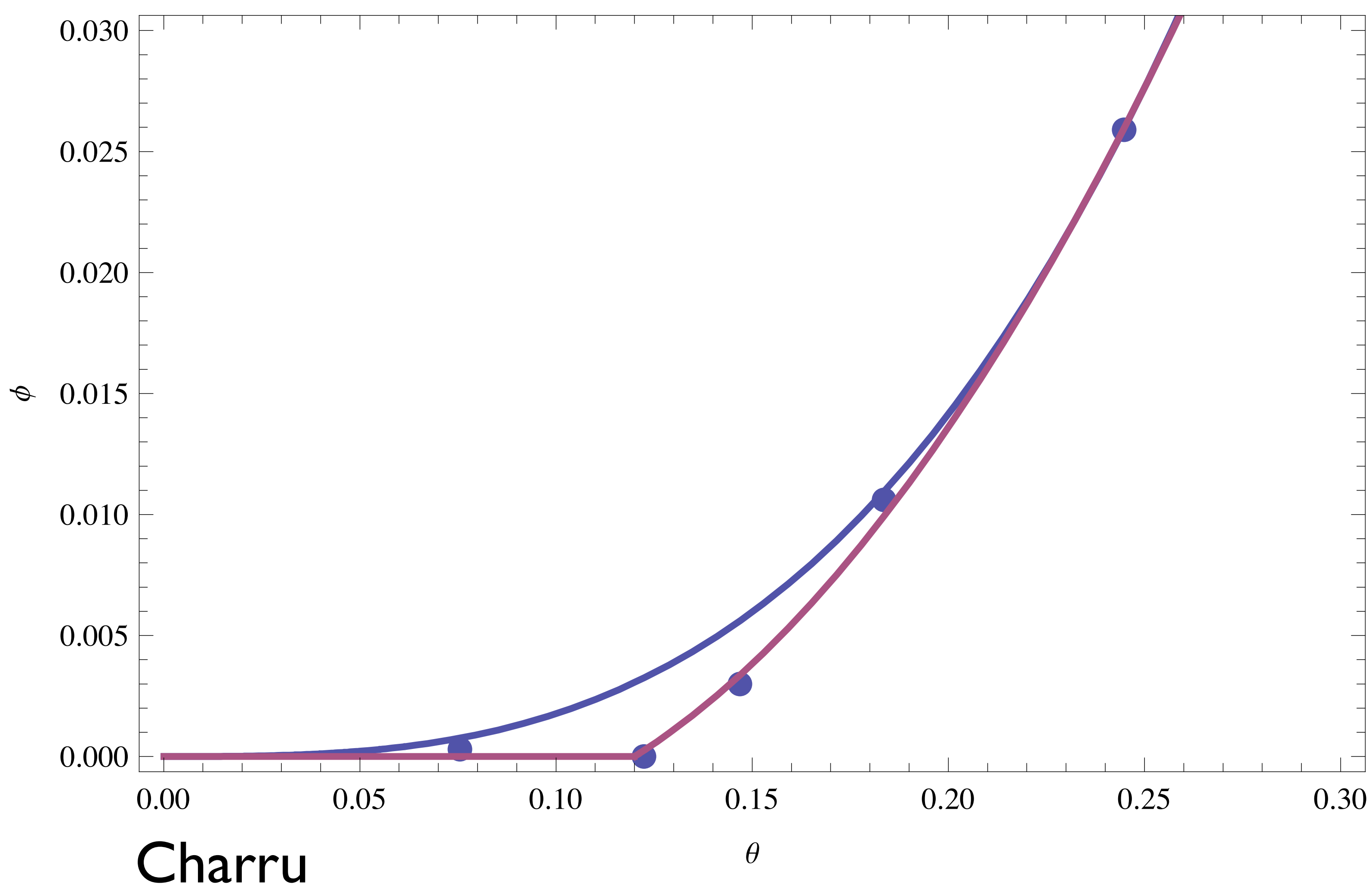

Charru

Erosion Model

In the literature one founds Charru /Izumi & Parker / Yang / Blondeau Du Boys

$$q_s = E\varpi(\tau^a(\tau - \tau_s)^b)$$

if $x > 0$ then $\varpi(x) = x$ else $\varpi(x) = 0$.

or with a slope correction for the threshold value:

a, E coefficients, $a = 0, b = 3$ or $a = b = 1$ or $a = 1/2, b = 1$ or ...

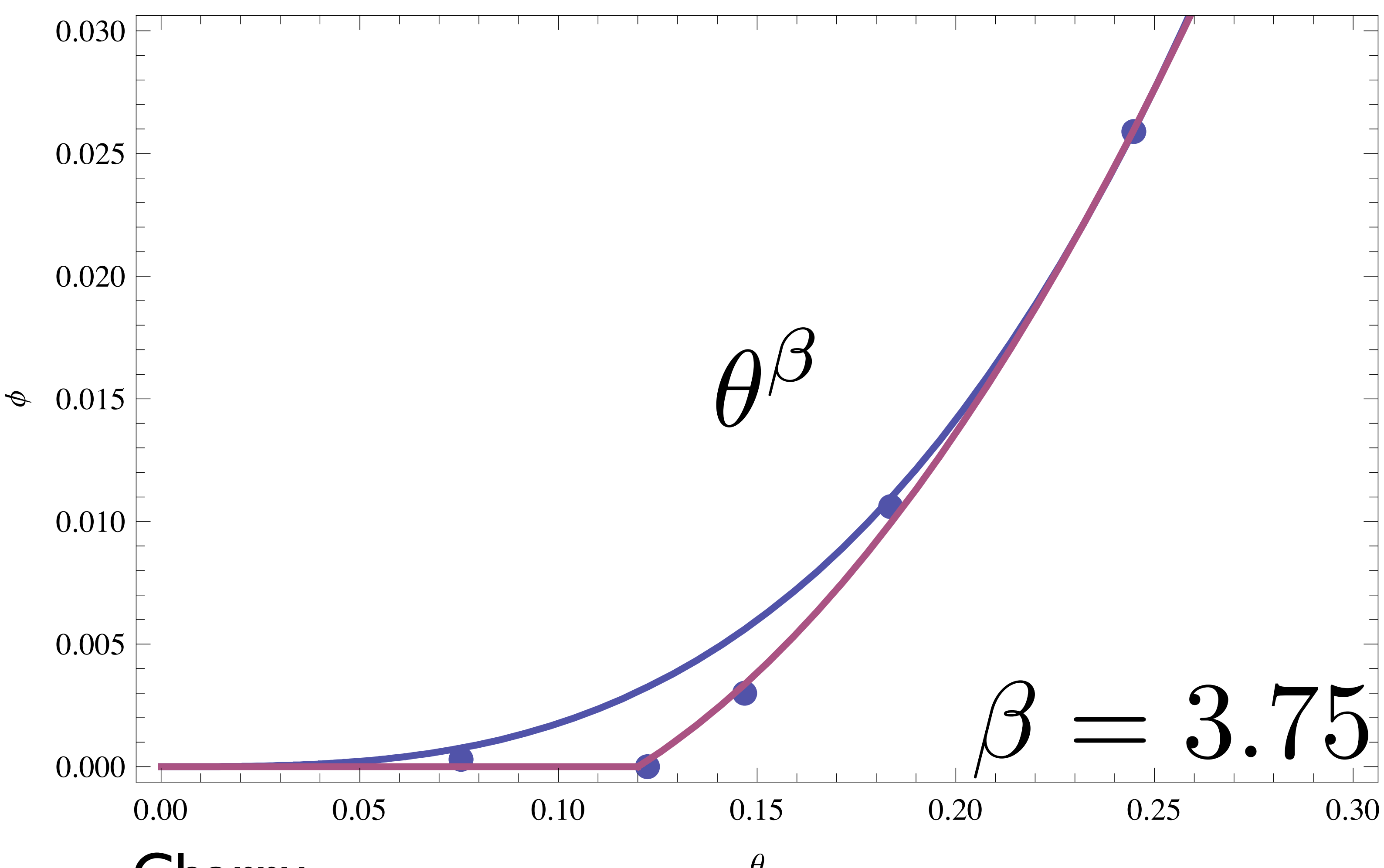

Charru

$$\vec{q} = \phi\theta^{\beta}\left(\frac{\vec{u}}{\|\vec{u}\|} - \gamma\vec{\nabla}h\right)$$

Bilan II

- threshold
- orders of magnitude
- experimental laws q(V,d,...)

Improving Exner law

$$\boxed{\begin{array}{cc} l_s\dfrac{\partial q}{\partial x} + q = q_s & \dfrac{\partial f}{\partial t} = -\dfrac{\partial q}{\partial x} \\ \multicolumn{2}{c}{q_s = E(\tau - \tau_s)_+} \end{array}}$$

Going back to mass conservation

(what goes in) - (what goes out)

Kroy/ Hermann/ Sauermann 02, Lagrée 03, Valance Langlois 05, Charru Hinch 06

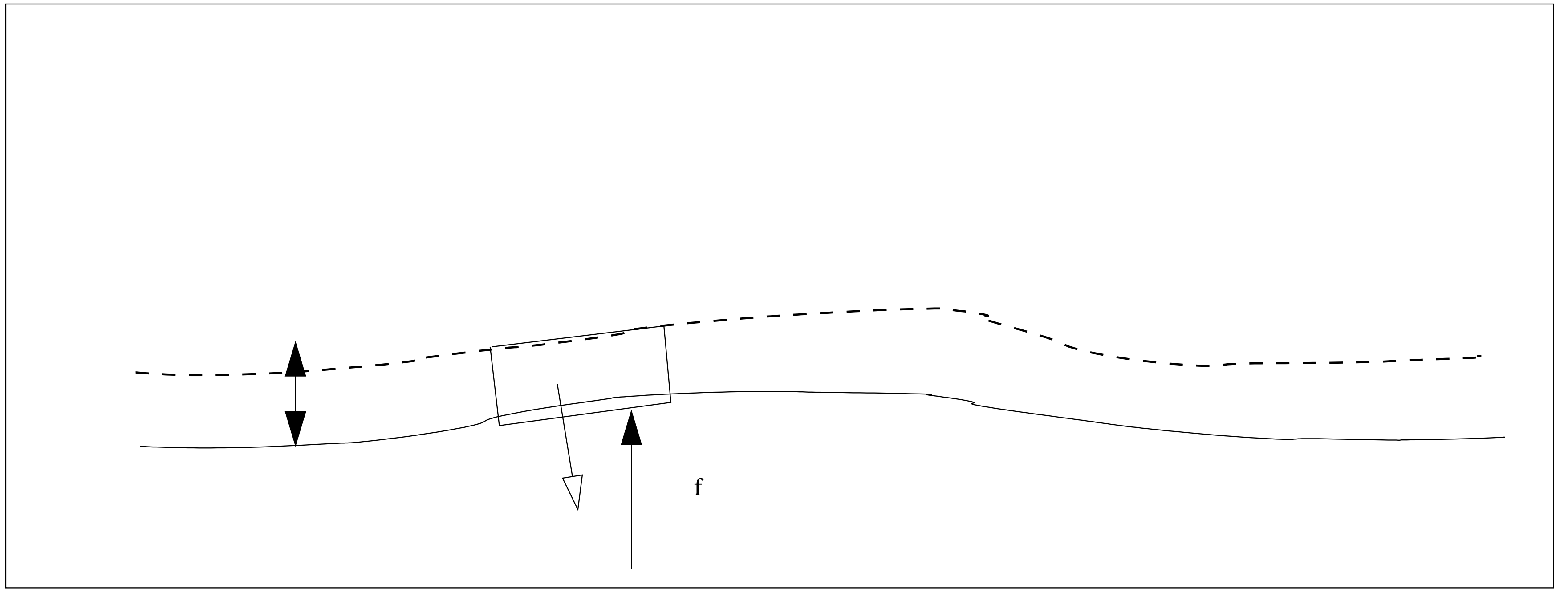

$$\frac{\partial R}{\partial t} = ... + \Gamma$$

$$\frac{\partial f}{\partial t} = -\Gamma$$

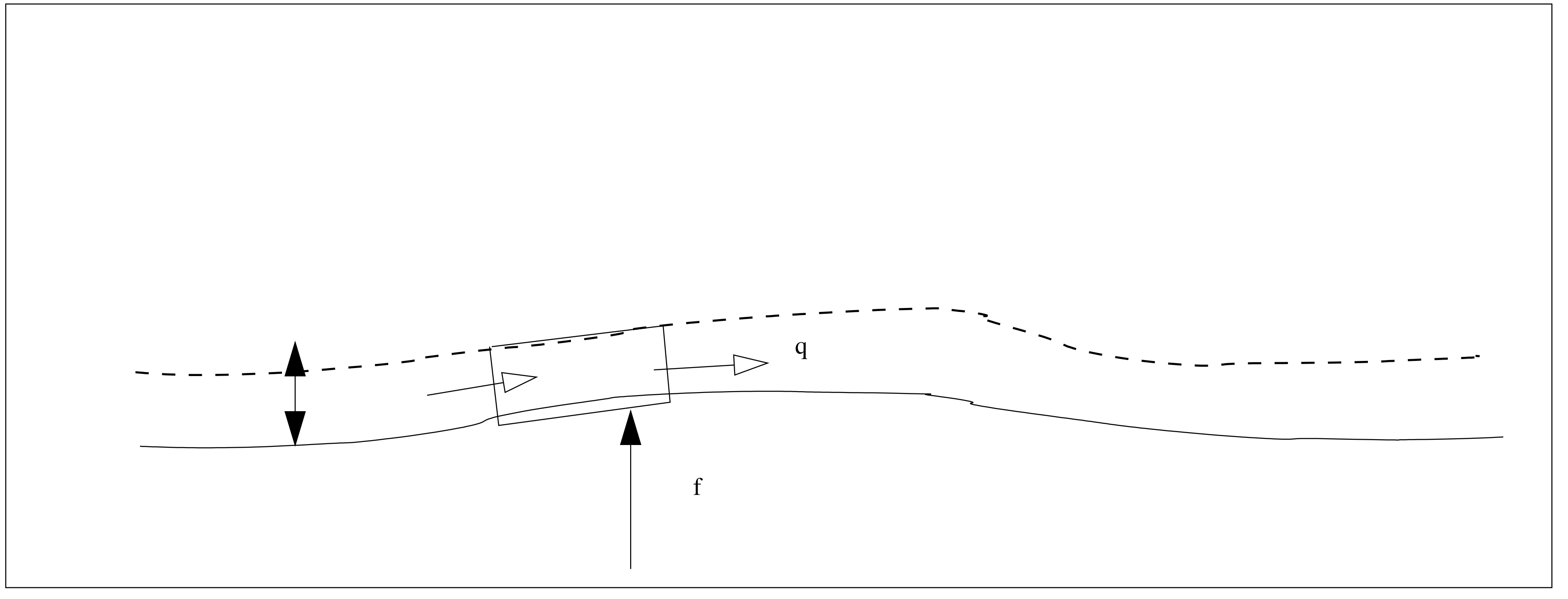

$$\frac{\partial R}{\partial t} = -\frac{\partial q}{\partial x} + \Gamma$$

$$\frac{\partial f}{\partial t} = -\Gamma$$

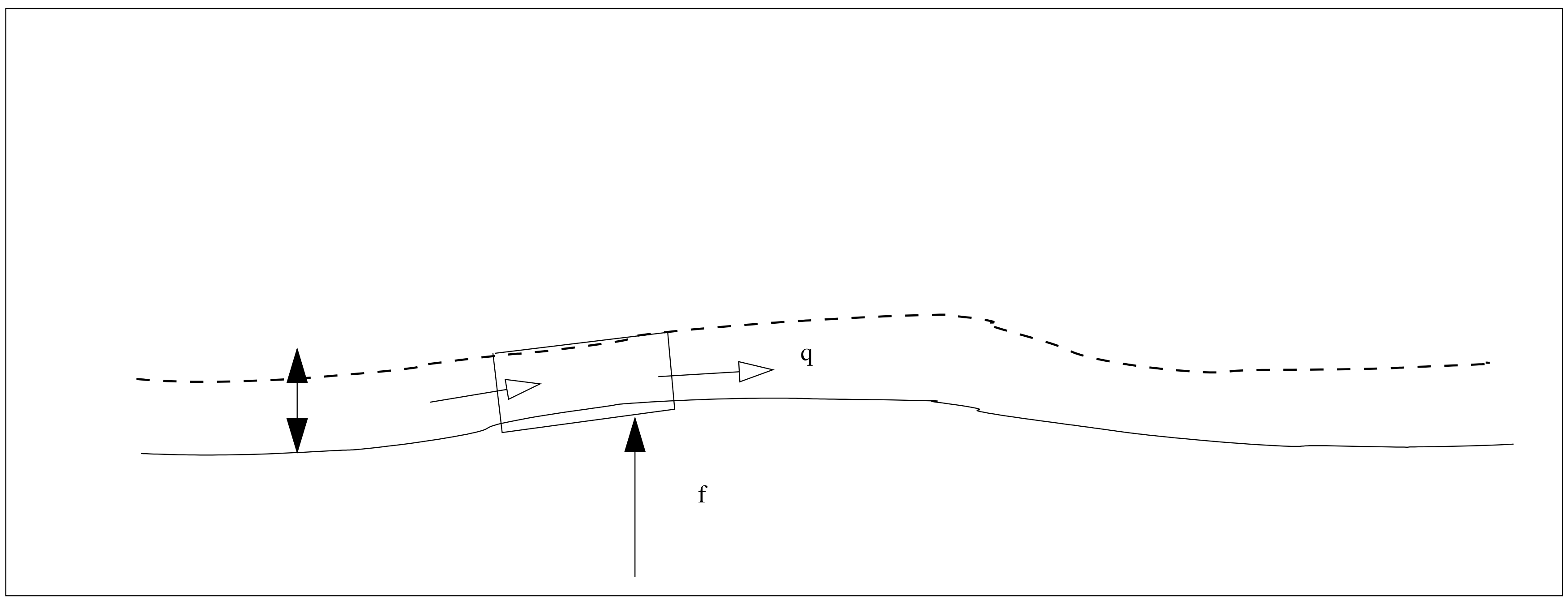

$$\frac{\partial R}{\partial t} = -\frac{\partial q}{\partial x} + \Gamma \qquad \frac{\partial f}{\partial t} = -\Gamma$$

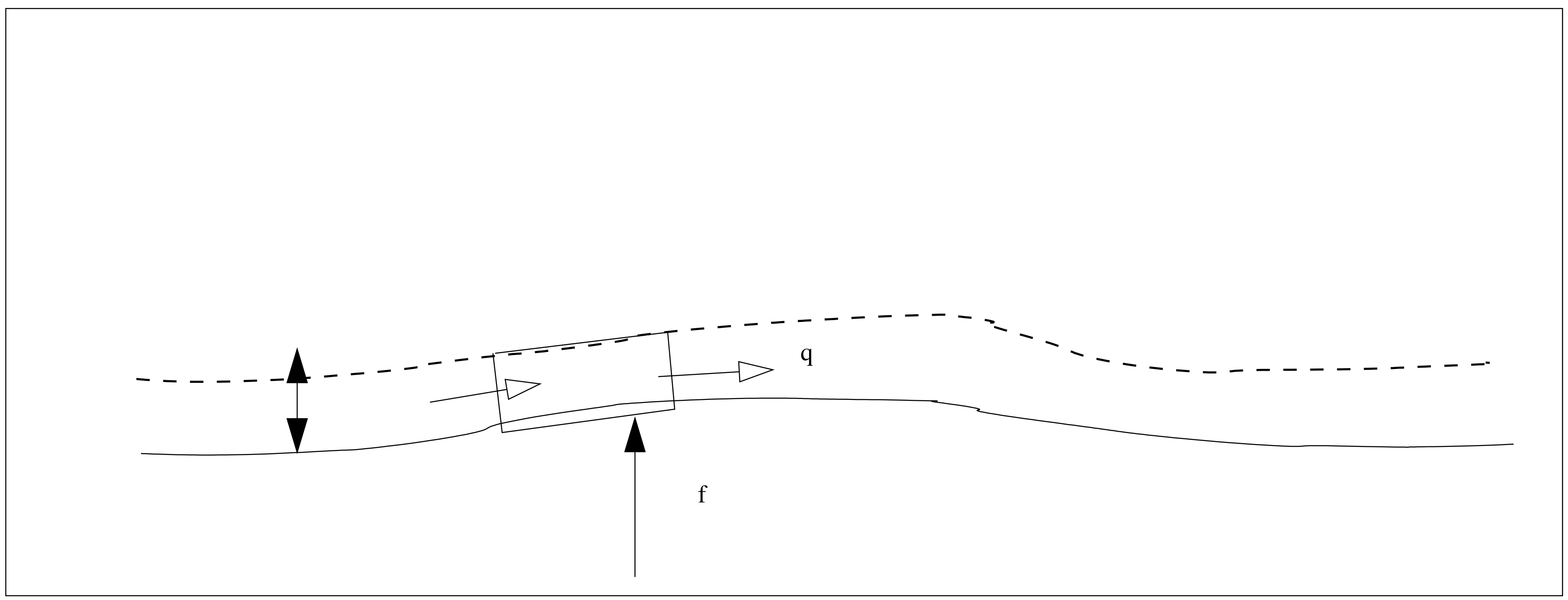

$$\frac{\partial R}{\partial t} = -\frac{\partial q}{\partial x} + \Gamma \qquad \frac{\partial f}{\partial t} = -\Gamma$$

$\Gamma =$ (érosion)-(déposition)

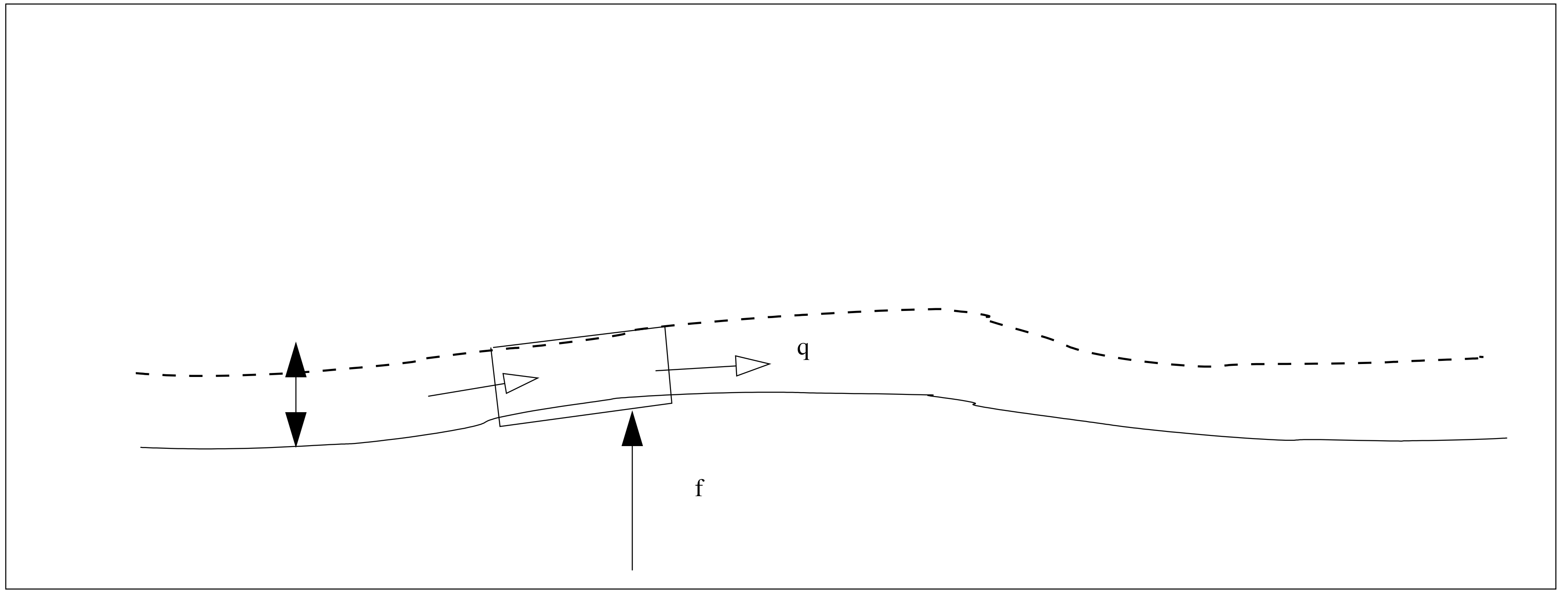

$$\frac{\partial R}{\partial t} = -\frac{\partial q}{\partial x} + \Gamma \qquad\qquad \frac{\partial f}{\partial t} = -\Gamma$$

$\Gamma =$ (érosion)-(déposition)

-(déposition) $\propto -R$ érosion $\propto (\tau - \tau_s)$ et $q \propto R\,\tau$

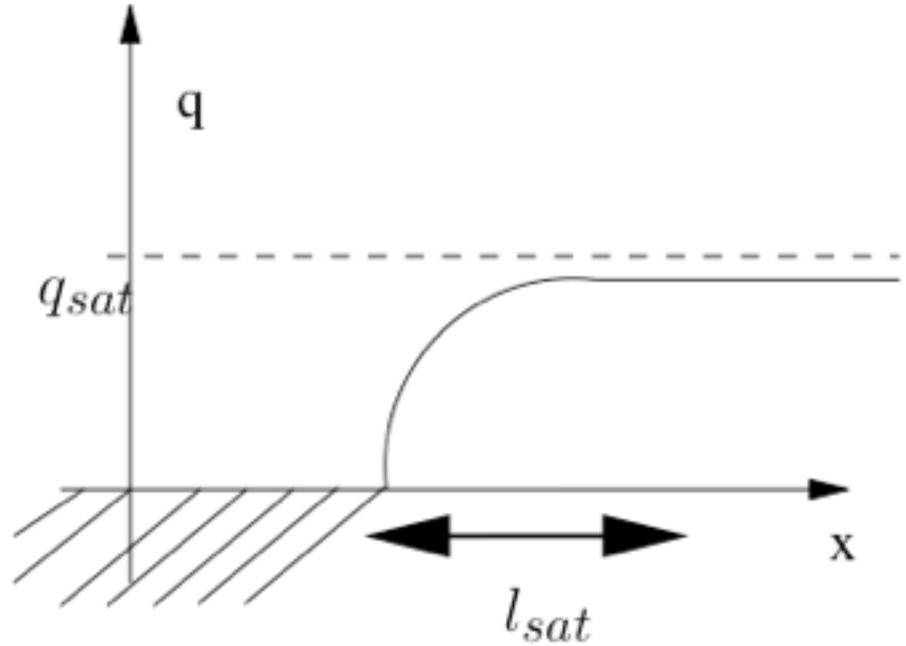

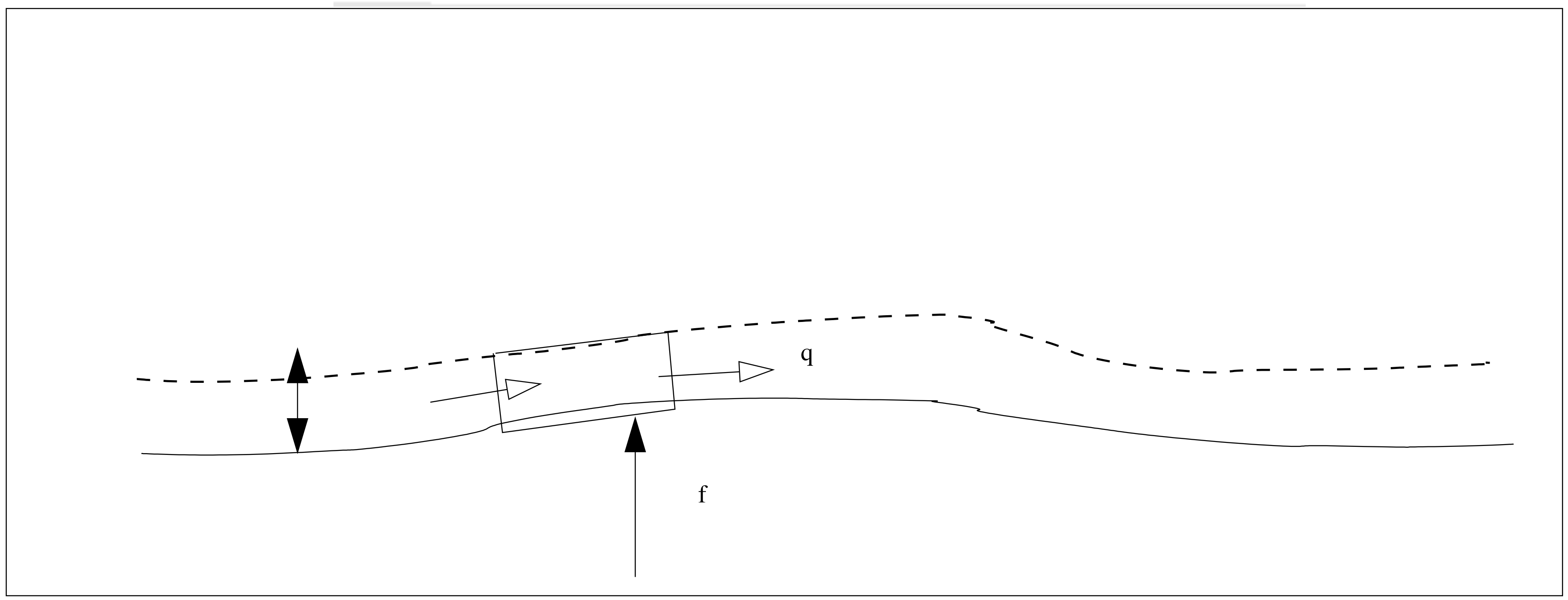

$$l_s \frac{\partial q}{\partial x} + q = q_s \qquad \frac{\partial f}{\partial t} = -\frac{\partial q}{\partial x}$$

$$q_s = E(\tau - \tau_s)_+$$

inspired from Sauerman Kroy Hermann 01: Andreotti Claudin Douady 02, Lagrée 03

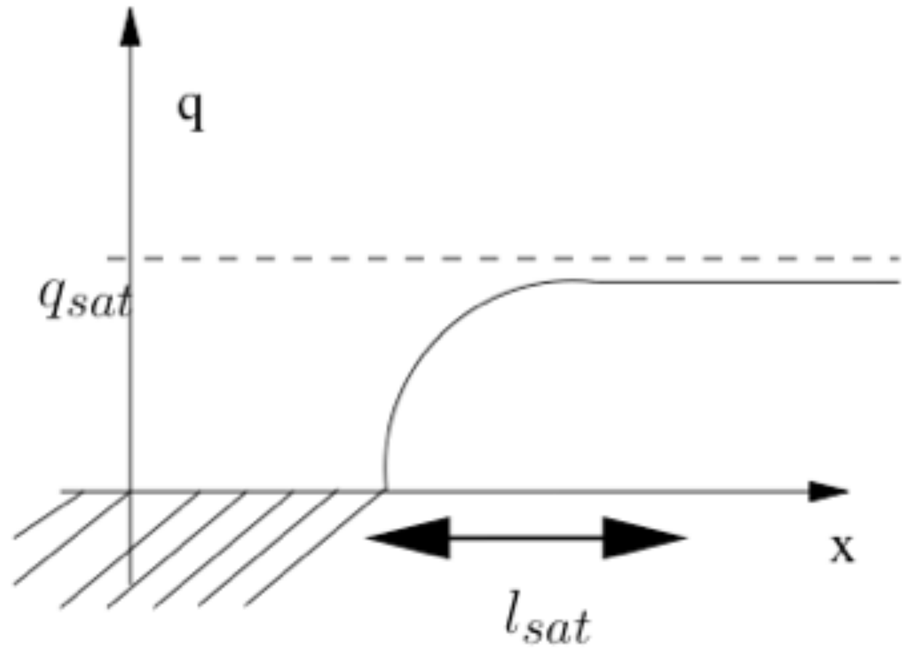

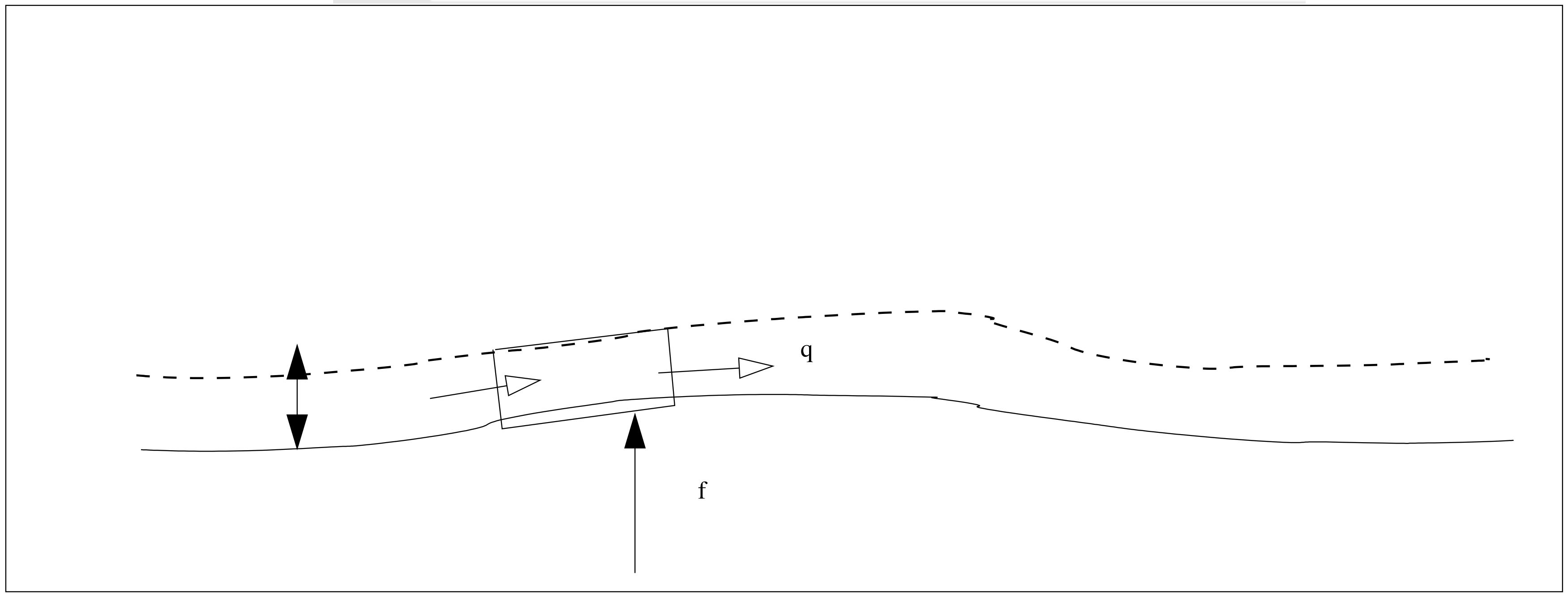

Du Boy (1879) :

“*une fois une certaine quantité de matières en mouvement sur le fond du lit, la vitesse des filets liquides devient trop faible pour entraîner davantage : le cours d'eau est alors saturé. Un cours d'eau non saturé tend à le devenir en entraînant une partie des matériaux qui composent son lit, et en choisissant de préférence les plus petits.*”

$$(4/3\pi(d/2)^3)\rho_p dv/dt = (4/3\pi(d/2)^3)(\rho_p - \rho)\, g - 6\pi\mu v(d/2)$$

$$\frac{dv}{dt} \simeq \frac{V_f - v}{T_{Stokes}}$$

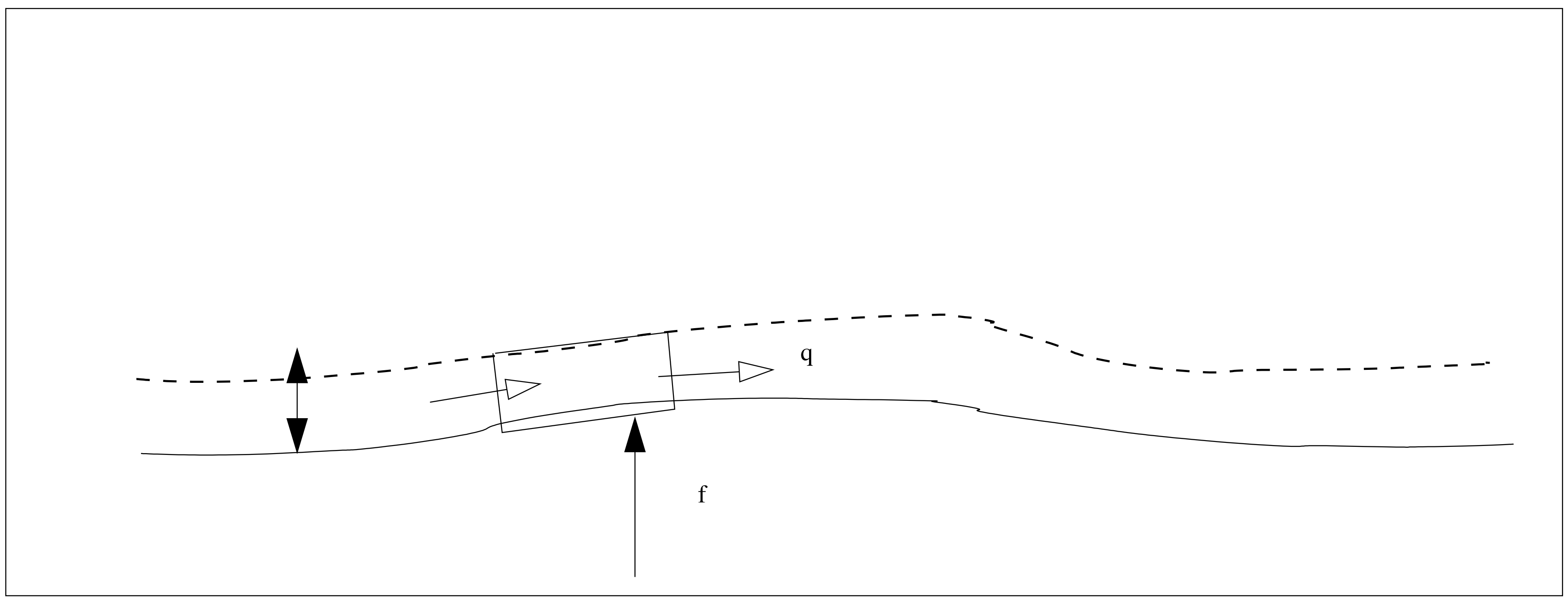

Characteristic length *d*

$$T_{Stokes} = \frac{\rho_p}{\rho}\frac{d^2}{\nu}, \quad \text{et} \quad V_f = \frac{(\rho_s - \rho)gd^2}{18\mu}$$

$$(4/3\pi d^3)\rho_p dv/dt = (4/3\pi d^3)(\rho_p - \rho)\, g - C_D \pi d^2 v^2$$

$$\frac{dv}{dt} \simeq \frac{V_f^2 - v^2}{l_{sat}}$$

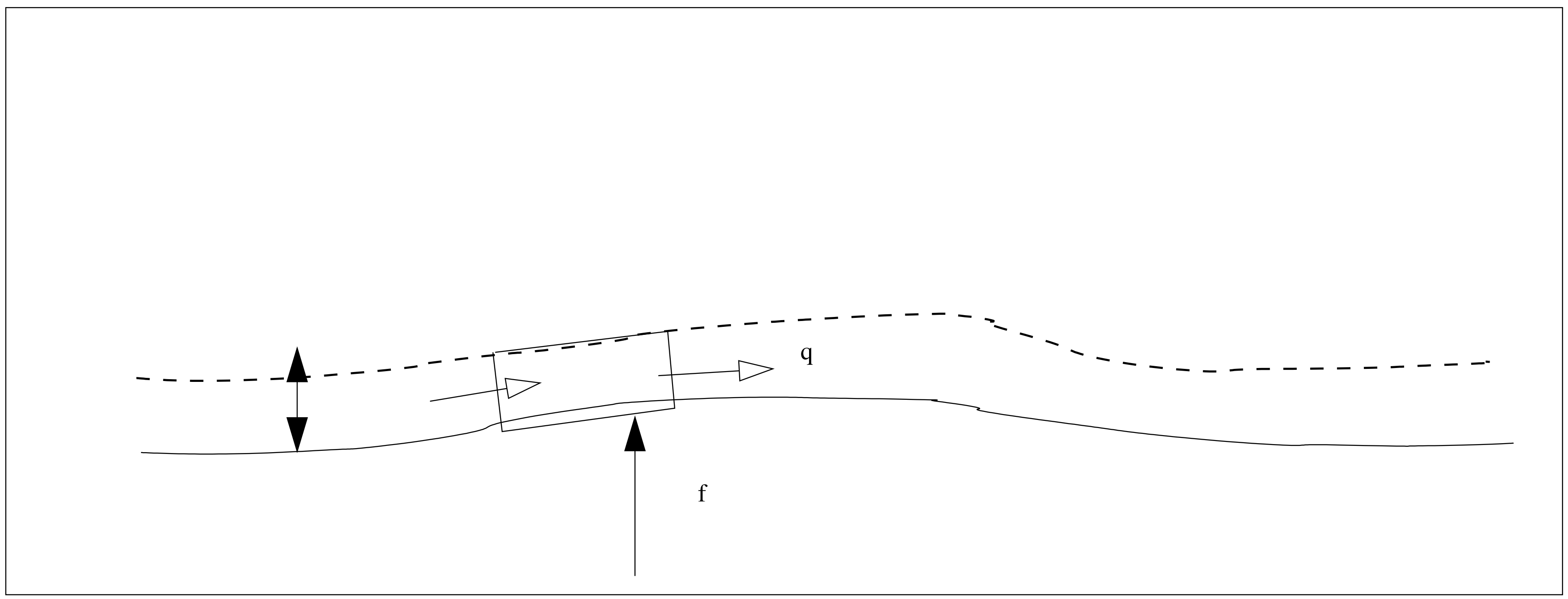

$$l_{sat} = \frac{\rho_p}{\rho}\, d. \quad \text{et} \quad V_f = \sqrt{\frac{4(\rho_s/\rho - 1)gd}{3c_d}}.$$

Notation «Charru»

$$\frac{\partial n}{\partial t} = \dot{n}_e - \dot{n}_d - \frac{\partial q}{\partial x} \qquad \phi \frac{\partial f}{\partial t} = \frac{\pi d^3}{6}(\dot{n}_e - \dot{n}_d)$$

$$\dot{n}_d = c_d \frac{V_s}{d} n \qquad \dot{n}_e = \frac{18 c_e V_s{}^3}{d}(c_g Sh - Sh_c) \qquad q = n c_u d \frac{\partial u}{\partial y}$$

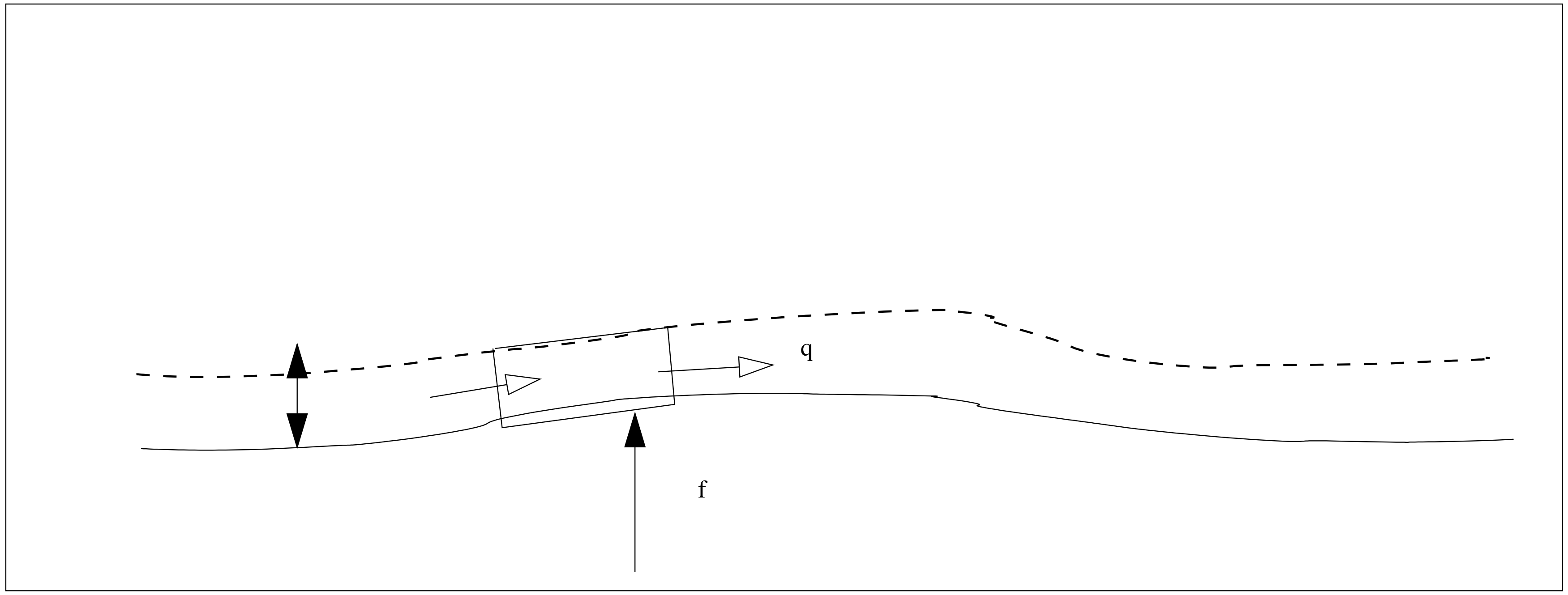

$$\frac{\partial R}{\partial t} = -\frac{\partial q}{\partial x} + \Gamma \qquad \frac{\partial f}{\partial t} = -\Gamma$$

$\Gamma =$ (érosion)-(déposition)

-(déposition) $\propto -R$ érosion $\propto (\tau - \tau_s)$ et $q \propto R\tau$

Bilan III

- threshold
- orders of magnitude
- experimental laws $q_s(V,d,\ldots)$ "saturated"
- mass balance
- new relation for actual flux q

$$l_s \frac{\partial q}{\partial x} + q = q_s \qquad\qquad \frac{\partial f}{\partial t} = -\frac{\partial q}{\partial x}$$

$$q_s = E(\tau - \tau_s)_+$$

The problem:

Simplified model of interaction: erodible bed/ flow

interaction: erodible bed/ flow
coupled problem
different time scales

The problem:

Simplified model of interaction: erodible bed/ flow

- simplified transport laws   slow bed evolution

- asymptotic models for the flow (Saint Venant, pure shear flow at large Reynolds)

The problem:

Simplified model of interaction: erodible bed/ flow

- simplified transport laws   slow bed evolution

- asymptotic models for the flow (Saint Venant, pure shear flow at large Reynolds)

=> good physics, good terms in the equation but maybe too simple...

easy model to solve

stability, pattern formation

conservation of mass of granulars bed load

$$\frac{\partial f}{\partial t} = -\frac{\partial q}{\partial x}.$$

f is the shape of the topography
q is the flux of sediment

Problem :
What is the relationship between q and the flow?
hint: the larger u the larger the erosion, the larger q
q seems to be proportional to the skin friction

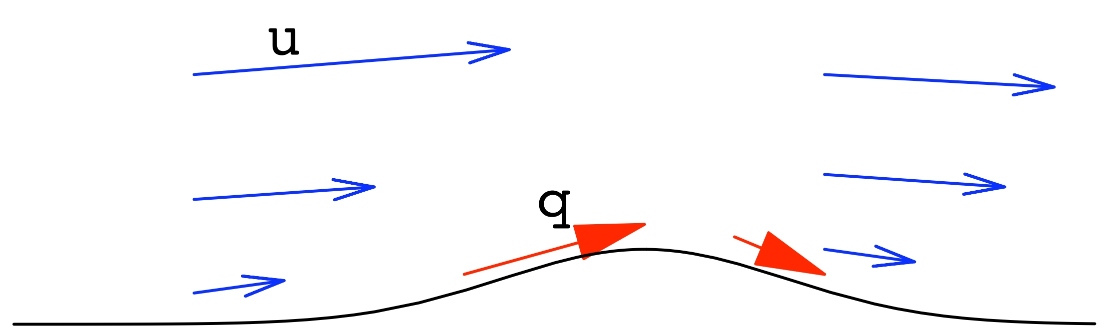

conservation of mass of granulars   bed load

$$\frac{\partial f}{\partial t} = -\frac{\partial q}{\partial x}.$$

Felix Maria von Exner-Ewarten
Vienna, 1876-1930
Austrian meteorologist and geophysicist

- crude mechanism $q \propto u$

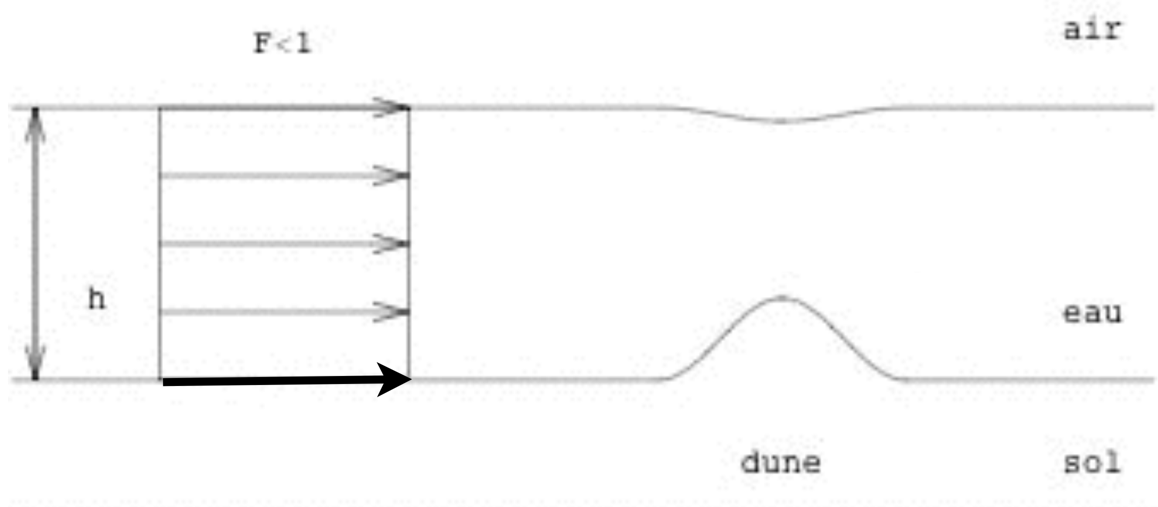

$$q \propto u$$

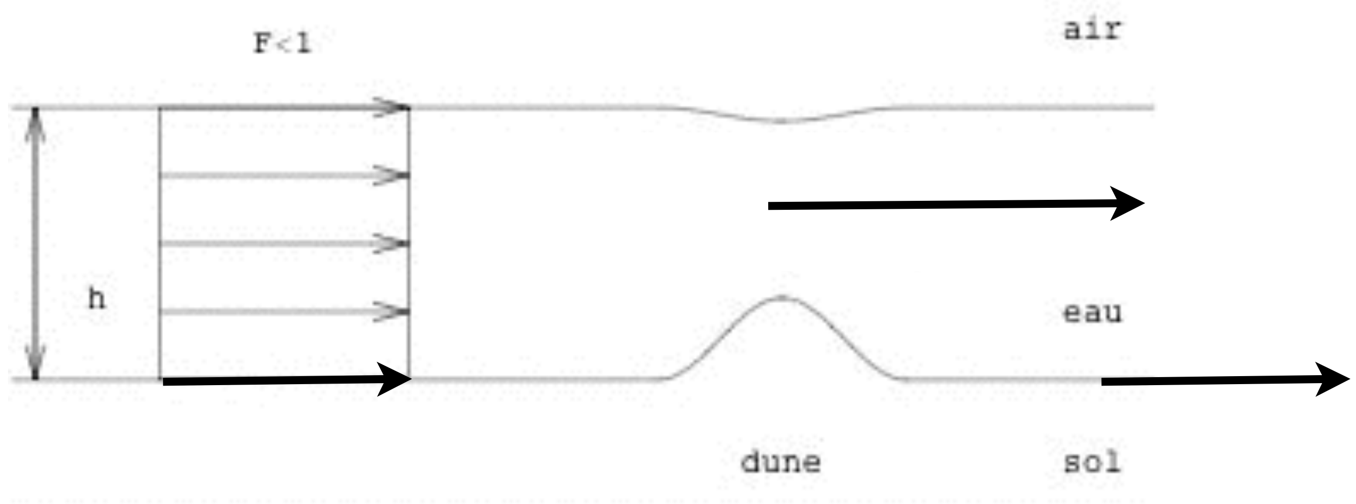

u increases & deacreases over the bump,

$$q \propto u$$

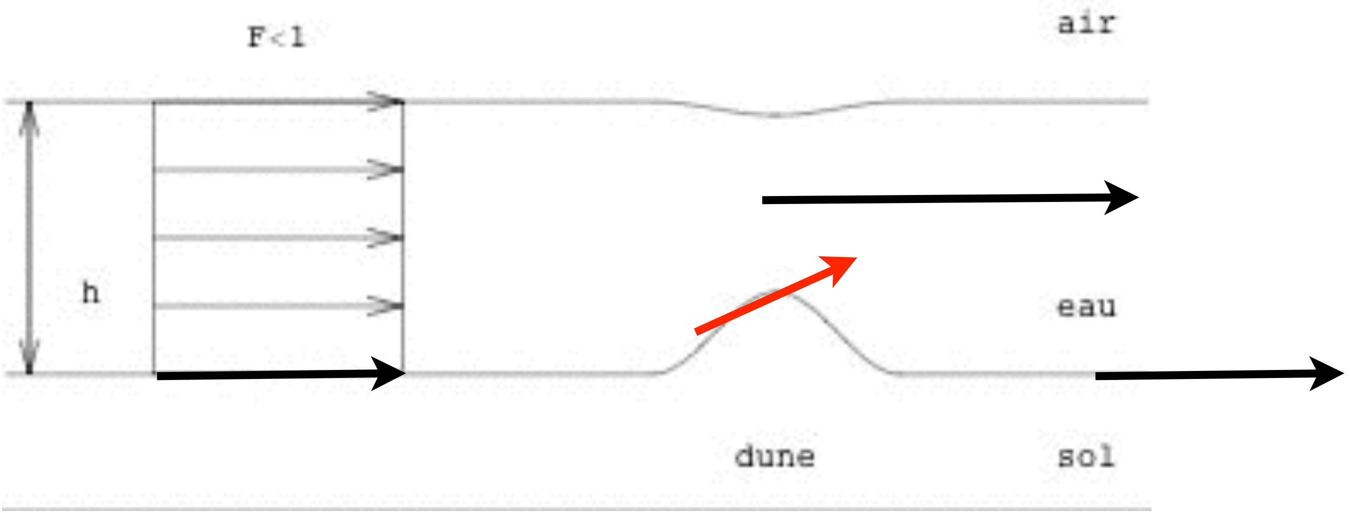

u increases & deacreases over the bump,

flux of granulars increases on the «wind» side

$$q \propto u \qquad \frac{\partial f}{\partial t} = -\frac{\partial q}{\partial x}$$

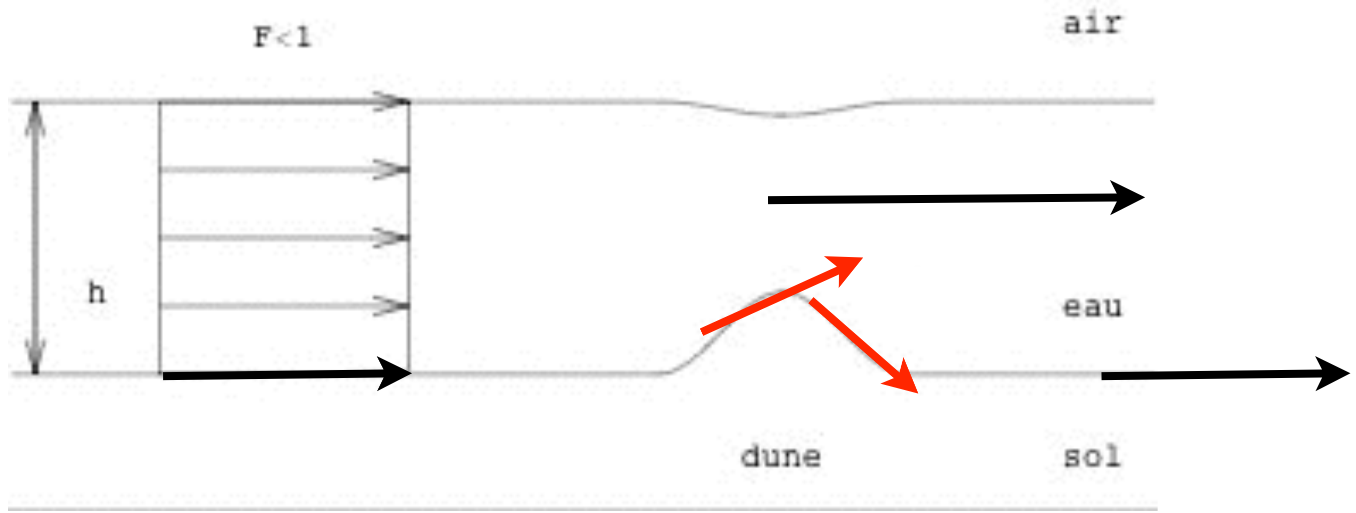

u increases & deacreases over the bump,

flux of granulars increases on the «wind» side

flux of granulars decreases on the «lee» side

$$q \propto u \qquad \frac{\partial f}{\partial t} = -\frac{\partial q}{\partial x}$$

$$\frac{\partial f}{\partial t} \propto -\frac{\partial u}{\partial x}$$

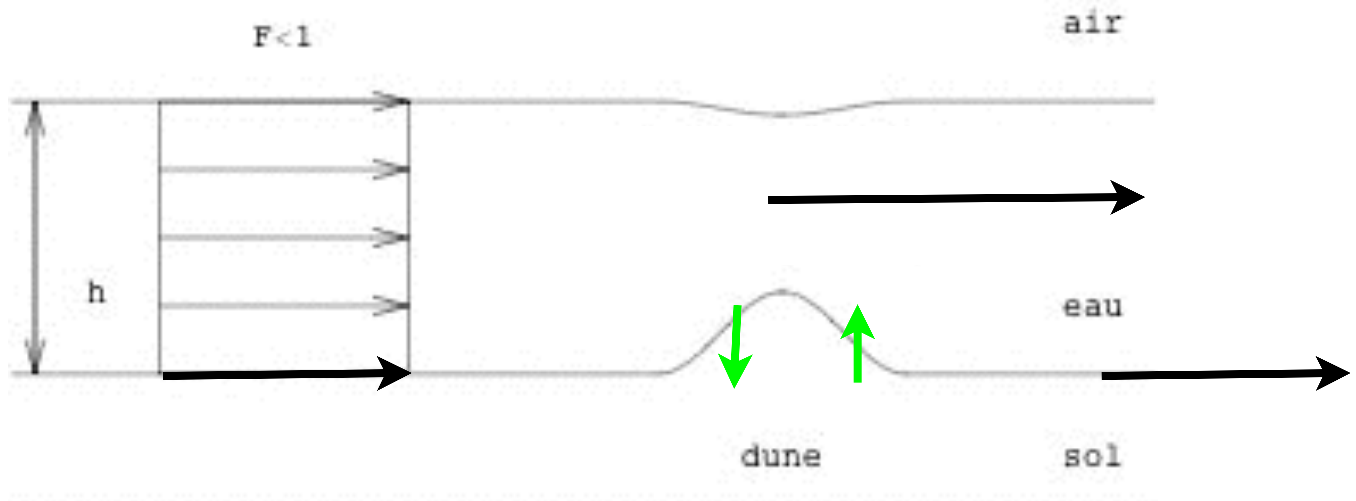

u increases & deacreases over the bump,

flux of granulars increases on the «wind» side

flux of granulars decreases on the «lee» side

the bump is eroded and sedimented

$$q \propto u \qquad \frac{\partial f}{\partial t} = -\frac{\partial q}{\partial x}$$

$$\frac{\partial f}{\partial t} \propto -\frac{\partial u}{\partial x}$$

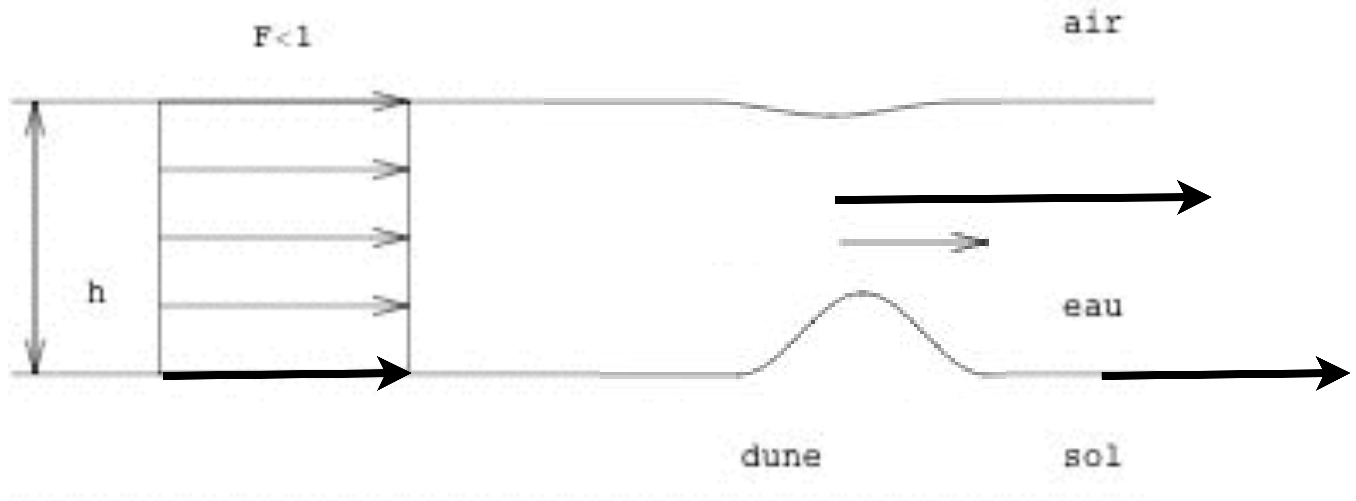

u increases & deacreases over the bump,

flux of granulars increases on the «wind» side

flux of granulars decreases on the «lee» side

the bump is eroded and sedimented

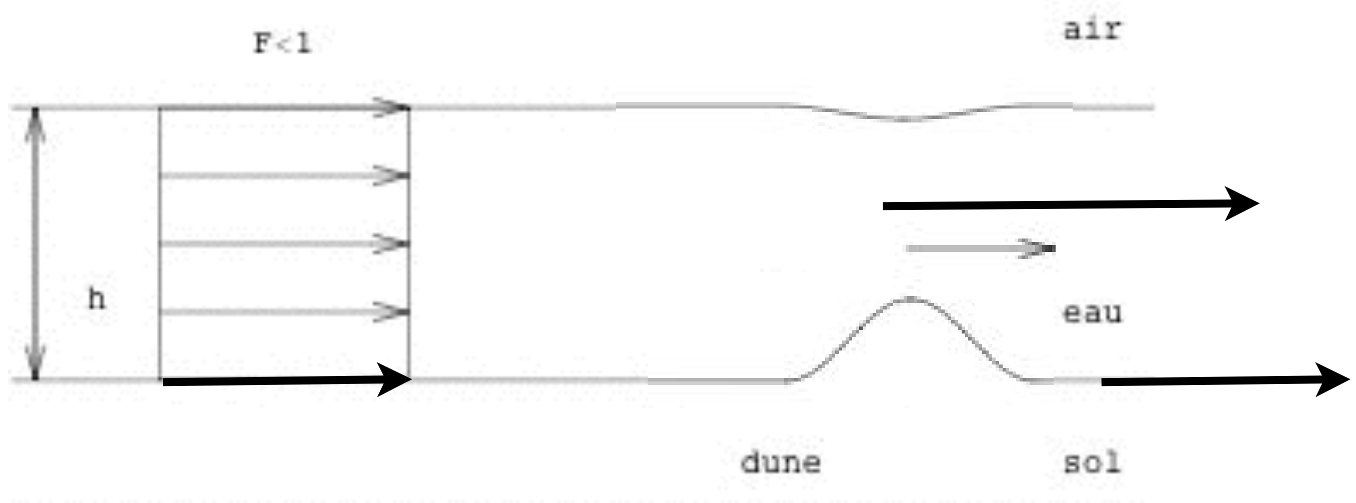

u increases & deacreases over the bump,

flux of granulars increases on the «wind» side

flux of granulars decreases on the «lee» side

the bump is eroded and sedimented

- a better mechanism $q \propto \mu \dfrac{\partial u}{\partial y}$

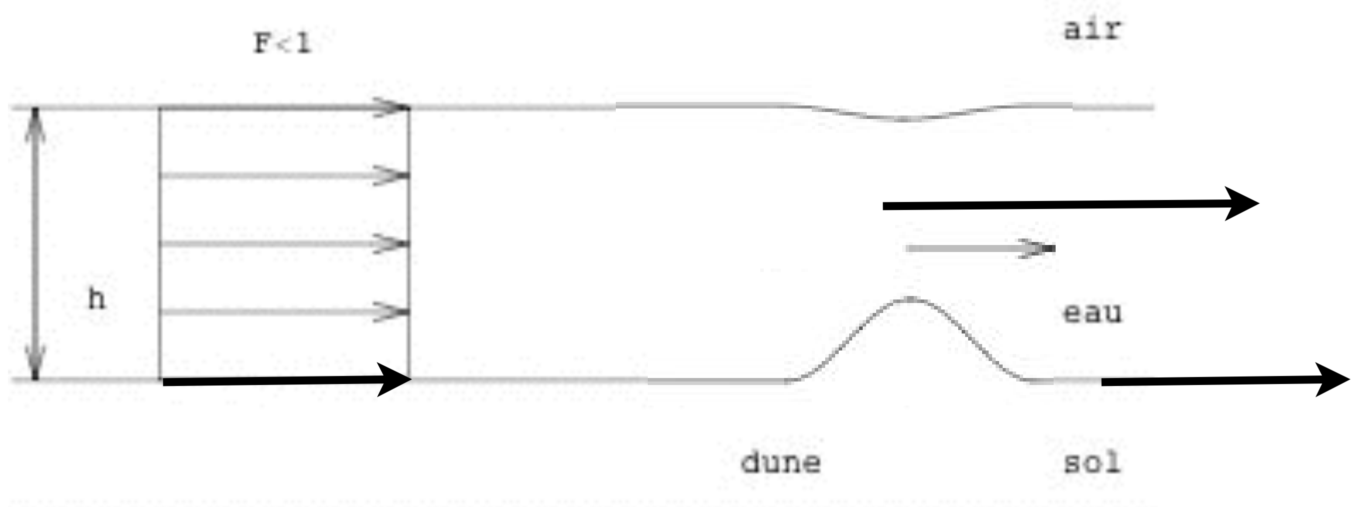

u increases & deacreases over the bump,

flux of granulars increases on the «wind» side

flux of granulars decreases on the «lee» side

the bump is eroded and sedimented

- case of the antidune!

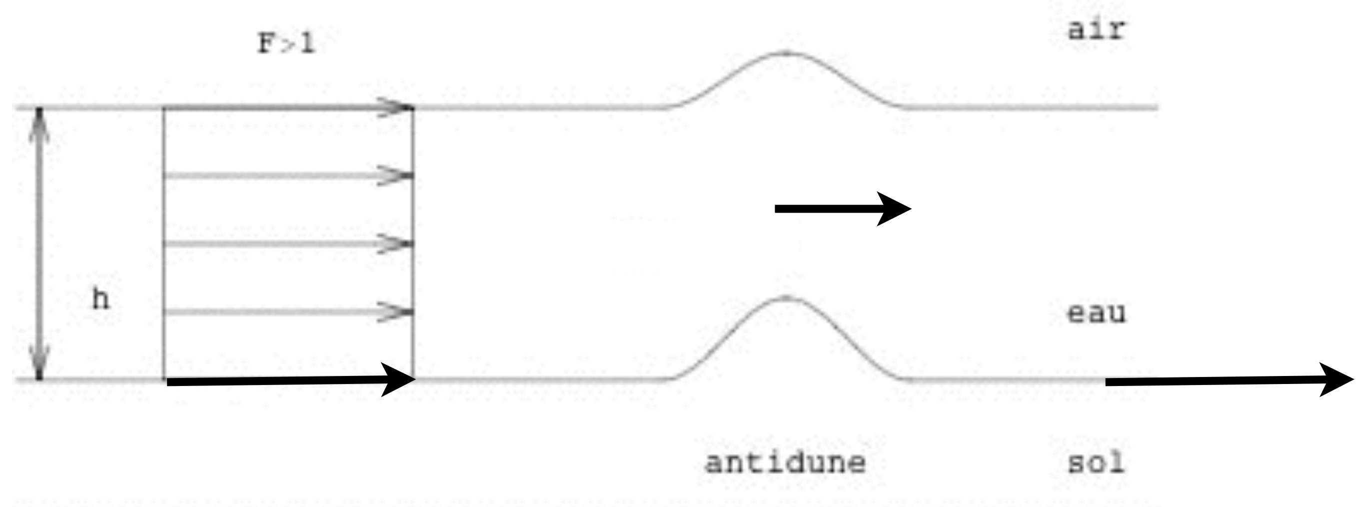

u increases & deacreases over the bump,

flux of granulars increases on the «wind» side

flux of granulars decreases on the «lee» side

the bump is eroded and sedimented

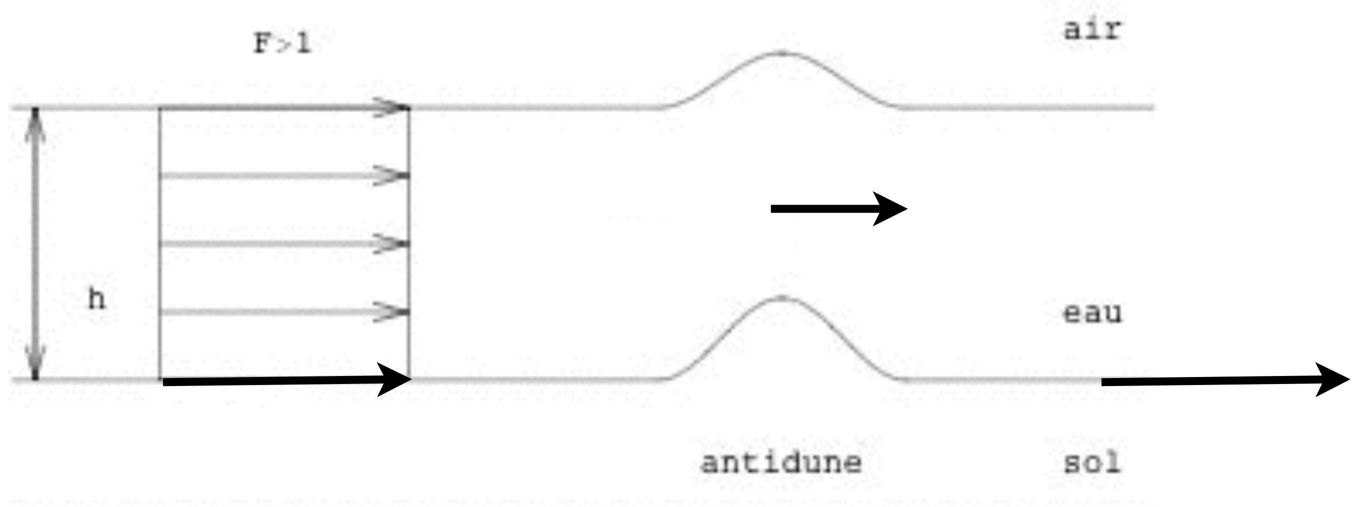

u increases & deacreases over the bump,

flux of granulars increases on the «wind» side

flux of granulars decreases on the «lee» side

the bump is eroded and sedimented

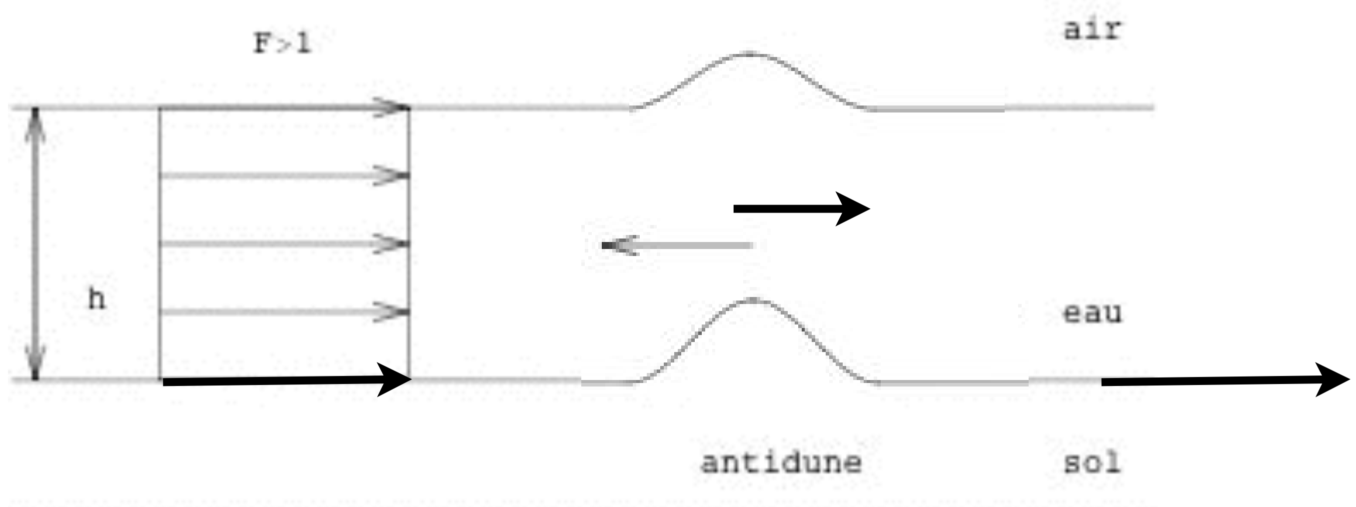

u increases & deacreases over the bump,

flux of granulars increases on the «wind» side

flux of granulars decreases on the «lee» side

the bump is eroded and sedimented

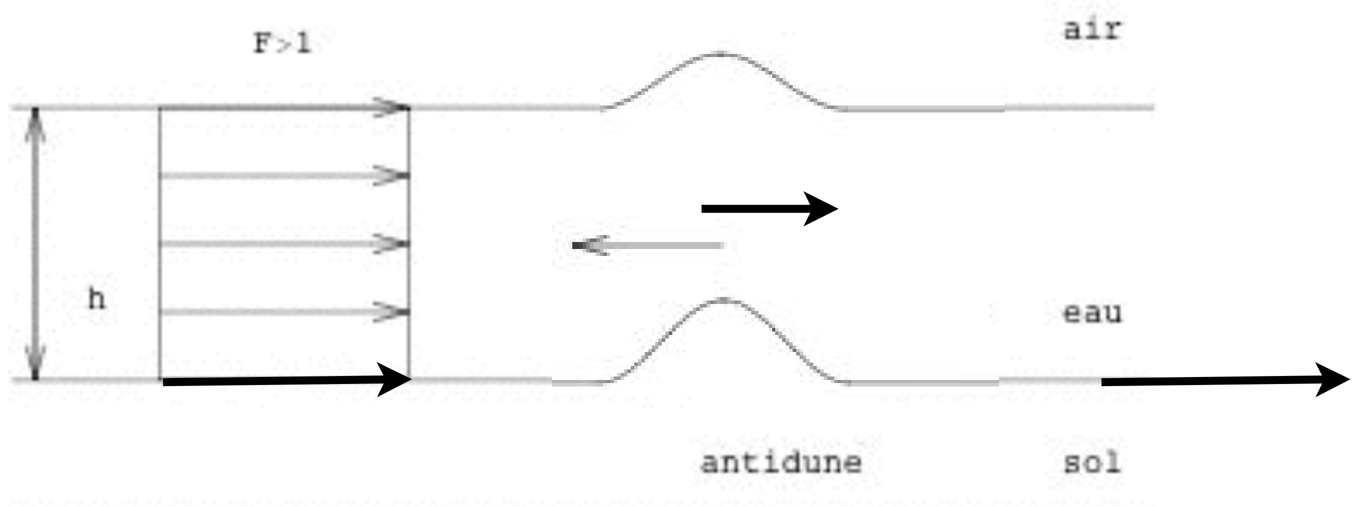

u increases & deacreases over the bump,

flux of granulars increases on the «wind» side

flux of granulars decreases on the «lee» side

the bump is eroded and sedimented

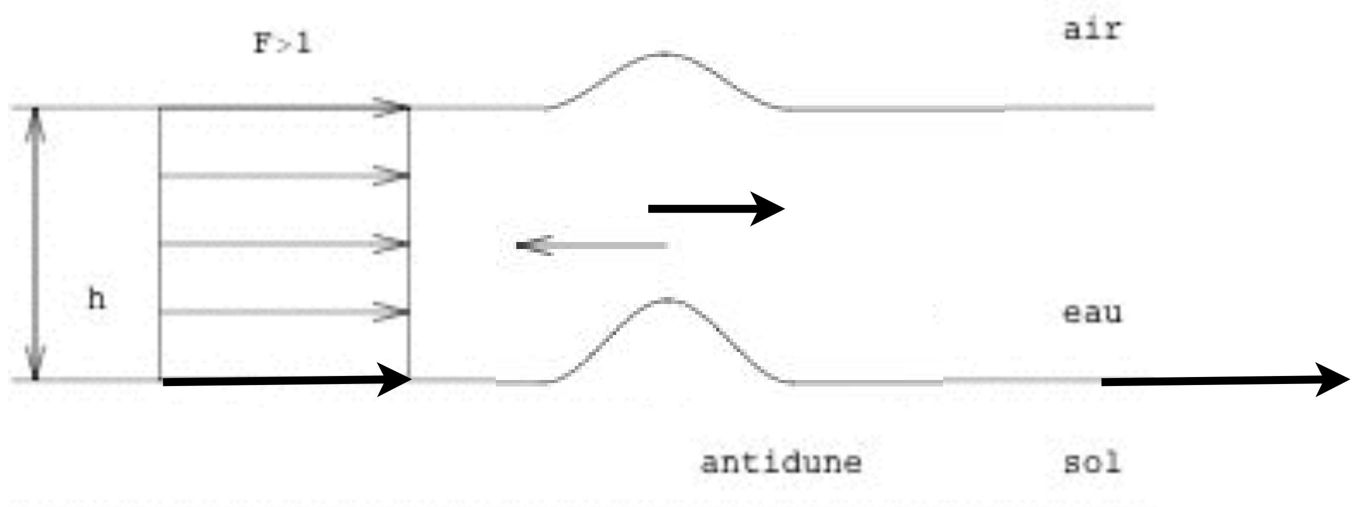

u increases & deacreases over the bump,

flux of granulars increases on the «wind» side

flux of granulars decreases on the «lee» side

the bump is eroded and sedimented

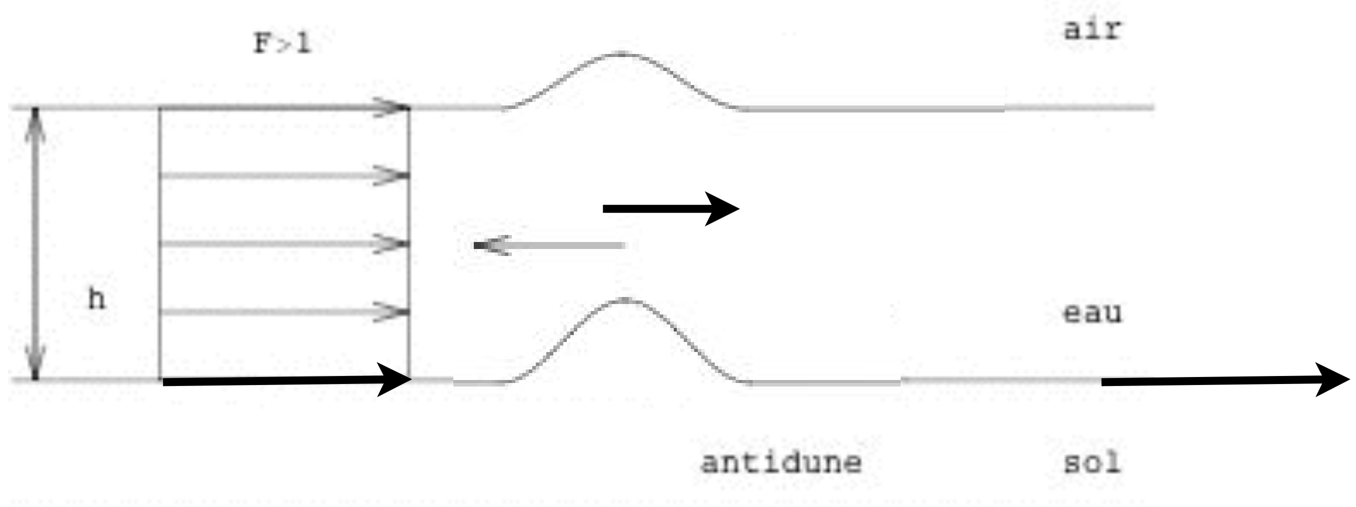

u increases & deacreases over the bump,

flux of granulars increases on the «wind» side

flux of granulars decreases on the «lee» side

the bump is eroded and sedimented

port An Dro Belle Ile

We have simple erosion law, the flow has to be calculated:

Saint Venant?

- **Saint Venant** Shallow Water

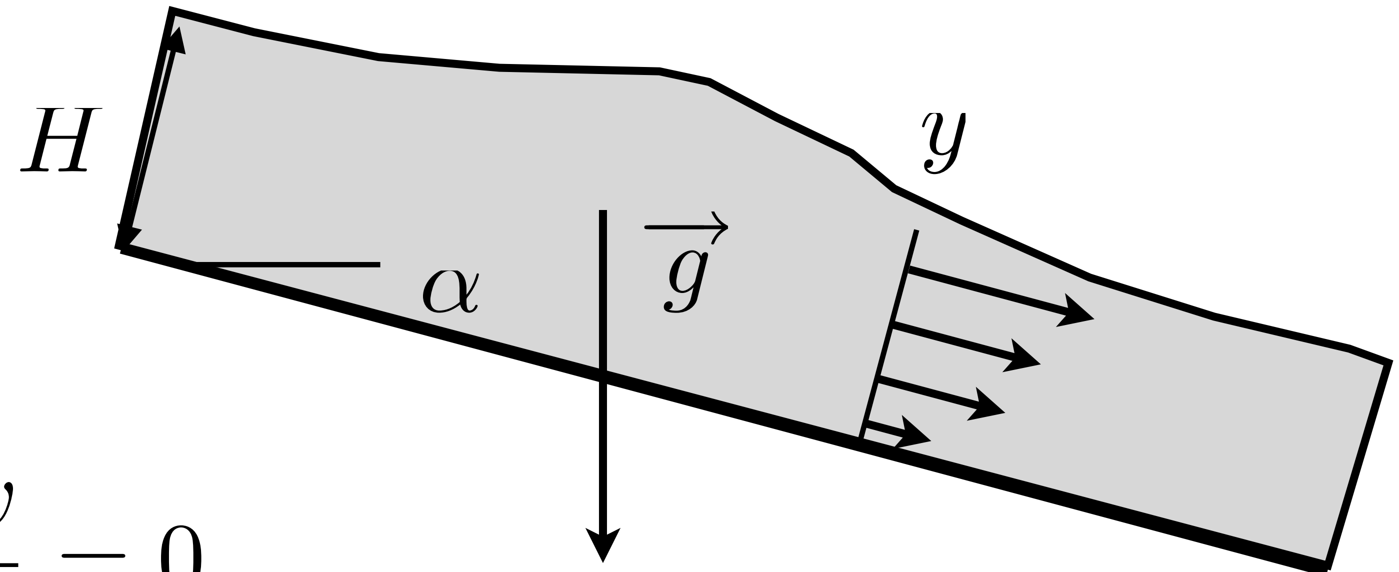

$$\frac{\partial u}{\partial x} + \frac{\partial v}{\partial y} = 0$$

$$\rho(\frac{\partial u}{\partial t} + u\frac{\partial u}{\partial x} + v\frac{\partial u}{\partial y}) = -\frac{\partial p}{\partial x} - \rho g sin(\alpha) + \mu(\frac{\partial^2 u}{\partial x^2} + \frac{\partial^2 u}{\partial y^2})$$

$$\rho(\frac{\partial v}{\partial t} + u\frac{\partial v}{\partial x} + v\frac{\partial v}{\partial y}) = -\frac{\partial p}{\partial y} - \rho g cos(\alpha) + \mu(\frac{\partial^2 v}{\partial x^2} + \frac{\partial^2 v}{\partial y^2})$$

- **Saint Venant** Shallow Water

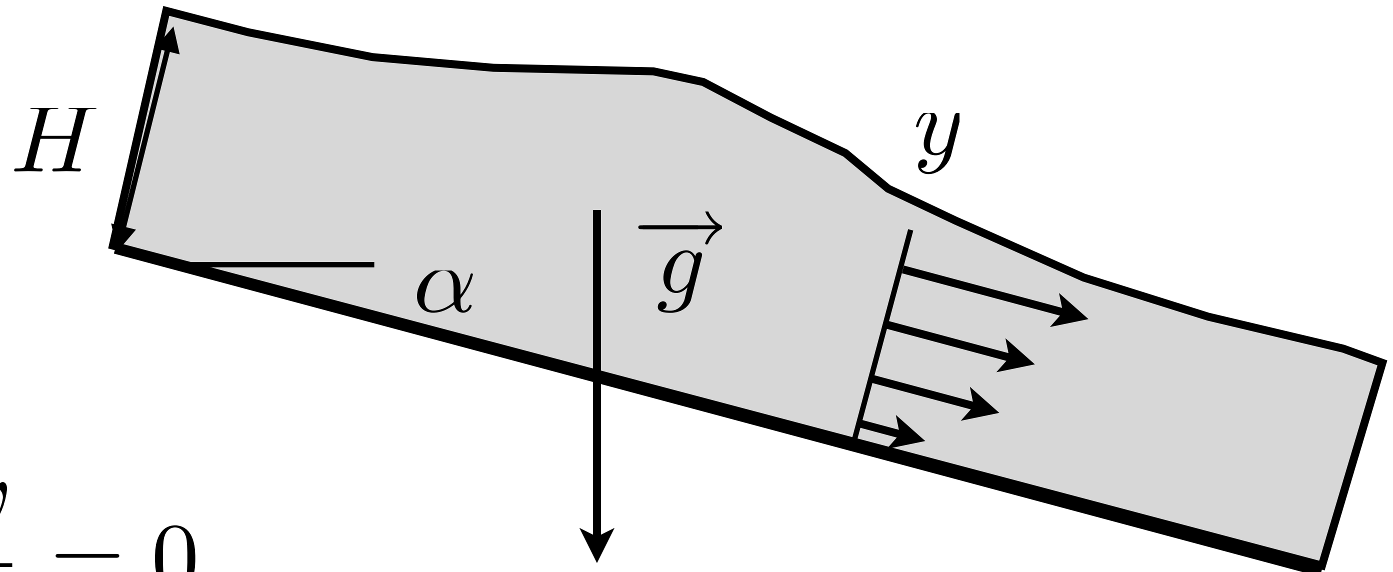

$$\varepsilon = H/L$$

$$\frac{\partial u}{\partial x} + \frac{\partial v}{\partial y} = 0$$

$$\rho(\frac{\partial u}{\partial t} + u\frac{\partial u}{\partial x} + v\frac{\partial u}{\partial y}) = -\frac{\partial p}{\partial x} - \rho g sin(\alpha) + \mu(\frac{\partial^2 u}{\partial x^2} + \frac{\partial^2 u}{\partial y^2})$$

$$\rho(\frac{\partial v}{\partial t} + u\frac{\partial v}{\partial x} + v\frac{\partial v}{\partial y}) = -\frac{\partial p}{\partial y} - \rho g cos(\alpha) + \mu(\frac{\partial^2 v}{\partial x^2} + \frac{\partial^2 v}{\partial y^2})$$

- **Saint Venant** Shallow Water

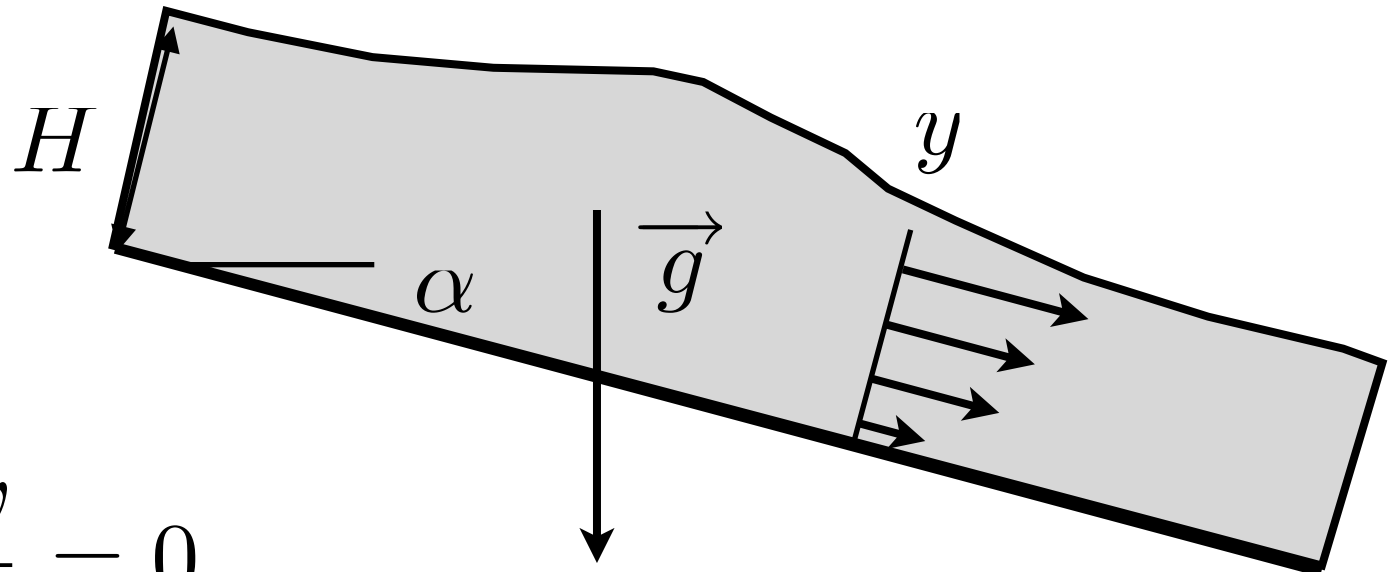

$$\varepsilon = H/L$$

$$\frac{\partial u}{\partial x} + \frac{\partial v}{\partial y} = 0$$

$$\rho(\frac{\partial u}{\partial t} + u\frac{\partial u}{\partial x} + v\frac{\partial u}{\partial y}) = -\frac{\partial p}{\partial x} - \rho g sin(\alpha) + \mu(\qquad + \frac{\partial^2 u}{\partial y^2})$$

$$0 \quad = -\frac{\partial p}{\partial y} - \rho g cos(\alpha)$$

- **Saint Venant** Shallow Water

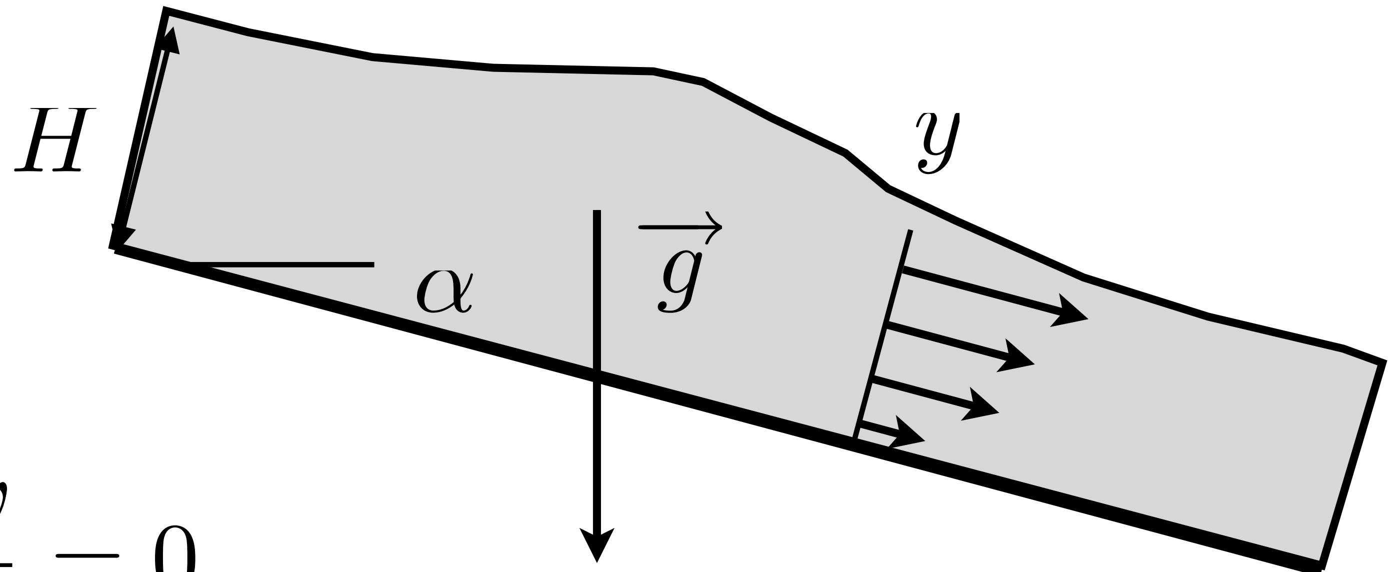

$$\varepsilon = H/L$$

$$\frac{\partial u}{\partial x} + \frac{\partial v}{\partial y} = 0$$

$$\rho\left(\frac{\partial u}{\partial t} + u\frac{\partial u}{\partial x} + v\frac{\partial u}{\partial y}\right) = -\frac{\partial p}{\partial x} - \rho g sin(\alpha) + \mu\left(\qquad + \frac{\partial^2 u}{\partial y^2}\right)$$

$$p = -\rho g \cos\alpha(\eta(x,t) - y)$$

- **Saint Venant** Shallow Water

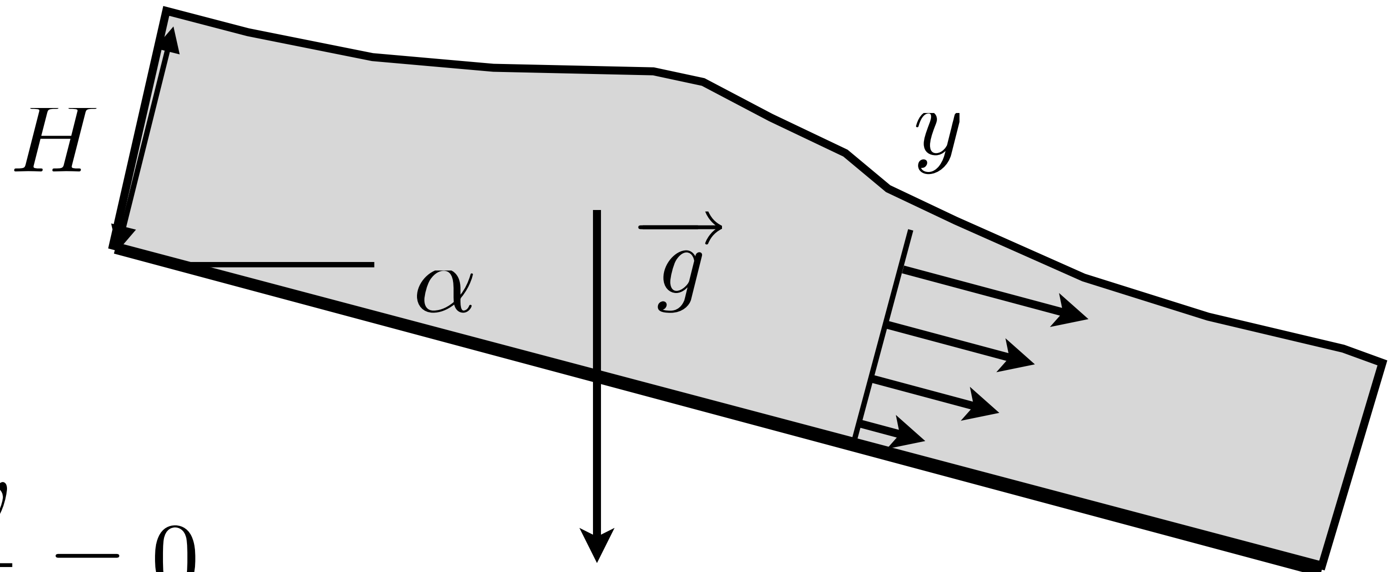

$$\varepsilon = H/L$$

$$\frac{\partial u}{\partial x} + \frac{\partial v}{\partial y} = 0$$

$$\rho(\frac{\partial u}{\partial t} + u\frac{\partial u}{\partial x} + v\frac{\partial u}{\partial y}) = -\rho g cos(\alpha)\frac{\partial \eta}{\partial x} - \rho g sin(\alpha) + \mu(\frac{\partial^2 u}{\partial y^2})$$

$$p = -\rho g \cos\alpha(\eta(x,t) - y)$$

- **Saint Venant** Shallow Water

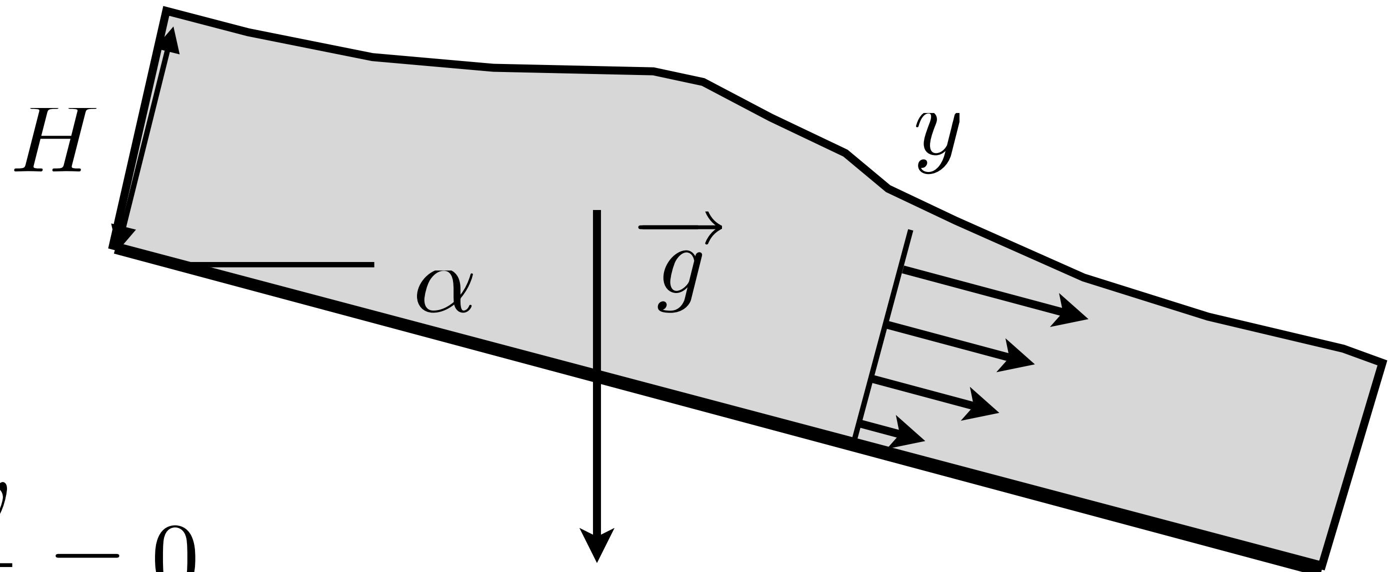

$$\varepsilon = H/L$$

$$\frac{\partial u}{\partial x} + \frac{\partial v}{\partial y} = 0$$

$$\rho(\frac{\partial u}{\partial t} + u\frac{\partial u}{\partial x} + v\frac{\partial u}{\partial y}) = -\rho g cos(\alpha)\frac{\partial \eta}{\partial x} - \rho g sin(\alpha) + \mu(\frac{\partial^2 u}{\partial y^2})$$

$$p = -\rho g \cos\alpha(\eta(x,t) - y)$$

- **Saint Venant** Shallow Water

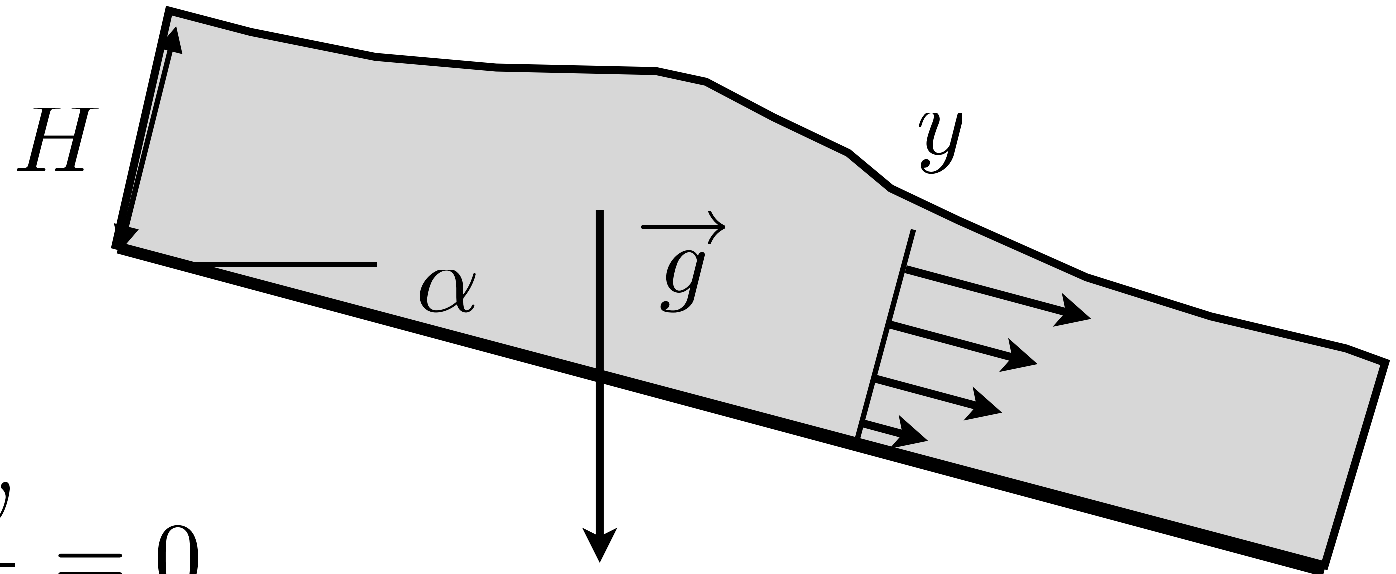

$$\varepsilon = H/L$$

$$\int dy \quad \frac{\partial u}{\partial x} + \frac{\partial v}{\partial y} = 0$$

$$\int dy \quad \rho(\frac{\partial u}{\partial t} + u\frac{\partial u}{\partial x} + v\frac{\partial u}{\partial y}) = -\rho g cos(\alpha)\frac{\partial \eta}{\partial x} - \rho g sin(\alpha) + \mu(\frac{\partial^2 u}{\partial y^2})$$

- **Saint Venant** Shallow Water

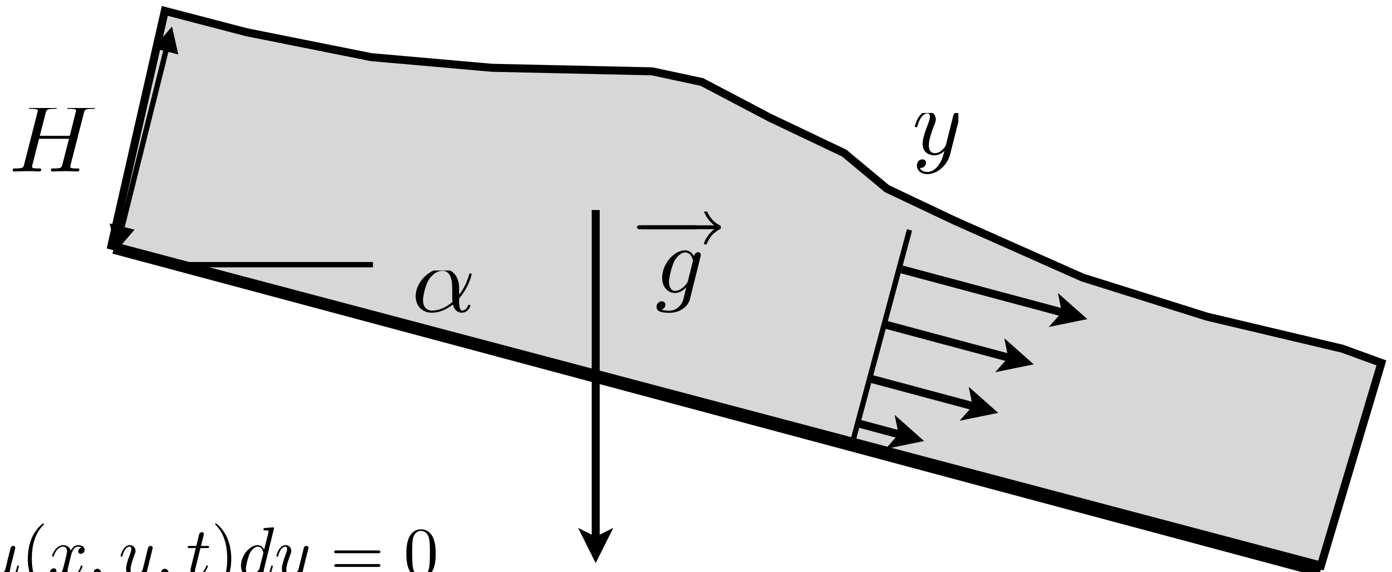

$$\varepsilon = H/L$$

$$\frac{\partial h}{\partial t} + \frac{\partial}{\partial x}\int_f^{\eta} u(x,y,t)dy = 0$$

$$\int dy \;\; \rho\left(\frac{\partial u}{\partial t} + u\frac{\partial u}{\partial x} + v\frac{\partial u}{\partial y}\right) = -\rho g cos(\alpha)\frac{\partial \eta}{\partial x} - \rho g sin(\alpha) + \mu\left(\frac{\partial^2 u}{\partial y^2}\right)$$

- **Saint Venant** Shallow Water

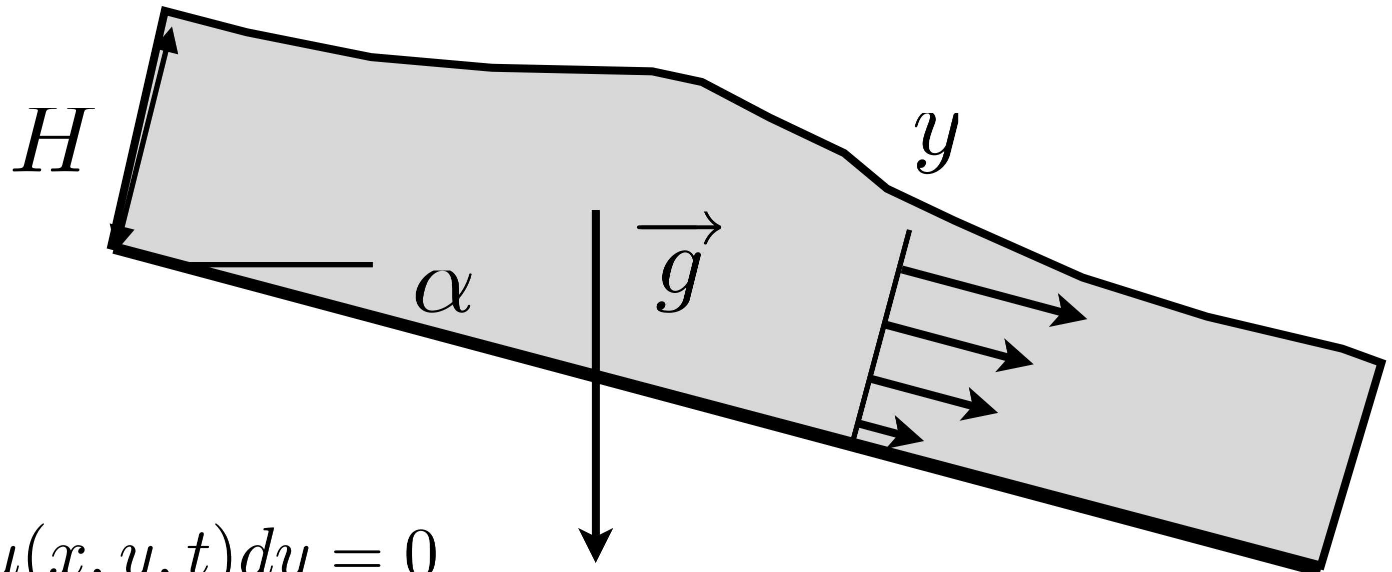

$$\varepsilon = H/L$$

$$\frac{\partial h}{\partial t} + \frac{\partial}{\partial x}\int_f^\eta u(x,y,t)dy = 0$$

$$\frac{\partial}{\partial t}\int_f^\eta u(x,y,t)dy + \frac{\partial}{\partial x}\left(\int_f^\eta u(x,y,t)^2 dy + cos(\alpha) g \frac{h^2}{2}\right) = -ghsin(\alpha) - \nu \frac{\partial u}{\partial y}\Big|_f$$

- **Saint Venant** Shallow Water

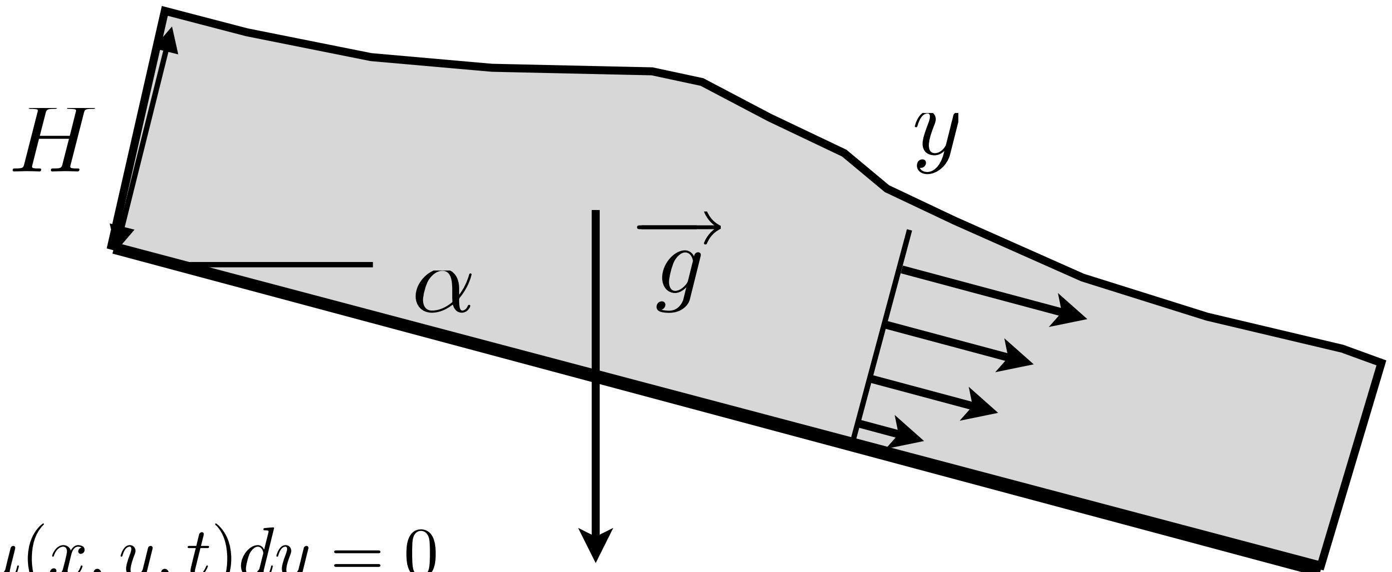

$$\varepsilon = H/L$$

$$\frac{\partial h}{\partial t} + \frac{\partial}{\partial x}\int_f^\eta u(x,y,t)dy = 0$$

$$\frac{\partial}{\partial t}\int_f^\eta u(x,y,t)dy + \frac{\partial}{\partial x}\left(\int_f^\eta u(x,y,t)^2 dy + cos(\alpha) g\frac{h^2}{2}\right) = -ghsin(\alpha) - \nu \frac{\partial u}{\partial y}|_f$$

Closure ?

- **Saint Venant** Shallow Water

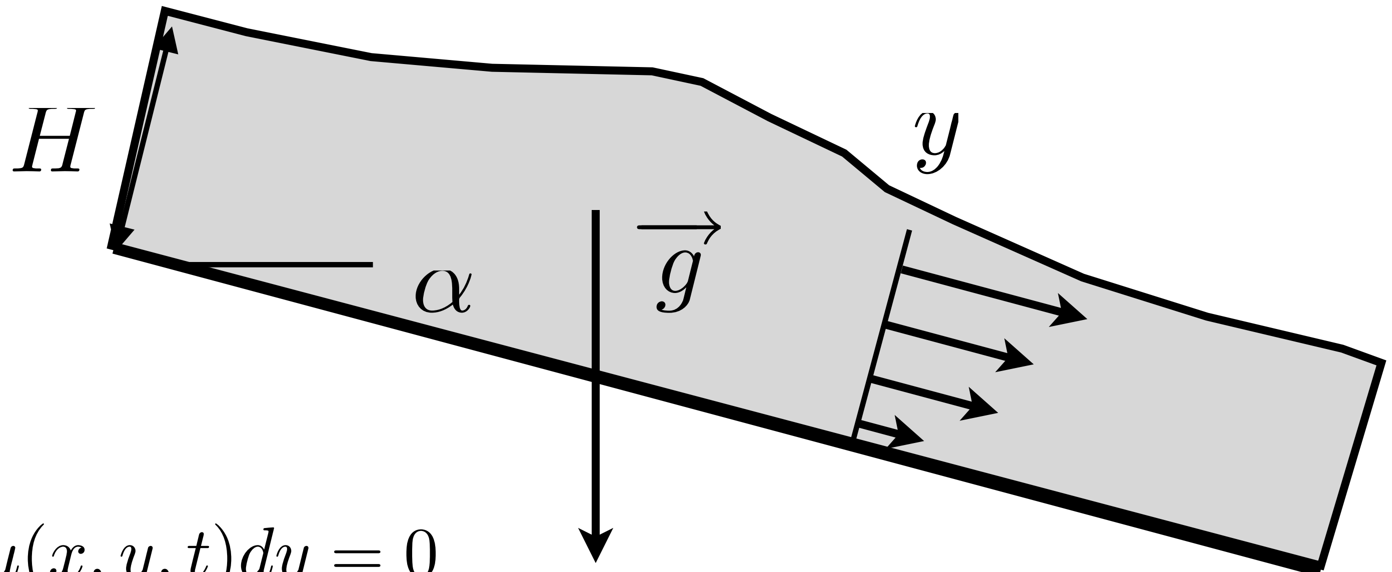

$$\varepsilon = H/L$$

$$\frac{\partial h}{\partial t} + \frac{\partial}{\partial x}\int_f^\eta u(x,y,t)dy = 0$$

$$\frac{\partial}{\partial t}\int_f^\eta u(x,y,t)dy + \frac{\partial}{\partial x}\left(\int_f^\eta u(x,y,t)^2 dy + cos(\alpha) g\frac{h^2}{2}\right) = -ghsin(\alpha) - \nu\frac{\partial u}{\partial y}|_f$$

Closure ?

$$0 = -\rho g sin(\alpha) + \mu\left(\frac{\partial^2 u}{\partial y^2}\right)$$ gives: $$u = -\frac{\rho g}{\mu} sin(\alpha) h^2 \frac{(2-y/h)(y/h)}{2}$$

- # Saint Venant Shallow Water

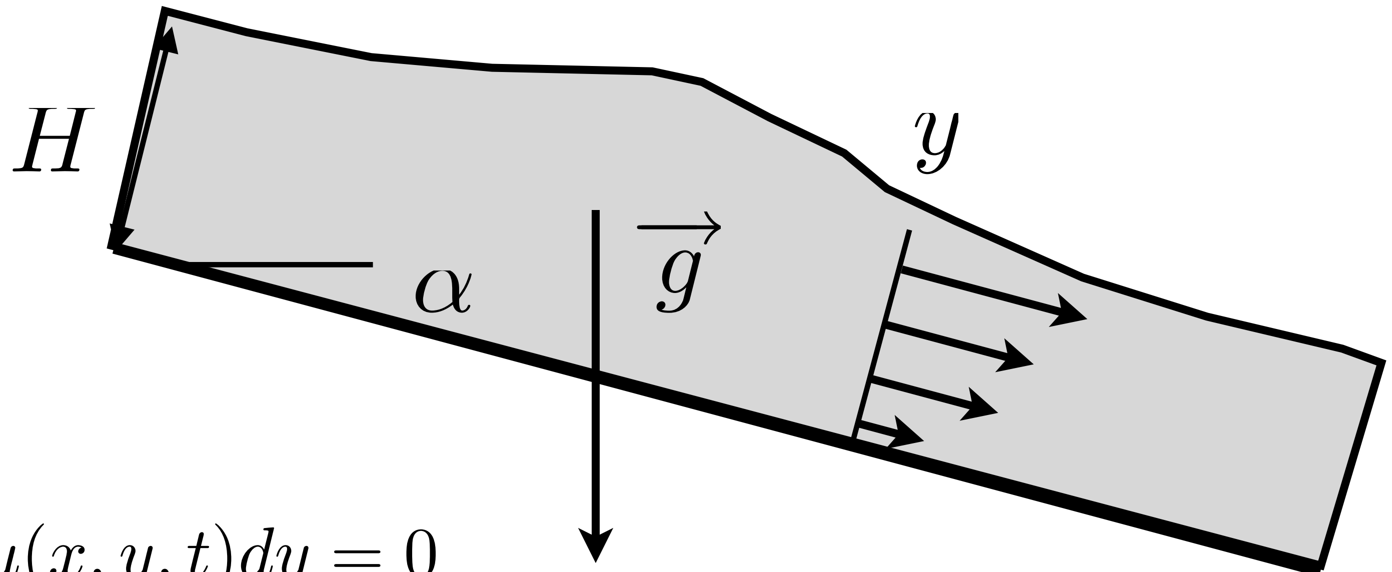

$$\varepsilon = H/L$$

$$\frac{\partial h}{\partial t} + \frac{\partial}{\partial x}\int_f^\eta u(x,y,t)dy = 0$$

$$\frac{\partial}{\partial t}\int_f^\eta u(x,y,t)dy + \frac{\partial}{\partial x}(\int_f^\eta u(x,y,t)^2 dy + cos(\alpha)g\frac{h^2}{2}) = -ghsin(\alpha) - \nu\frac{\partial u}{\partial y}|_f$$

suppose $$u(x,y,t) = U(x,t)\frac{3(2-y/h)(y/h)}{2}$$

the transverse shape is always a half-Poiseuille

- Saint Venant Shallow Water

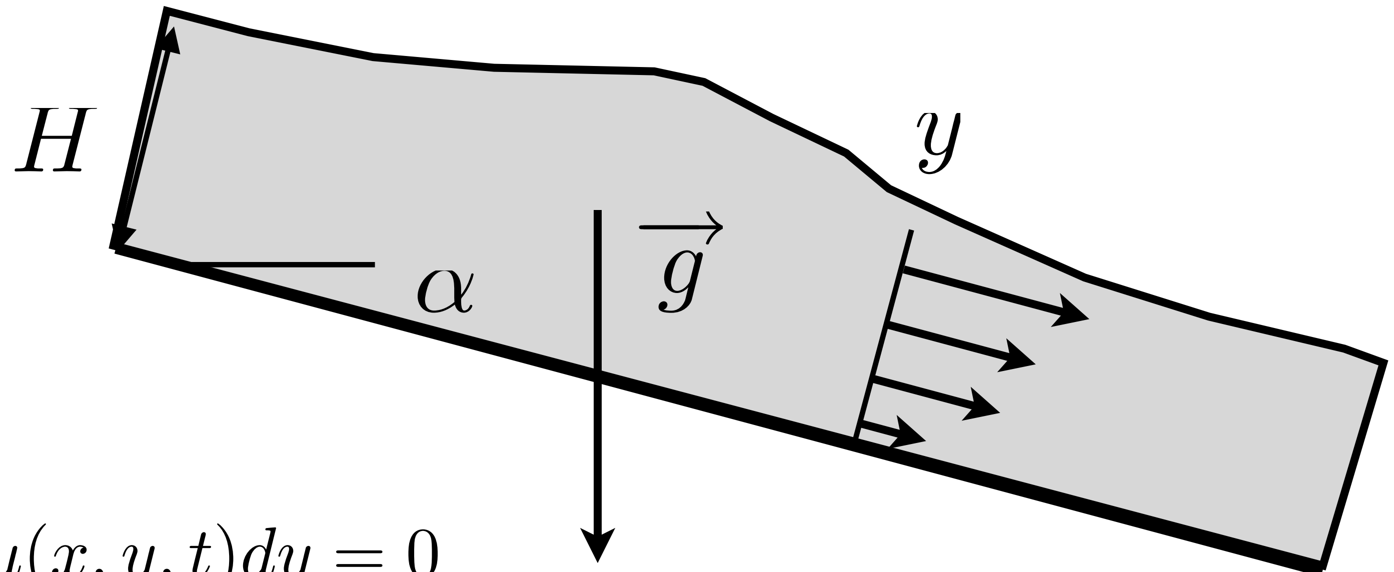

$$\varepsilon = H/L$$

$$\frac{\partial h}{\partial t} + \frac{\partial}{\partial x}\int_f^\eta u(x,y,t)dy = 0$$

$$\frac{\partial}{\partial t}\int_f^\eta u(x,y,t)dy + \frac{\partial}{\partial x}(\int_f^\eta u(x,y,t)^2 dy + cos(\alpha) g\frac{h^2}{2}) = -ghsin(\alpha) - \nu\frac{\partial u}{\partial y}|_f$$

suppose $$u(x,y,t) = U(x,t)\frac{3(2-y/h)(y/h)}{2}$$

$$\int u(x,y,t)dy = [\int \frac{3(2-y/h)(y/h)}{2}dy/h](U(x,t)^2 h) = \frac{3}{3}(U(x,t)h)$$

- **Saint Venant** Shallow Water

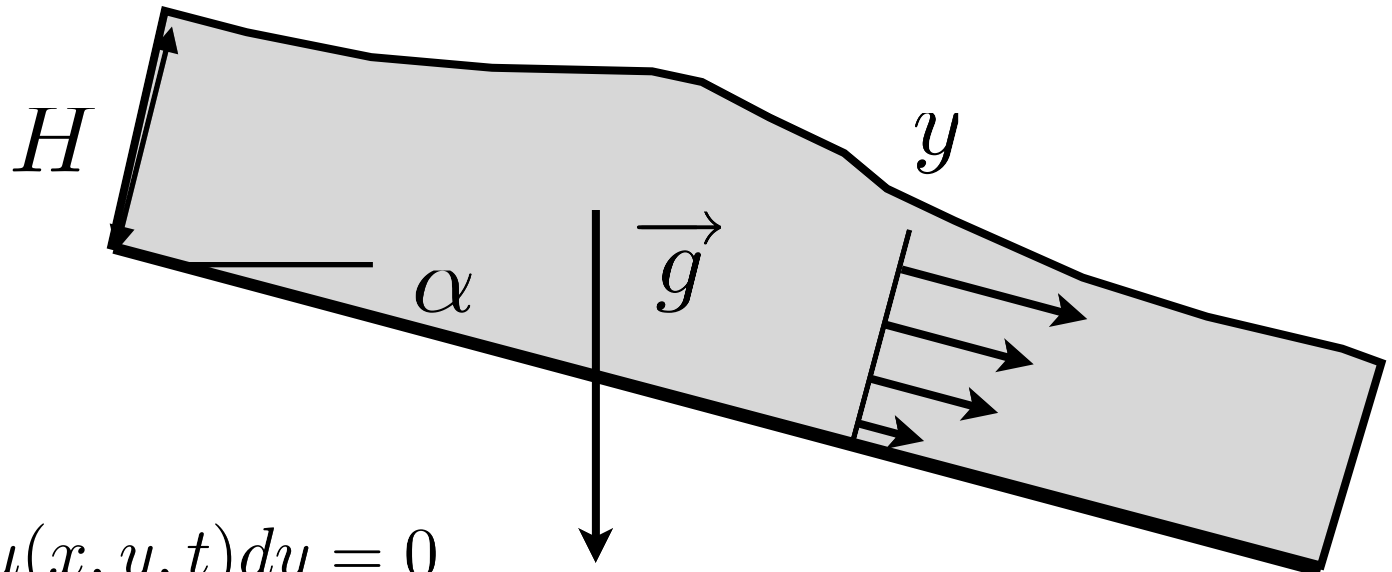

$$\varepsilon = H/L$$

$$\frac{\partial h}{\partial t} + \frac{\partial}{\partial x}\int_f^\eta u(x,y,t)dy = 0$$

$$\frac{\partial}{\partial t}\int_f^\eta u(x,y,t)dy + \frac{\partial}{\partial x}\left(\int_f^\eta u(x,y,t)^2 dy + cos(\alpha) g\frac{h^2}{2}\right) = -ghsin(\alpha) - \nu\frac{\partial u}{\partial y}|_f$$

suppose $$u(x,y,t) = U(x,t)\frac{3(2-y/h)(y/h)}{2}$$

$$\int u(x,y,t)dy = [\int \frac{3(2-y/h)(y/h)}{2}dy/h](U(x,t)^2 h) = \frac{3}{3}(U(x,t)h)$$

- **Saint Venant** Shallow Water

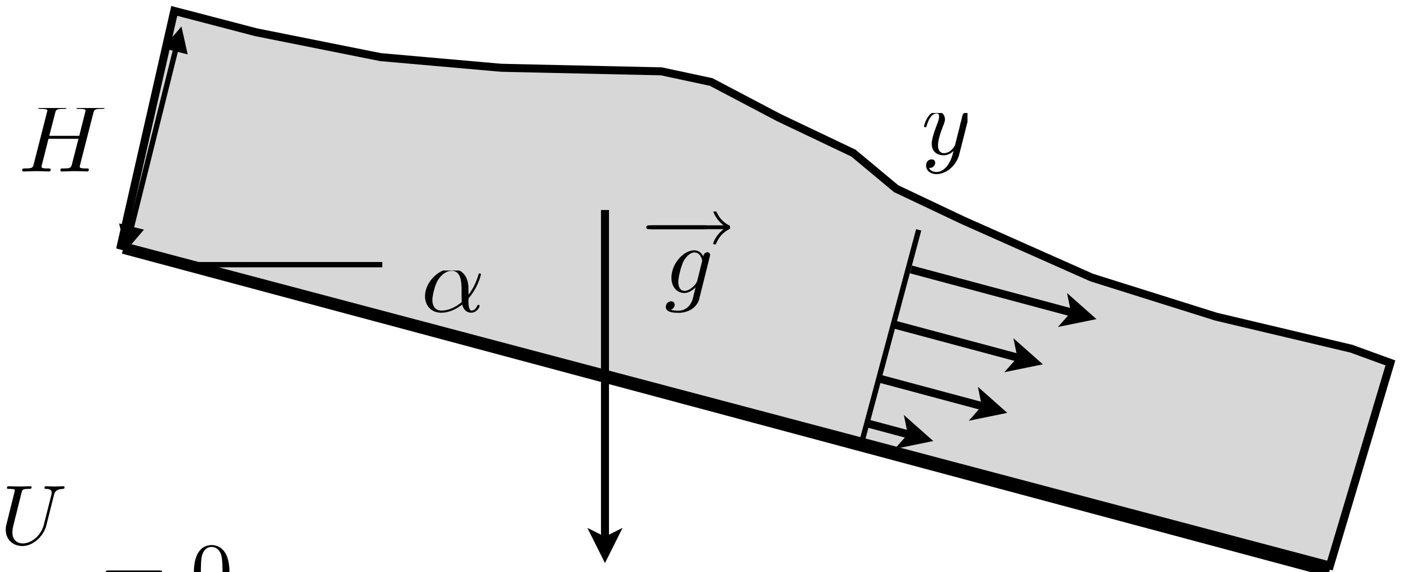

$$\varepsilon = H/L$$

$$\frac{\partial h}{\partial t} + \frac{\partial hU}{\partial x} = 0$$

$$\frac{\partial}{\partial t}\int_f^\eta u(x,y,t)dy + \frac{\partial}{\partial x}\left(\int_f^\eta u(x,y,t)^2 dy + cos(\alpha) g \frac{h^2}{2}\right) = -ghsin(\alpha) - \nu \frac{\partial u}{\partial y}|_f$$

suppose $$u(x,y,t) = U(x,t)\frac{3(2-y/h)(y/h)}{2}$$

$$\int u(x,y,t)dy = [\int \frac{3(2-y/h)(y/h)}{2} dy/h](U(x,t)^2 h) = \frac{3}{3}(U(x,t)h)$$

- **Saint Venant** Shallow Water

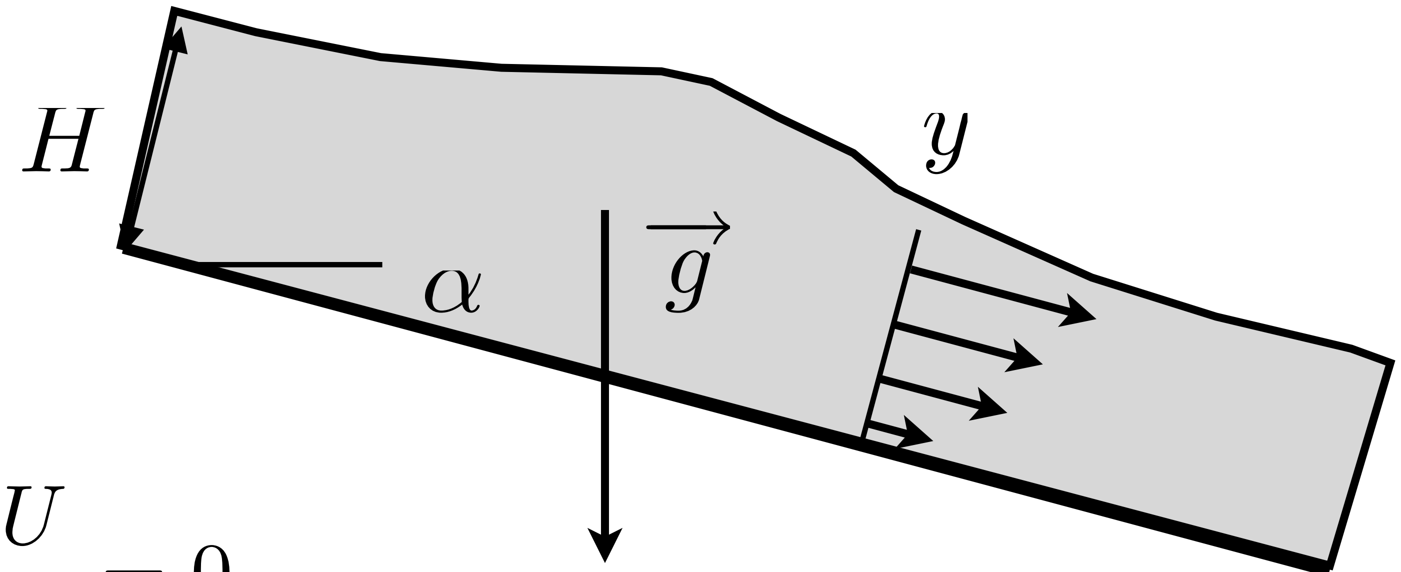

$$\varepsilon = H/L$$

$$\frac{\partial h}{\partial t} + \frac{\partial hU}{\partial x} = 0$$

$$\frac{\partial}{\partial t}\int_f^\eta u(x,y,t)dy + \frac{\partial}{\partial x}(\int_f^\eta u(x,y,t)^2 dy + cos(\alpha)g\frac{h^2}{2}) = -ghsin(\alpha) - \nu\frac{\partial u}{\partial y}|_f$$

suppose $$u(x,y,t) = U(x,t)\frac{3(2-y/h)(y/h)}{2}$$

- **Saint Venant** Shallow Water

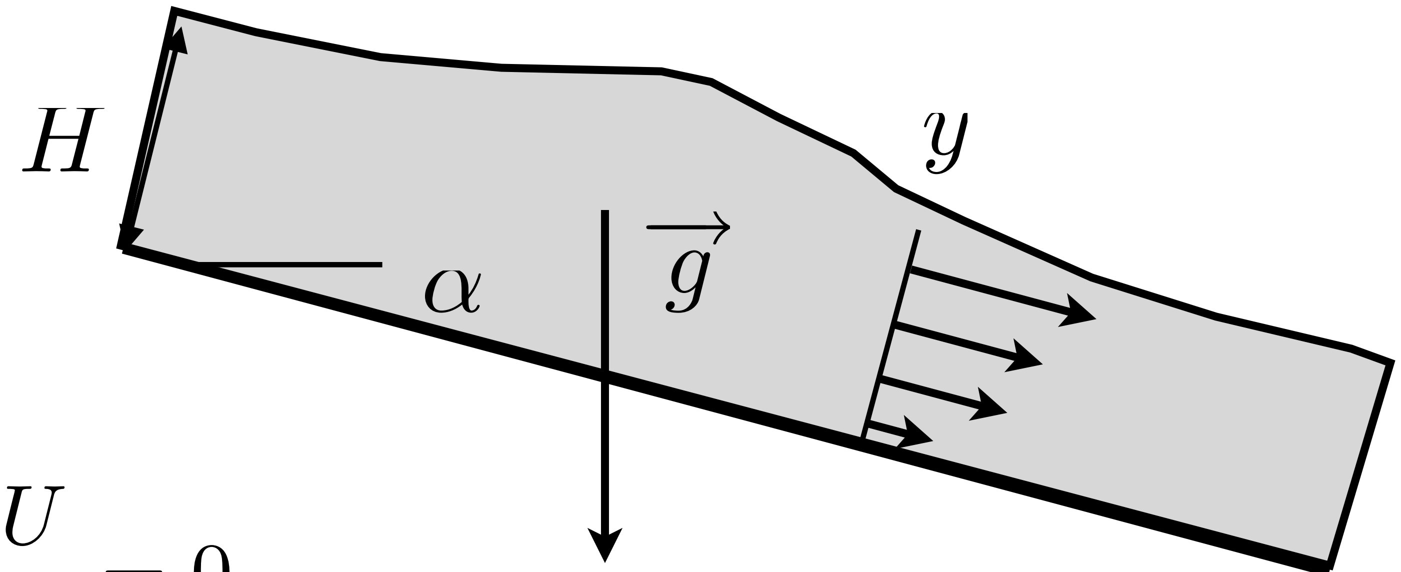

$$\varepsilon = H/L$$

$$\frac{\partial h}{\partial t} + \frac{\partial hU}{\partial x} = 0$$

$$\frac{\partial}{\partial t}\int_f^\eta u(x,y,t)dy + \frac{\partial}{\partial x}\left(\int_f^\eta u(x,y,t)^2 dy + cos(\alpha) g \frac{h^2}{2}\right) = -ghsin(\alpha) - \nu \frac{\partial u}{\partial y}|_f$$

suppose $\quad u(x,y,t) = U(x,t)\dfrac{3(2-y/h)(y/h)}{2}$

$$\int u(x,y,t)^2 dy = [\int \left(\frac{3(2-y/h)(y/h)}{2} dy/h\right)^2](U(x,t)^2 h) = \frac{6}{5}(U(x,t)^2 h)$$

$$\nu \frac{\partial u}{\partial y} = \nu [\frac{-3}{h}](U(x,t)) = -3\nu \frac{U(x,t)}{h}$$

- Saint Venant Shallow Water

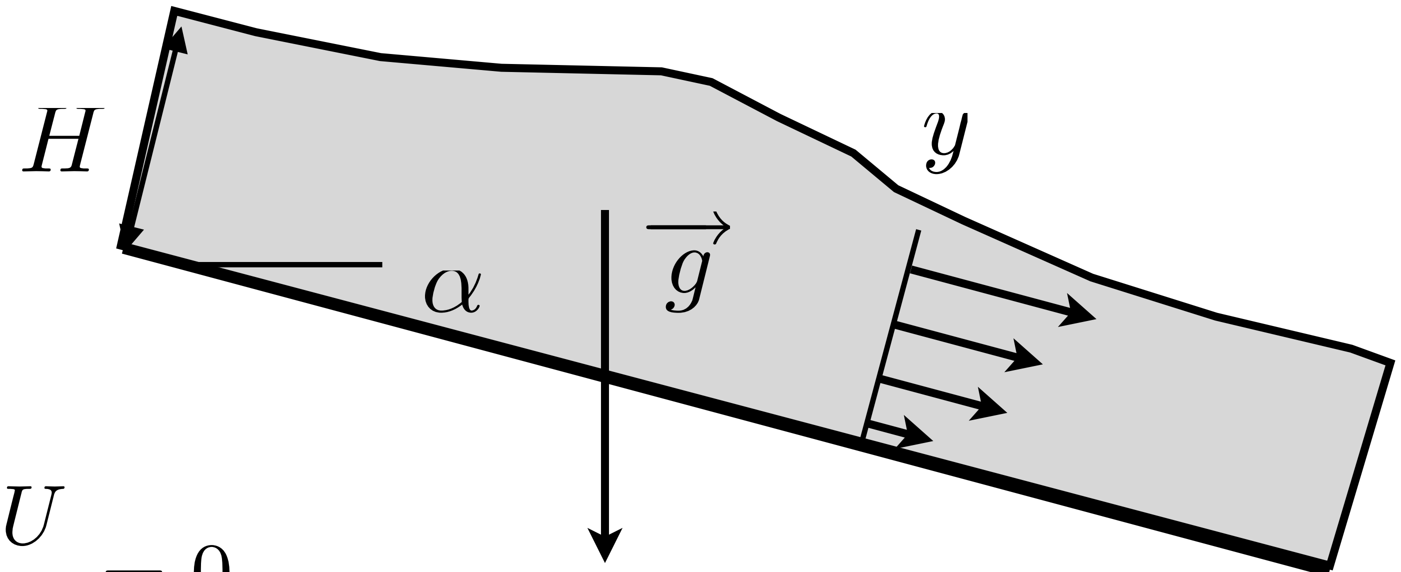

$$\varepsilon = H/L$$

$$\frac{\partial h}{\partial t} + \frac{\partial hU}{\partial x} = 0$$

$$\frac{\partial hU}{\partial t} + \frac{6}{5}\frac{\partial hU^2}{\partial x} = -ghcos(\alpha)\frac{\partial \eta}{\partial x} - ghsin(\alpha) - 3\nu(\frac{U}{h})$$

- **Saint Venant** Shallow Water

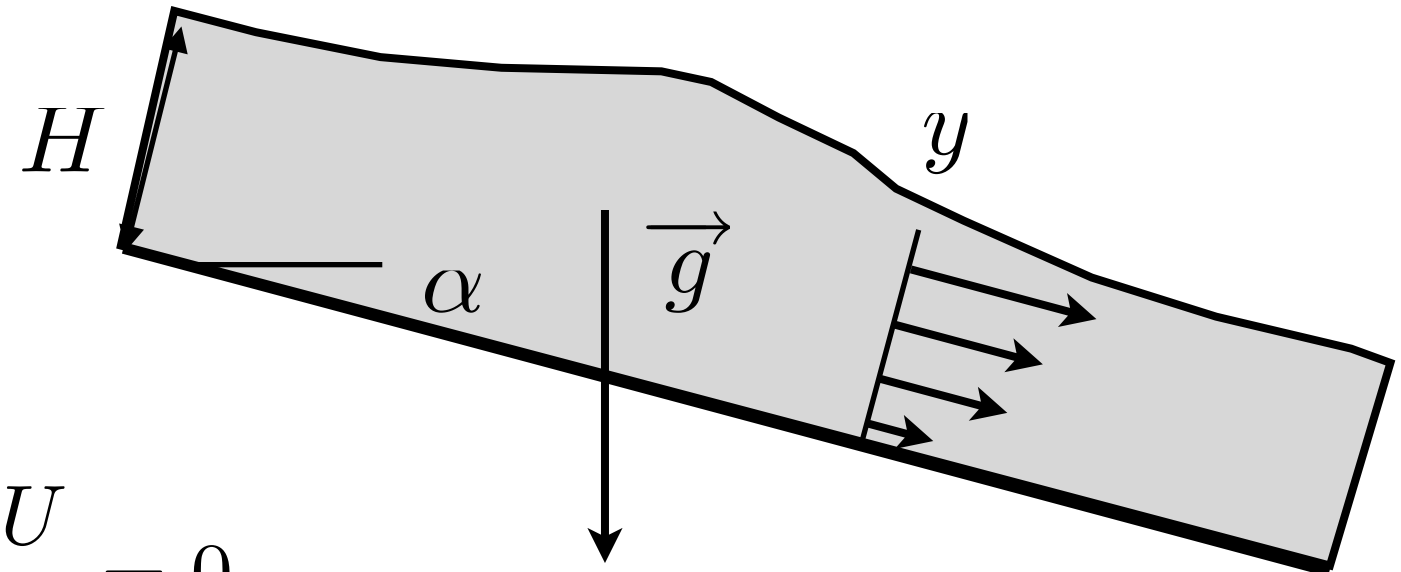

$$\varepsilon = H/L$$

$$\frac{\partial h}{\partial t} + \frac{\partial hU}{\partial x} = 0$$

$$\frac{\partial hU}{\partial t} + \frac{6}{5}\frac{\partial hU^2}{\partial x} = -ghcos(\alpha)\frac{\partial \eta}{\partial x} - ghsin(\alpha) - 3\nu(\frac{U}{h})$$

Turbulent??

- **Saint Venant** Shallow Water

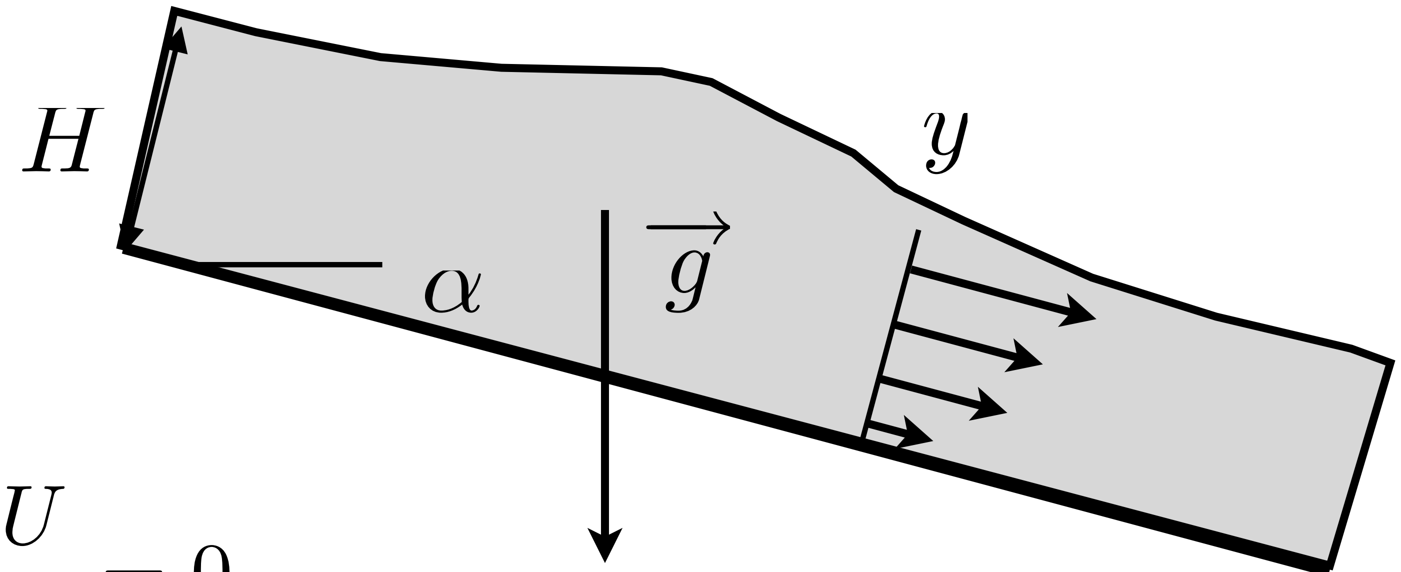

$$\varepsilon = H/L$$

$$\frac{\partial h}{\partial t} + \frac{\partial hU}{\partial x} = 0$$

$$\frac{\partial hU}{\partial t} + \frac{6}{5}\frac{\partial hU^2}{\partial x} = -ghcos(\alpha)\frac{\partial \eta}{\partial x} - ghsin(\alpha) - 3\nu(\frac{U}{h})$$ Laminar

- **Saint Venant** Shallow Water

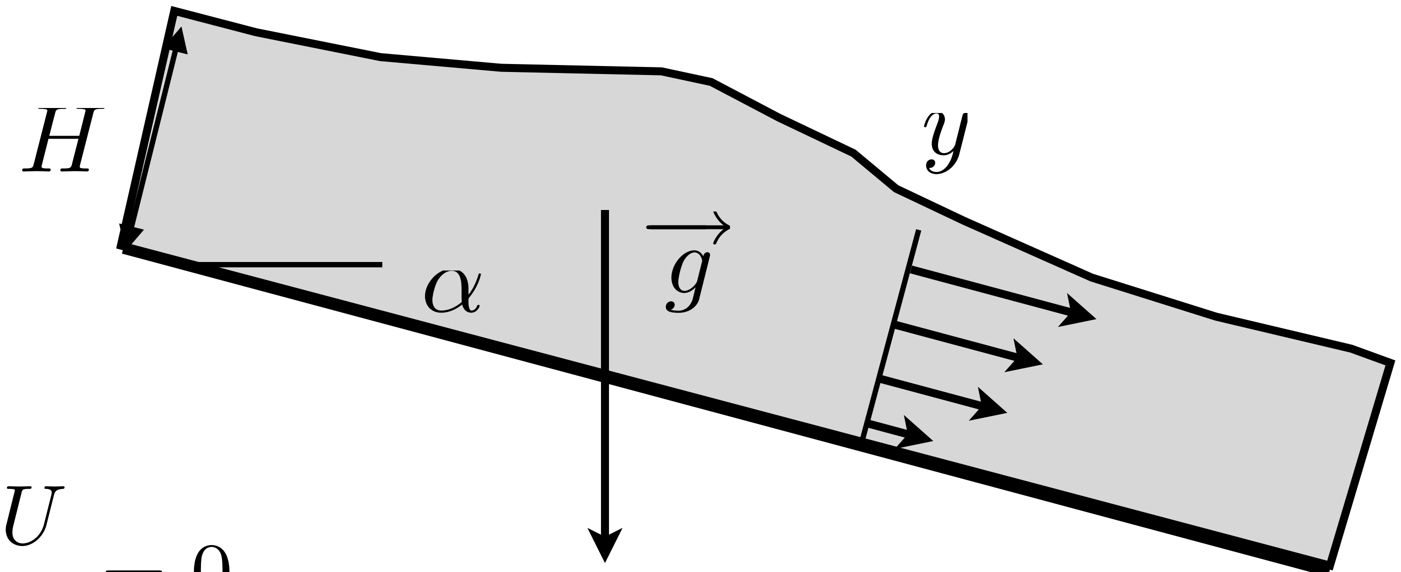

$$\varepsilon = H/L$$

$$\frac{\partial h}{\partial t} + \frac{\partial hU}{\partial x} = 0$$

$$\frac{\partial hU}{\partial t} + \frac{6}{5}\frac{\partial hU^2}{\partial x} = -ghcos(\alpha)\frac{\partial \eta}{\partial x} - ghsin(\alpha) - 3\nu(\frac{U}{h})$$ Laminar

$$\frac{\partial hU}{\partial t} + \frac{\partial hU^2}{\partial x} = -ghcos(\alpha)\frac{\partial \eta}{\partial x} - ghsin(\alpha) - \frac{c_f}{2}U^2$$ Turbulent

- **Saint Venant** Shallow Water

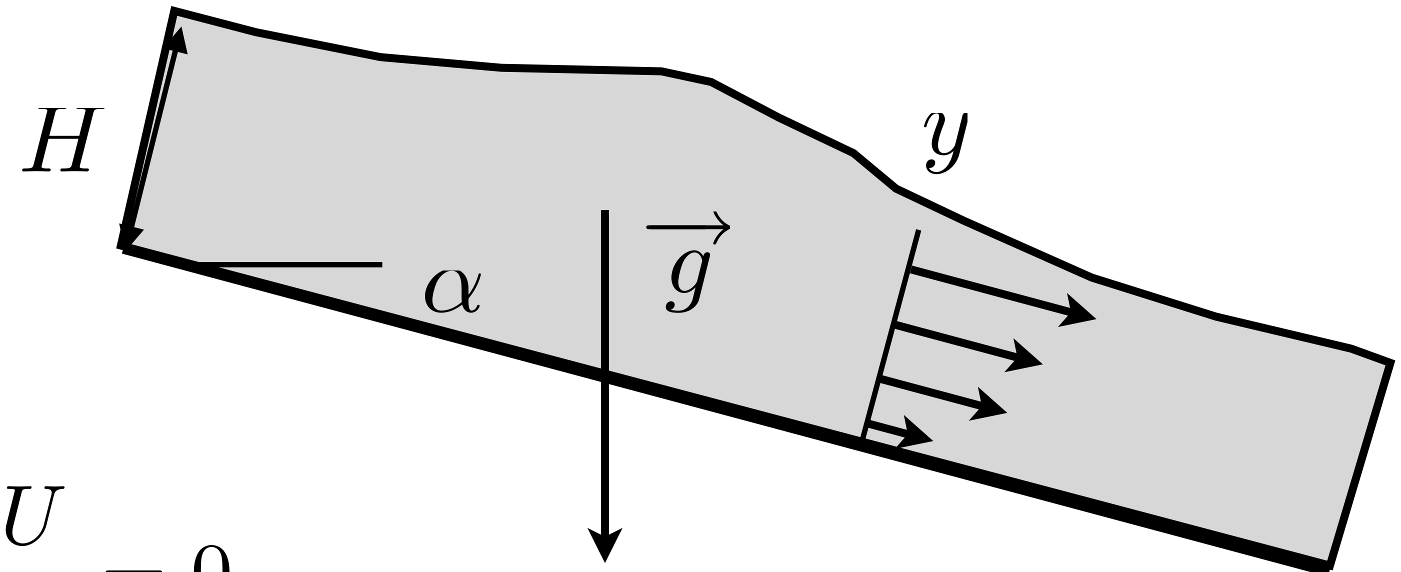

$$\varepsilon = H/L$$

$$\frac{\partial h}{\partial t} + \frac{\partial hU}{\partial x} = 0$$

$$\frac{\partial hU}{\partial t} + \frac{6}{5}\frac{\partial hU^2}{\partial x} = -ghcos(\alpha)\frac{\partial \eta}{\partial x} - ghsin(\alpha) - 3\nu(\frac{U}{h})$$ Laminar

$$\frac{\partial hU}{\partial t} + \frac{\partial hU^2}{\partial x} = -ghcos(\alpha)\frac{\partial \eta}{\partial x} - ghsin(\alpha) - \frac{c_f}{2}U^2$$ Turbulent

$$-\frac{c_f}{2}U^2 = -\frac{g}{C_c^2}(U/h)^2$$

Chézy coeff.

$$C_C = \sqrt{8g}(2log(12.7R_h/k_h))$$

$$C_C = \frac{1}{n_{GM}}(h)^{1/6}$$

- **Saint Venant** Shallow Water

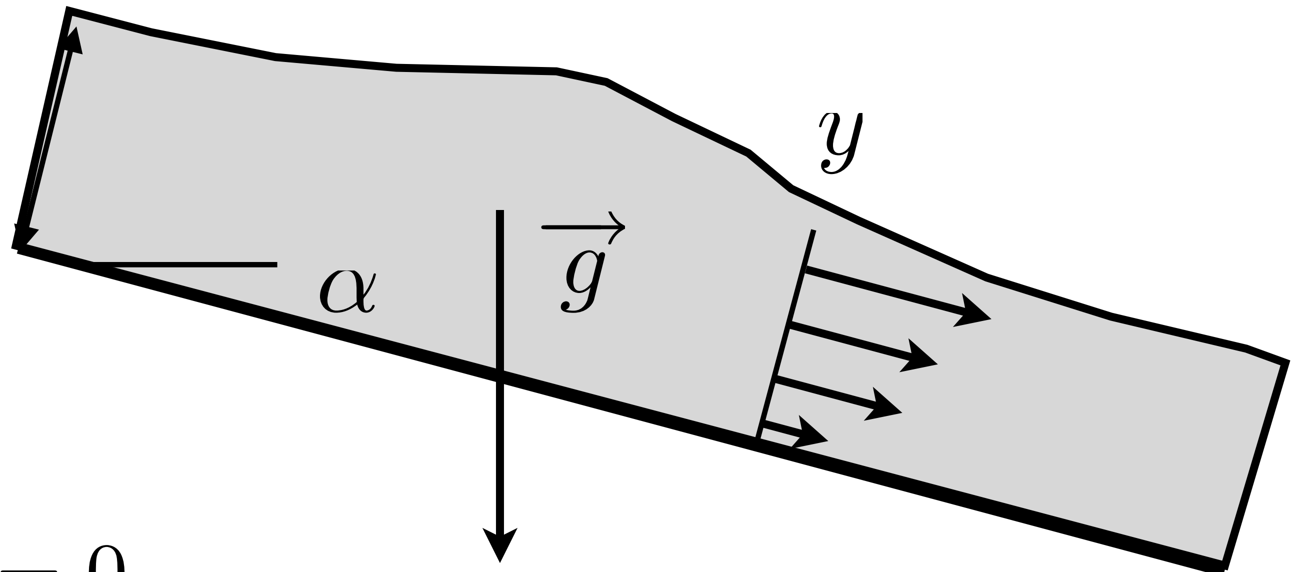

$$\varepsilon = H/L$$

$$\frac{\partial h}{\partial t} + \frac{\partial hU}{\partial x} = 0$$

$$\frac{\partial hU}{\partial t} + \frac{6}{5}\frac{\partial hU^2}{\partial x} = -ghcos(\alpha)\frac{\partial \eta}{\partial x} - ghsin(\alpha) - 3\nu(\frac{U}{h})$$ Laminar

$$\frac{\partial hU}{\partial t} + \frac{\partial hU^2}{\partial x} = -ghcos(\alpha)\frac{\partial \eta}{\partial x} - ghsin(\alpha) - \frac{c_f}{2}U^2$$ Turbulent

$$-\frac{c_f}{2}U^2 = -\frac{g}{C_c^2}(U/h)^2$$

Chézy coeff.

$$C_C = \sqrt{8g}(2log(12.7R_h/k_h))$$

$$C_C = \frac{1}{n_{GM}}(h)^{1/6}$$

Saint-Venant approach

Flow Model

(Navier Stokes)

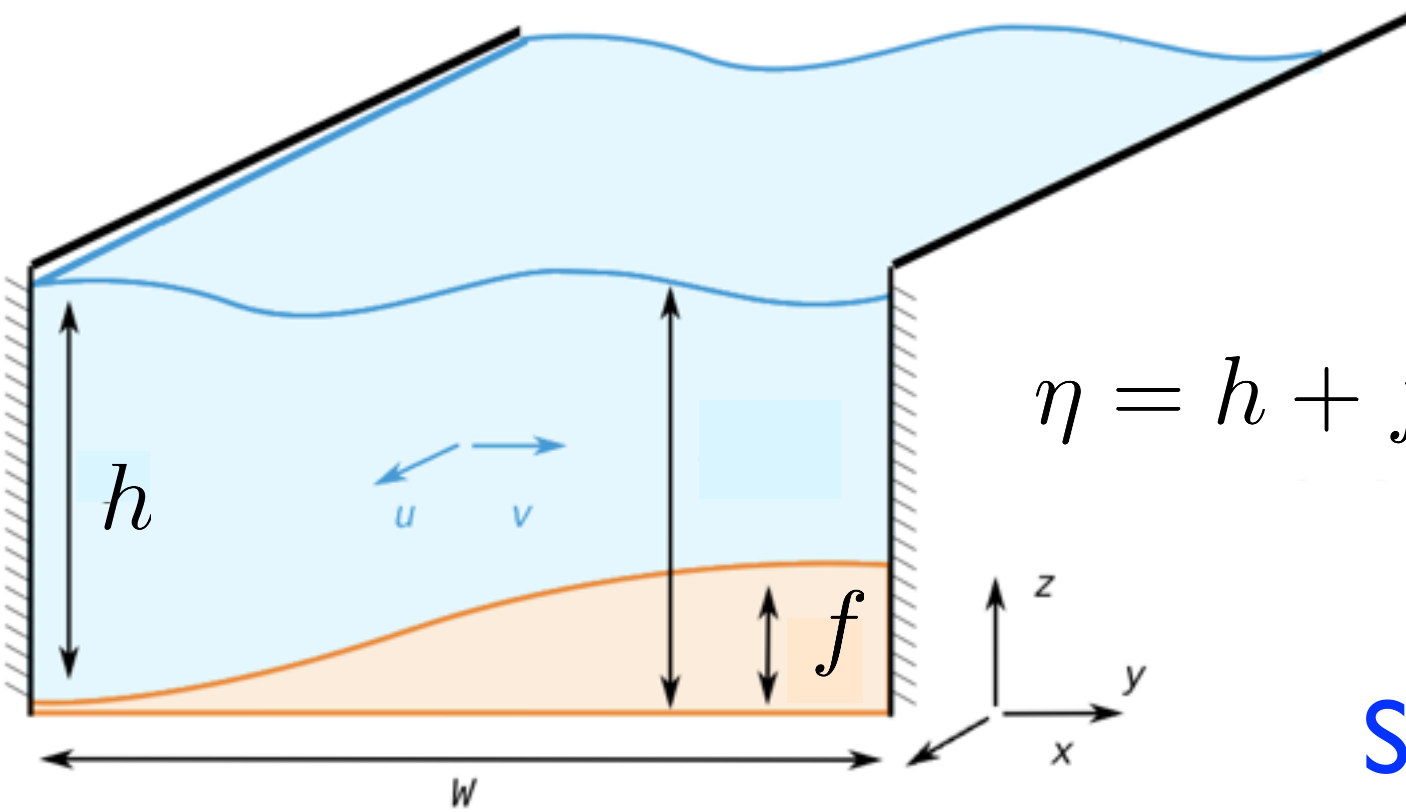

$$\eta = h + f$$

Shallow water - Saint Venant

Saint-Venant approach

Flow Model

$$\int_{z=f}^{z=\eta} dz \qquad \text{(Navier Stokes)}$$

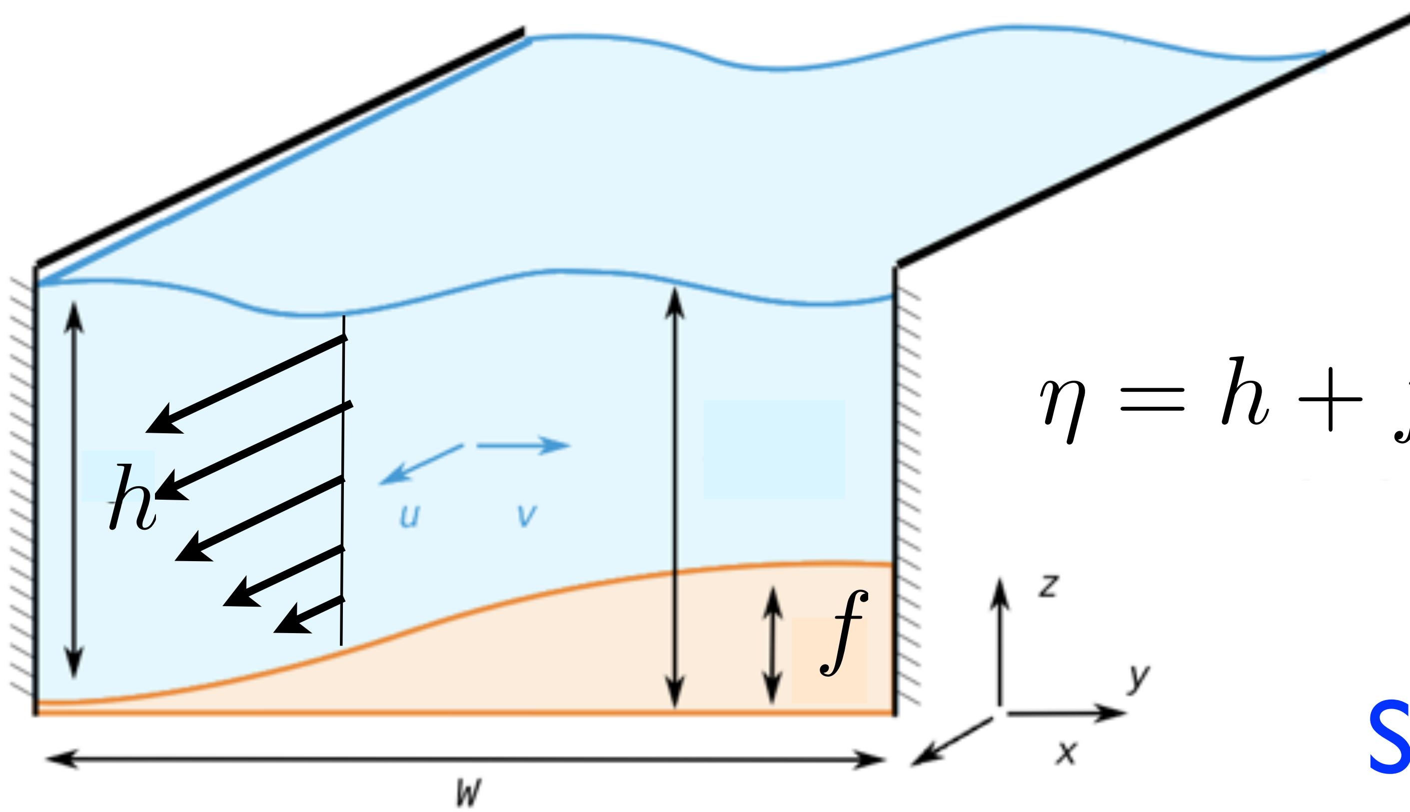

$$\eta = h + f$$

+Poiseuille profile

+ hydrostatic balance

Shallow water - Saint Venant

Saint-Venant approach

Flow Model

$$\frac{6}{5}(\overrightarrow{u}\cdot\overrightarrow{\nabla})\overrightarrow{u} = -g(\overrightarrow{\nabla}\eta + sin(\theta)\overrightarrow{e}_x) - \frac{3\nu\overrightarrow{u}}{(h)^2}$$

$$\overrightarrow{\nabla}\cdot(h\overrightarrow{u}) = 0$$

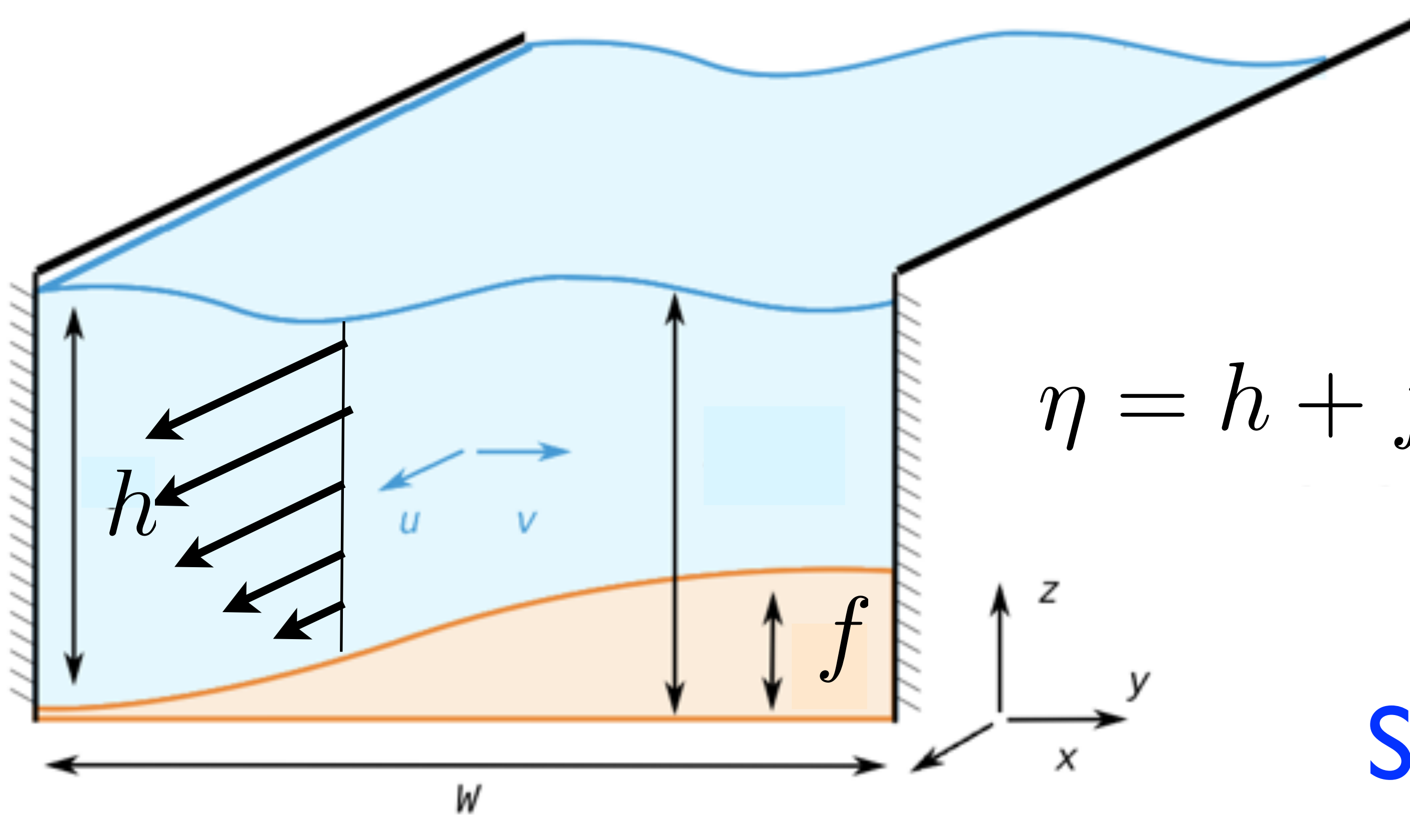

$$\eta = h + f$$

+Poiseuille profile

+ hydrostatic balance

Shallow water - Saint Venant

Saint-Venant approach

Flow Model

$$\frac{6}{5}(\overrightarrow{u}\cdot\overrightarrow{\nabla})\overrightarrow{u} = -g(\overrightarrow{\nabla}\eta + sin(\theta)\overrightarrow{e}_x) - \frac{3\nu\overrightarrow{u}}{(h)^2}$$

$$\overrightarrow{\nabla}\cdot(h\overrightarrow{u}) = 0$$

$$u \rightarrow \frac{h_0^2 g S}{3\nu}$$

$$(x, y) \rightarrow h_0$$

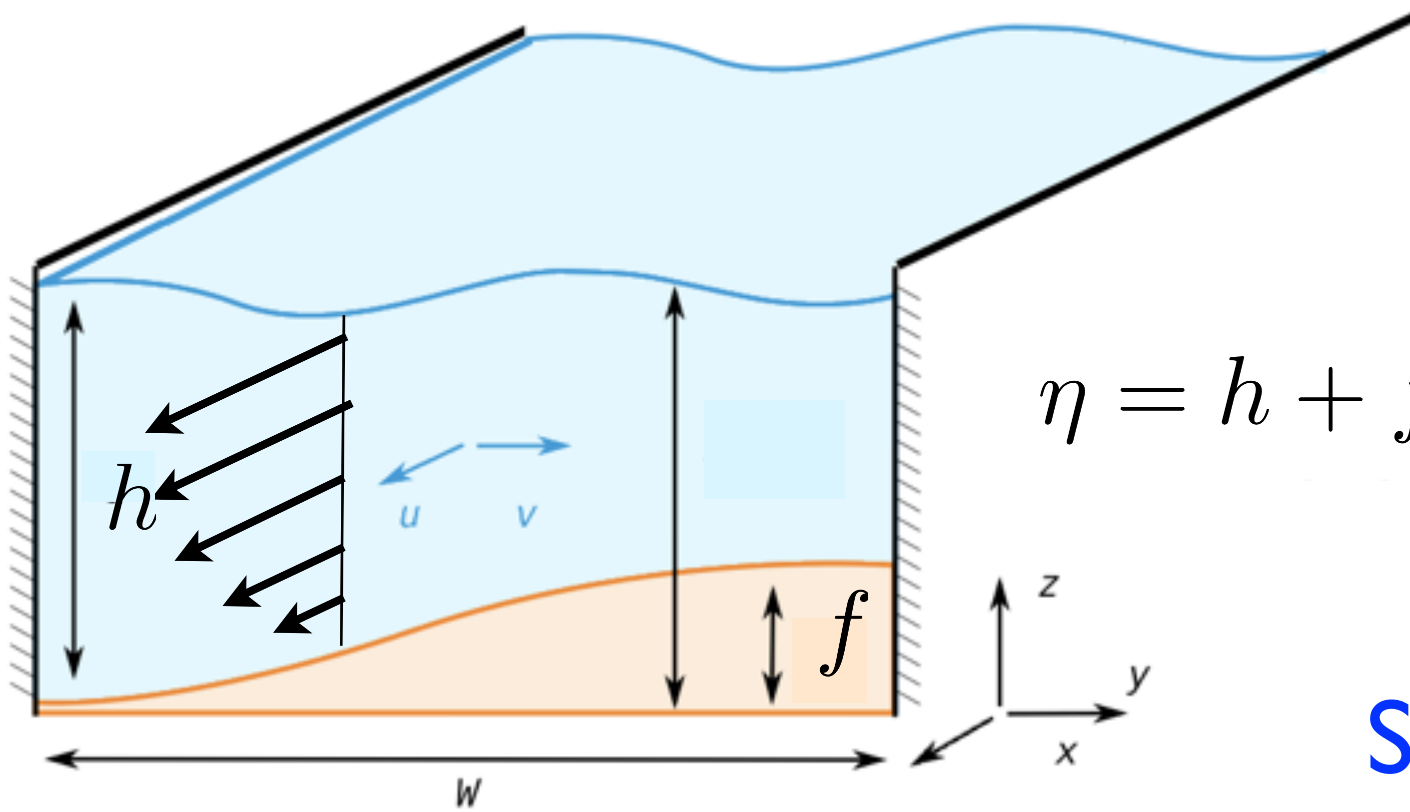

$$\eta = h + f$$

Shallow water - Saint Venant

Saint-Venant approach

Flow Model

laminar $$\frac{6}{5}F^2 u_k \partial_k u_i = S\delta_{i1} - \partial_i(h+f) - S\frac{u_i}{h^2}$$

$$\partial_k(hu_k) = 0$$

$$F^2 = \frac{U_0}{gh_0}$$

$$\mathrm{Re} = \frac{3F^2}{S}.$$

$$\boxed{\tau_i = \frac{u_i}{h}}$$

Saint-Venant approach

Flow Model

laminar $$\frac{6}{5}F^2 u_k \partial_k u_i = S\delta_{i1} - \partial_i(h+f) - S\frac{u_i}{h^2}$$

turbulent $$F^2 u_k \partial_k u_i = S\delta_{i1} - \partial_i(h+f) - S\frac{||u||}{h}u_i$$

$$\partial_k(hu_k) = 0$$

$$F^2 = \frac{U_0}{gh_0}$$

$$\mathrm{Re} = \frac{3F^2}{S}.$$

$$\boxed{\tau_i = ||u||u_i}$$

Saint-Venant approach

Flow Model

laminar $$\frac{6}{5}F^2 u_k \partial_k u_i = S\delta_{i1} - \partial_i(h+f) - S\frac{u_i}{h^2}$$

$$\partial_k(hu_k) = 0$$

$$F^2 = \frac{U_0}{gh_0}$$

$$\mathrm{Re} = \frac{3F^2}{S}.$$

$$\boxed{\tau_i = \frac{u_i}{h}}$$

testing Saint Venant + erosion

bars?

coupled system

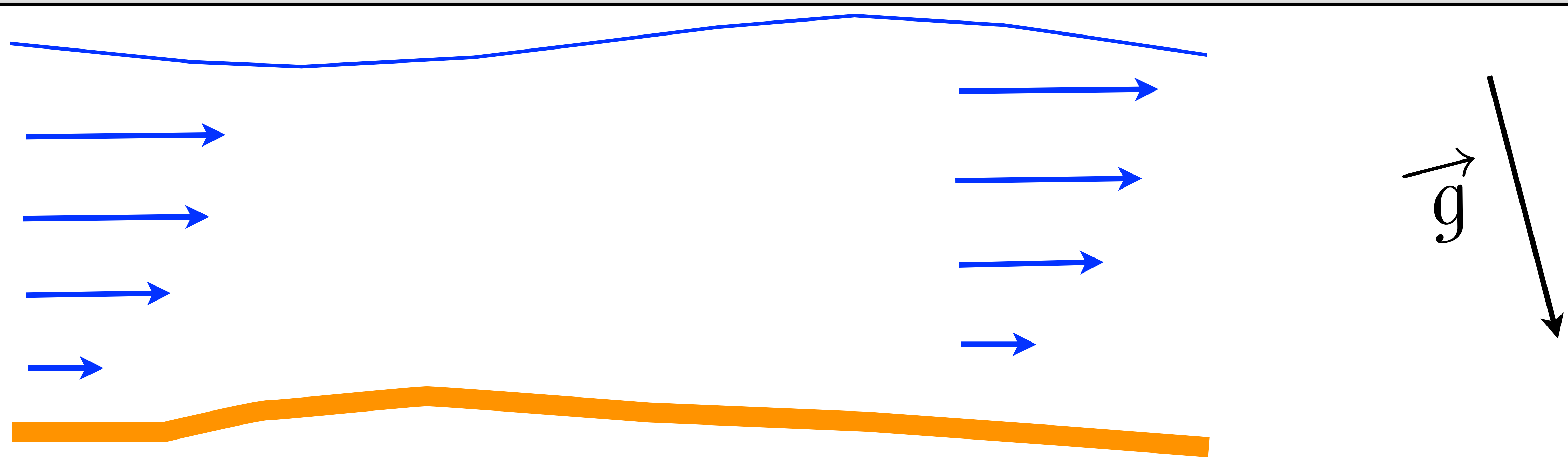

Navier Stokes

coupled system

Saint Venant

$$\frac{6}{5}(\overrightarrow{u}\cdot\overrightarrow{\nabla})\overrightarrow{u} = -g(\overrightarrow{\nabla}\eta + sin(\theta)\overrightarrow{e}_x) - \frac{3\nu\overrightarrow{u}}{(h)^2}$$

Mass conservation of fluid

$$\overrightarrow{\nabla}\cdot(h\overrightarrow{u}) = 0$$

$$\vec{q} = \phi\theta^{\beta}\left(\frac{\vec{u}}{\|\vec{u}\|} - \gamma\vec{\nabla}h\right)$$

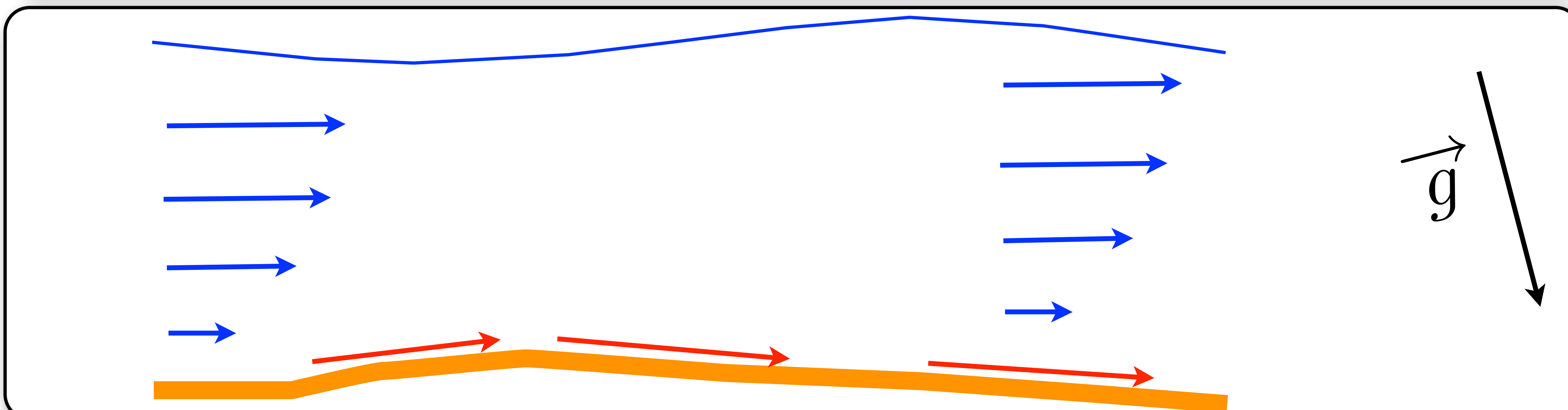

Navier Stokes

coupled system

Saint Venant

$$\frac{6}{5}(\overrightarrow{u}\cdot\overrightarrow{\nabla})\overrightarrow{u} = -g(\overrightarrow{\nabla}\eta + sin(\theta)\overrightarrow{e}_x) - \frac{3\nu\overrightarrow{u}}{(h)^2}$$

Mass conservation of fluid

$$\overrightarrow{\nabla}\cdot(h\overrightarrow{u}) = 0$$

$$\vec{q} = \phi\theta^{\beta}\left(\frac{\vec{u}}{\|\vec{u}\|} - \gamma\vec{\nabla}h\right)$$

$$\frac{\partial f}{\partial t} = -\overrightarrow{\nabla}\cdot\overrightarrow{q}$$

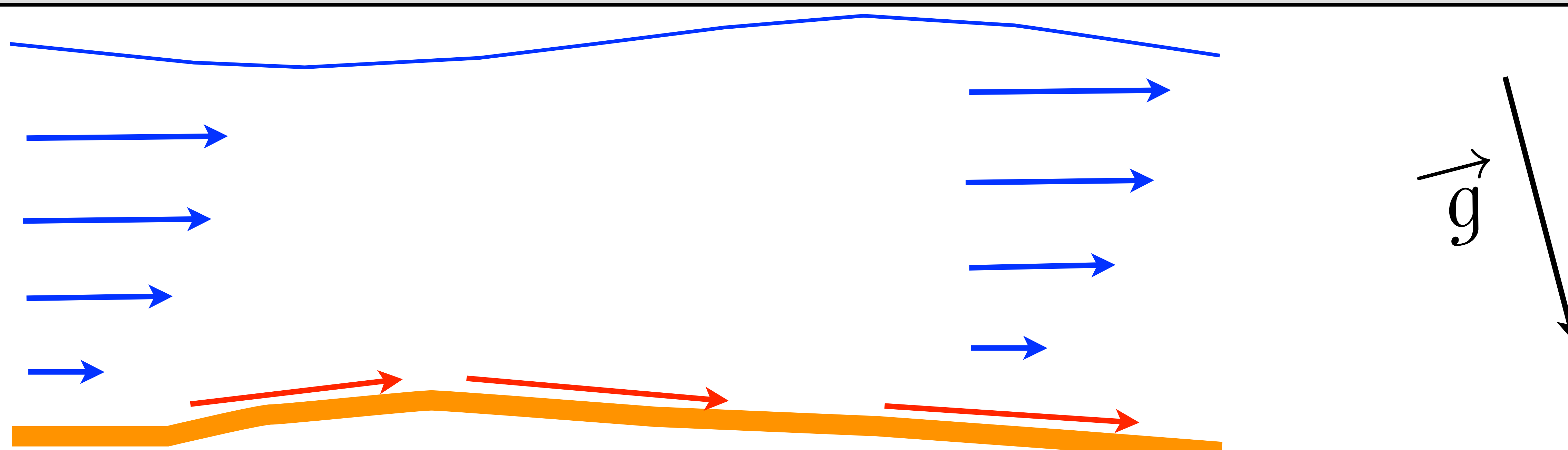

Navier Stokes — coupled system — Saint Venant

$$\frac{6}{5}(\overrightarrow{u}\cdot\overrightarrow{\nabla})\overrightarrow{u} = -g(\overrightarrow{\nabla}\eta + sin(\theta)\overrightarrow{e}_x) - \frac{3\nu\overrightarrow{u}}{(h)^2}$$

Mass conservation of fluid

$$\overrightarrow{\nabla}\cdot(h\overrightarrow{u}) = 0$$

$$\vec{q} = \phi\theta^{\beta}\left(\frac{\vec{u}}{\|\vec{u}\|} - \gamma\vec{\nabla}h\right)$$

$$\frac{\partial f}{\partial t} = -\overrightarrow{\nabla}\cdot\overrightarrow{q}$$

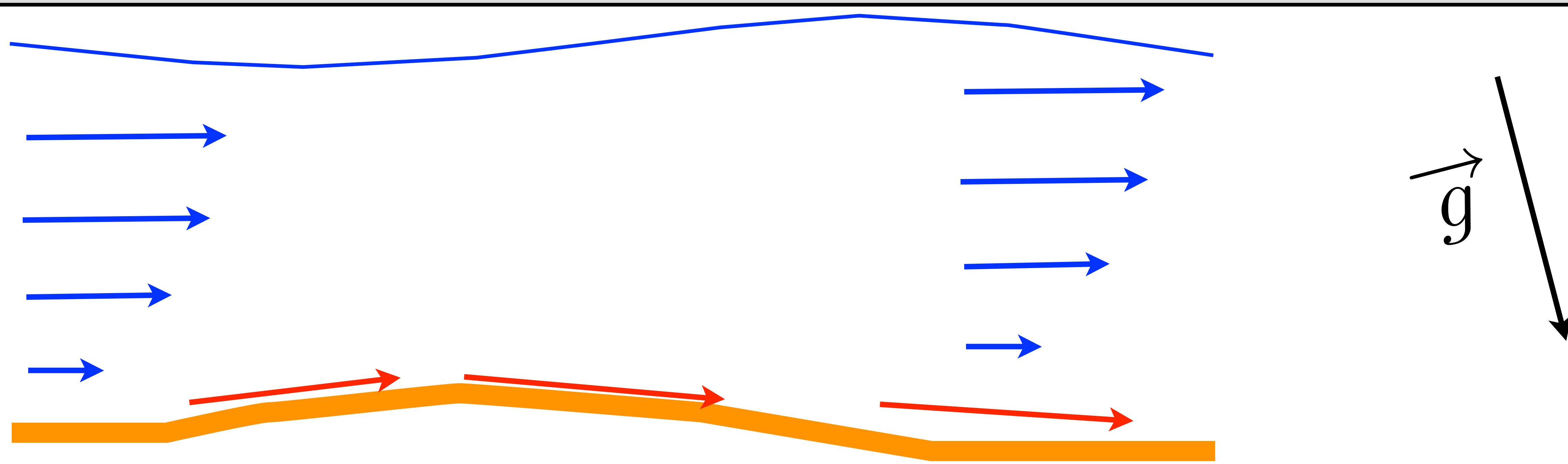

Navier Stokes

coupled system

Saint Venant

$$\frac{6}{5}(\overrightarrow{u}\cdot\overrightarrow{\nabla})\overrightarrow{u} = -g(\overrightarrow{\nabla}\eta + sin(\theta)\overrightarrow{e}_x) - \frac{3\nu\overrightarrow{u}}{(h)^2}$$

Mass conservation of fluid

$$\overrightarrow{\nabla}\cdot(h\overrightarrow{u}) = 0$$

$$\vec{q} = \phi\theta^{\beta}\left(\frac{\vec{u}}{\|\vec{u}\|} - \gamma\vec{\nabla}h\right)$$

$$\frac{\partial f}{\partial t} = -\overrightarrow{\nabla}\cdot\overrightarrow{q}$$

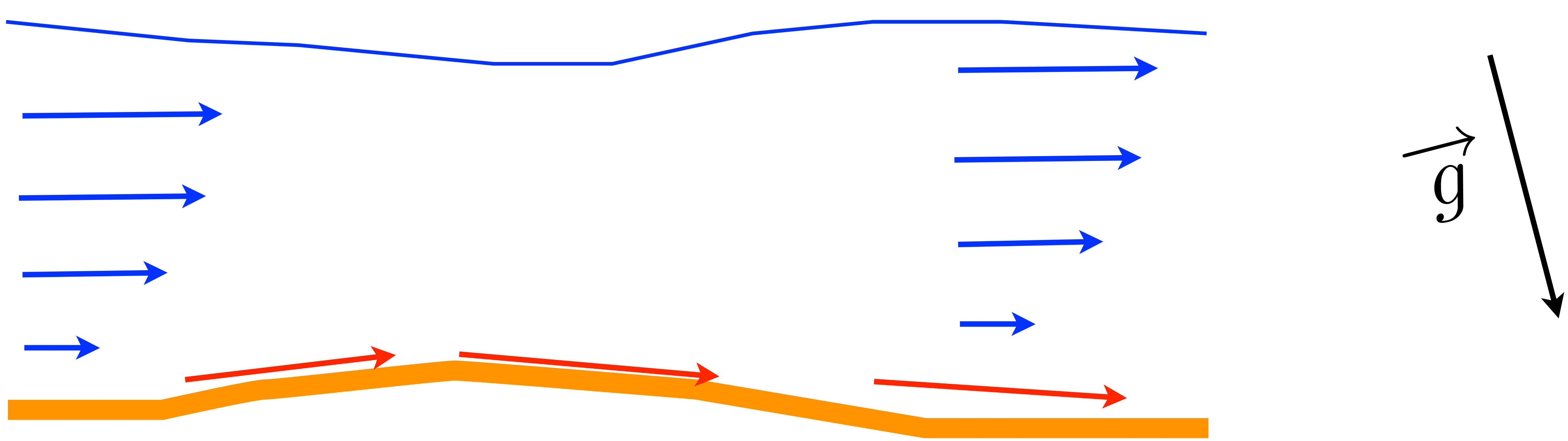

Navier Stokes

coupled system

Saint Venant

$$\frac{6}{5}(\overrightarrow{u} \cdot \overrightarrow{\nabla})\overrightarrow{u} = -g(\overrightarrow{\nabla}\eta + sin(\theta)\overrightarrow{e}_x) - \frac{3\nu\overrightarrow{u}}{(h)^2}$$

Mass conservation of fluid

$$\overrightarrow{\nabla} \cdot (h\overrightarrow{u}) = 0$$

$$\vec{q} = \phi\theta^{\beta}\left(\frac{\vec{u}}{\|\vec{u}\|} - \gamma\vec{\nabla}h\right)$$

$$\frac{\partial f}{\partial t} = -\overrightarrow{\nabla} \cdot \overrightarrow{q}$$

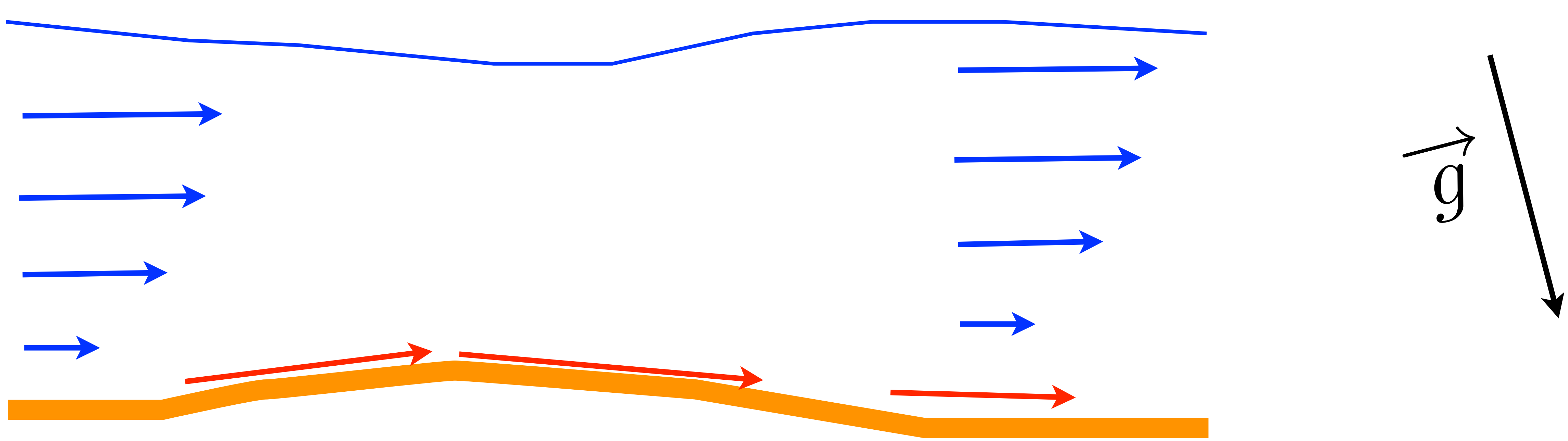

Navier Stokes

coupled system

Saint Venant

$$\frac{6}{5}(\overrightarrow{u}\cdot\overrightarrow{\nabla})\overrightarrow{u} = -g(\overrightarrow{\nabla}\eta + sin(\theta)\overrightarrow{e}_x) - \frac{3\nu\overrightarrow{u}}{(h)^2}$$

Mass conservation of fluid

$$\overrightarrow{\nabla}\cdot(h\overrightarrow{u}) = 0$$

$$\vec{q} = \phi\theta^{\beta}\left(\frac{\vec{u}}{\|\vec{u}\|} - \gamma\vec{\nabla}h\right)$$

$$\frac{\partial f}{\partial t} = -\overrightarrow{\nabla}\cdot\overrightarrow{q}$$

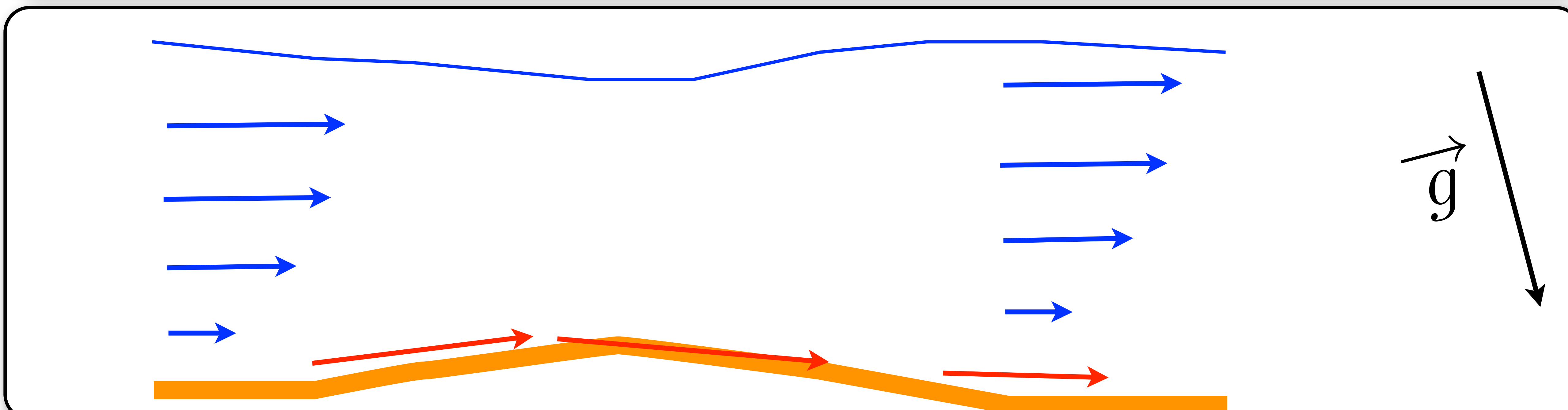

Linear Stability

Basic flow

$$u_0 = 1,\, d_0 = 1$$

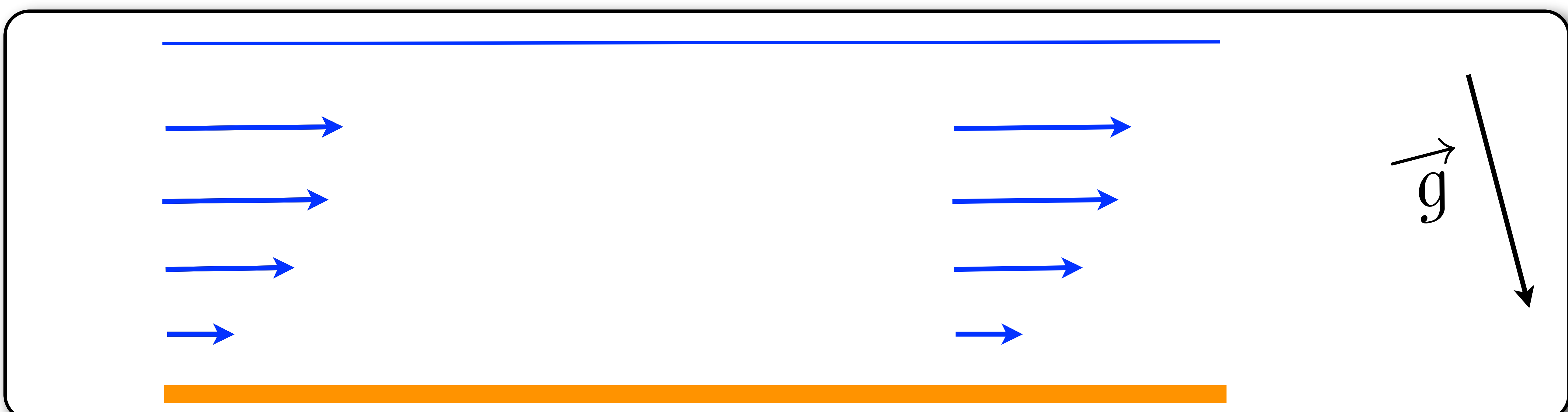

Linear Stability

Basic flow $u_0 = 1,\ d_0 = 1$

perturbations $\propto \exp(i(k_l x_l - \omega t))$

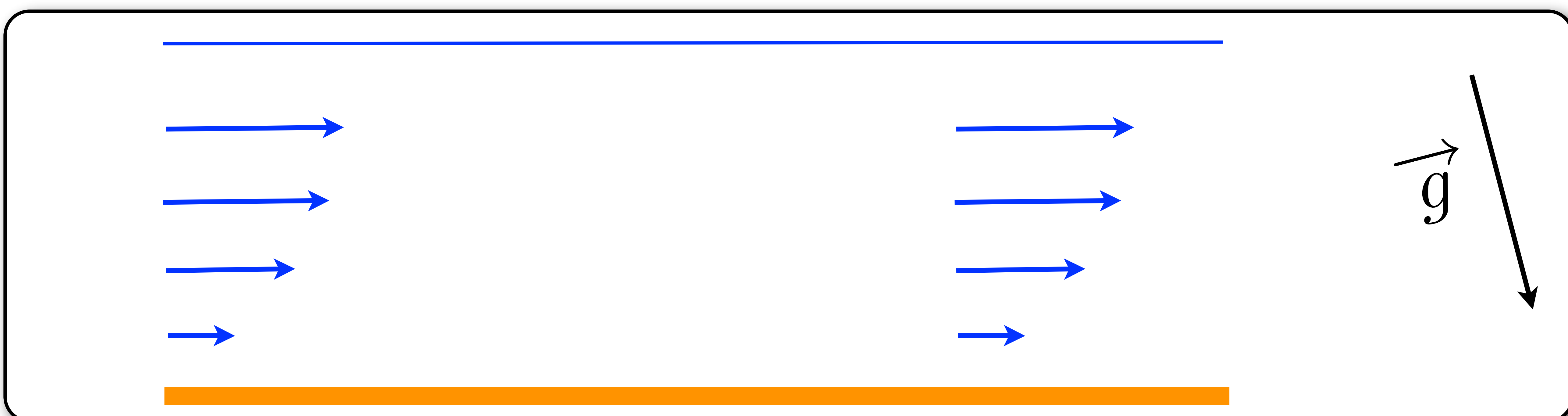

Linear Stability

Basic flow $u_0 = 1,\ d_0 = 1$

perturbations $\propto \exp(i(k_l x_l - \omega t))$

dispersion relation

$$
\begin{aligned}
\omega = \Big(& -36iF^4k_x^3\big(k_x^2+k_y^2\big)\gamma + 30iF^2k_x\big(k_x^4\gamma + 2k_x^2k_y^2\gamma + k_y^4\gamma \\
& + 2ik_x^3(\beta + S(2+\beta)\gamma) + ik_xk_y^2(1+\beta+S(4+\beta)\gamma)\big) \\
& + 25S\big(k_x^4\gamma + 2k_x^2k_y^2\gamma + k_y^4\gamma - ik_xk_y^2(-3+\beta)(1+S\gamma) \\
& + ik_x^3(2\beta + S(3+2\beta)\gamma)\big)\Big)\Big/ \\
& \Big(\big(6F^2k_x - 5iS\big)\Big(\big(-5+6F^2\big)k_x^2 - 5k_y^2 - 15ik_xS\big)(1+S\gamma)\Big)
\end{aligned}
$$

$$\beta = \frac{\theta_0 \phi'(\theta_0)}{\phi(\theta_0)}$$

Linear Stability   2D $\int(3D)$

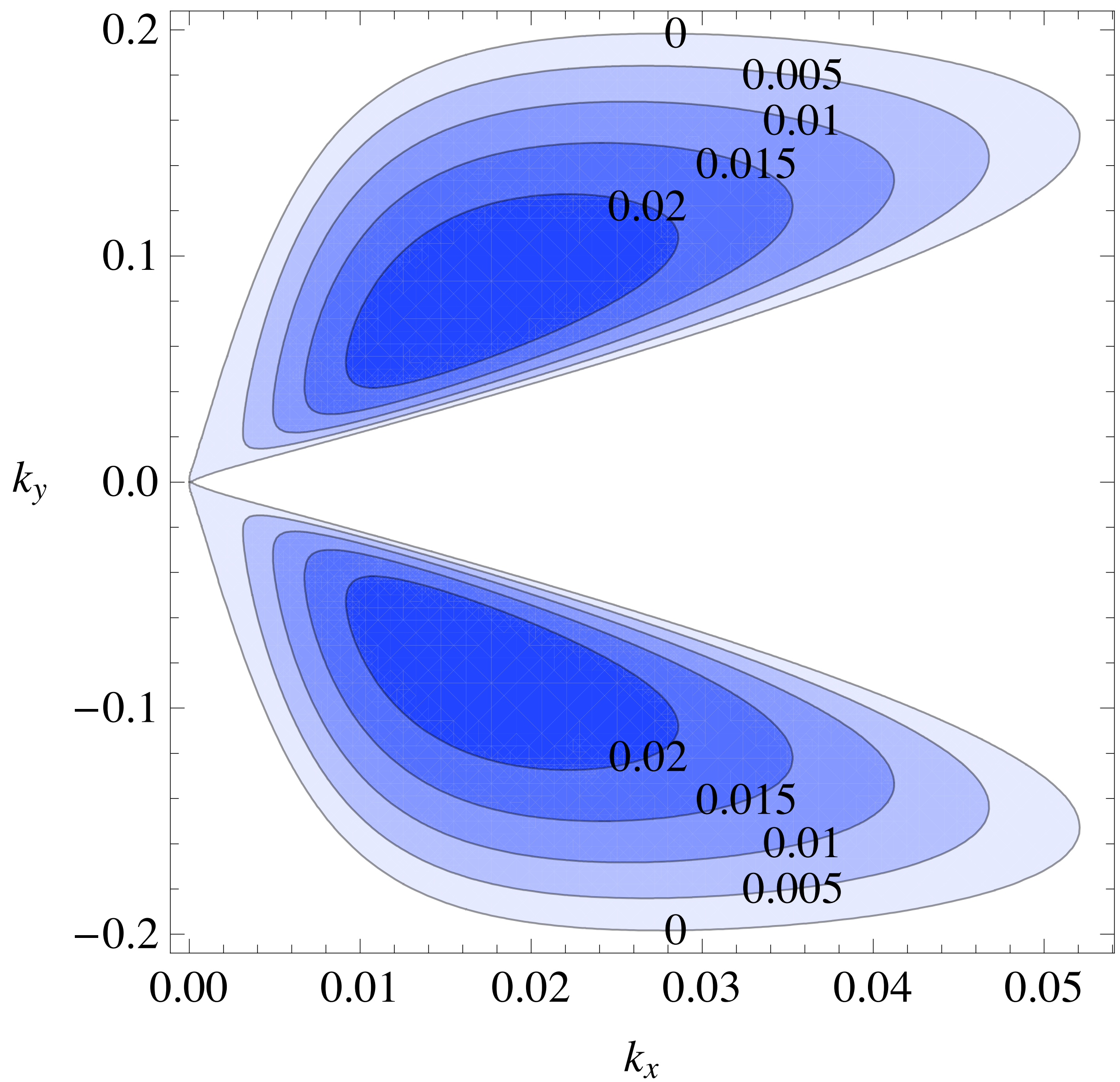

Mussel Curve

Linear Stability

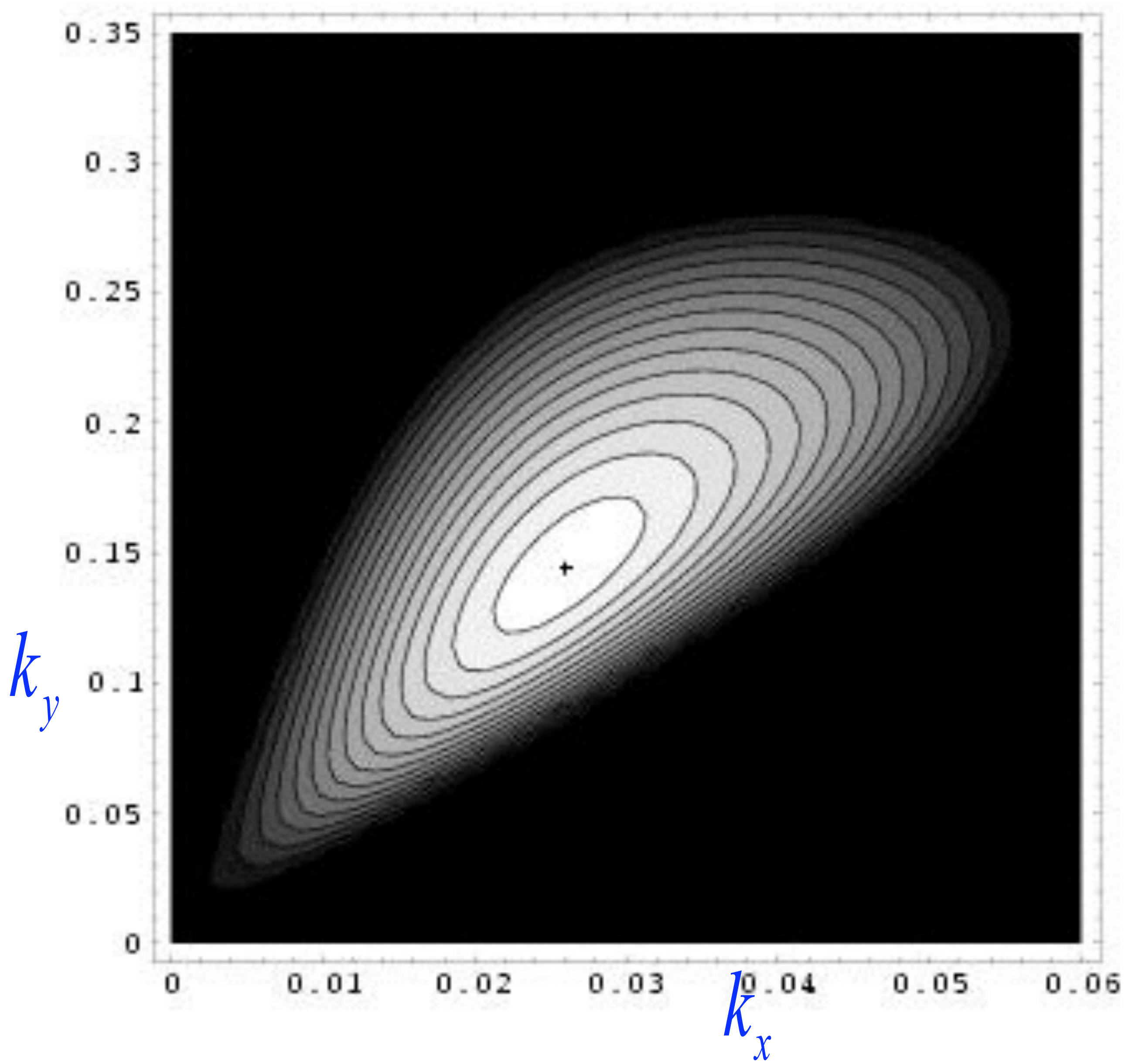

2 D Instability : inclindes bancs

No 1D instability (k_y=0):

$$F = 1,5 \quad \varphi = 3°$$

$$\beta = 3,75 \quad \gamma = 1$$

Linear Stability

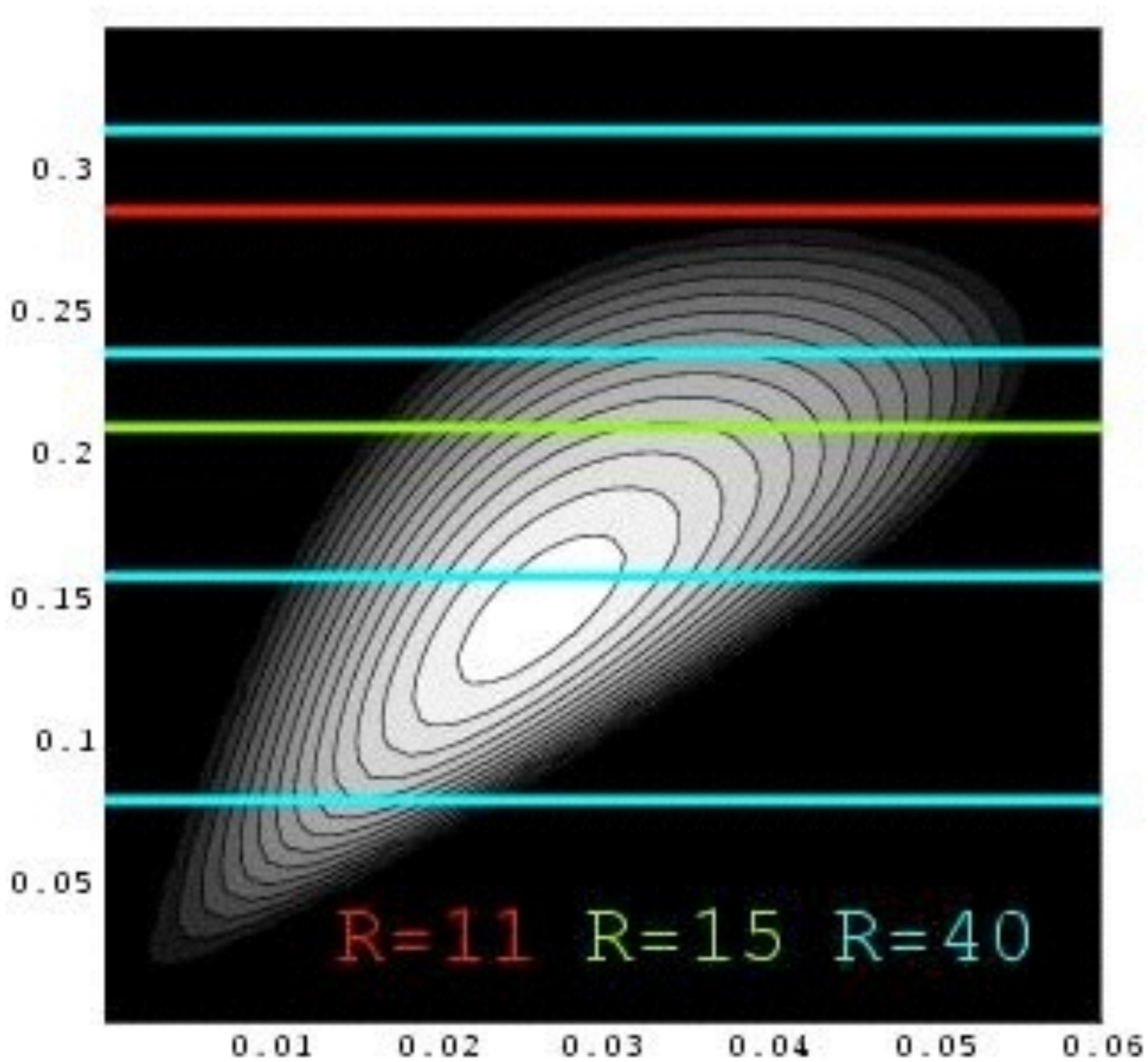

width of the river R promotes the modes

$$F = 1{,}5 \quad \varphi = 3^\circ$$

$$\beta = 3{,}75 \quad \gamma = 1$$

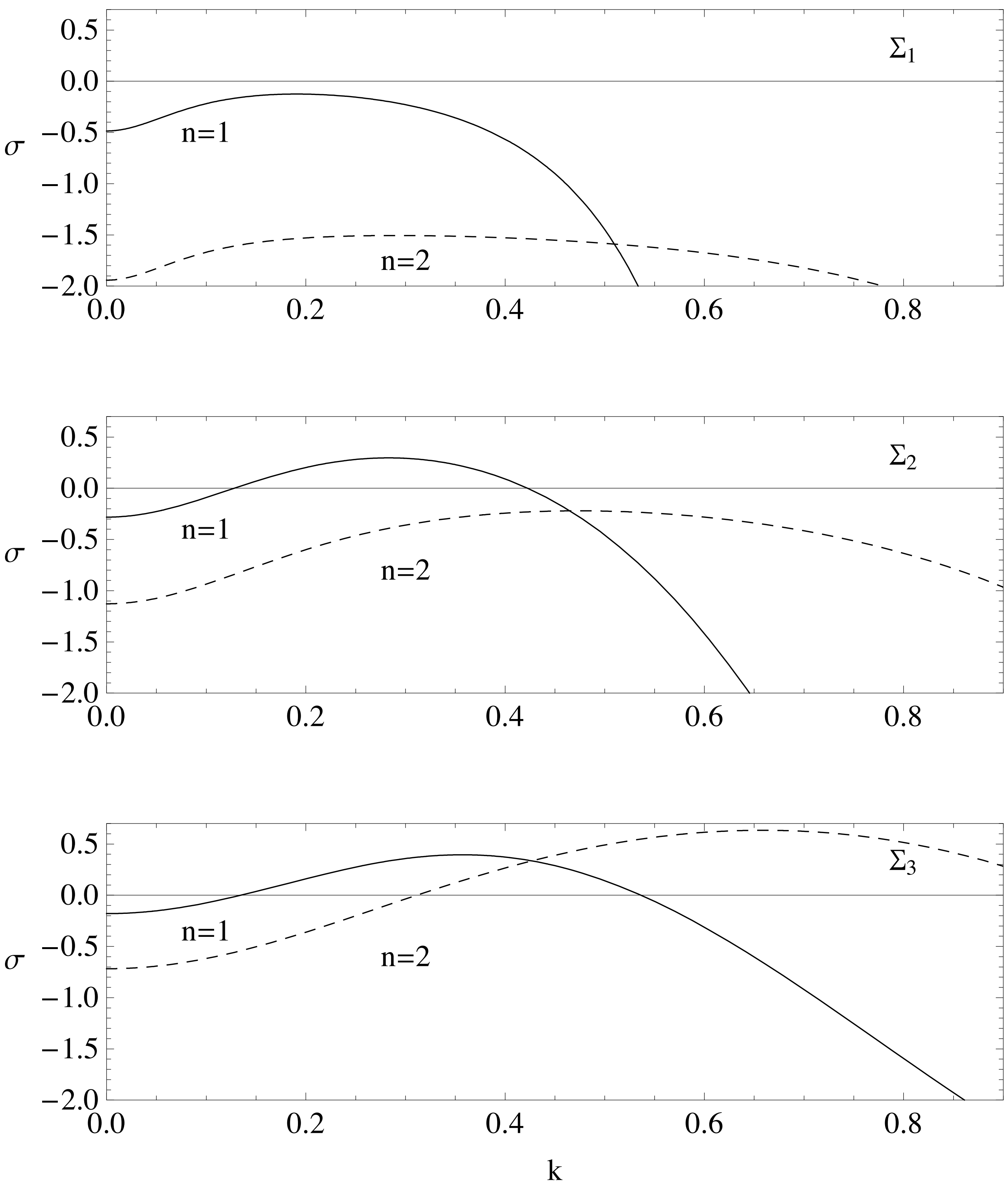

Σ1
n=1
n=2
Σ2
n=1
n=2
Σ3
n=1
n=2
σ
k

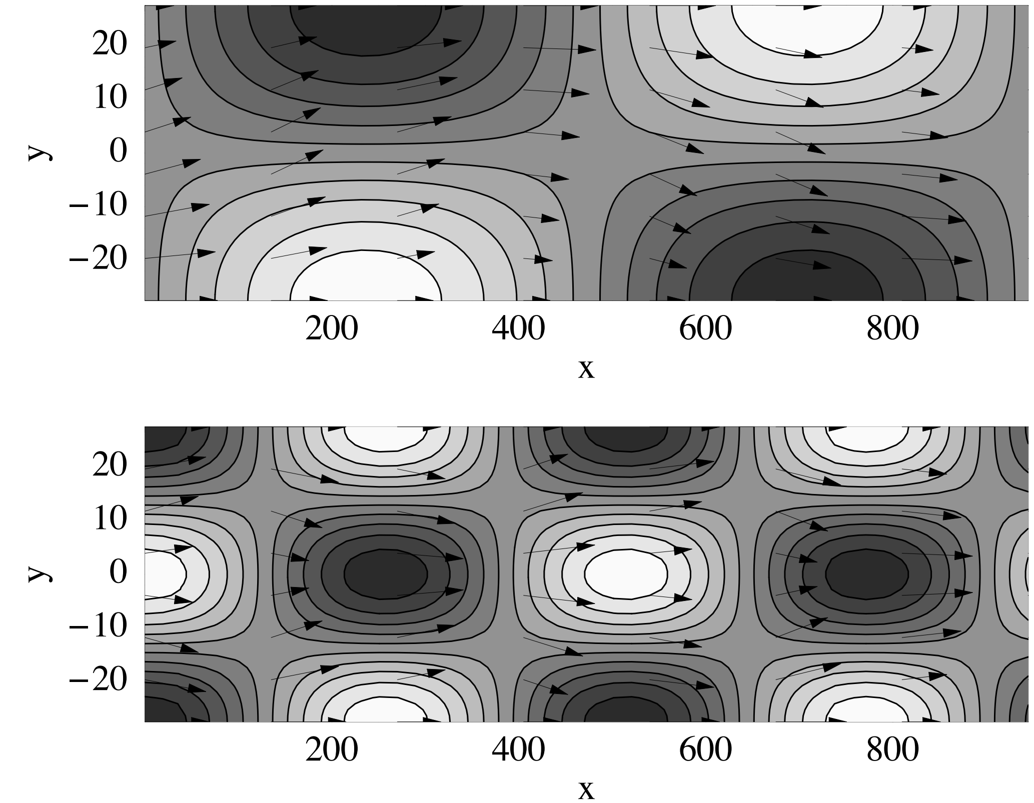

y
x

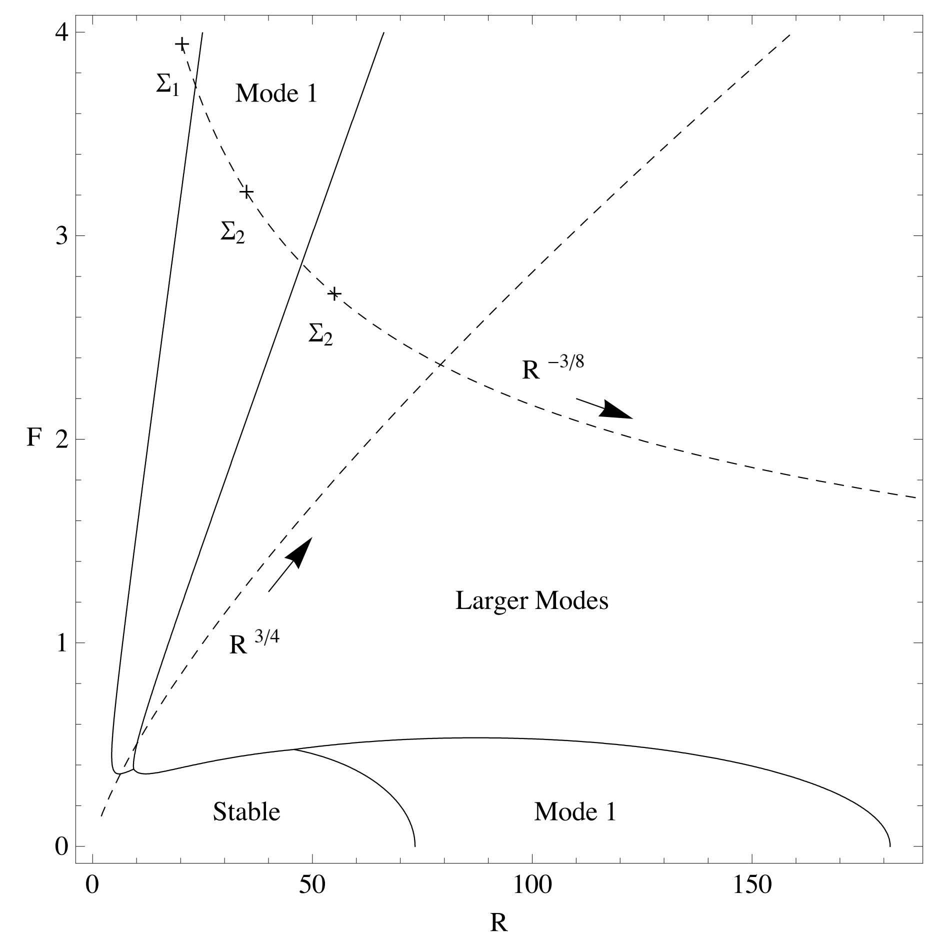

Σ1
Mode 1
Σ2
Σ2
R −3/8
F
Larger Modes
R 3/4
Stable
Mode 1
R

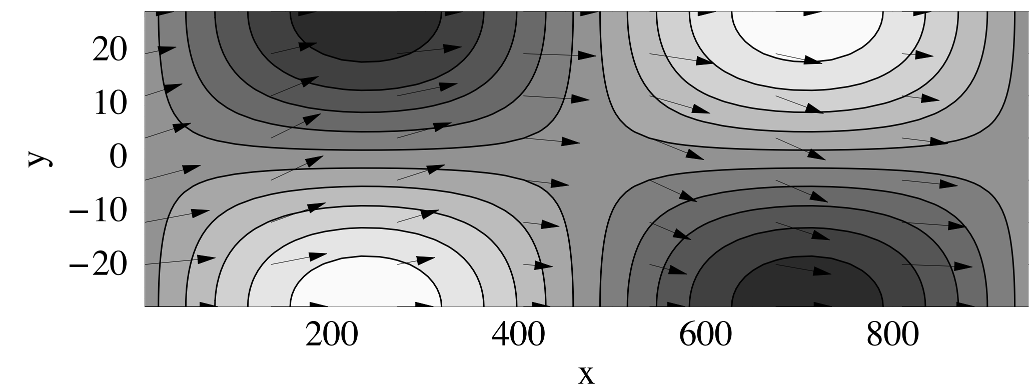

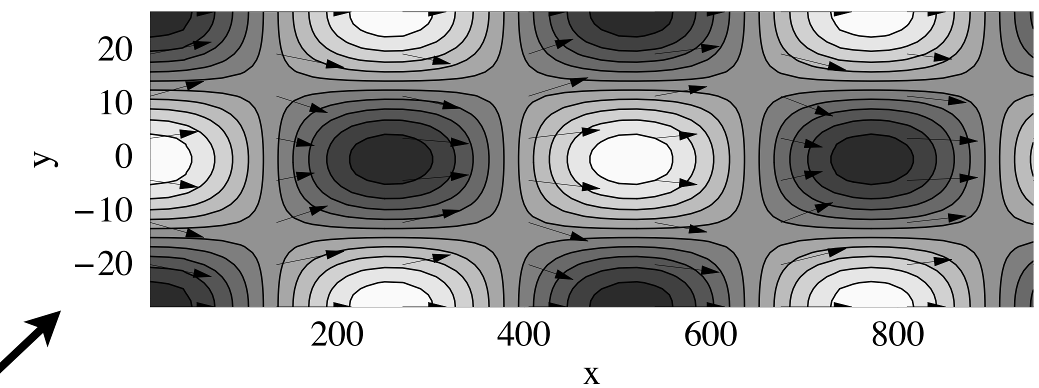

meander

braided river

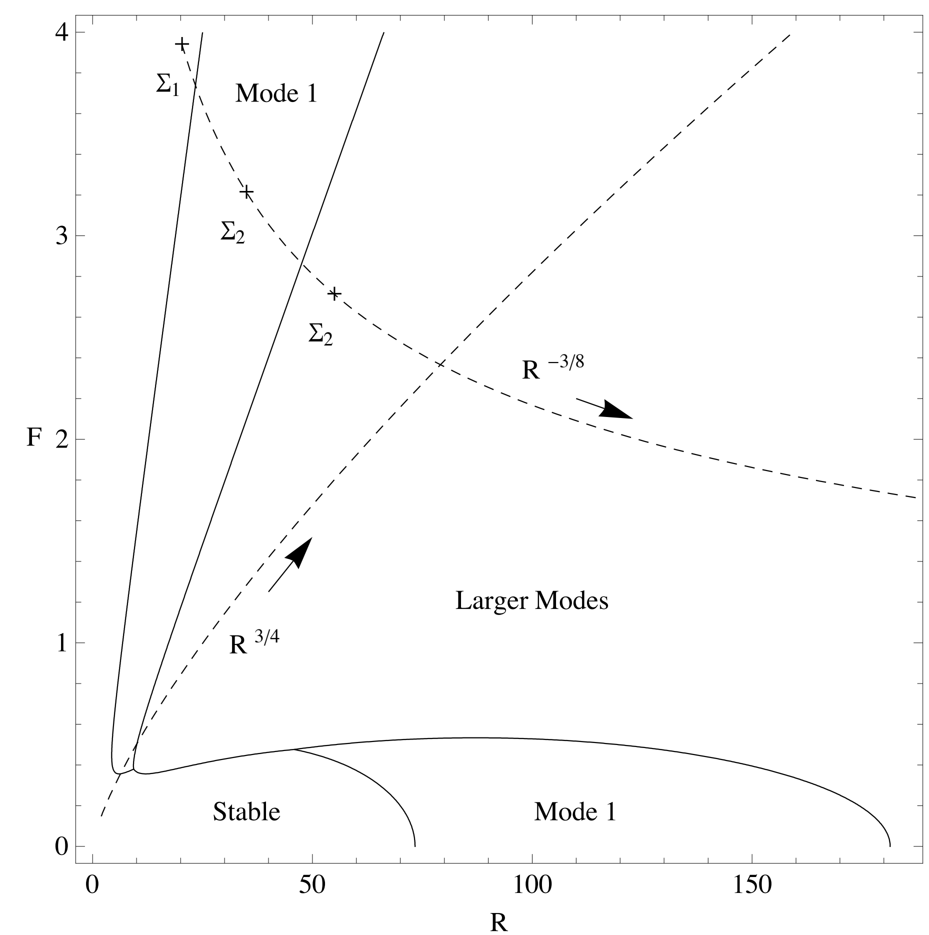

- Saint Venant + erosion gives alternate bars
- now we look at the evolution of those bars

small film of water

beach of Santa Barbara CA

small film of water

RHOMBOID RIPPLE MARK.

A. O. WOODFORD.

Bucher (p. 153, 1919) has proposed the term "*rhomboid (current-) ripple*" for "*small rhomboidal, scale-like tongues of sand*, arranged in a reticular pattern" produced experimentally by Engels (1905) as the first effect of transportation by a water current in gentle, uniform flow. But violent currents in water also impress rhomboidal patterns on sand, and hence, in this paper, the term *rhomboid ripple mark* will be used in a descriptive sense, to include all sharply rhomboid patterns developed on the surface of a mobile sediment. An example is given in Fig. 1. Braided rills which are not sharply and regularly rhomboid in pattern, are not included. Neither are the numerous V-shaped grooves which spread from the snouts of partly buried sand crabs (Hippidae, *Emerita analoga* in California), and which may in combination suggest an irregularly rhombic pattern.

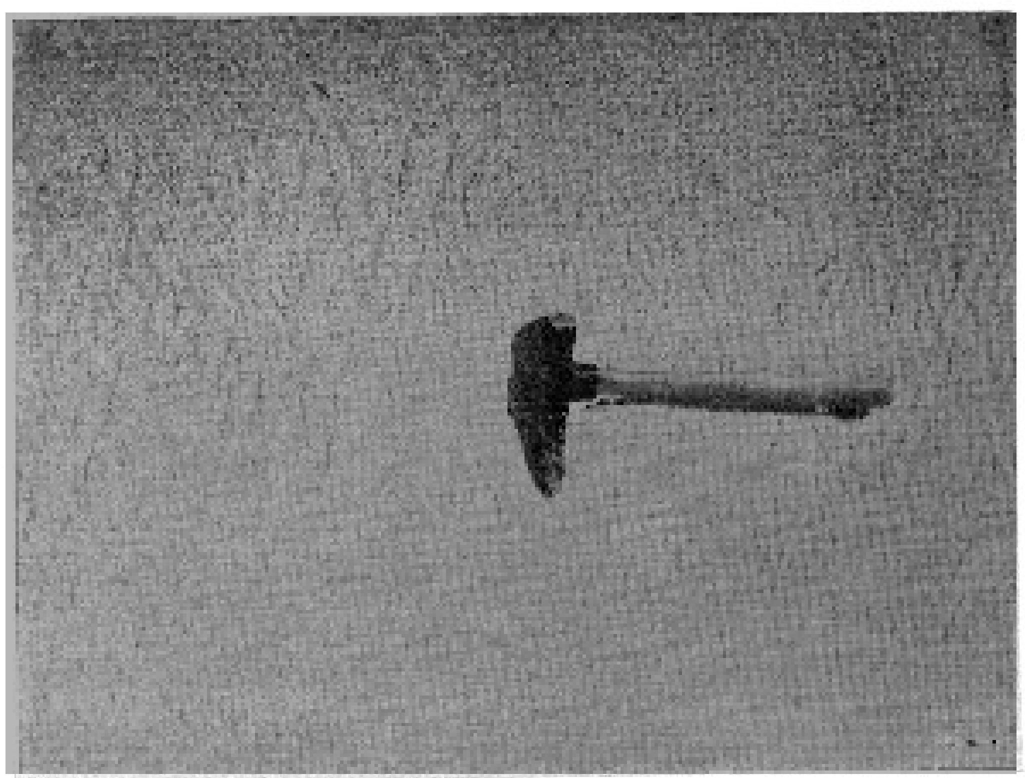

Fig. 1. Rhomboid ripple mark, Laguna Beach, Calif., March 29, 1933. The hammer gives the scale.

Several authors (Kindle: p. 34 and pl. 19b, 1917; Johnson: pp. 515-517, 1919; Kindle and Bucher: pp. 655, 656, 1932) describe and figure rhomboid ripple marks from modern beaches. In 1917 Kindle ascribed the imbricated pattern to, "The action of very small waves lapping and crossing each other from opposite sides of a miniature spit," but in 1932 Kindle and Bucher were inclined to explain the pattern in the light of the Engels' experiment mentioned above. Johnson calls the structures "backwash marks," and says (p. 517, 1919): "The thin sheet of water returning down the beach slope appeared to be split into diverging minor currents by every patch of more compact sand or particle of coarser material which impeded its progress, and the crossing of these minor currents resulted in the criss-cross pattern in the sand."

INTERFERENCE PATTERN UNDER RAPID FLOW.

The rhomboid pattern formed on sand looks very much like an interference effect. Therefore, before describing the

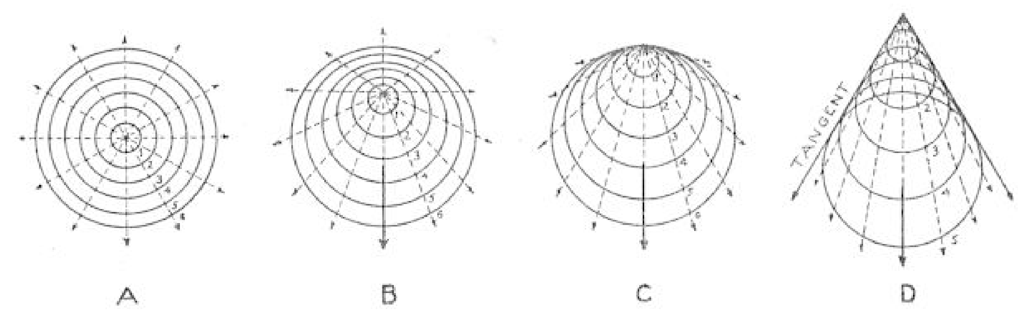

Fig. 2. Schematic sketches showing wave impulses spreading from a point, affected by various rates of flow. See text for explanation. After Rehbock.

observed pattern in detail, there will be presented some generalities concerning the waves which may form in water currents.

First of all, the distinction must be made between *tranquil flow* and *rapid flow* (Rehbock: 1930; Bakhmeteff: 1932). In tranquil flow, the average velocity of the water is less than the wave velocity for the given depth; in rapid flow it is greater. The effect on waves is shown in Fig. 2, after Rehbock. If a pebble is tossed into quiet water, concentric waves are produced (A). If the water is in tranquil flow, the ripples are distorted (B). If a certain critical velocity is equaled or exceeded, the waves cannot be propagated upstream, but only down (C and D). In D there is suggested a cause for the


gutter
sidewalk

Chang Simons JFM 70

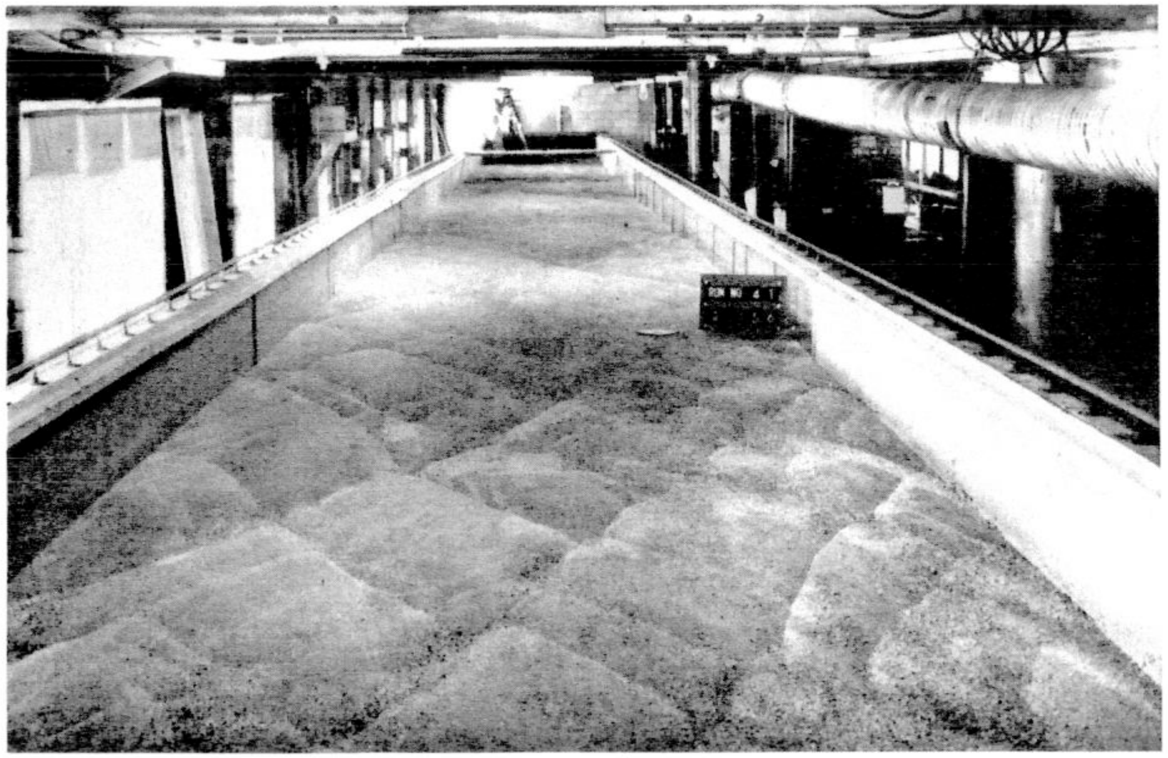

(c)

FIGURE 2. Diagonal bed patterns in a laboratory flume with large width to depth ratios and with the flow nearly critical. (a) Froude number = 0·92, width to depth ratio = 24. (b) Froude number = 0·83, width to depth ratio = 28·5. (c) Froude number = 1·12, width to depth ratio = 18.

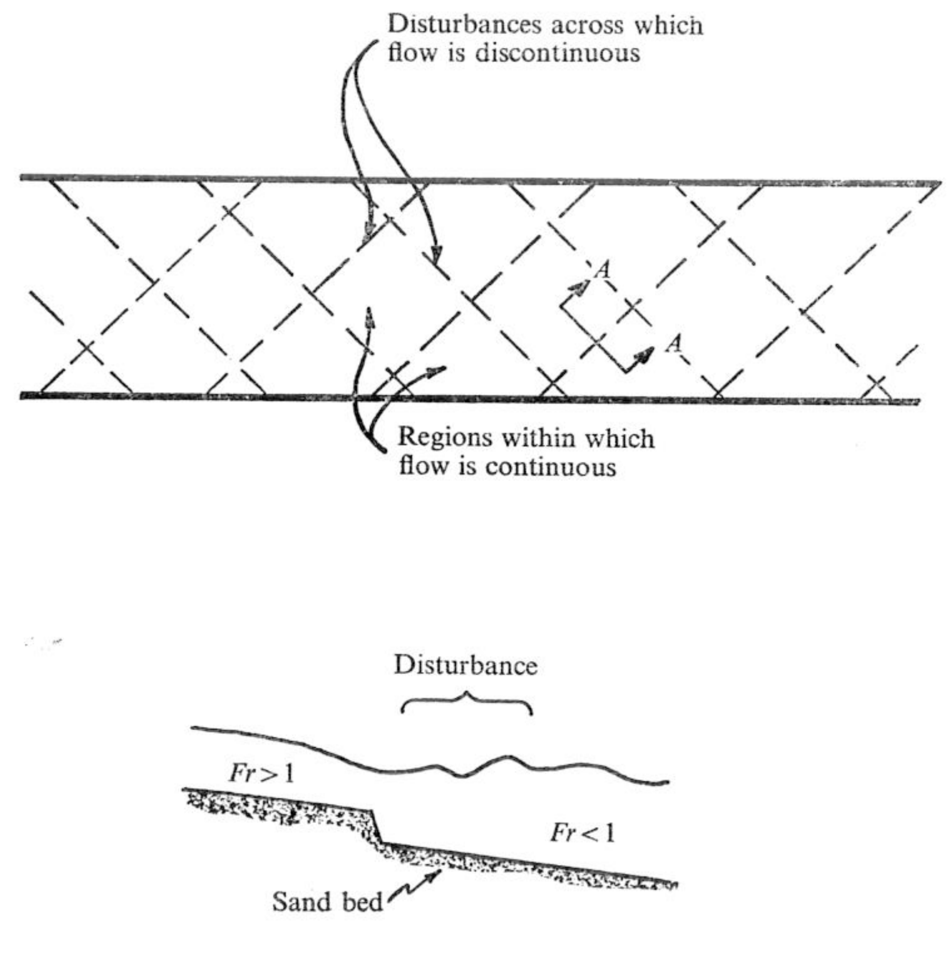

Section A–A

Schematic drawing showing diagonal lines in shallow channel flow with Froude number near unity.

$$N = \begin{vmatrix} U & W & 0 & 0 & g & 0 & 0 & 0 \\ 0 & 0 & U & W & 0 & g & 0 & 0 \\ h & 0 & 0 & h & U & W & 0 & 0 \\ 0 & \dfrac{Wq_1}{U^2} & 0 & -\dfrac{q_1}{U} & 0 & 0 & -1 & -\dfrac{W}{U} \\ dx & dz & 0 & 0 & 0 & 0 & 0 & 0 \\ 0 & 0 & dx & dz & 0 & 0 & 0 & 0 \\ 0 & 0 & 0 & 0 & dx & dz & 0 & 0 \\ 0 & 0 & 0 & 0 & 0 & 0 & dx & dz \end{vmatrix}.$$


IPGP Saint-Maur

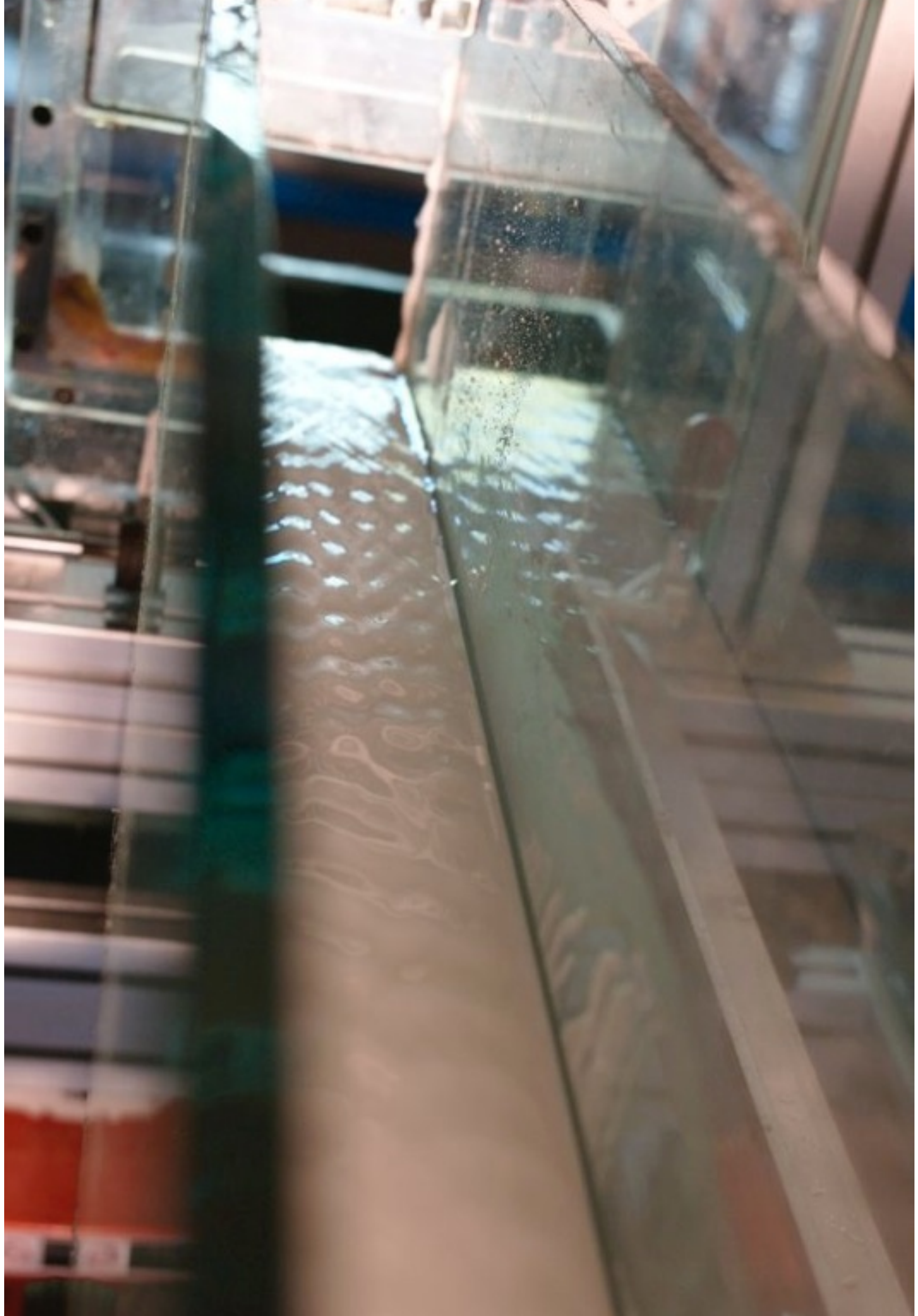

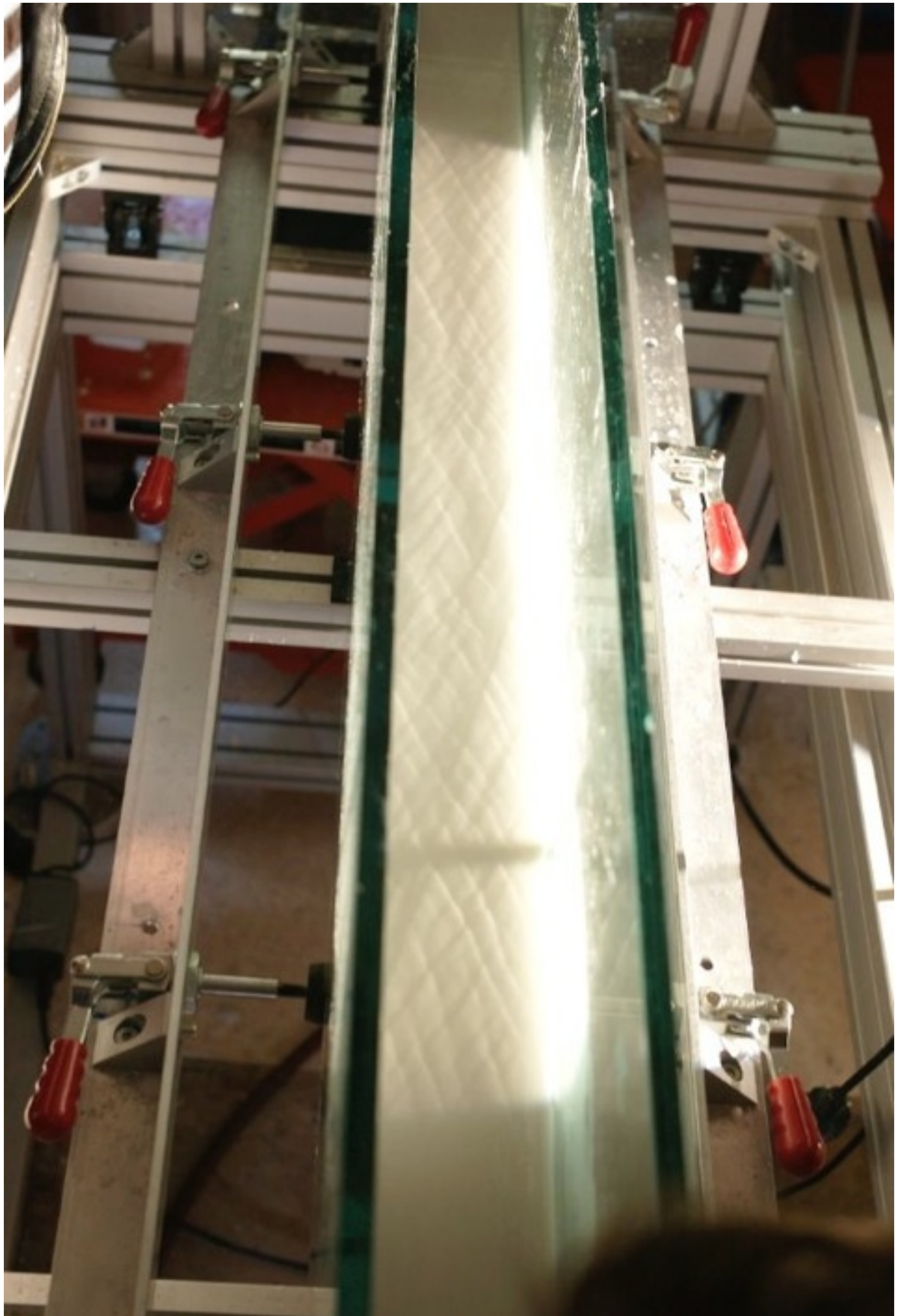

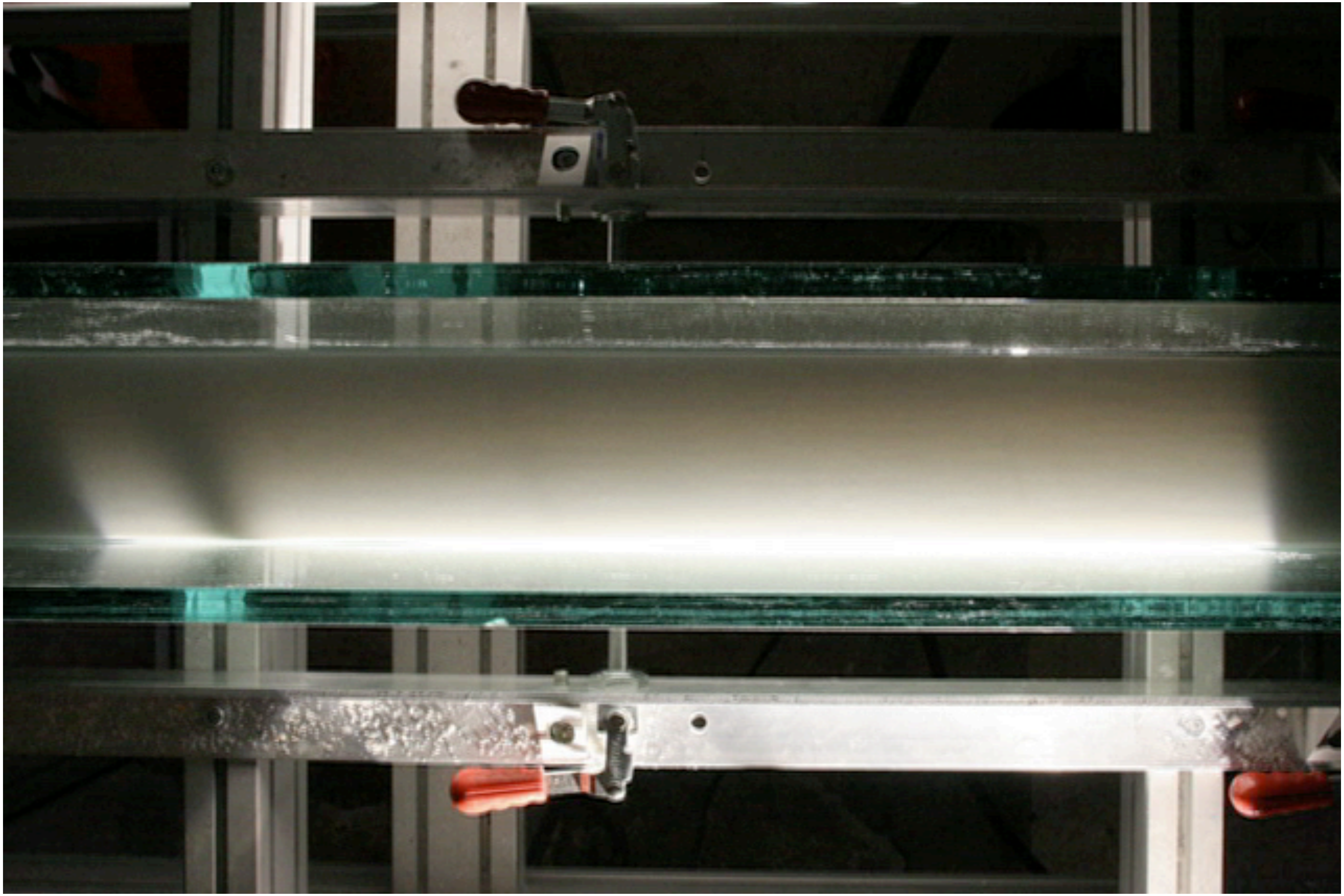

apparition des chevrons (lecture en boucle)

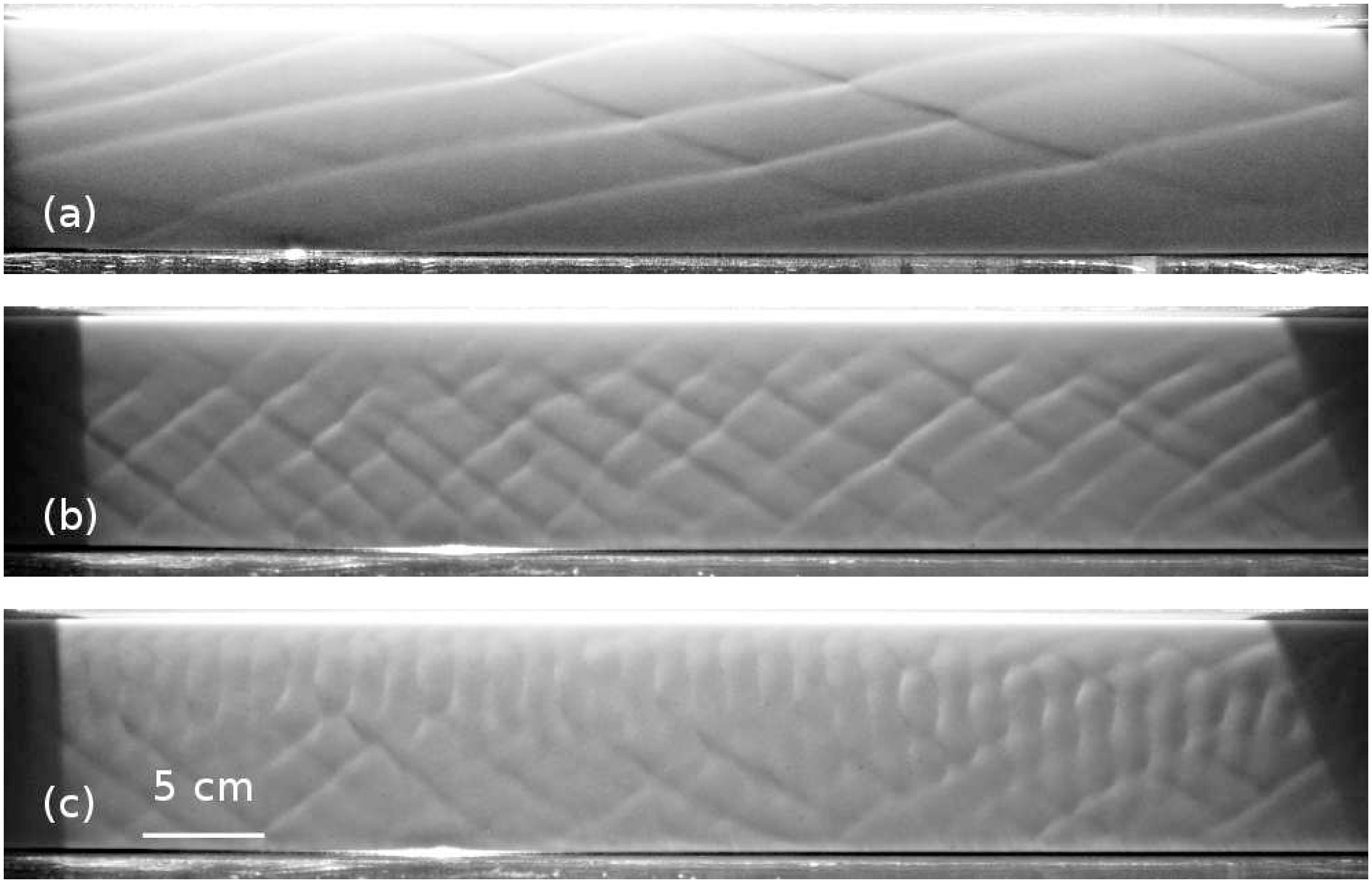
(a)
(b)
(c)
5 cm

evolution of a periodic bed with an initial random noise
it gives inclined waves and rhomboid shape

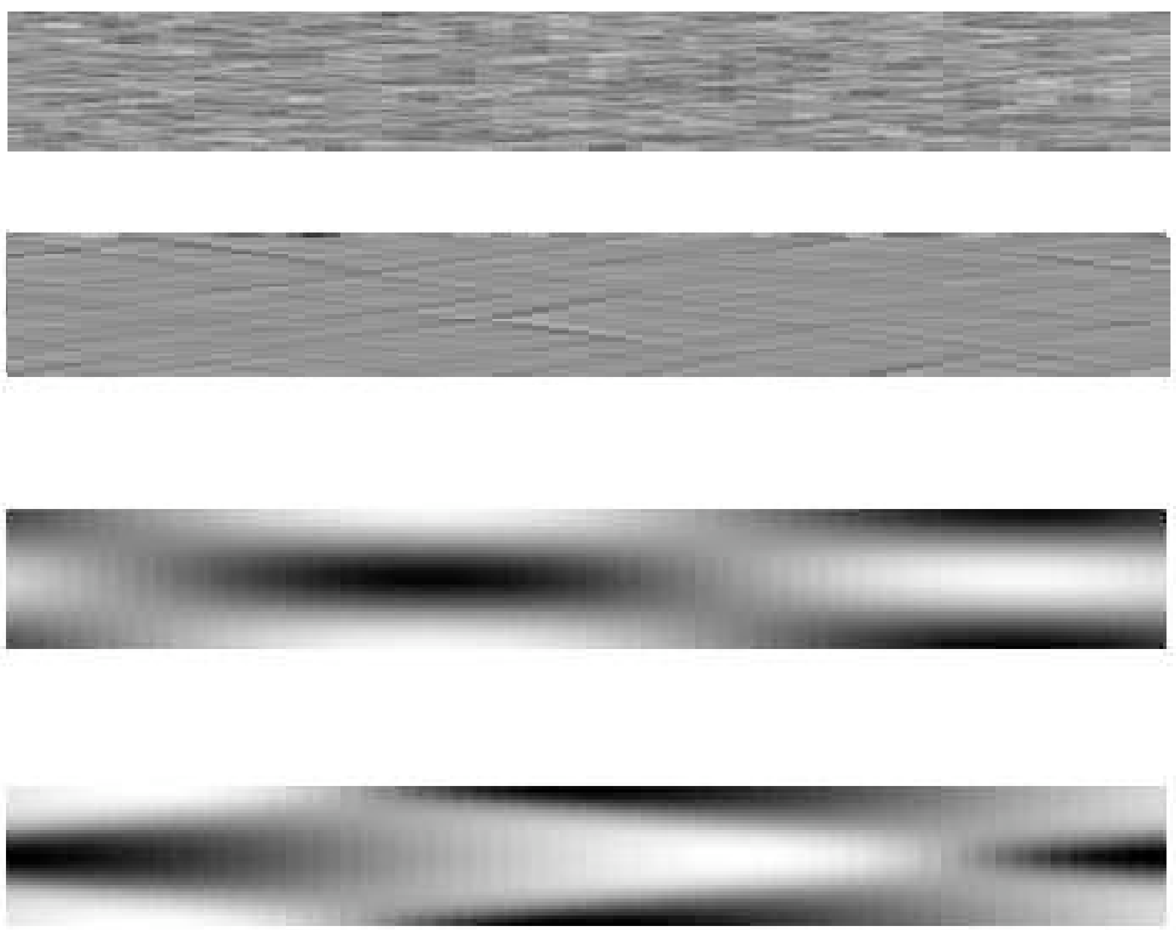

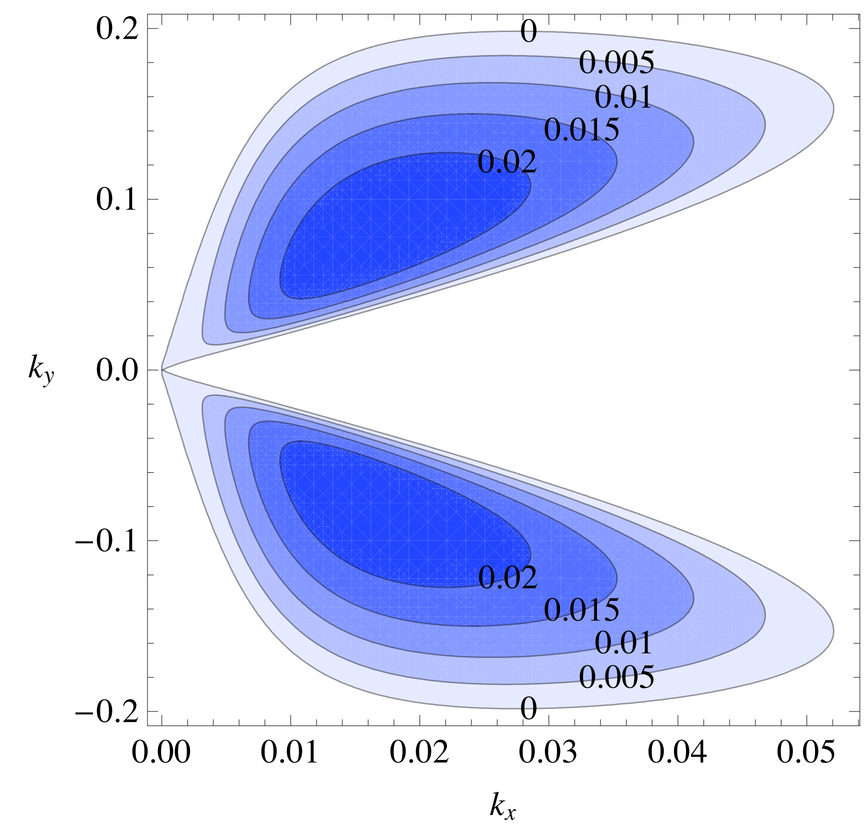

Fourier/ non linearity (θ^{β}), periodicity in x et y

Inclined ripples and diamond pattern

at first

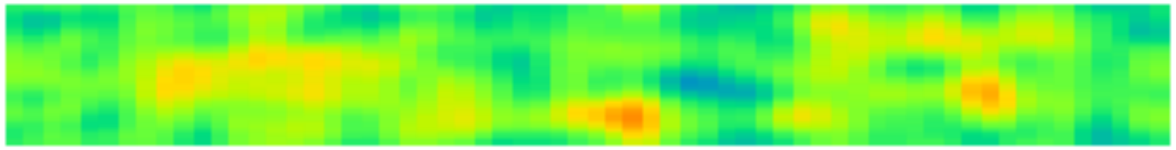

next

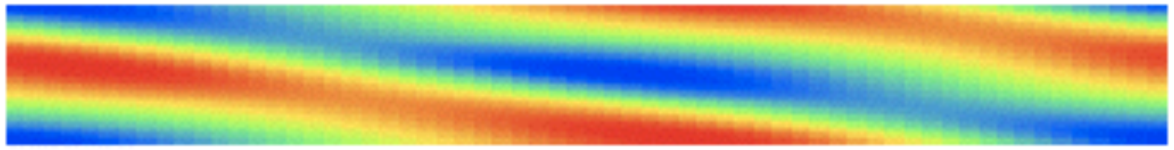

Fourier FFT/ non linearity (θ^{β}), full periodicity

Inclined ripples and diamond pattern

at first

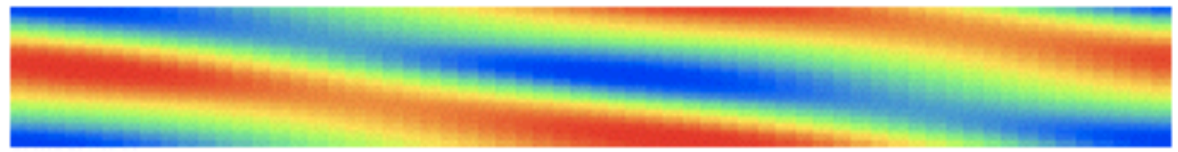

next

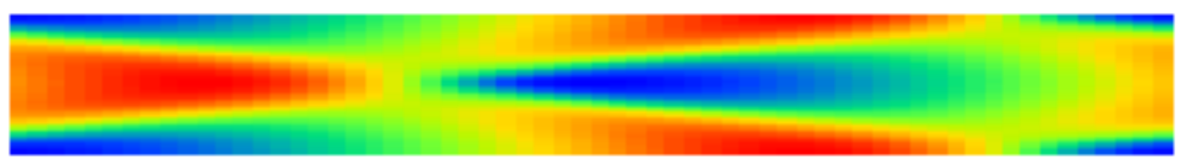

Fourier FFT/ non linearity (θ^{β}), full periodicity

comparisons mesurements vs theory

$$\alpha \approx \arcsin \frac{0.463}{F},$$

$$\alpha = \arcsin \frac{1}{F},$$

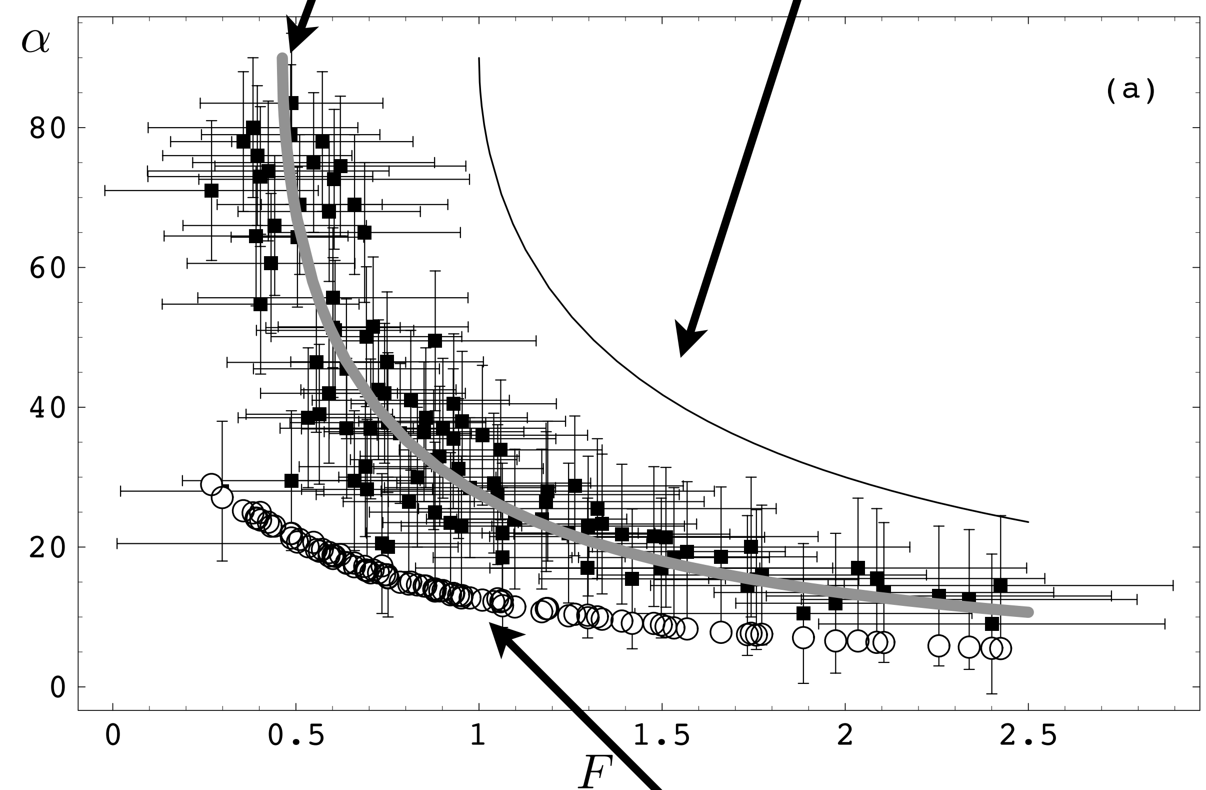

Saint Venant

problems with Saint Venant

$\alpha \approx \arcsin \frac{0.463}{F}$, $\alpha = \arcsin \frac{1}{F}$,

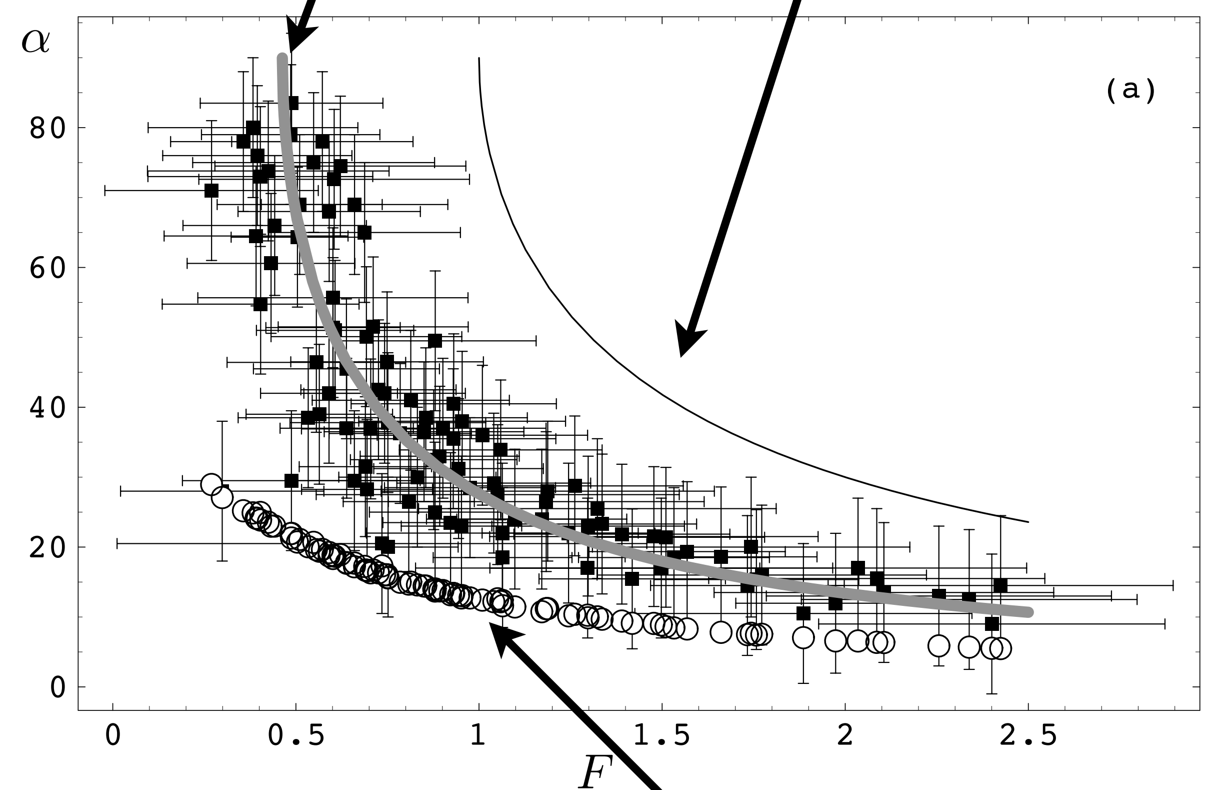

Saint Venant

up to now only qualitative results: realistic trends but:

Saint Venant is not enough precise for the bars...

is Saint Venant good for the dunes?

testing Saint Venant + erosion

dune?

Linear Stability 1D $\int$(2D)

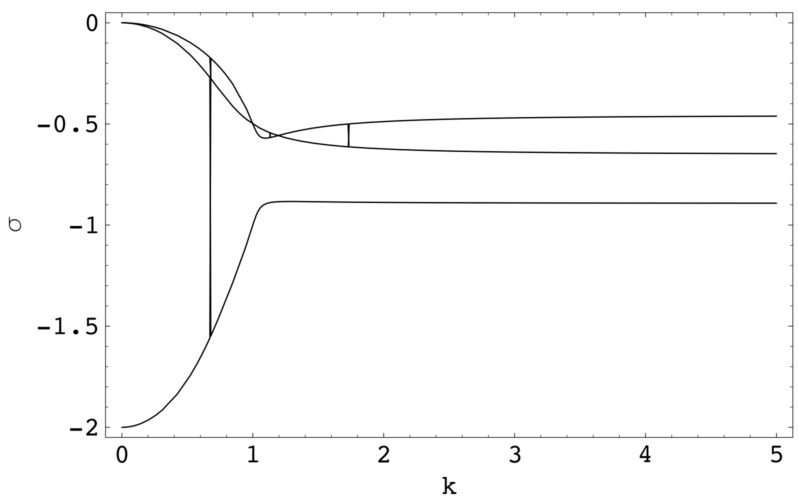

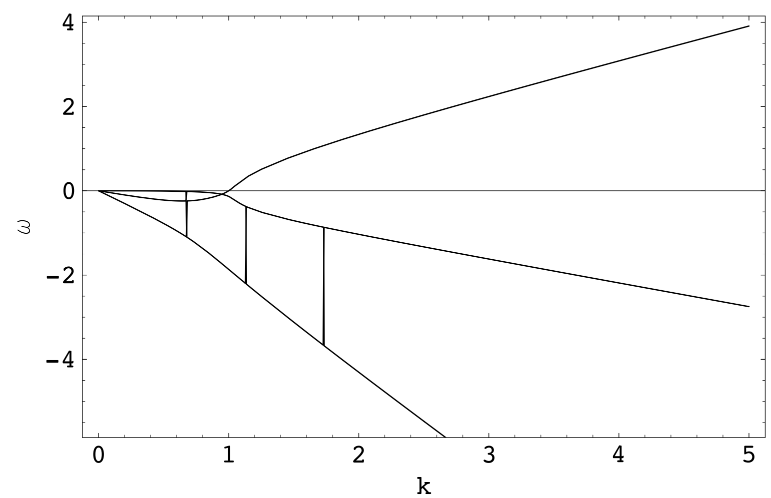

no dunes in 2D

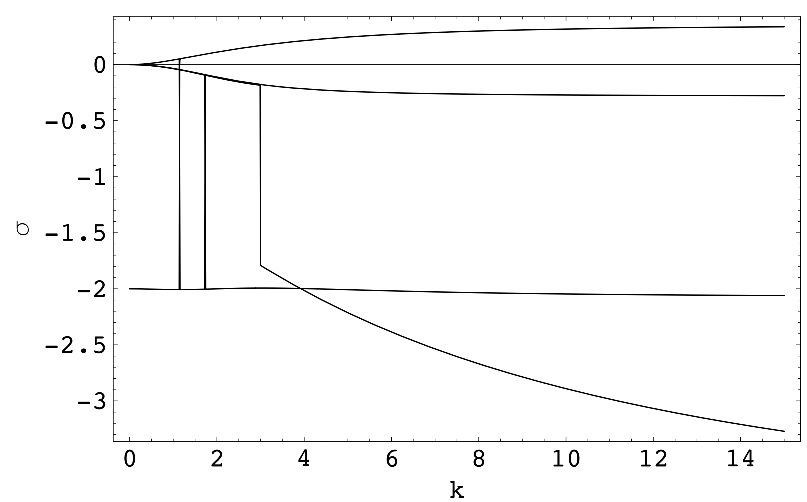

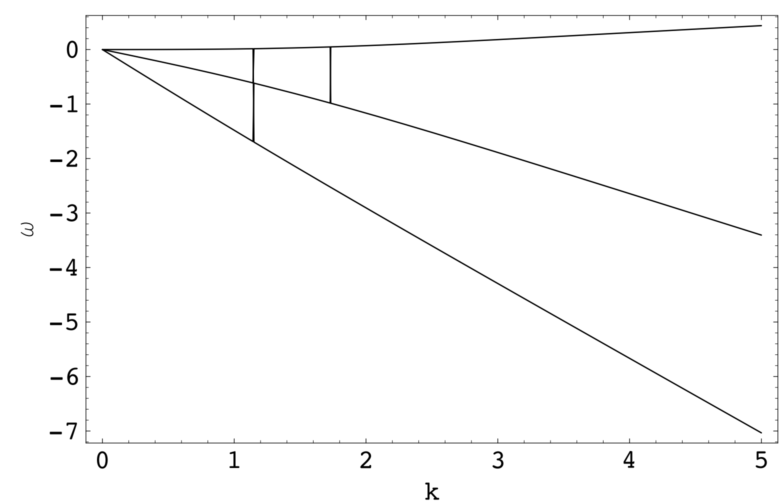

antidunes in 2D

Linear Stability 1D $\int$(2D)

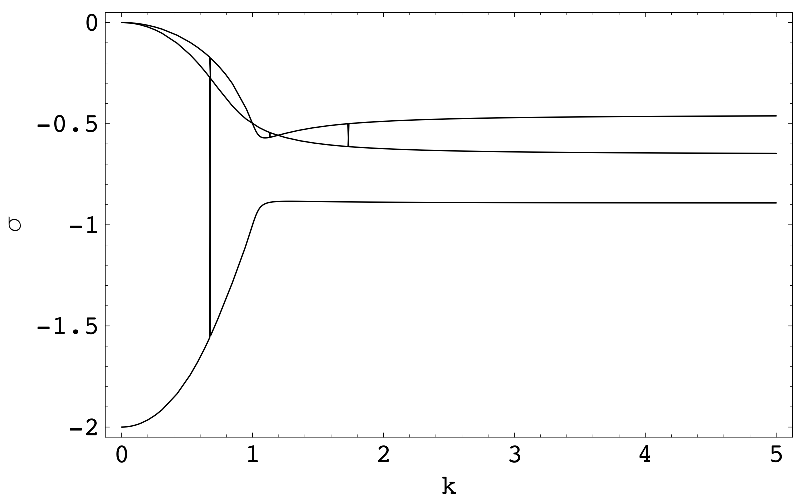

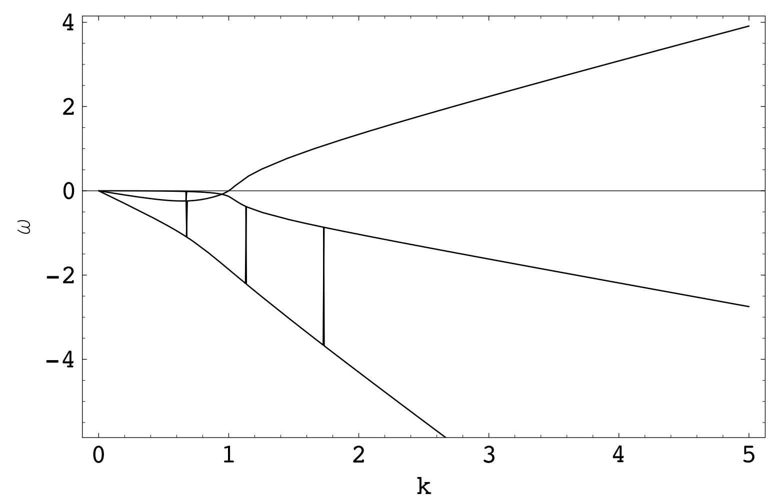

no dunes in 2D

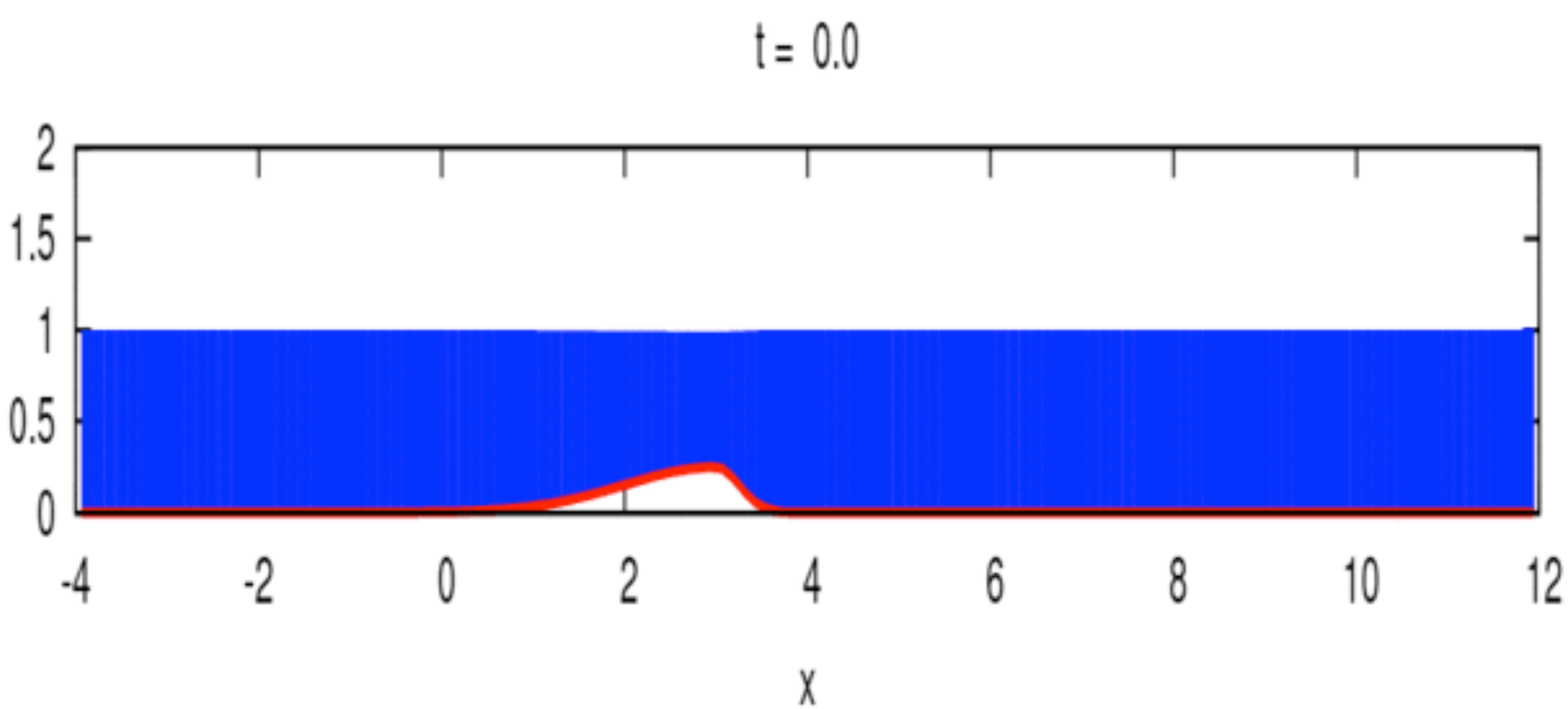

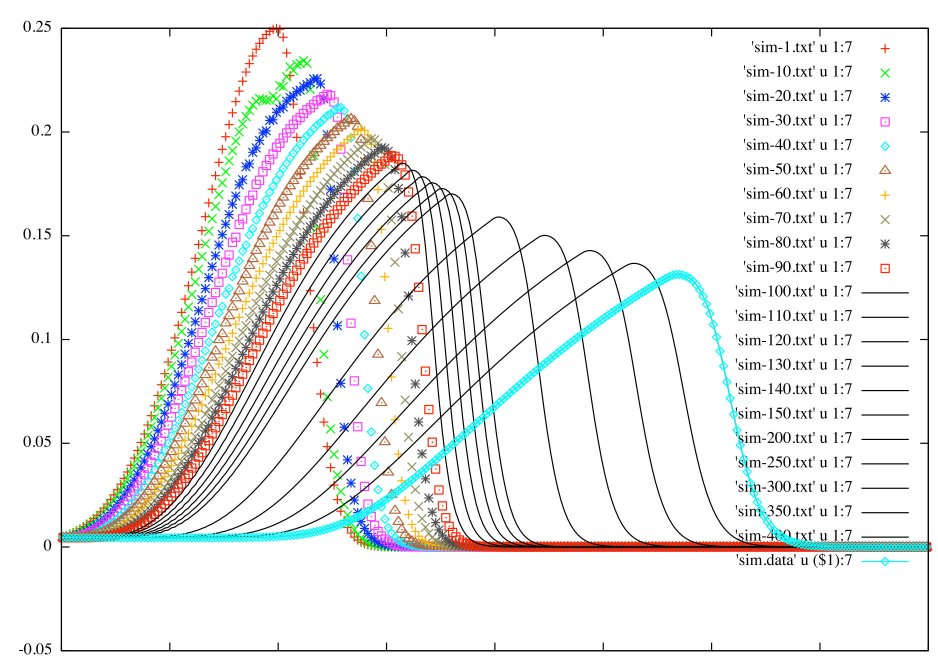

example: coupling of *Gerris* (St Venant Finite volumes) and erodible bed

Bilan IV

- Saint Venant is qualitatively good
- Shallow Water does not allow for dunes/ripples

find a better model to estimate the shear

Viscous effects are important near the wall

Perturbation of a shear flow Non linear resolution (with flow separation) possible

It is called Double Deck (Triple Deck)

Introduced by Neiland 69 Stewartson 69 Smith 80...

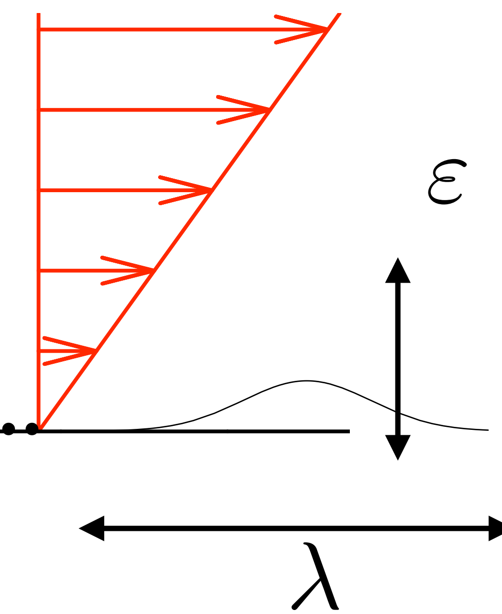

near the wall the velocity is small

$u \sim \varepsilon$

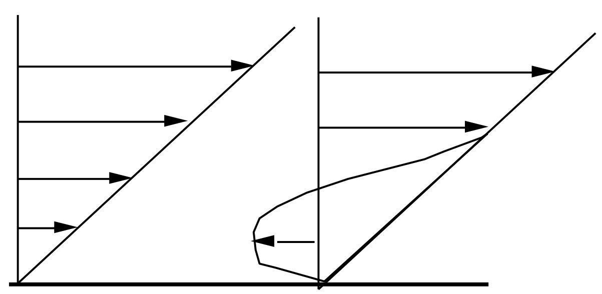

$\Delta u \sim \varepsilon$

convection-diffusion balance

$$u\frac{\partial u}{\partial x} \simeq \frac{1}{Re}\frac{\partial^2 u}{\partial y^2}$$

$$\frac{\varepsilon}{\lambda} = \frac{1}{Re}\frac{1}{\varepsilon^2}$$

size of the bump

$$\varepsilon^3 = \frac{\lambda}{Re}$$

Viscous effects are important near the wall
Perturbation of a shear flow Non linear resolution
(with flow separation) possible

It is called Double Deck (Triple Deck)
Introduced by Neiland 69 Stewartson 69 Smith 80...

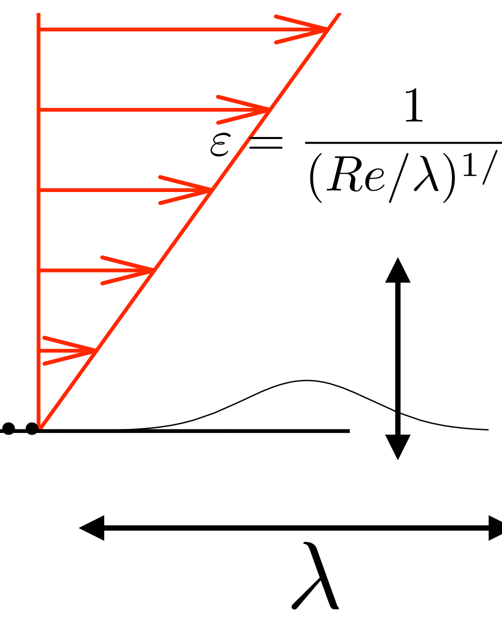

$$
\begin{aligned}
\frac{\partial}{\partial x}u + \frac{\partial}{\partial y}v &= 0, \\
u\frac{\partial}{\partial x}u + v\frac{\partial}{\partial y}u &= -\frac{d}{dx}p + \frac{\partial^2}{\partial y^2}u. \\
u(x, y = f(x)) &= 0, \qquad v(x, y = f(x)) = 0 \\
\& \qquad \lim_{y\to\infty} u(x, y) &= y.
\end{aligned}
$$

Prandtl equations with different BC

Viscous effects are important near the wall
Perturbation of a shear flow Non linear resolution (with flow separation) possible

It is called Double Deck (Triple Deck)
Introduced by Neiland 69 Stewartson 69 Smith 80...

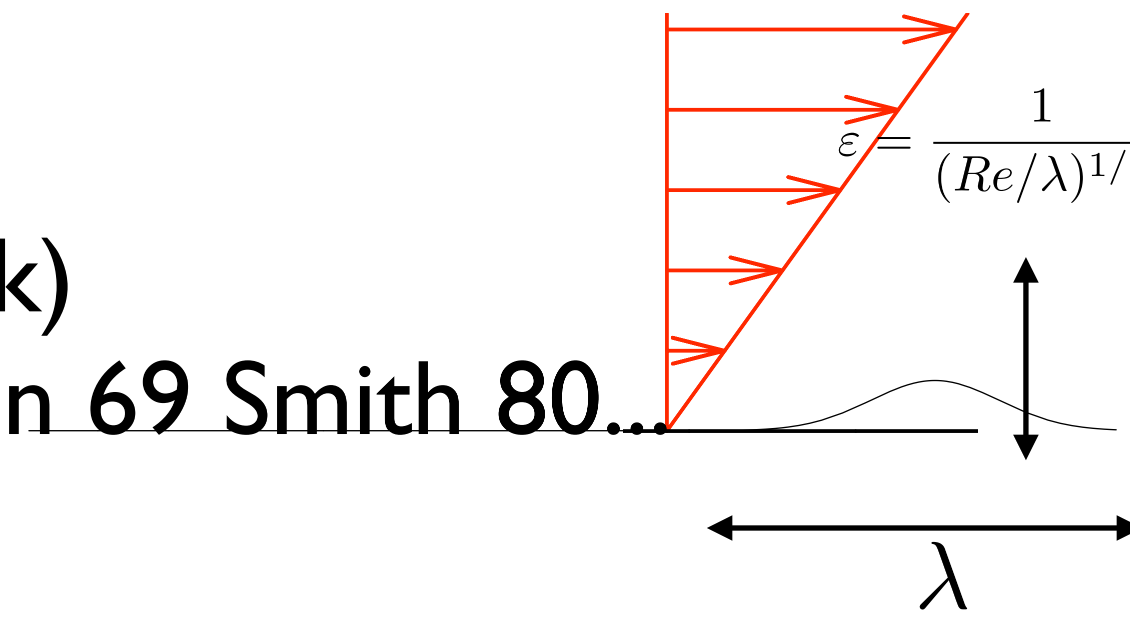

$$
\begin{aligned}
\frac{\partial}{\partial x}u + \frac{\partial}{\partial y}v &= 0, \\
u\frac{\partial}{\partial x}u + v\frac{\partial}{\partial y}u &= -\frac{d}{dx}p + \frac{\partial^2}{\partial y^2}u. \\
u(x, y = f(x)) &= 0, \qquad v(x, y = f(x)) = 0 \\
\& \qquad \lim_{y\to\infty} u(x, y) &= y.
\end{aligned}
$$

we linearize

$$u = y + u_1 \quad v = v_1$$

Viscous effects are important near the wall

Perturbation of a shear flow Non linear resolution (with flow separation) possible

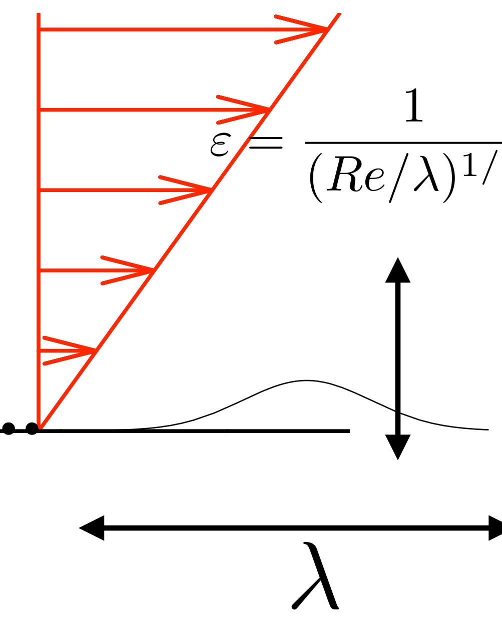

It is called Double Deck (Triple Deck)

Introduced by Neiland 69 Stewartson 69 Smith 80...

$$
\begin{aligned}
\frac{\partial}{\partial x}u + \frac{\partial}{\partial y}v &= 0, \\
u\frac{\partial}{\partial x}u + v\frac{\partial}{\partial y}u &= -\frac{d}{dx}p + \frac{\partial^2}{\partial y^2}u. \\
u(x, y = f(x)) &= 0, \qquad v(x, y = f(x)) = 0 \\
\& \qquad \lim_{y\to\infty} u(x, y) &= y.
\end{aligned}
$$

we linearize

$$u = y + u_1 \quad v = v_1$$

we look at solution in Fourier space

$$u_1 \to e^{-ikx}\hat{u}_1(y)$$

Viscous effects are important near the wall

Perturbation of a shear flow Non linear resolution (with flow separation) possible

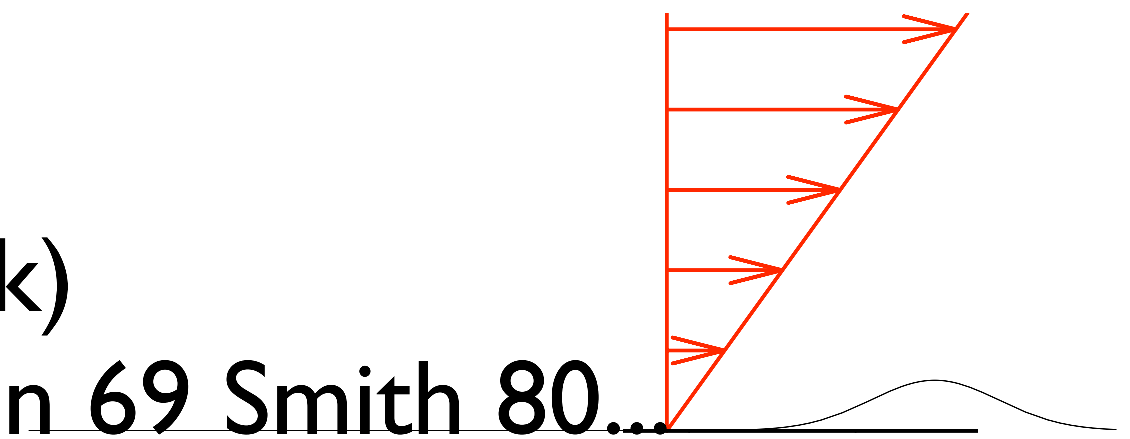

It is called Double Deck (Triple Deck)

Introduced by Neiland 69 Stewartson 69 Smith 80...

linear solution

$$\begin{cases} -ik\hat{u}_1 + \dfrac{\partial \hat{v}_1}{\partial y} = 0, \\ -iky\hat{u}_1 + \hat{v}_1 = ik\hat{p}_1 \quad + \dfrac{\partial^2 \hat{u}_1}{\partial y^2}, \end{cases}$$

$$u_1 \to e^{-ikx}\hat{u}_1(y)$$

Viscous effects are important near the wall

Perturbation of a shear flow Non linear resolution (with flow separation) possible

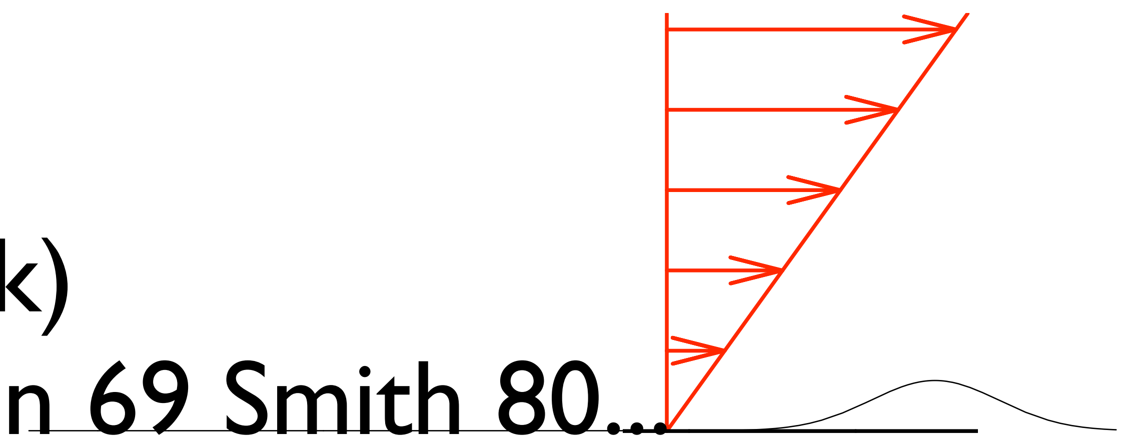

It is called Double Deck (Triple Deck)

Introduced by Neiland 69 Stewartson 69 Smith 80...

linear solution

$$\begin{cases} -ik\hat{u}_1 + \dfrac{\partial \hat{v}_1}{\partial y} = 0, \\ -iky\hat{u}_1 + \hat{v}_1 = ik\hat{p}_1 \quad + \dfrac{\partial^2 \hat{u}_1}{\partial y^2}, \end{cases}$$

$$\downarrow$$

$$-iky\hat{\tau}_1 = \frac{\partial^2 \hat{\tau}_1}{\partial y^2} \longrightarrow Ai((-ik)^{1/3} y)$$

Viscous effects are important near the wall
Perturbation of a shear flow Non linear resolution (with flow separation) possible

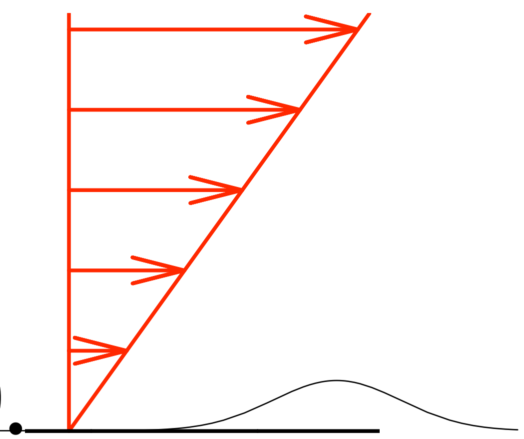

It is called Double Deck (Triple Deck)
Introduced by Neiland 69 Stewartson 69 Smith 80.

linear solution

in terms of Airy function

$$Ai((-ik)^{1/3}y)$$

this gives the final “exact” linear solution

$$\tau = \mu U_0'(\bar{U}_S'(1+(\frac{U_0'}{\nu\lambda})^{1/3}H\tilde{c})), \text{with } \tilde{c} = FT^{-1}[FT[\tilde{f}]3Ai(0)(-(i2\pi\tilde{k})\bar{U}_S')^{1/3}]$$

Viscous effects are important near the wall

Perturbation of a shear flow Non linear resolution (with flow separation) possible

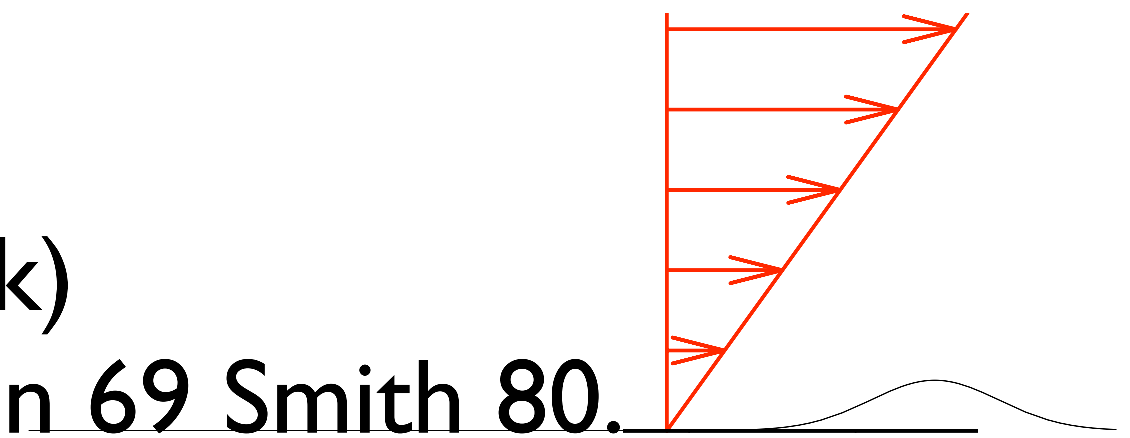

It is called Double Deck (Triple Deck)

Introduced by Neiland 69 Stewartson 69 Smith 80.

linear solution

in terms of Airy function

this gives the final "exact" linear solution

$$\tau = \mu U_0'(\bar{U}_S'(1 + (\frac{U_0'}{\nu\lambda})^{1/3} H\tilde{c})), \text{with } \tilde{c} = FT^{-1}[FT[\tilde{f}]3Ai(0)(-(i2\pi\tilde{k})\bar{U}_S')^{1/3}]$$

very similar to Fowler / Azerad Bouharguane

$$\frac{\partial^{1/3}}{\partial x^{1/3}} \qquad \int_0^\infty \frac{f'(x-\xi)}{\xi^{1/3}} d\xi$$

We have defined a linear solution of the response of a flow to topography

We are able to compute the shear stress

Shear Stress is important for sedimentation

let us test it on an erodible bed

Completely erodible soil, Linear Stability

Solution of

$$\tau = TF^{-1}[(3Ai(0))(-ik)^{1/3}TF[f]]$$
$$l_s\frac{\partial q}{\partial x} + q = \varpi(\tau - \tau_s - \Lambda\frac{\partial f}{\partial x})$$
$$\frac{\partial f}{\partial t} = -\frac{\partial q}{\partial x}$$

this is a model problem, not the reality
BUT it gives some ideas, and is qualitatively consistent
with the experiments

Completely erodible soil, Linear Stability

$Re(\sigma(k))$

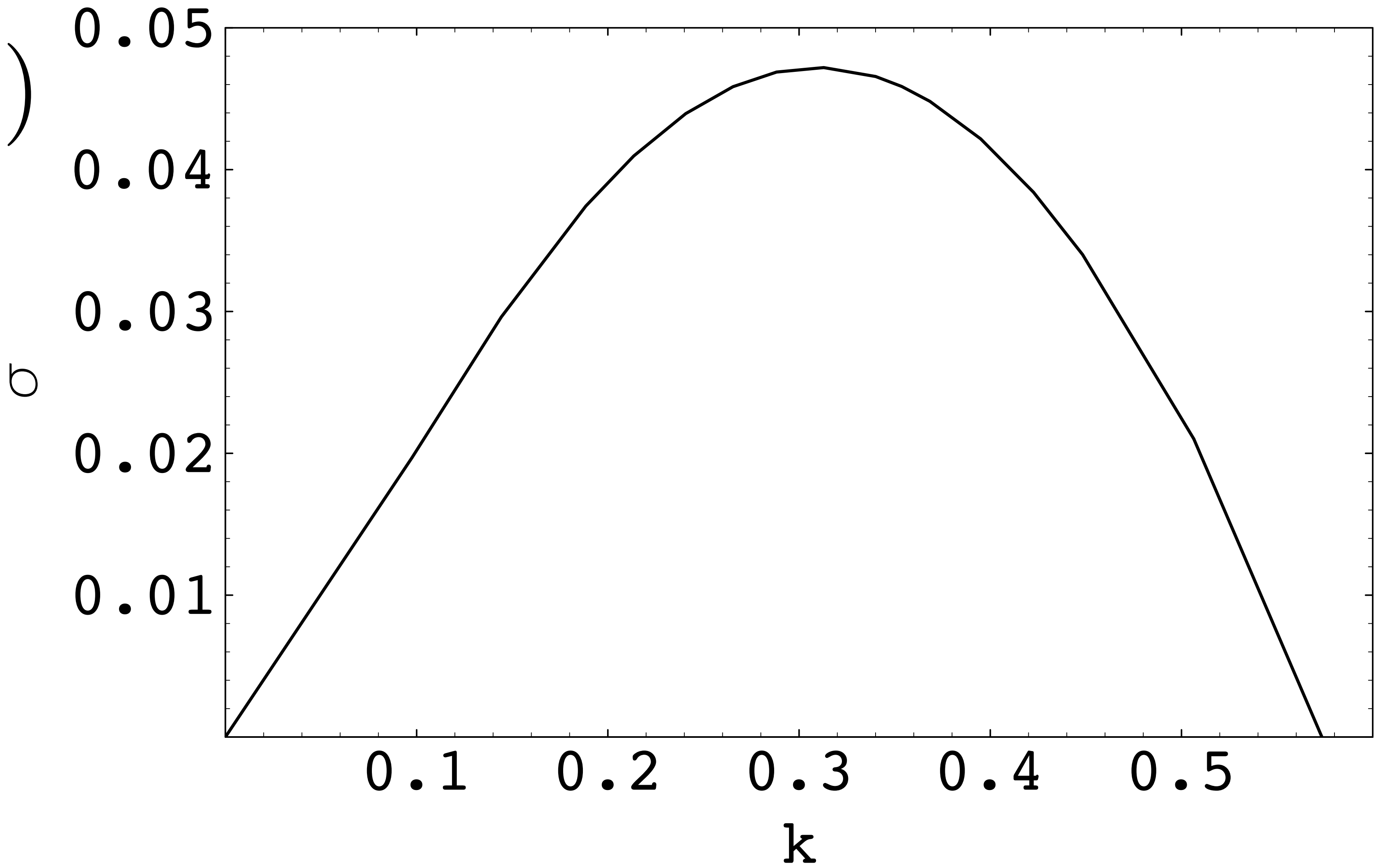

$$e^{\sigma t - ikx}$$

$\Lambda = 0,\ l_s$ increases

$$\tau = TF^{-1}[(3Ai(0))(-ik)^{1/3}TF[f]]$$

$$l_s \frac{\partial q}{\partial x} + q = \varpi(\tau - \tau_s - \Lambda \frac{\partial f}{\partial x})$$

$$\frac{\partial f}{\partial t} = -\frac{\partial q}{\partial x}$$

Fourier

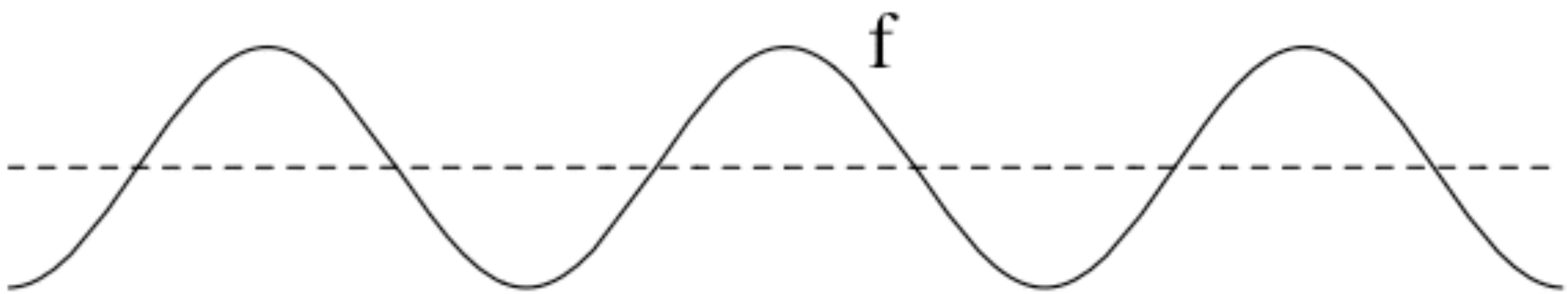

$$e^{\sigma t - ikx}$$

$$Re(\sigma(k))$$

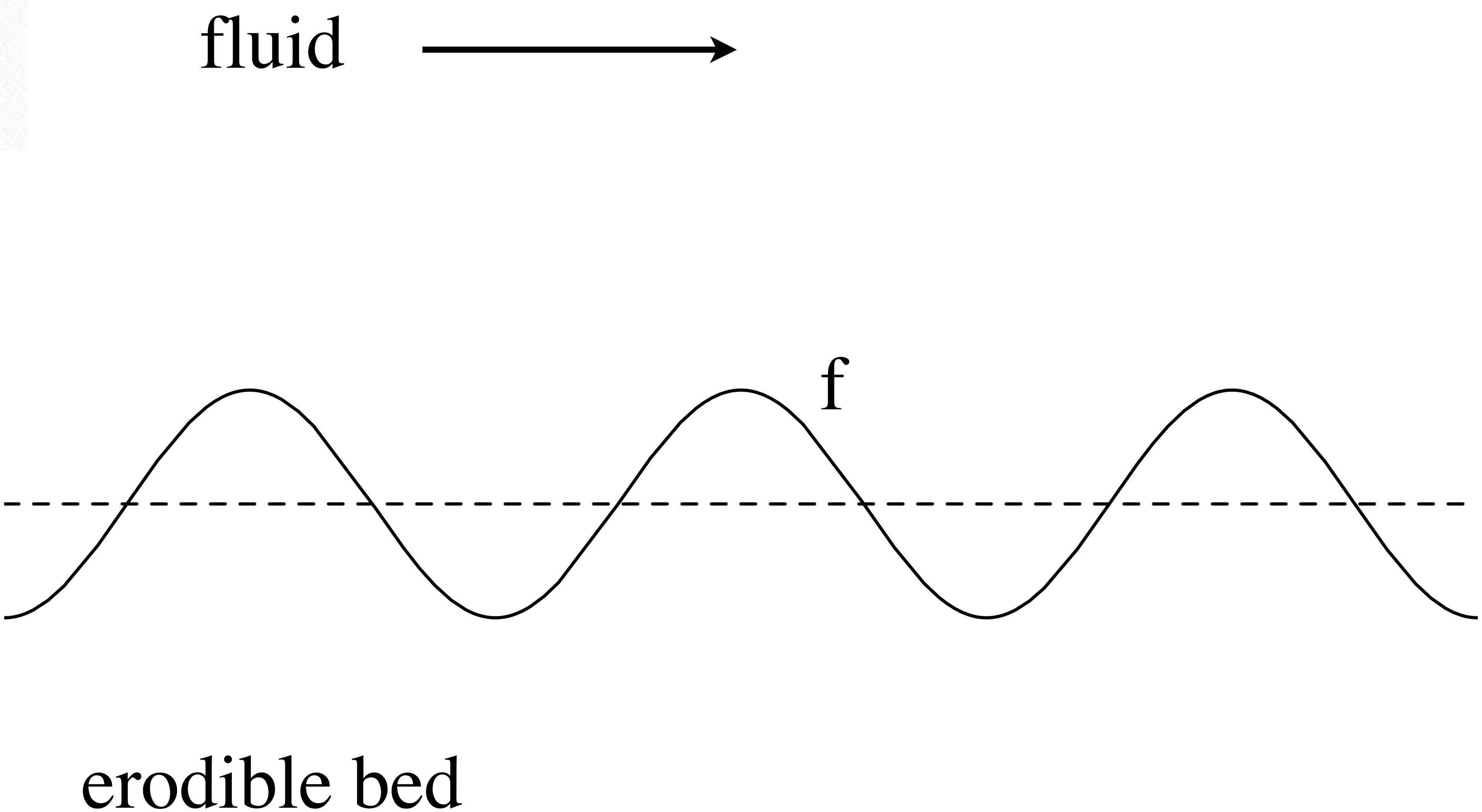
fluid
f
erodible bed

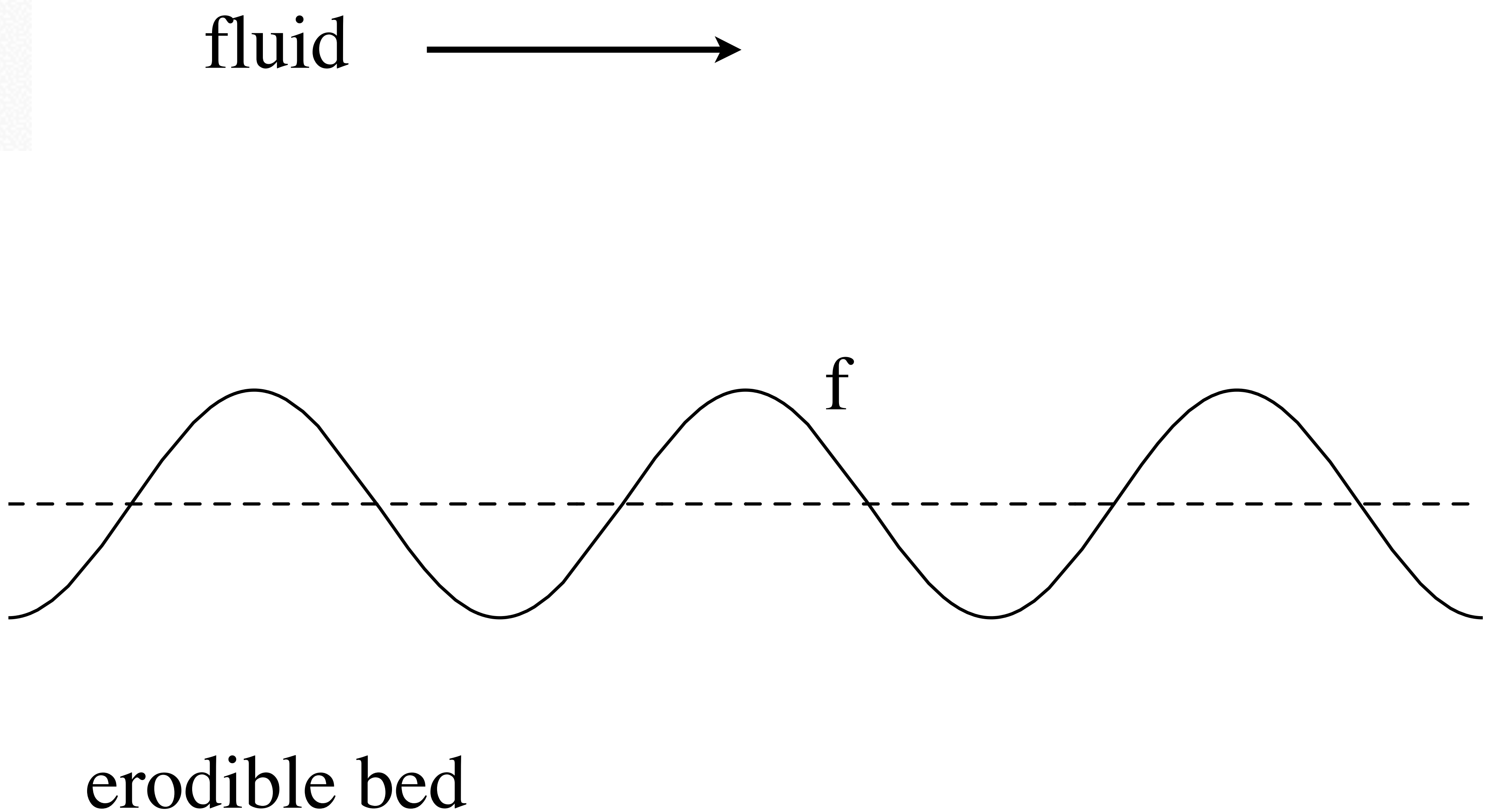

the bed

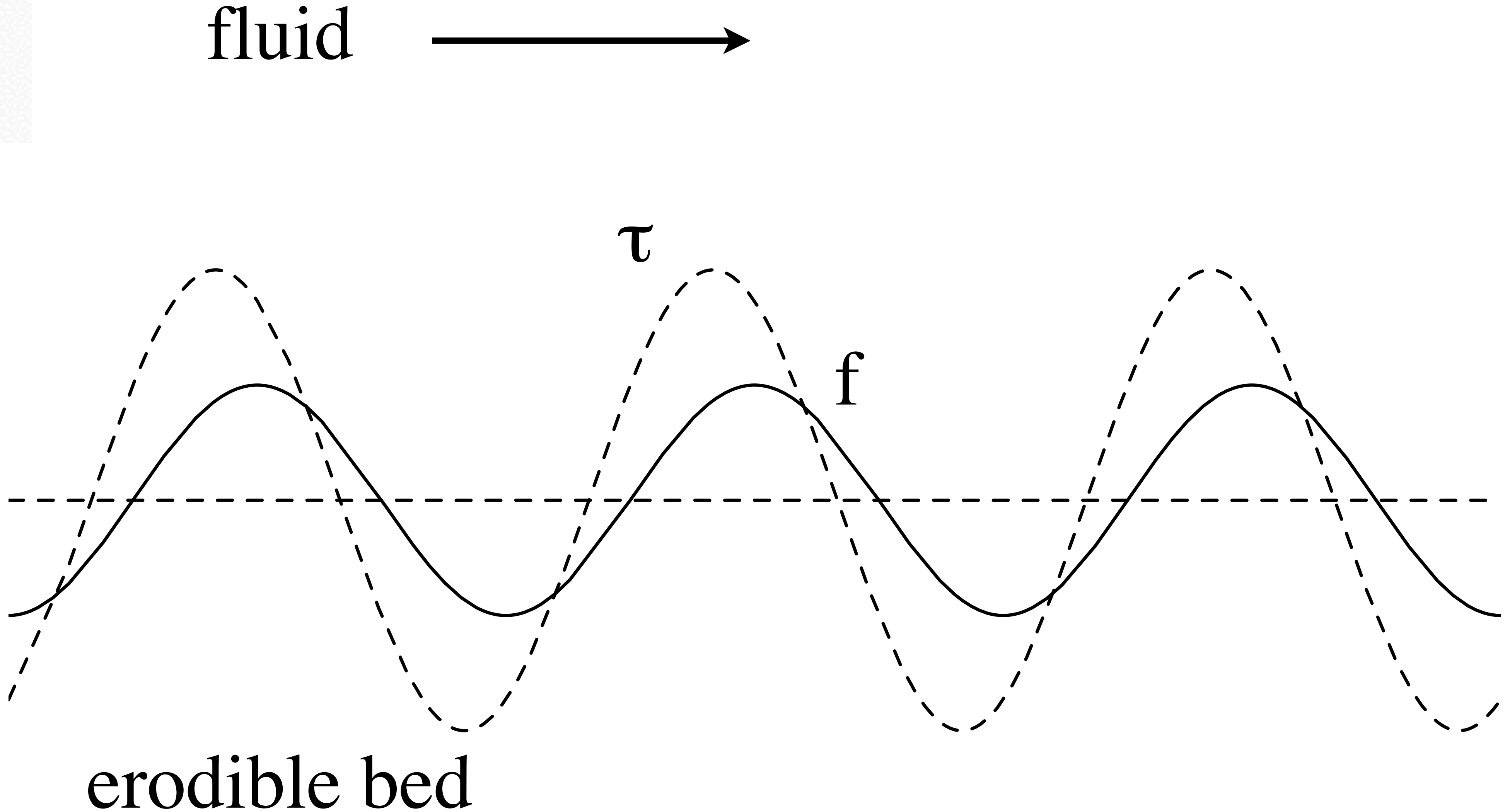

the bed The shear stress

fluid

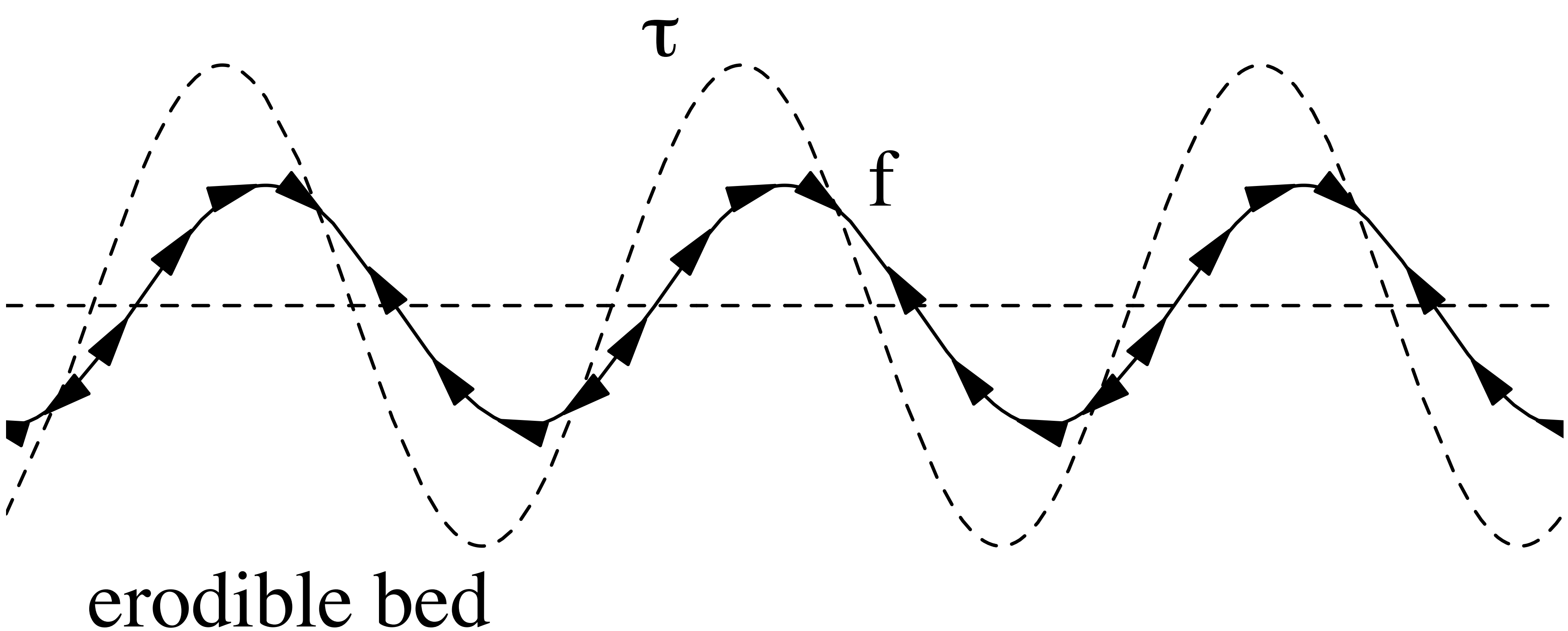

the bed The shear stress

The flux

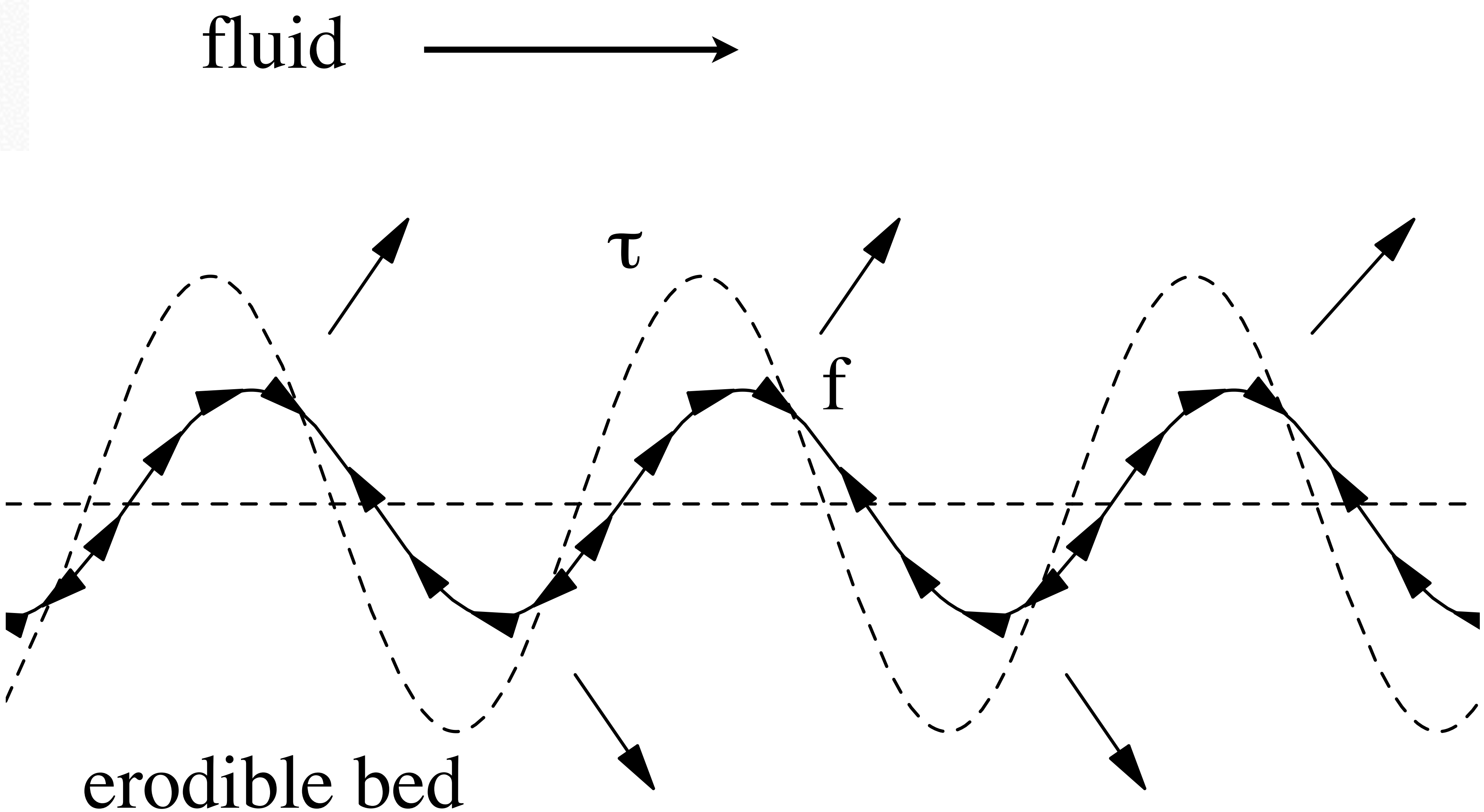

flux is positive after the top of the ripple

increase of the shear stress

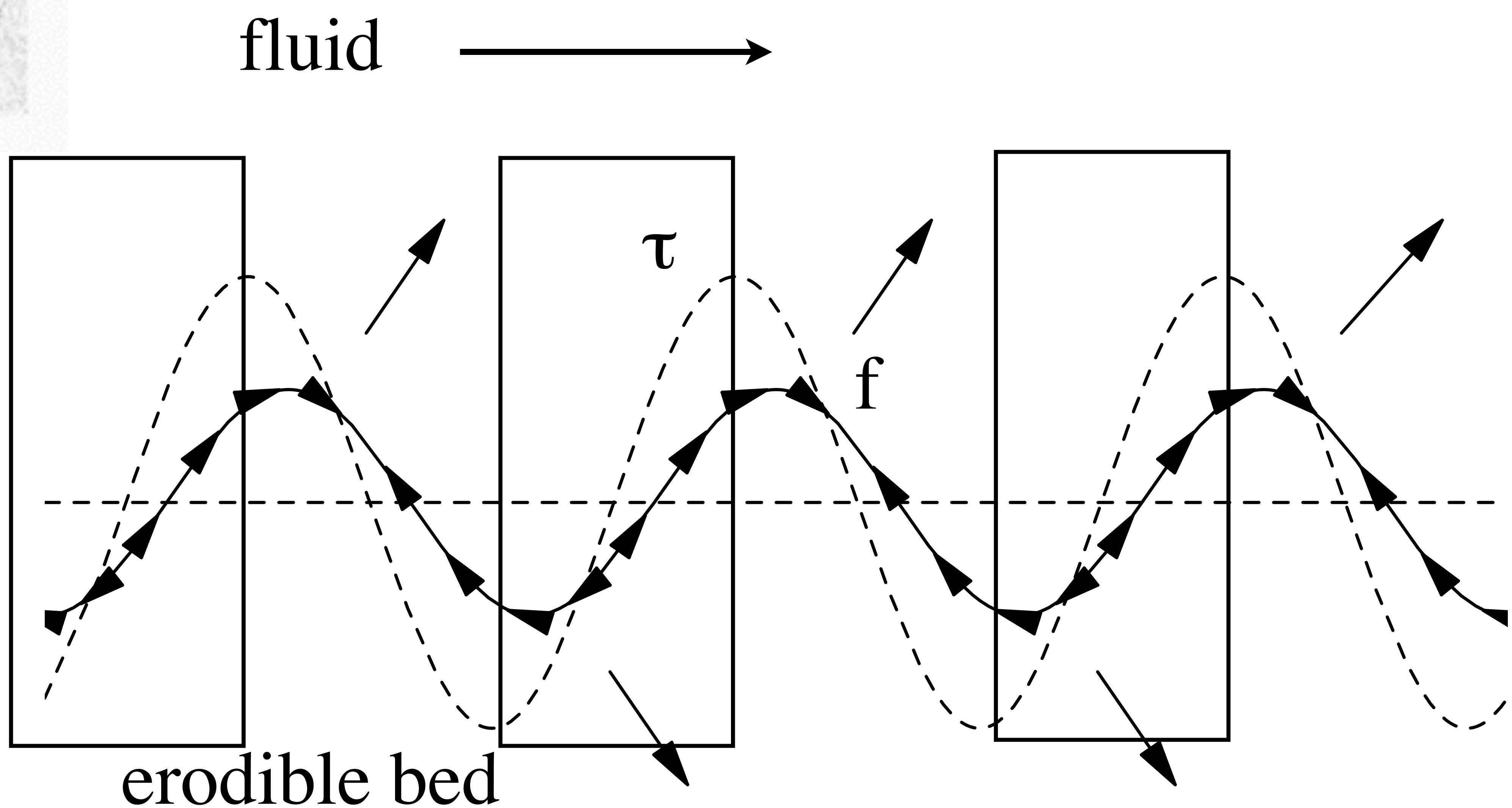

flux is positive after the top of the ripple

increase of the shear stress

erosion

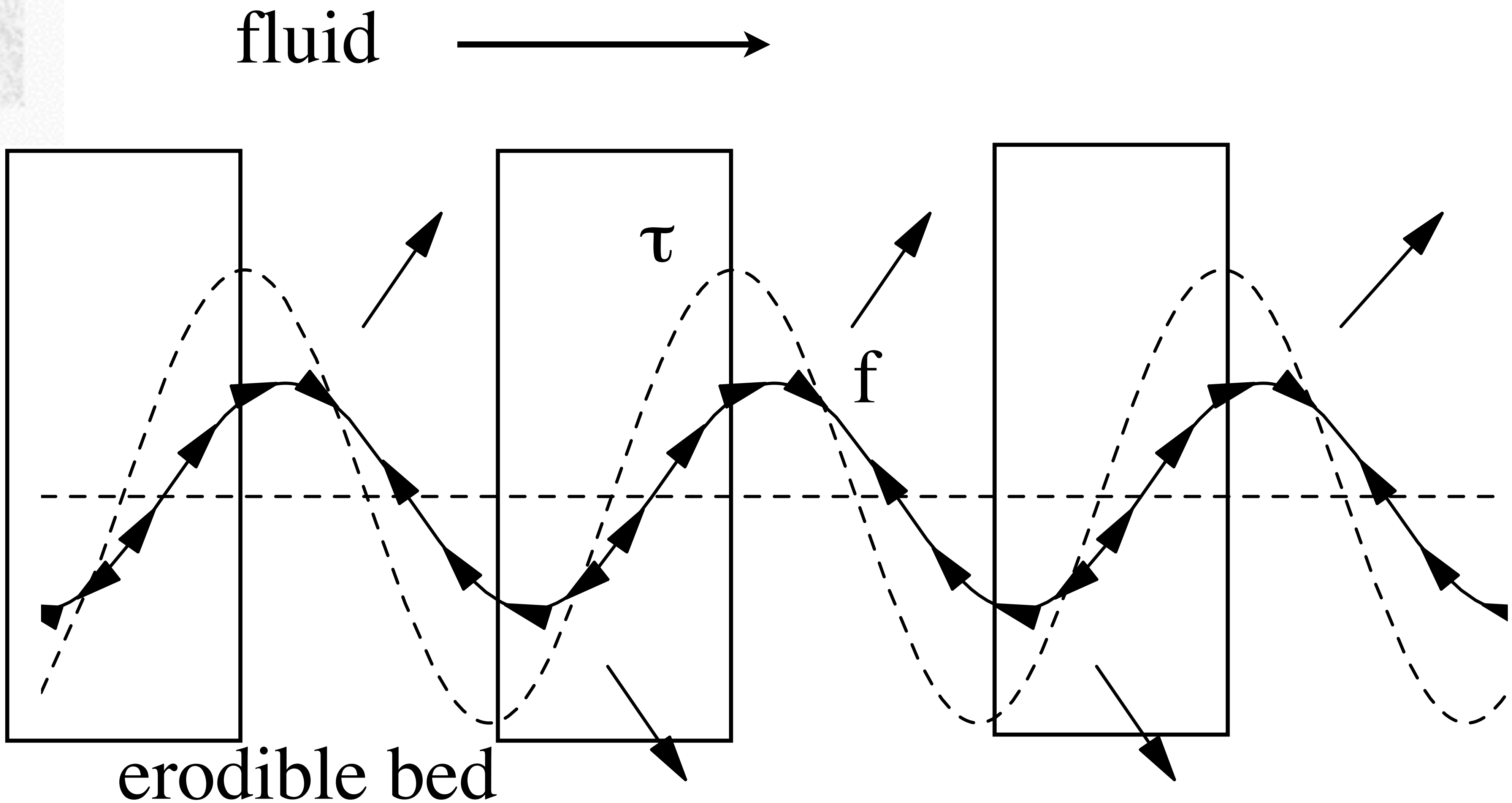

flux is positive after the top of the ripple

increase of the shear stress

erosion

decrease of the shear stress

fluid

deposition

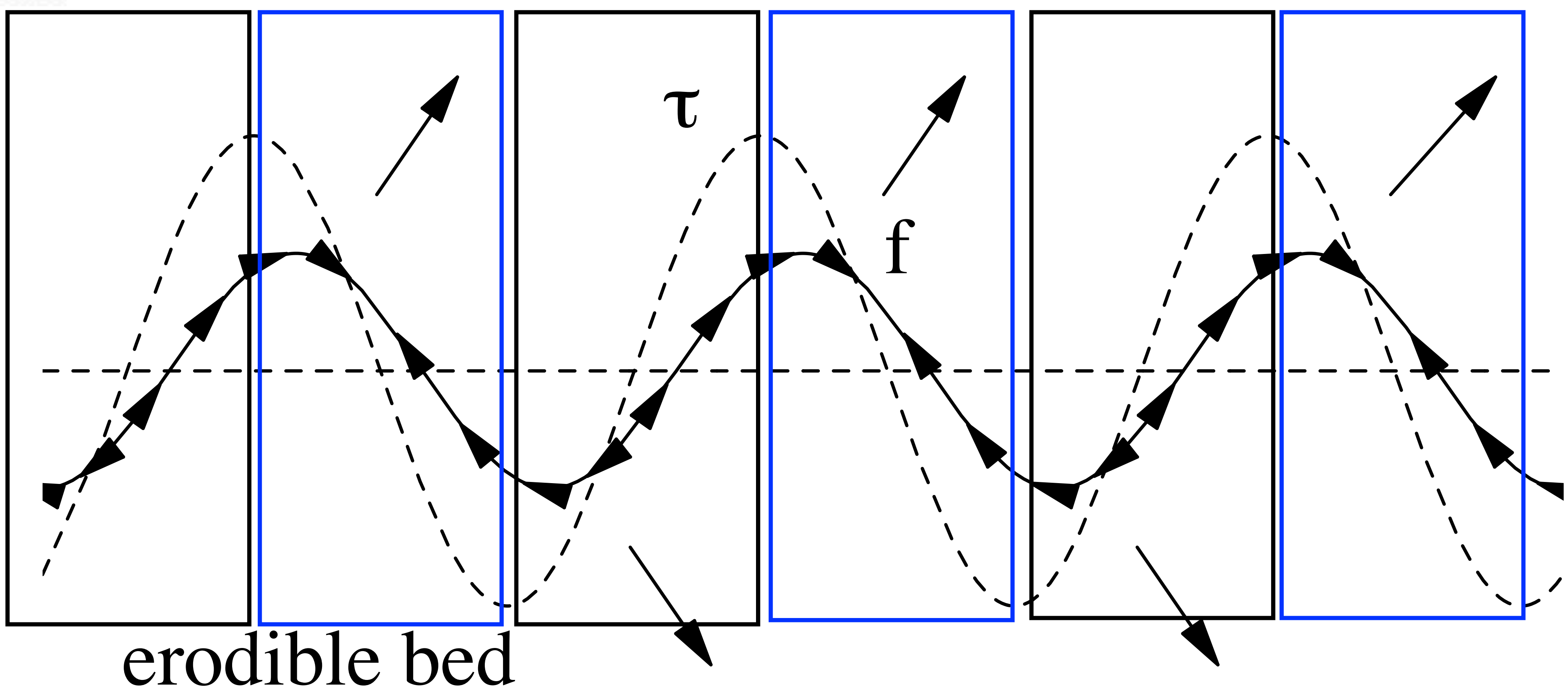

flux is positive after the top of the ripple

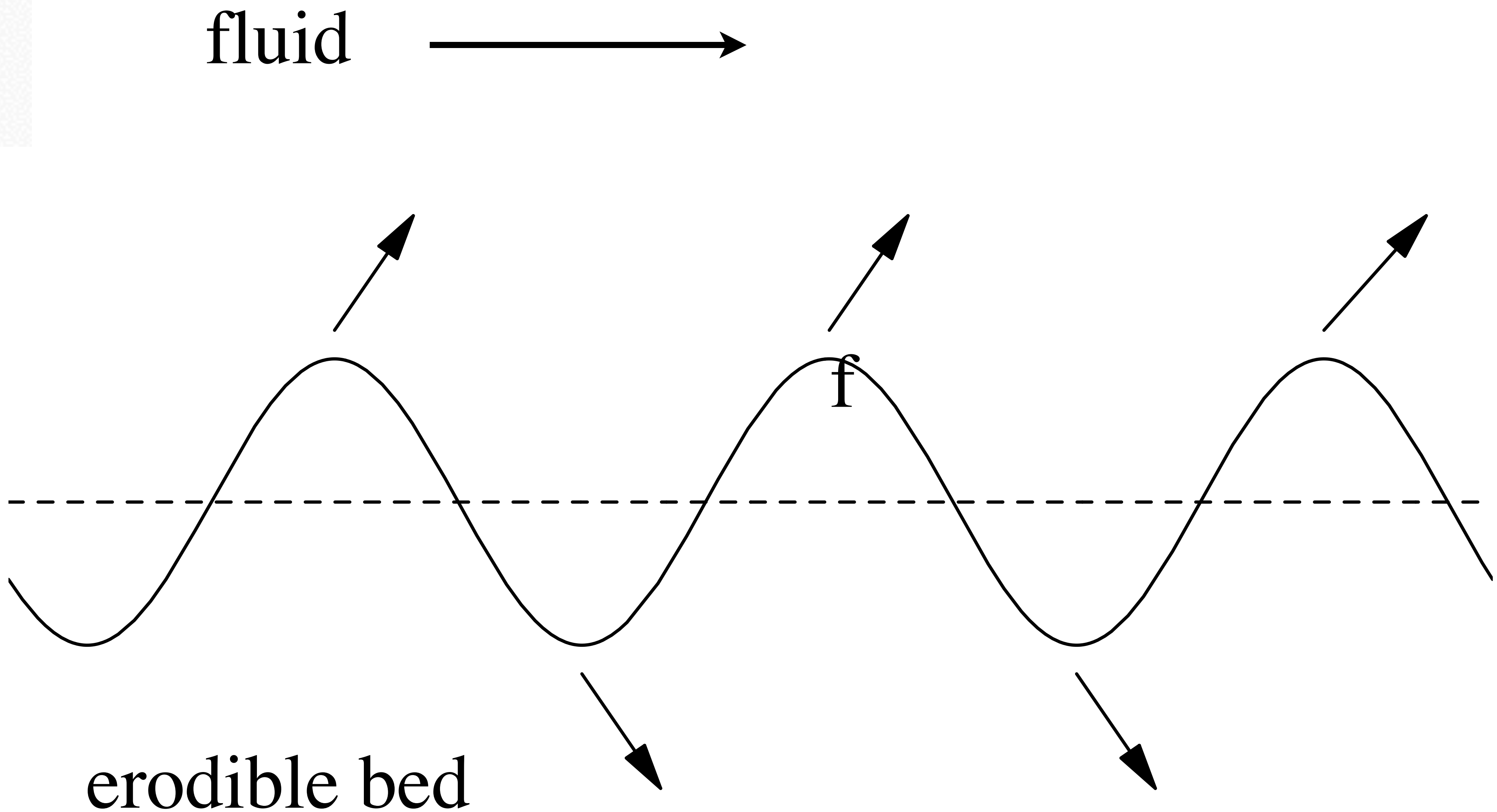
fluid
f
erodible bed

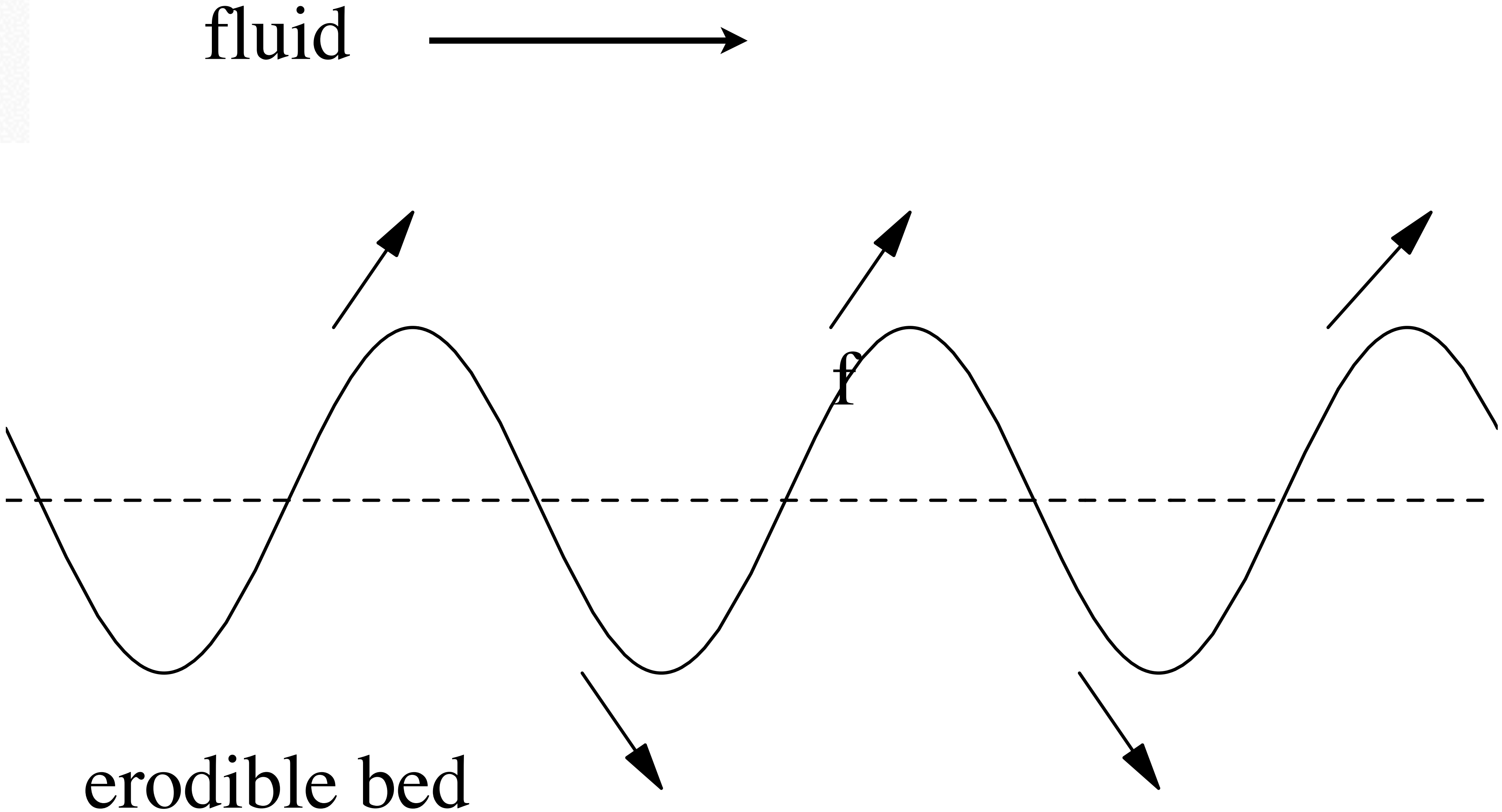

This is an instability

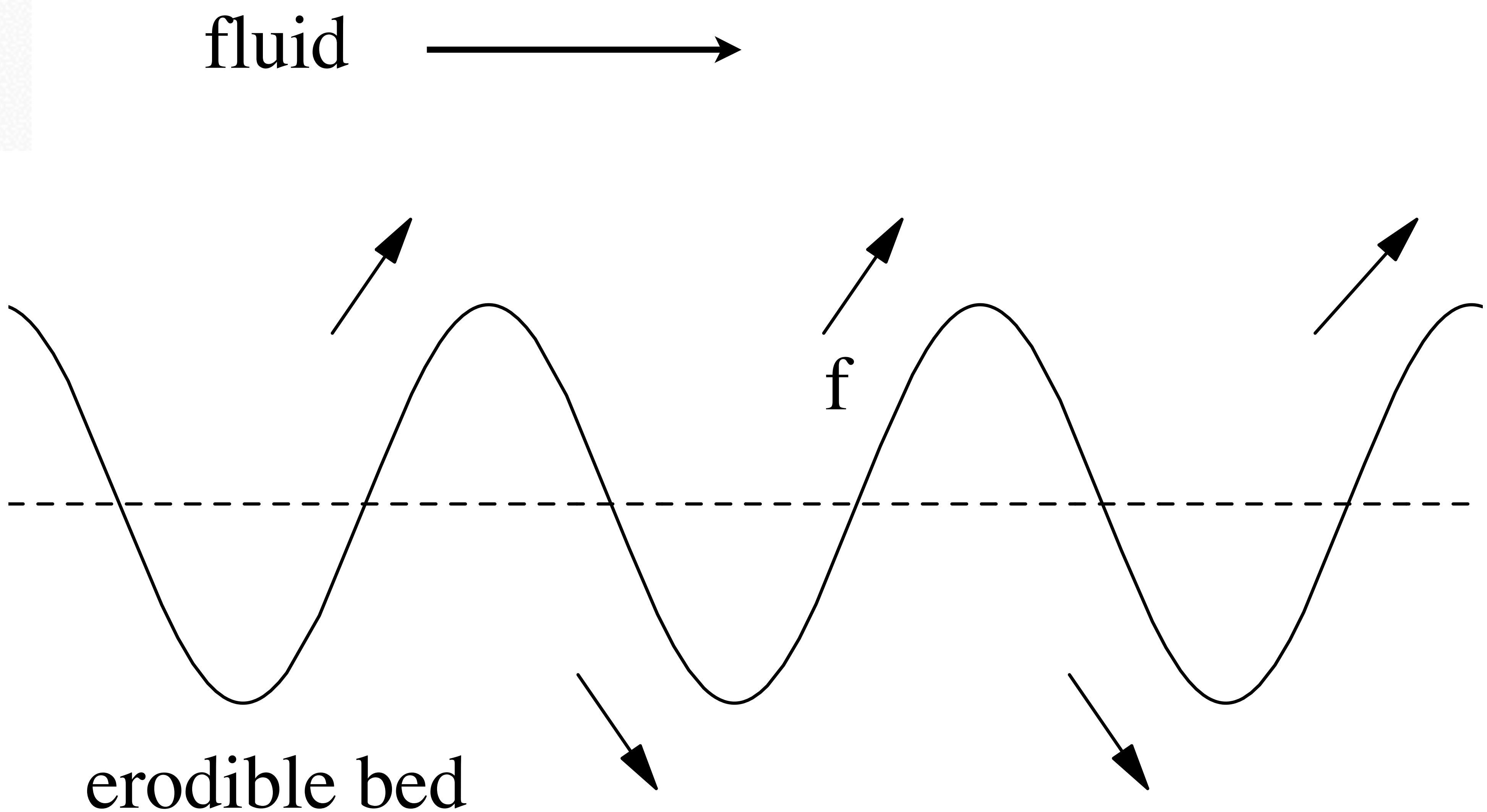

This is an instability

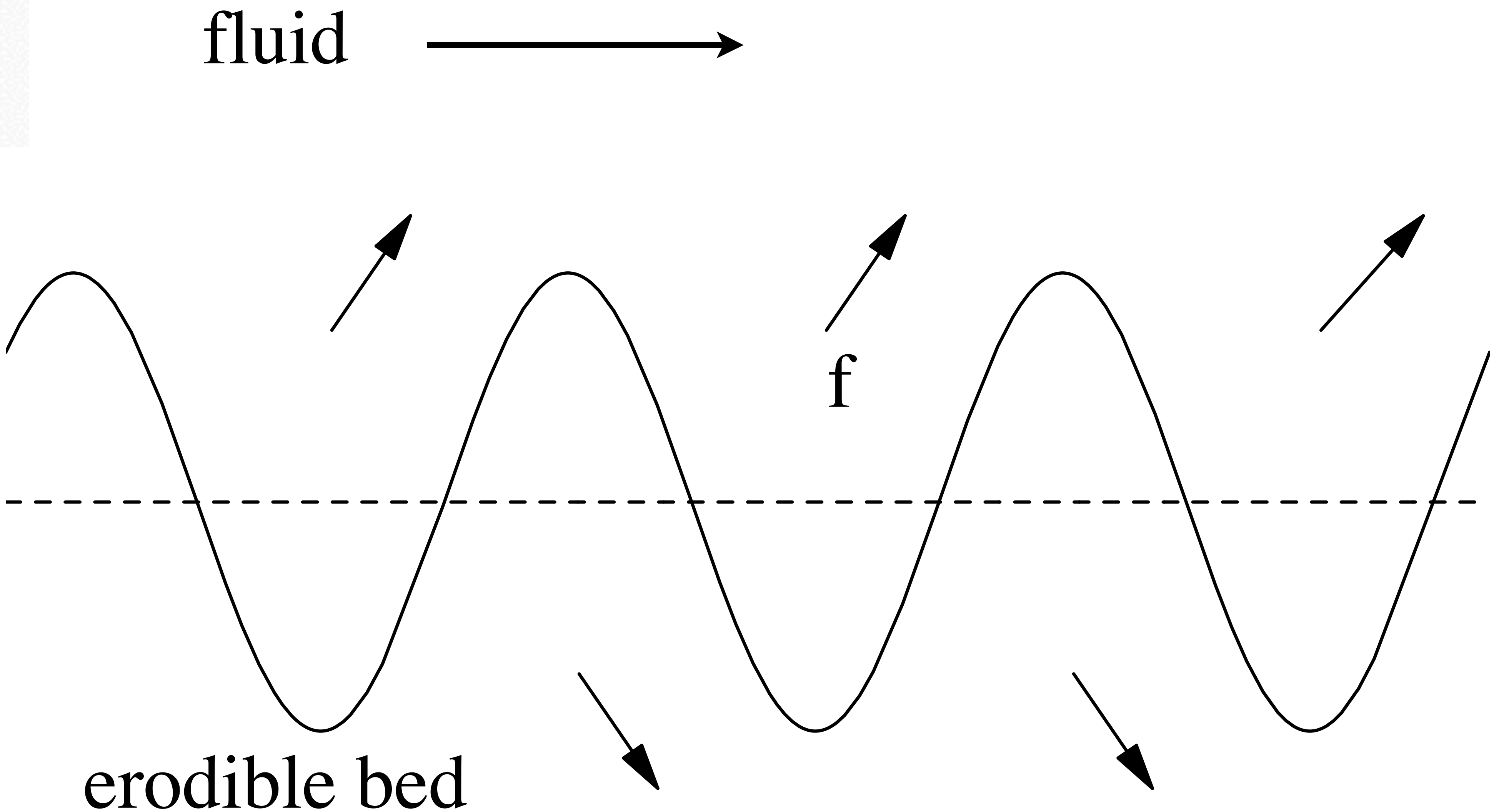

This is an instability

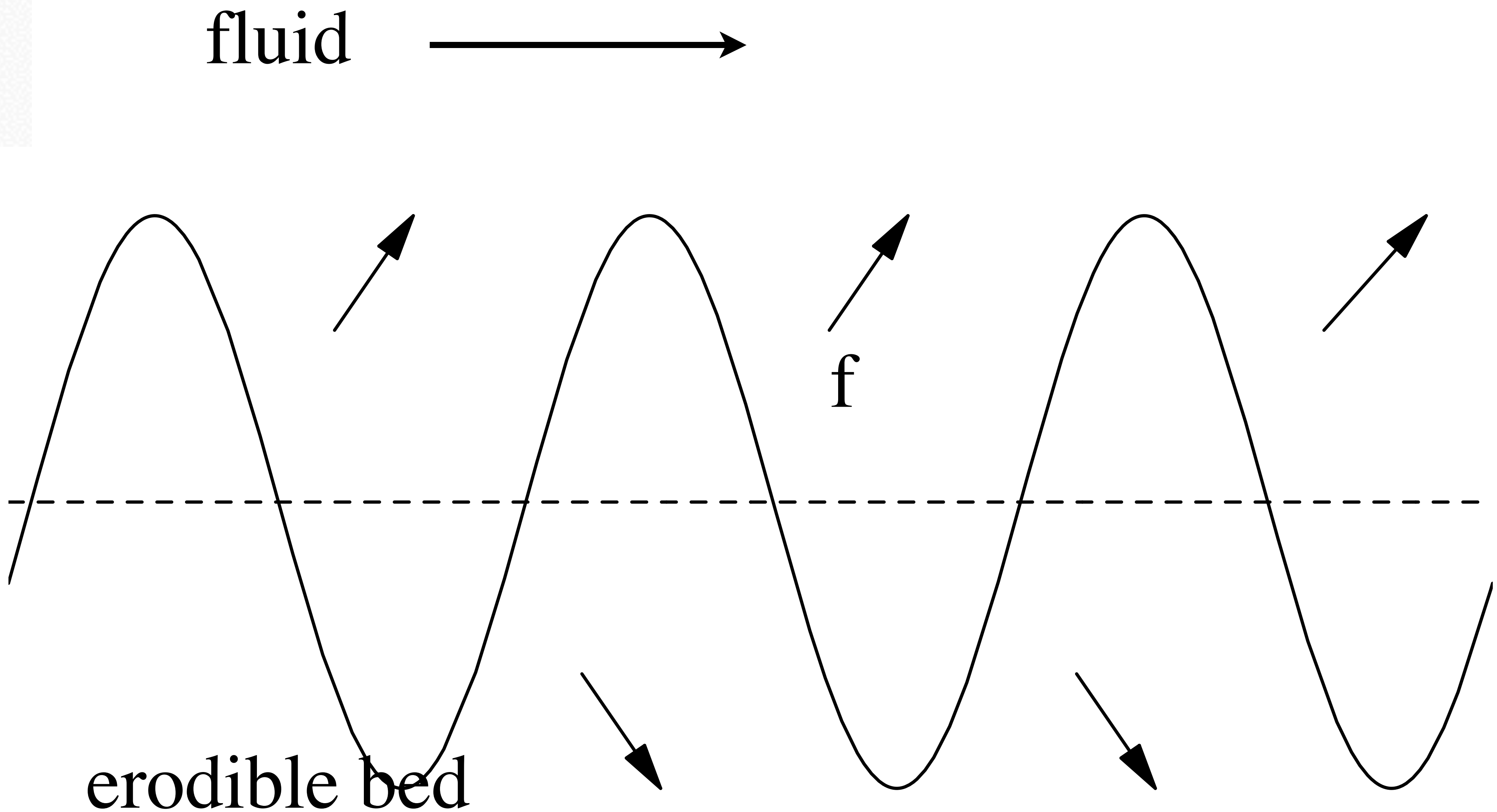

This is an instability

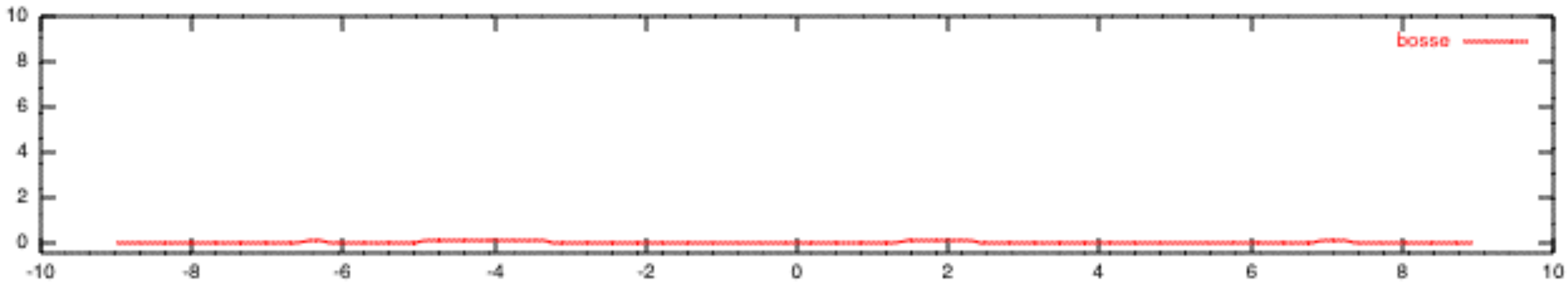

numerical simulation FFT

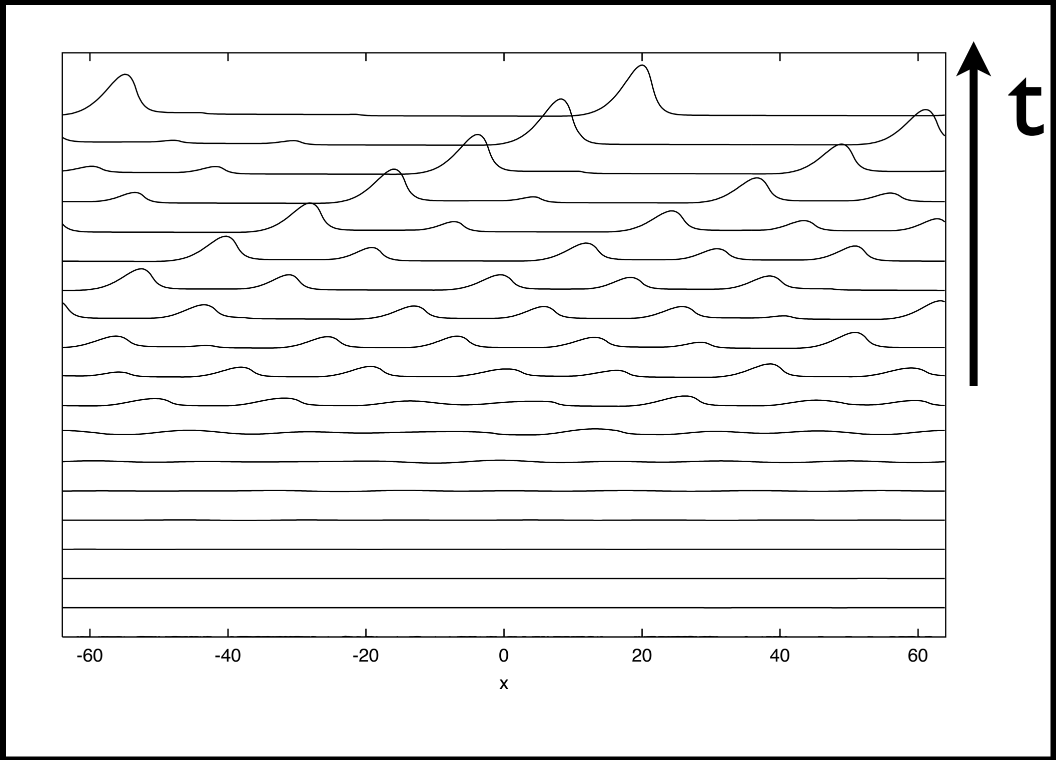

t
-60
-40
-20
0
20
40
60
x

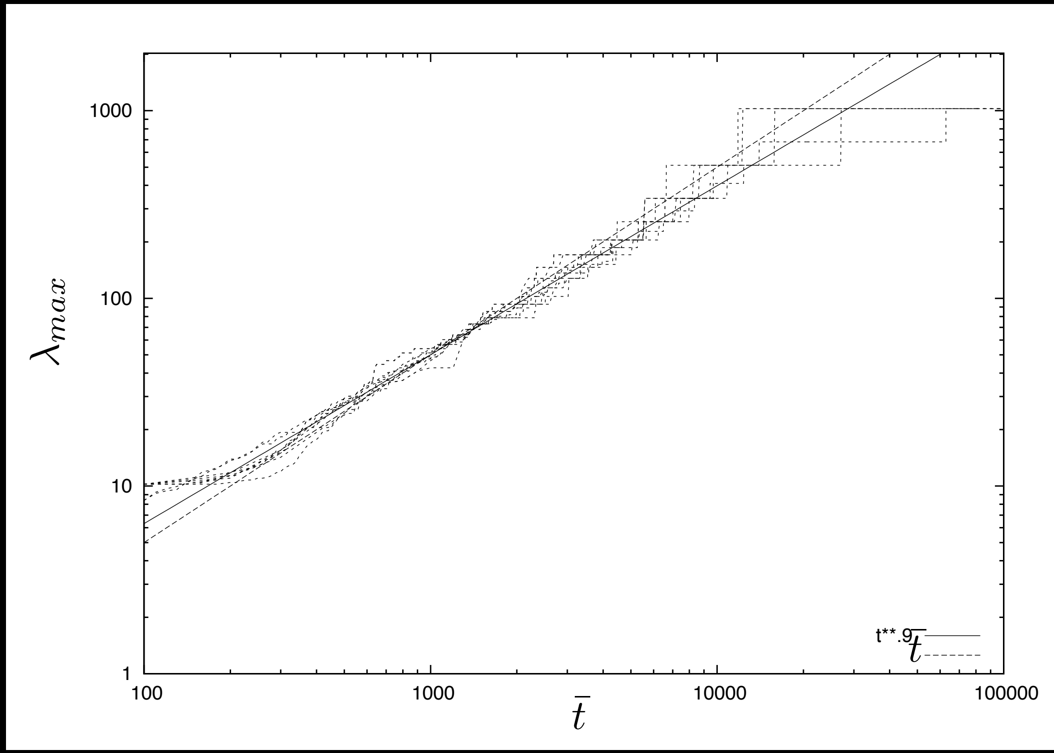

λ_{max}
1000
100
10
1
100
1000
10000
100000
$\bar{t}$
t**.9
$\bar{t}$

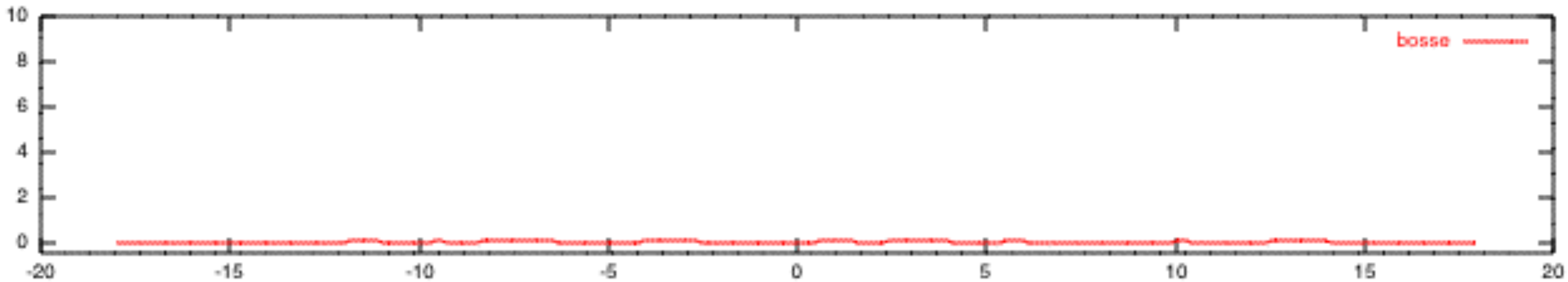

bosse
10
8
6
4
2
0
-20
-15
-10
-5
0
5
10
15
20

coarsening

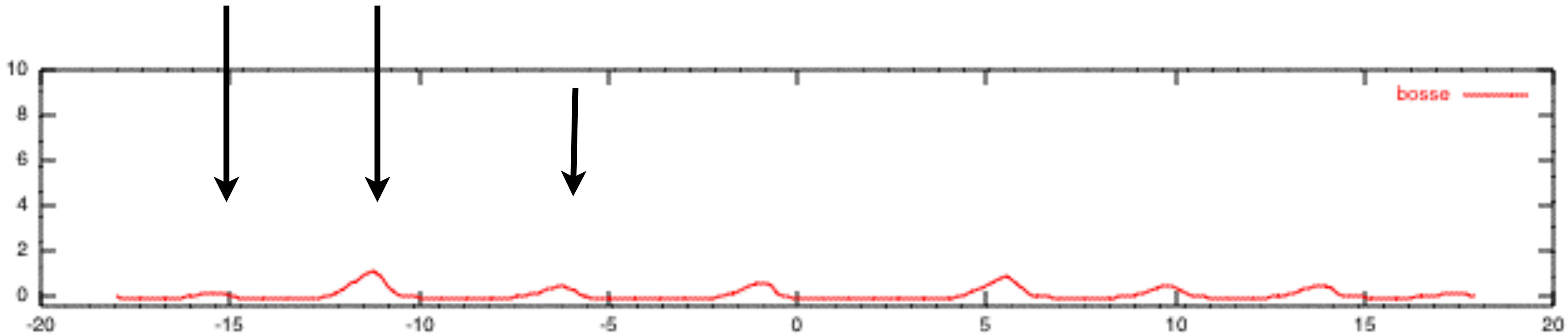

coarsening

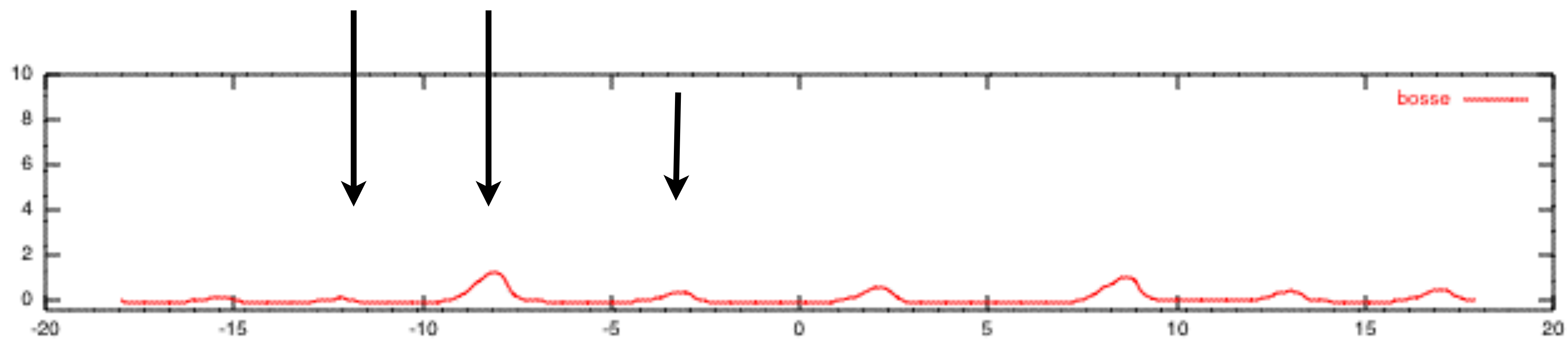

coarsening

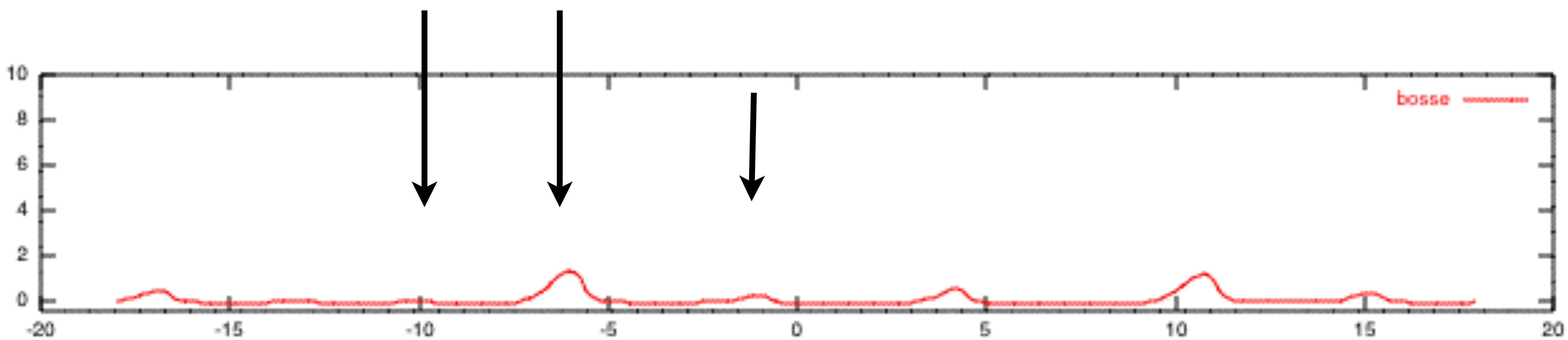

coarsening

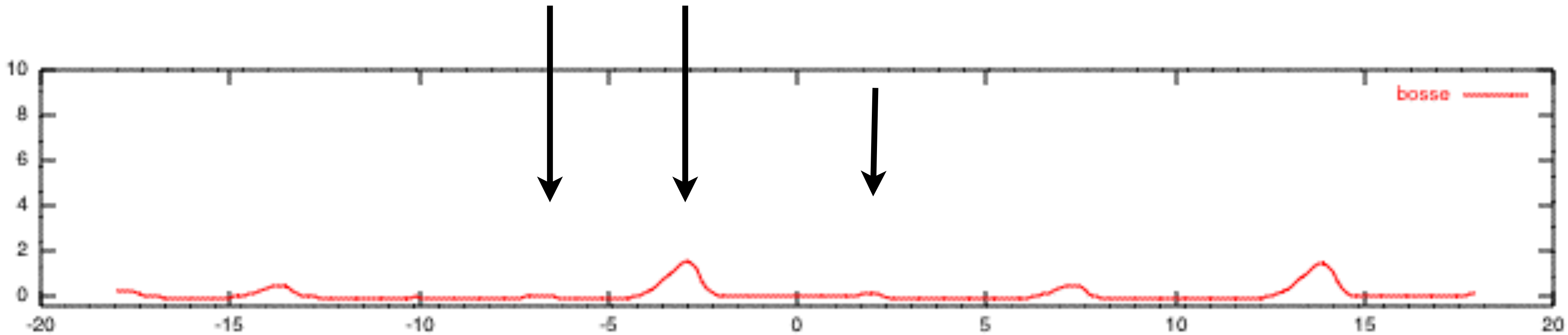

coarsening

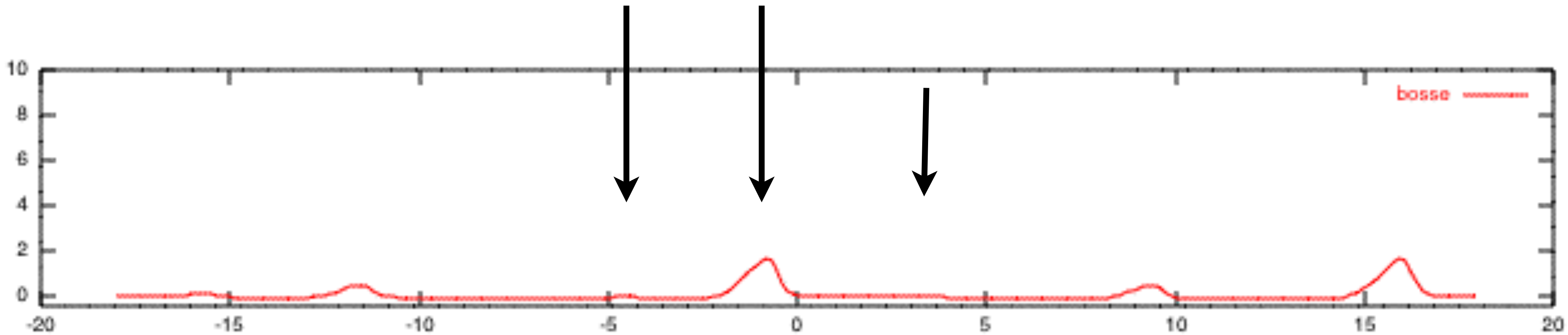

coarsening

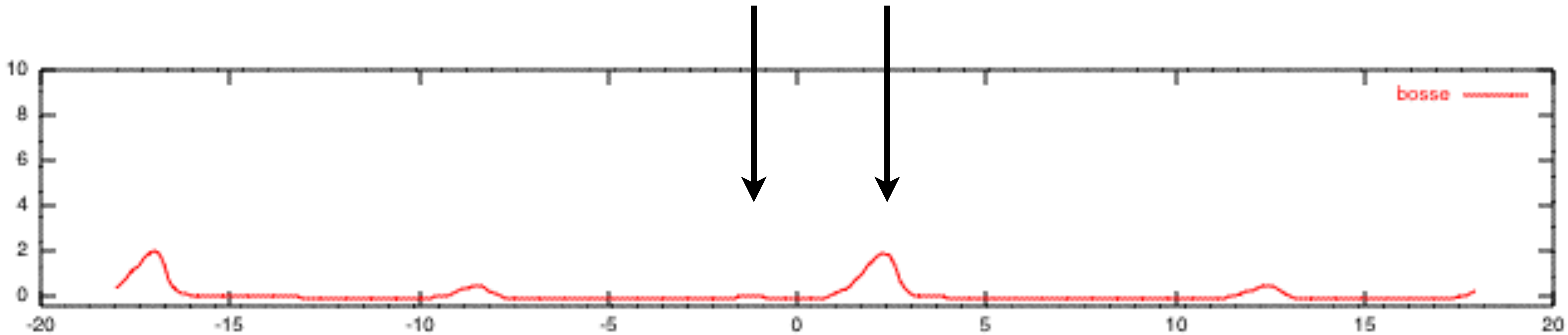

coarsening

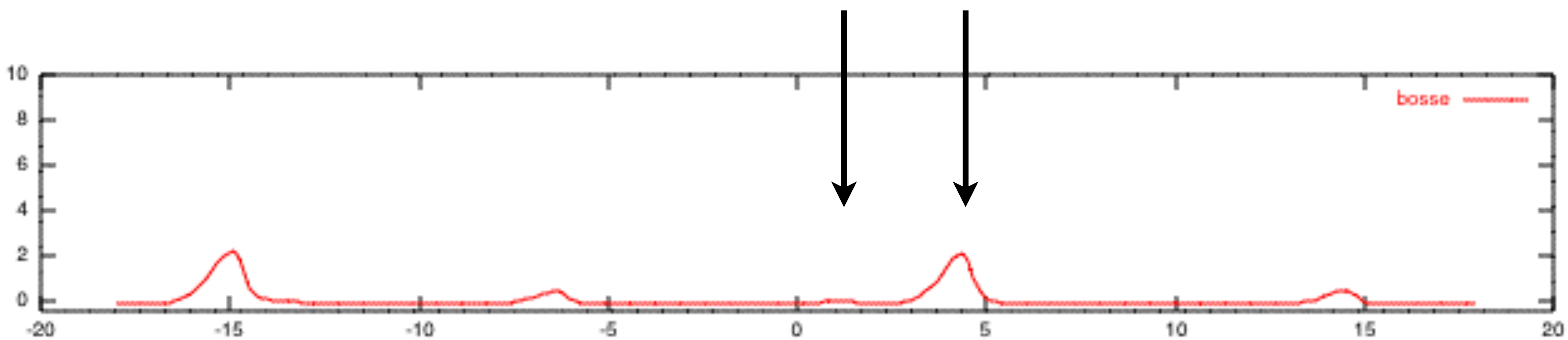

coarsening

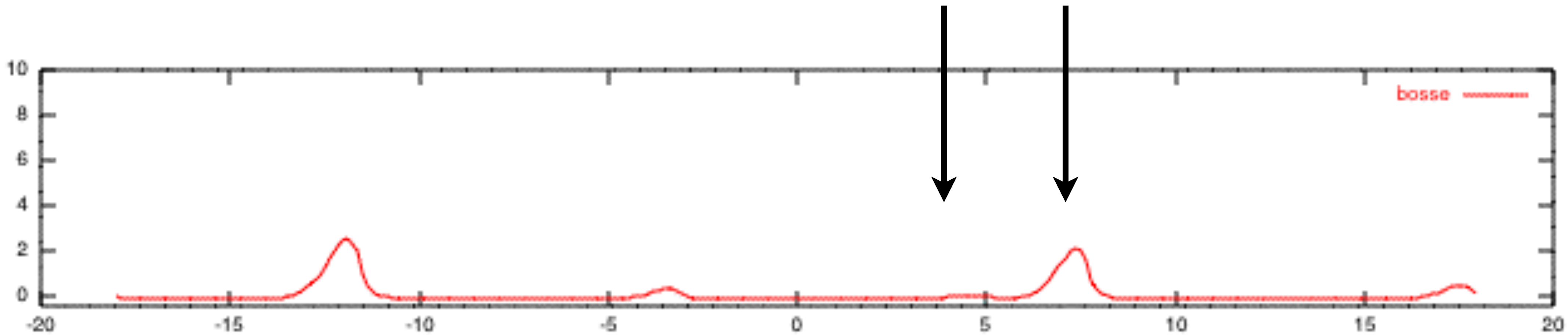

coarsening

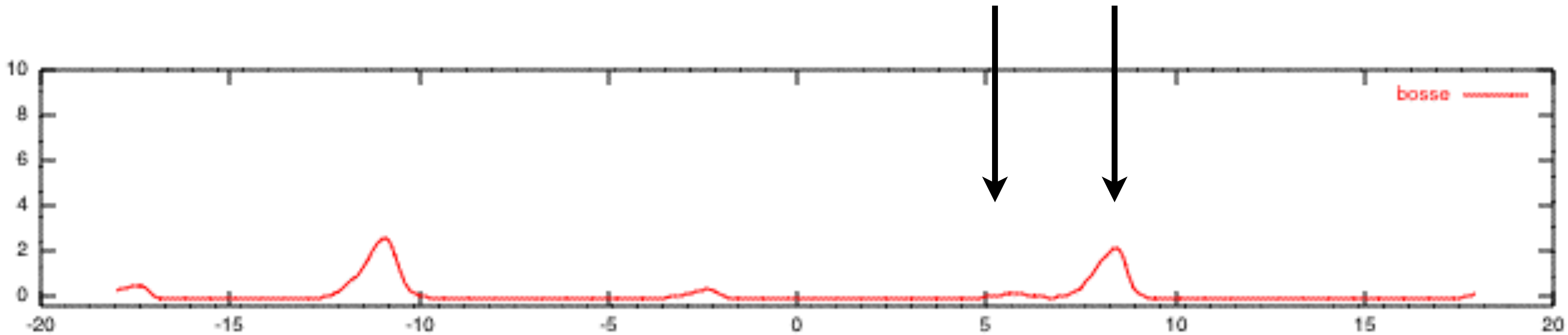

coarsening

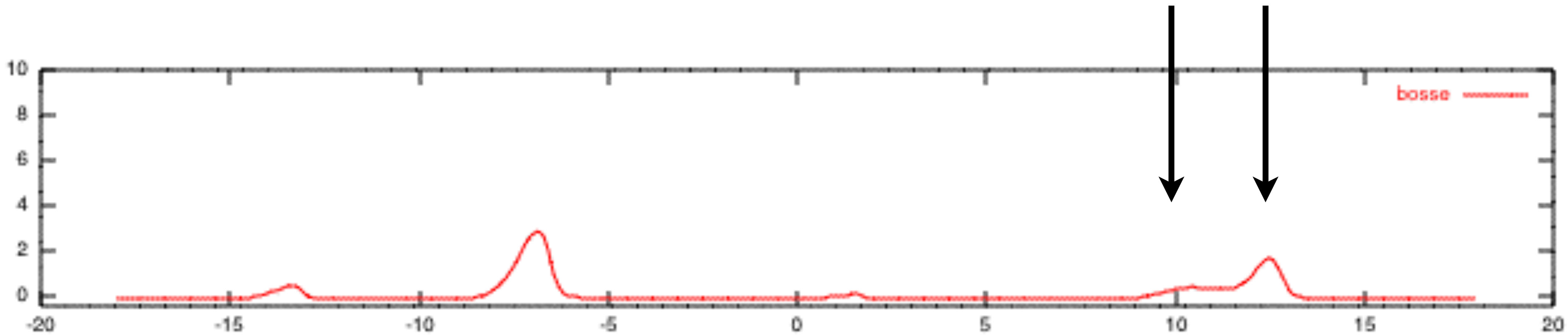

coarsening

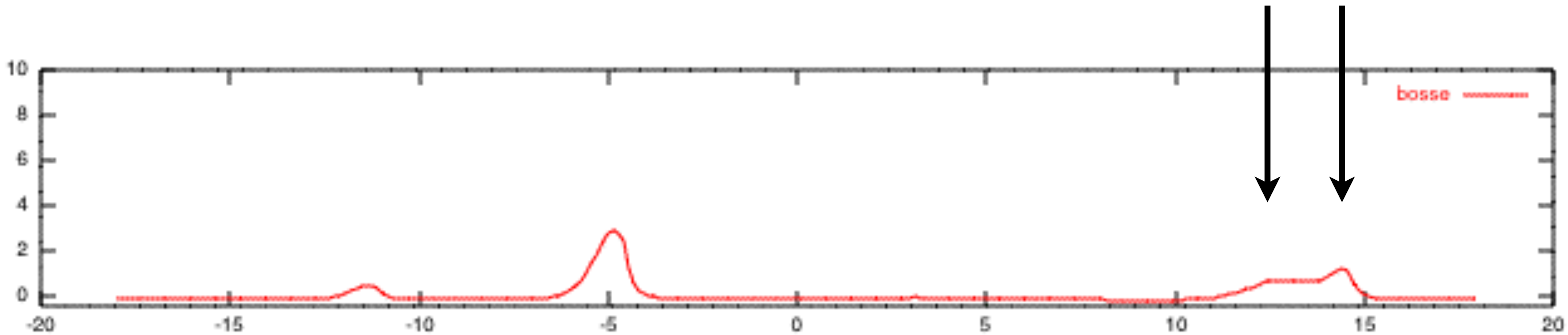

coarsening

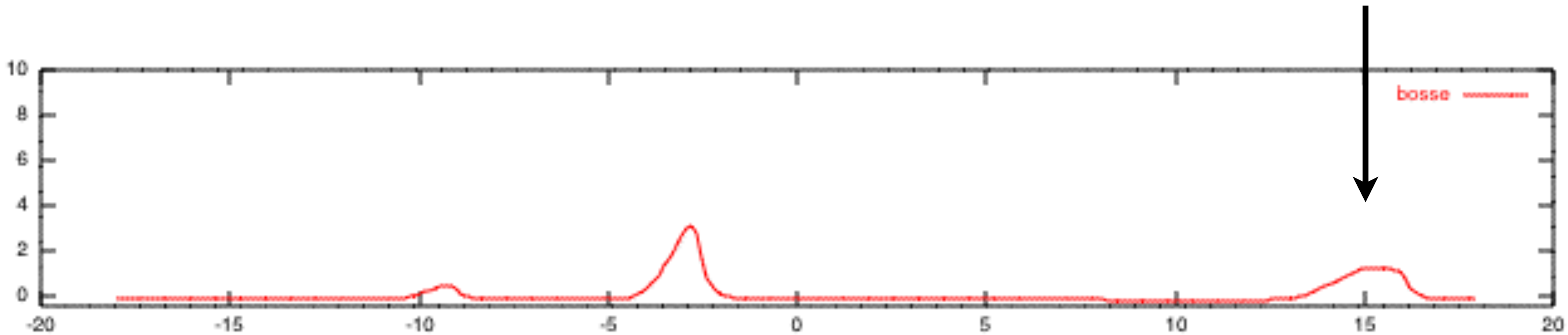

coarsening

a model for ripple instability,

non linearities allow ripples to merge,
they are less and less ripples;

this is observed experimentally

“Dunes”

Final bump: a model ”dune”

(Kouakou & Lagrée 06) Coarsening process
There is less and less ripple in the computational box
(here constant shear)

Final bump: a model ”dune”

At the end of coarsening, there is only one ripple.

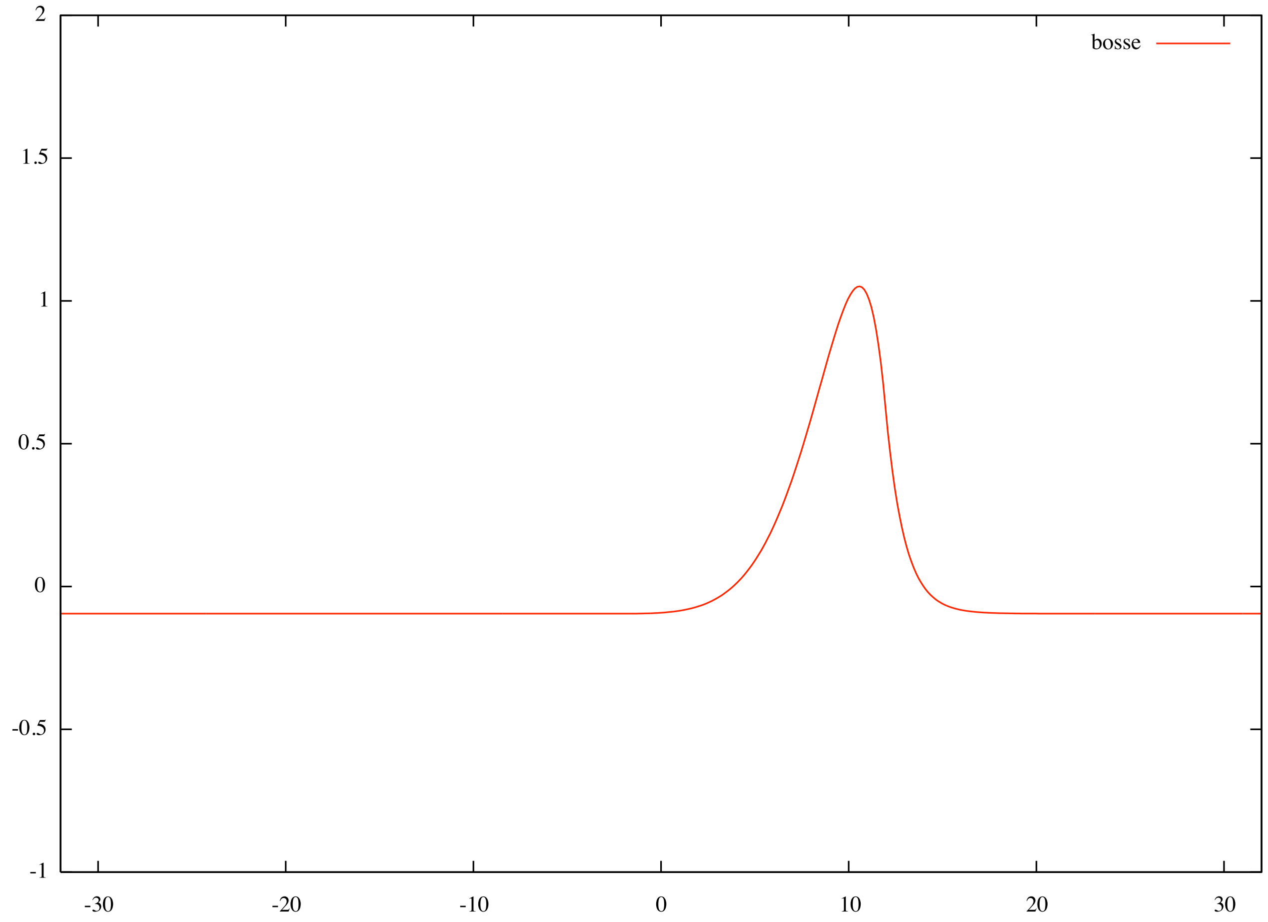

Final bump: a model ”dune”

At the end of coarsening, there is only one ripple.

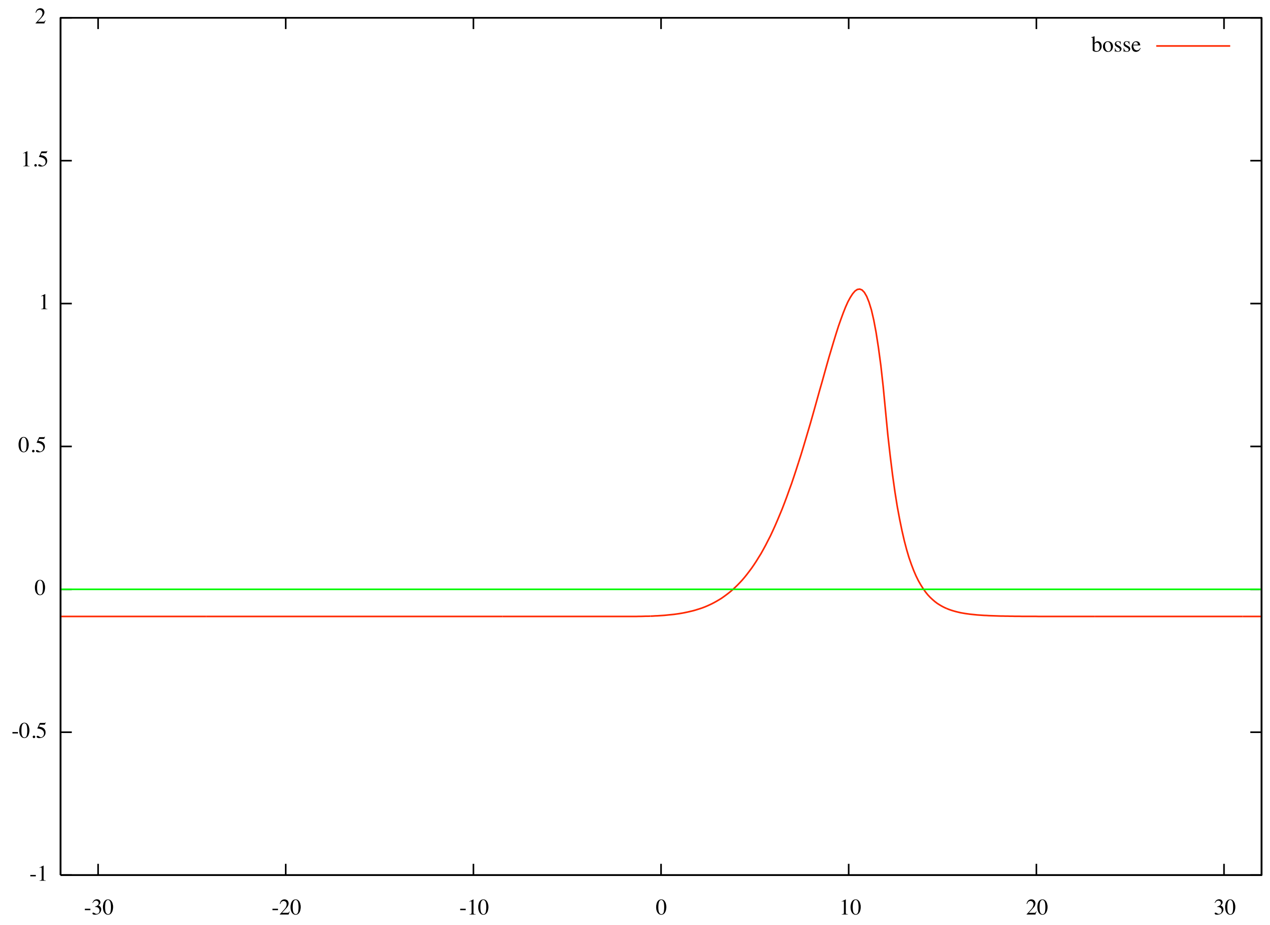

Final bump: a model "dune"

At the end of coarsening, there is only one ripple.

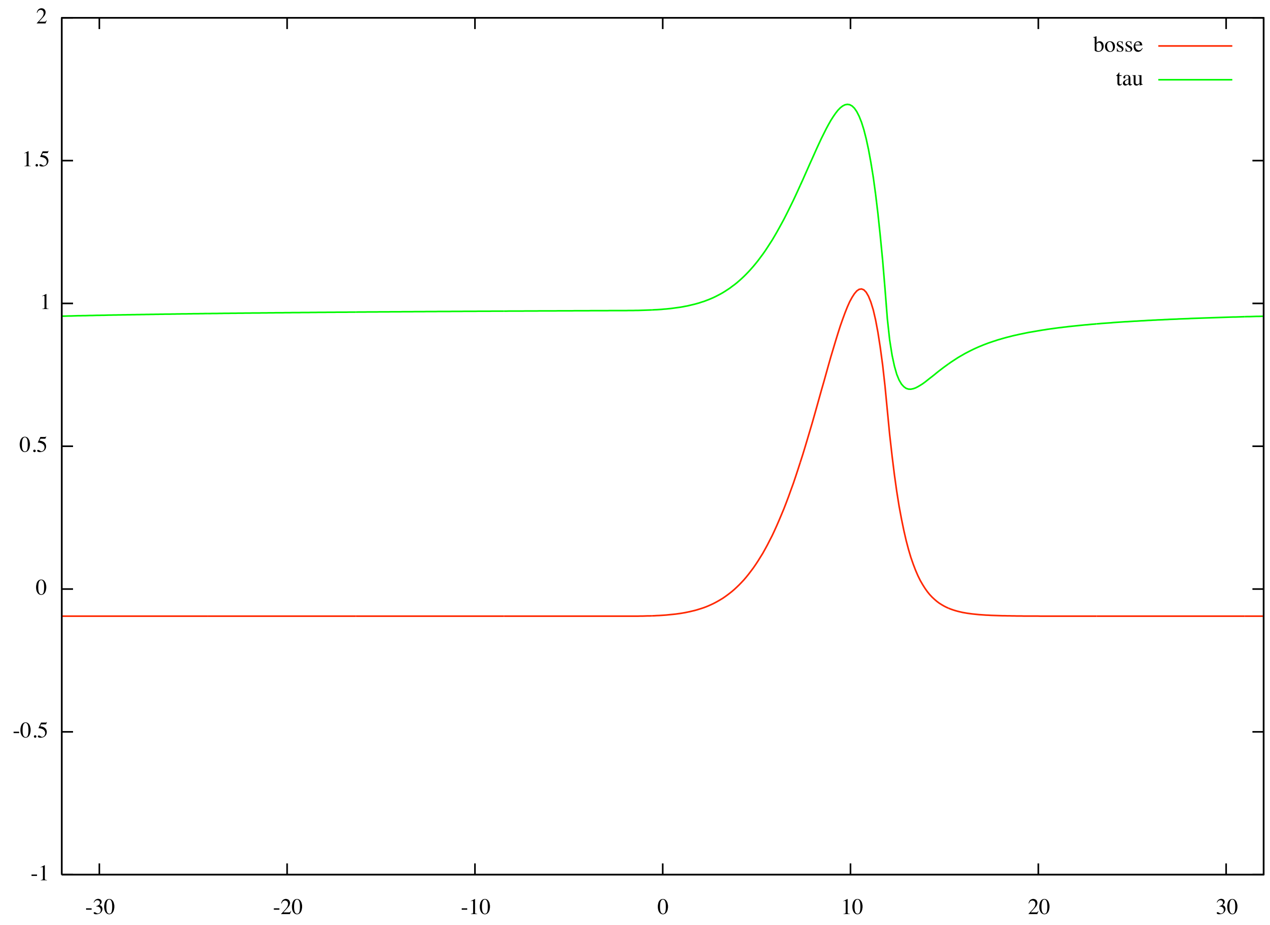

Final bump: a model ”dune”

At the end of coarsening, there is only one ripple.

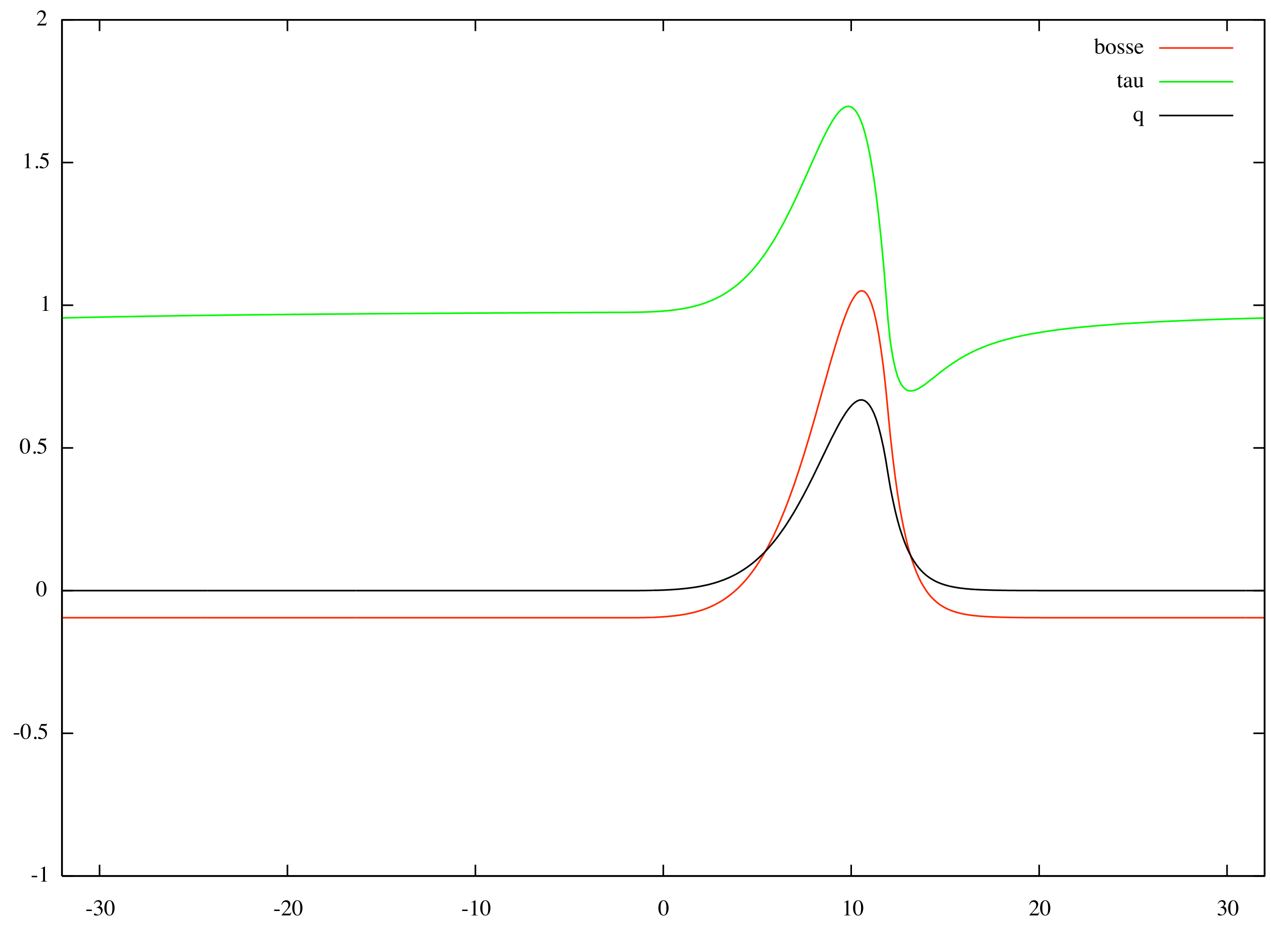

double deck shear

$$\tau = TF^{-1}[(3Ai(0))(-ik)^{1/3}TF[f]]$$

$$l_s\frac{\partial q}{\partial x} + q = \varpi(\tau - \tau_s - \Lambda\frac{\partial f}{\partial x})$$

$$\frac{\partial f}{\partial t} = -\frac{\partial q}{\partial x}$$

conserved mass

$$\int f dx$$

erodible hump on a non erodible bed

Example of displacement of a "dune"

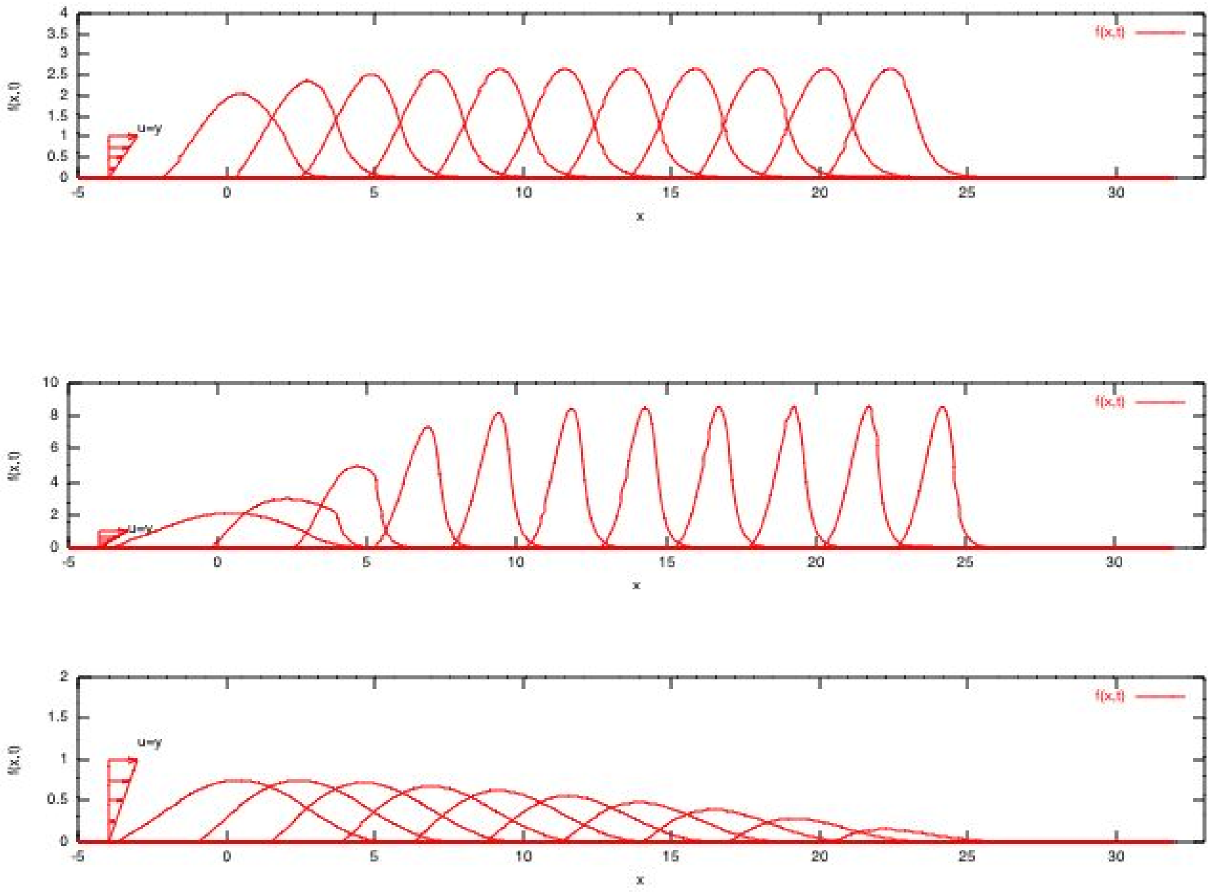

erodible hump on a non erodible bed

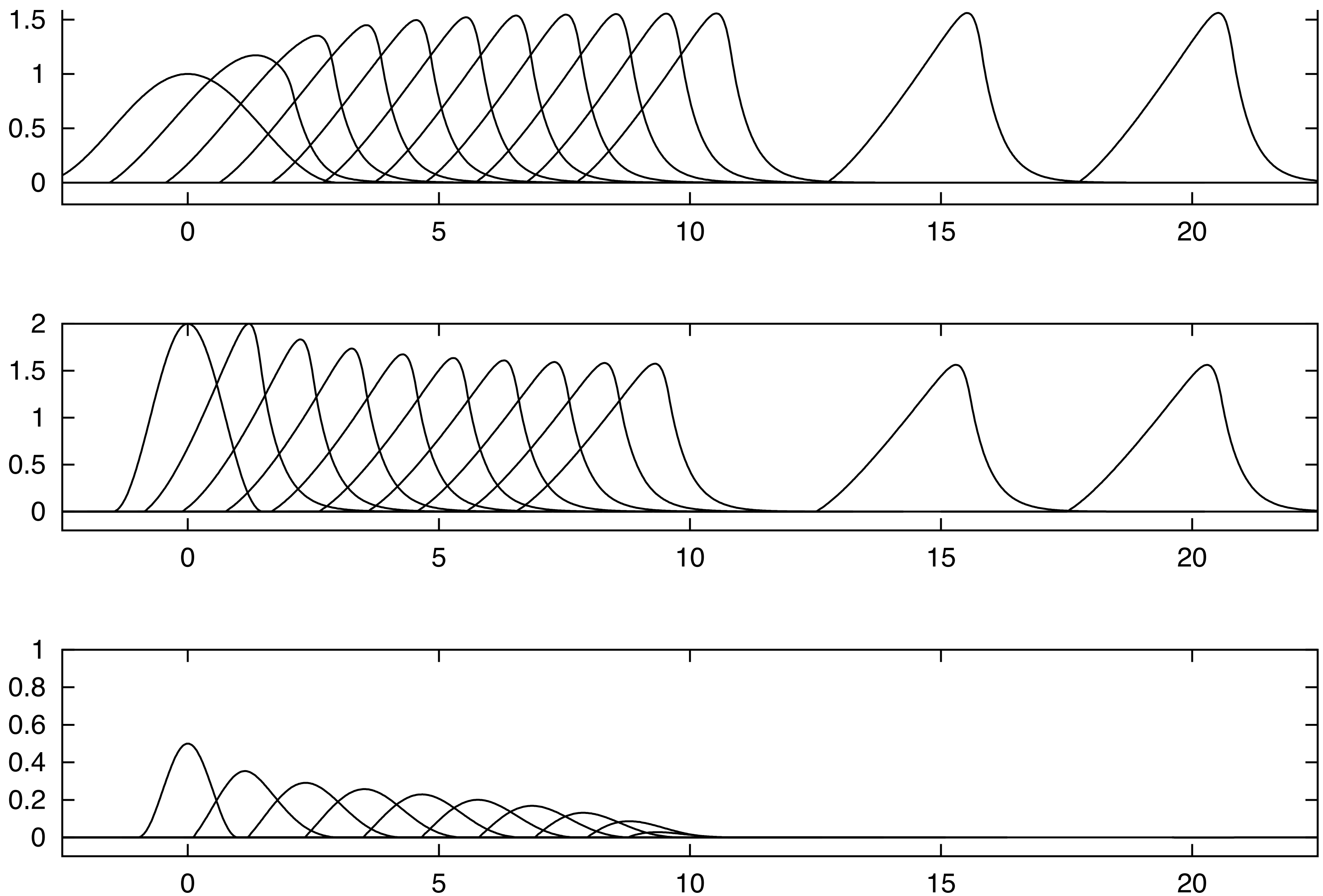

Fig. 4. The non-linear Double Deck evolution of three "dunes", for $\bar{t} = 0, 1, 2, ..., 10$, $\bar{t} = 15$, and $\bar{t} = 20$. Two upper curves: $\bar{m} = 3$ is conserved, $\bar{\tau}_s = 0.9$, and $1/\bar{l}_s = 2.5$, but two different initial shapes leading to the same final solution. Lower curve: $\bar{m} = 0.5$; when the initial mass is too small, the "dune" is washed, it loses mass.

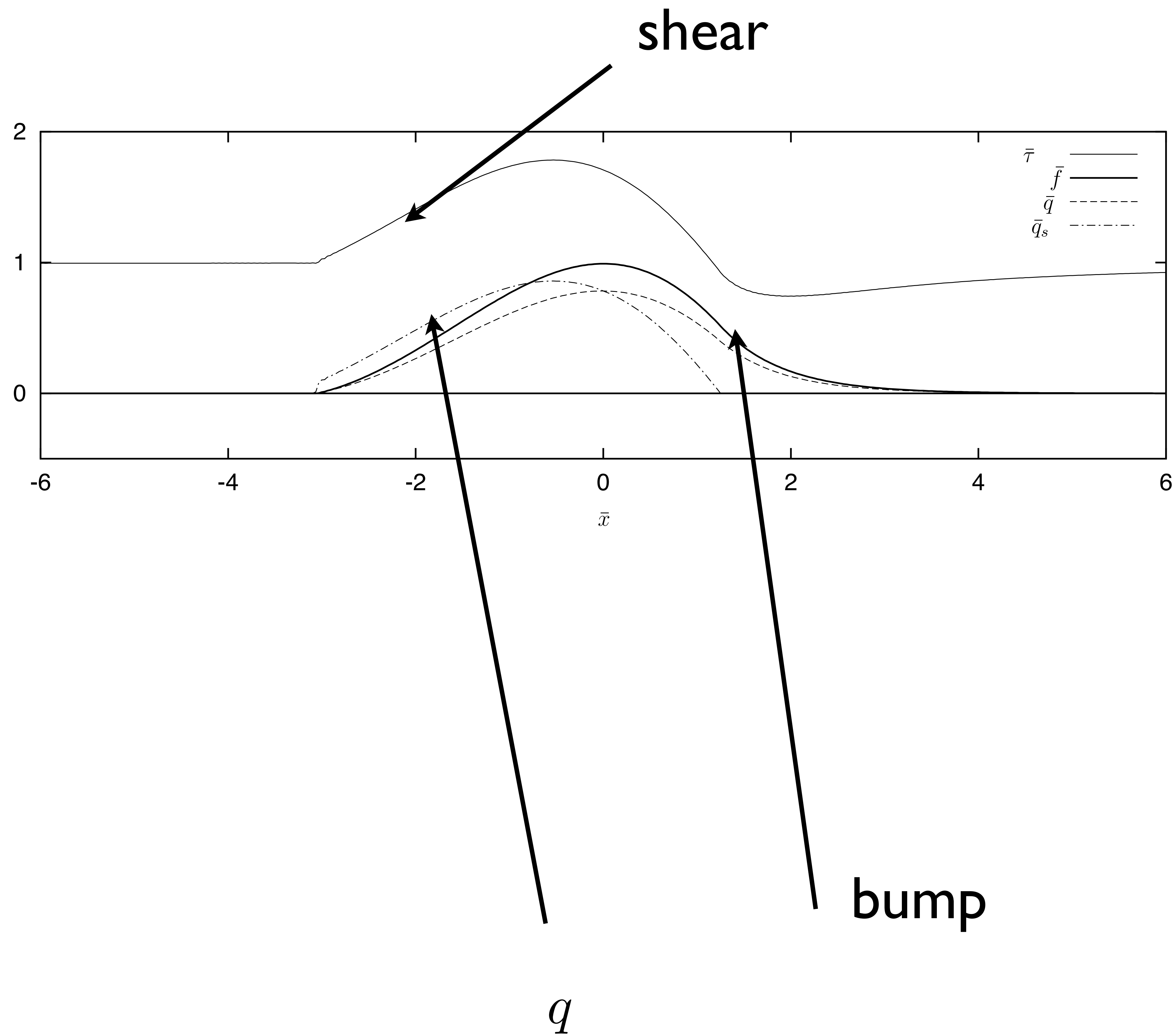

shear
q
bump
$\bar{\tau}$
$\bar{f}$
$\bar{q}$
$\bar{q}_s$
2
1
0
-6
-4
-2
0
2
4
6
$\bar{x}$

small bump

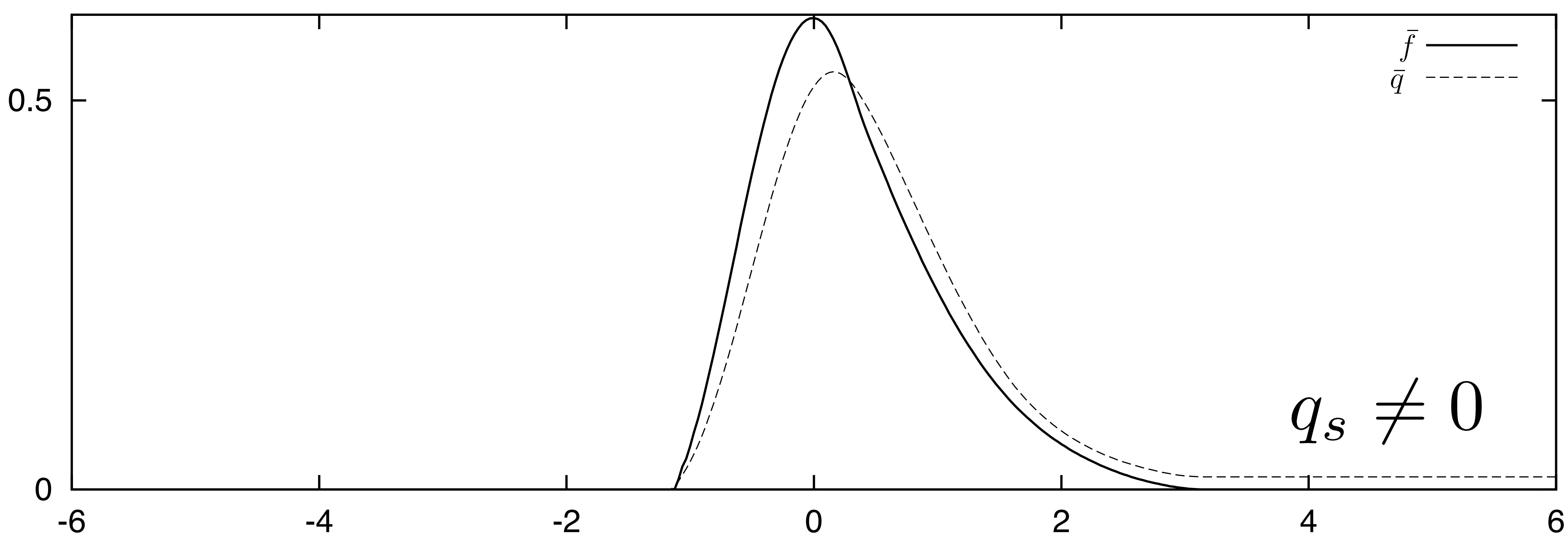

small bump loose mass

Self Similarity

rescaling $x = Lx^*$, we have $f = L^{1/3} f^*$ so that τ is invariant

$$\tau = L^{-1/3} L^{1/3} TF^{-1}[(3Ai(0))(-ik^*)^{1/3} TF[f^*]] = \tau^*$$

$$q = q^*$$

$\int f dx = m$ so $L^{4/3} = m$ with $\int f^* dx^* = 1$

$$(\frac{l_s}{m^{3/4}})\frac{\partial q^*}{\partial x^*} + q^* = \varpi(\tau^* - \tau_s)$$

$$\frac{\partial f^*}{\partial t^*} = -\frac{\partial q^*}{\partial x^*}$$

$t = mt^*$ so $c = m^{-1/4} c^*$

$1/c$ proportional to $m^{1/4}$ and function $l_s^{-1} m^{3/4}$

Self Similarity

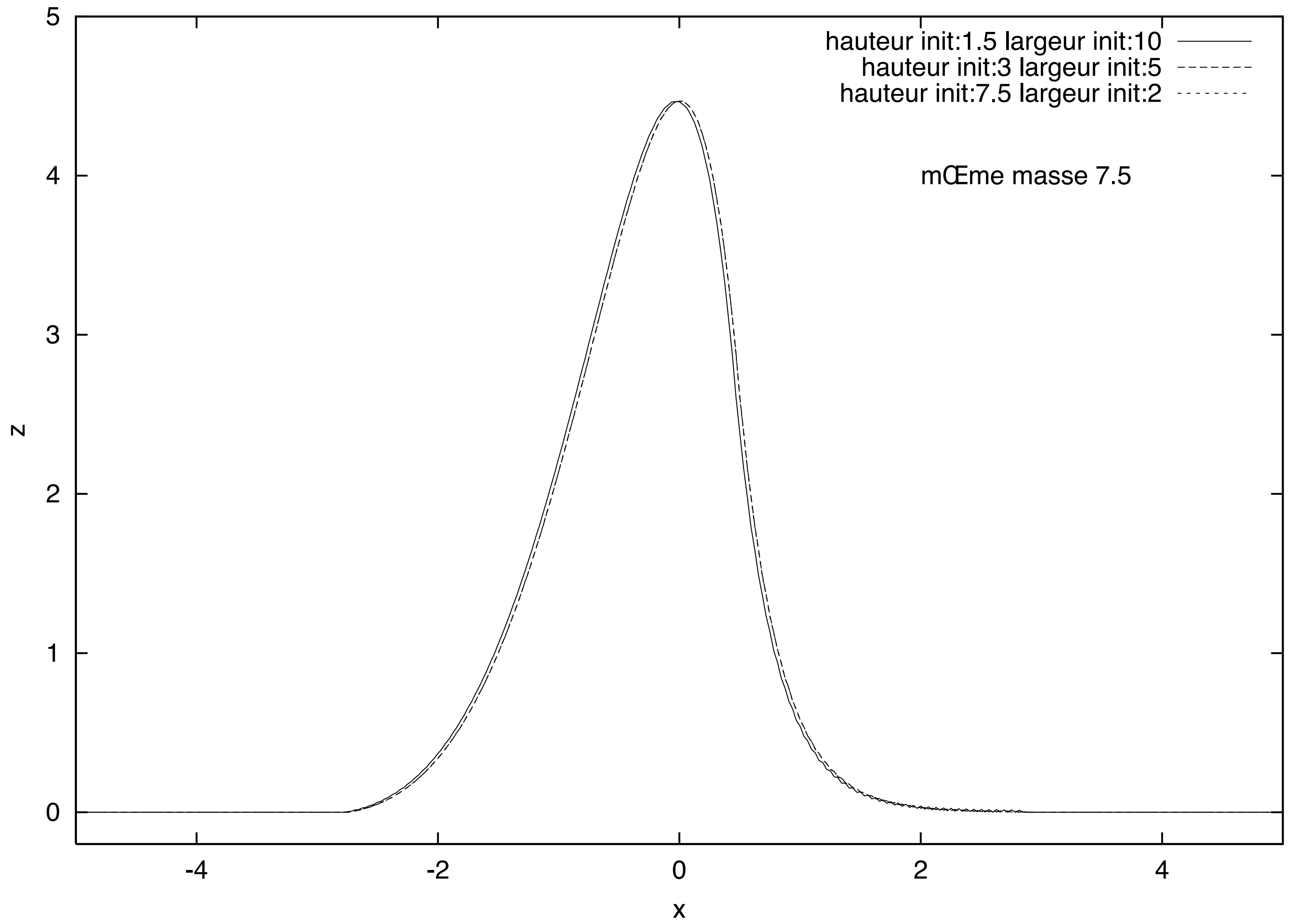

two different initial bumps of same m lead to the same final state

Self Similarity

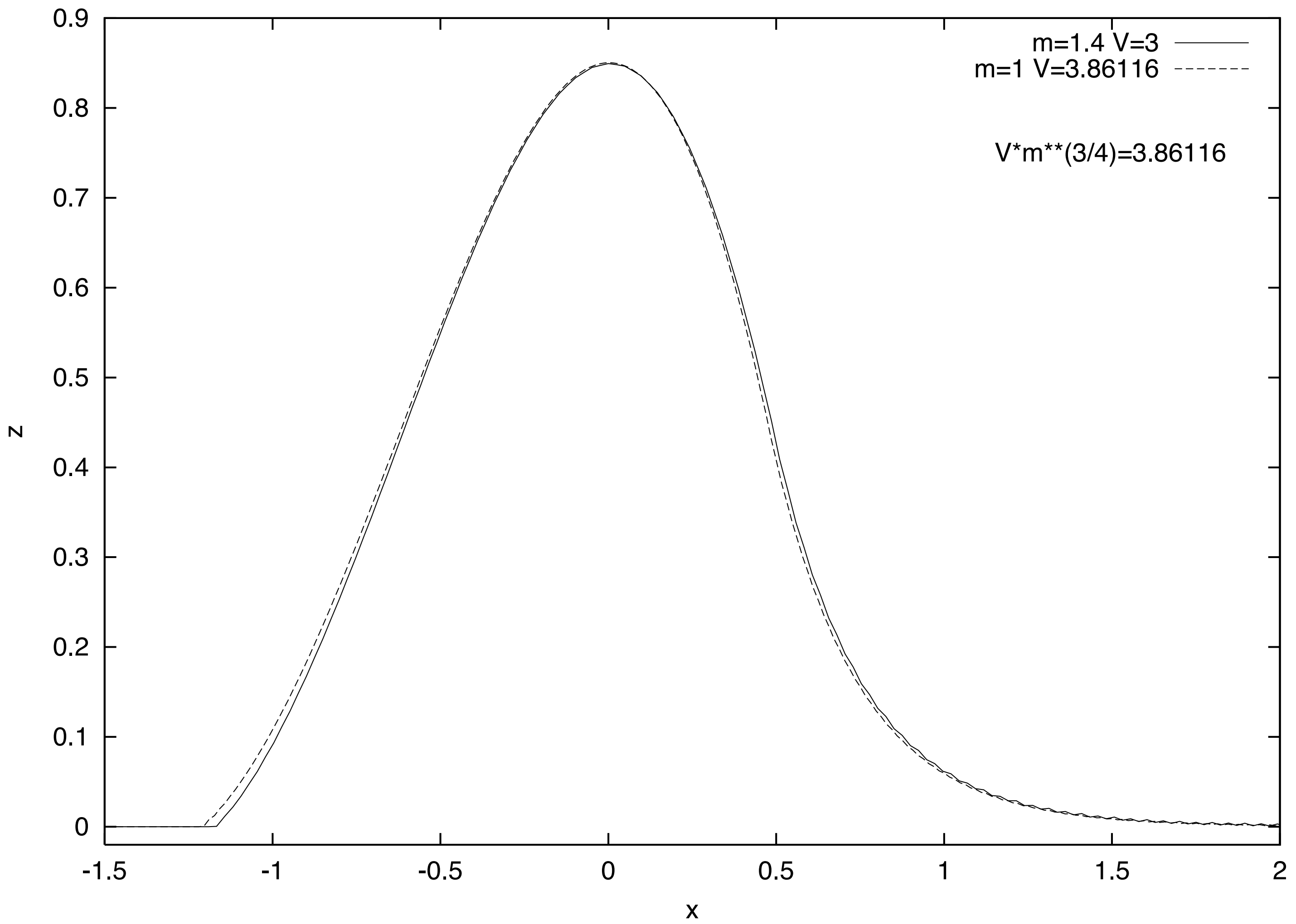

two cases of same $l_s^{-1} m^{3/4}$.

Self Similarity

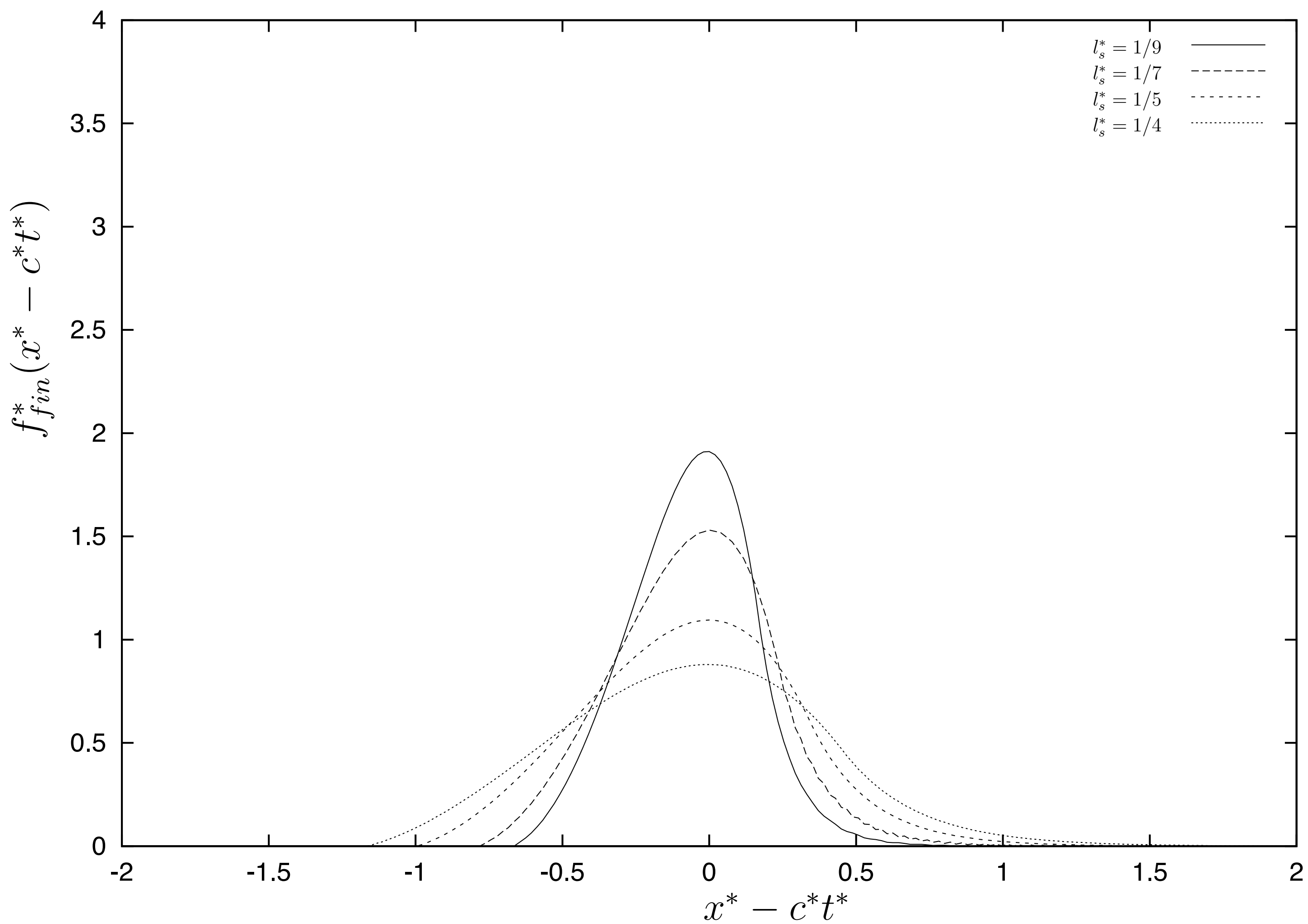

Fig. 8. "Dunes" of unit mass with $l_s^* = 1/4, 1/5, 1/7, 1/9$ $(\tau_s = 0.9)$. The smaller l_s^* is, the thinner and higher the "dune" is.

selfsimilarity, unit mass $m = 1$, different $l_s^{-1} m^{3/4}$.

q proportional only to skin friction

$= \tau - \tau_s - \Lambda \frac{\partial f}{\partial x}$ new similarity $\Lambda m^{-1/4}$, $c = m^{-1/4}$

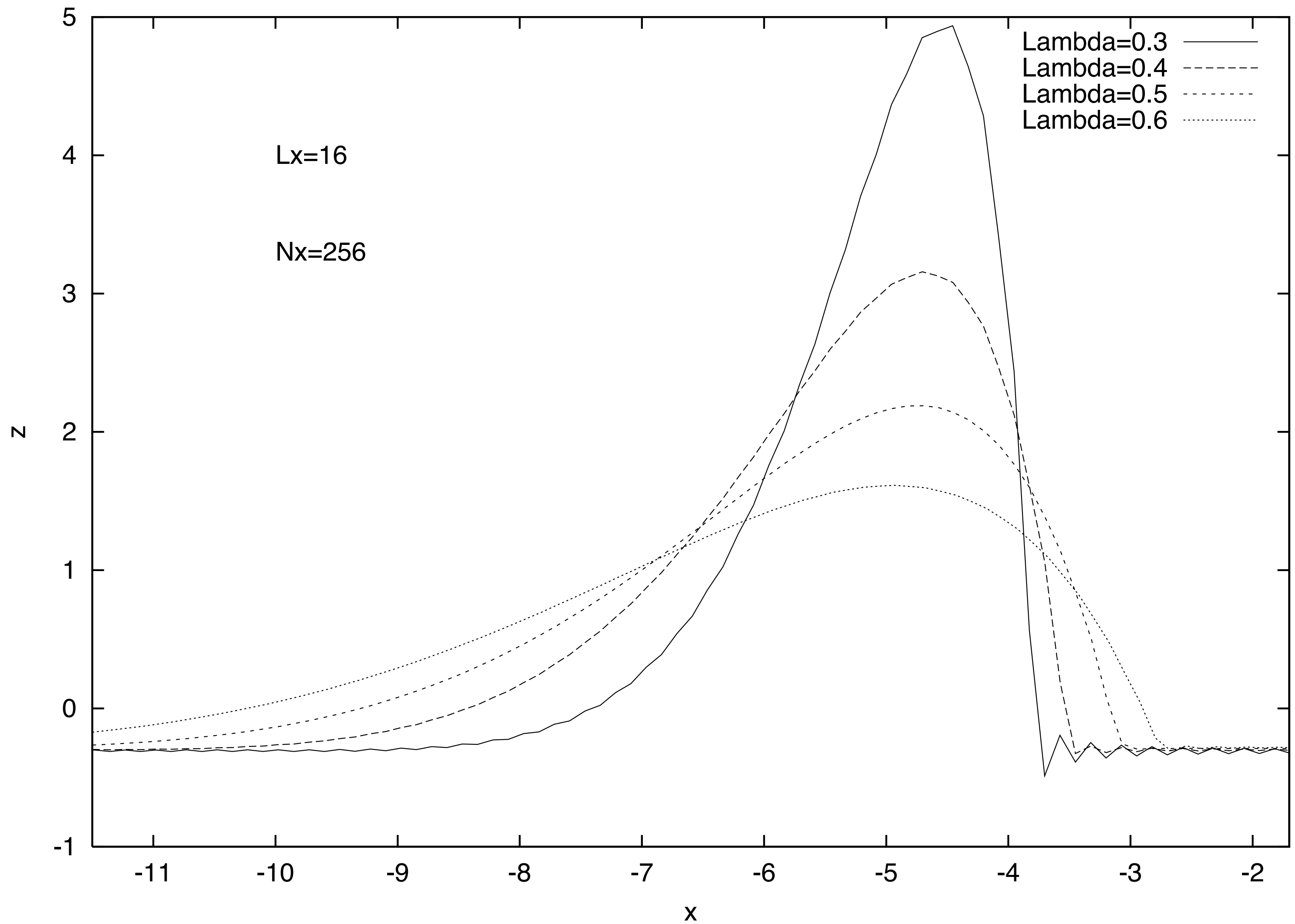

Influence of Λ linear case $x = m^{3/4} x^*$ and $f = m^{1/4} f^*$ seems to be no $q = \tau - \tau_s$ solution.

formes finales lin/ non lin

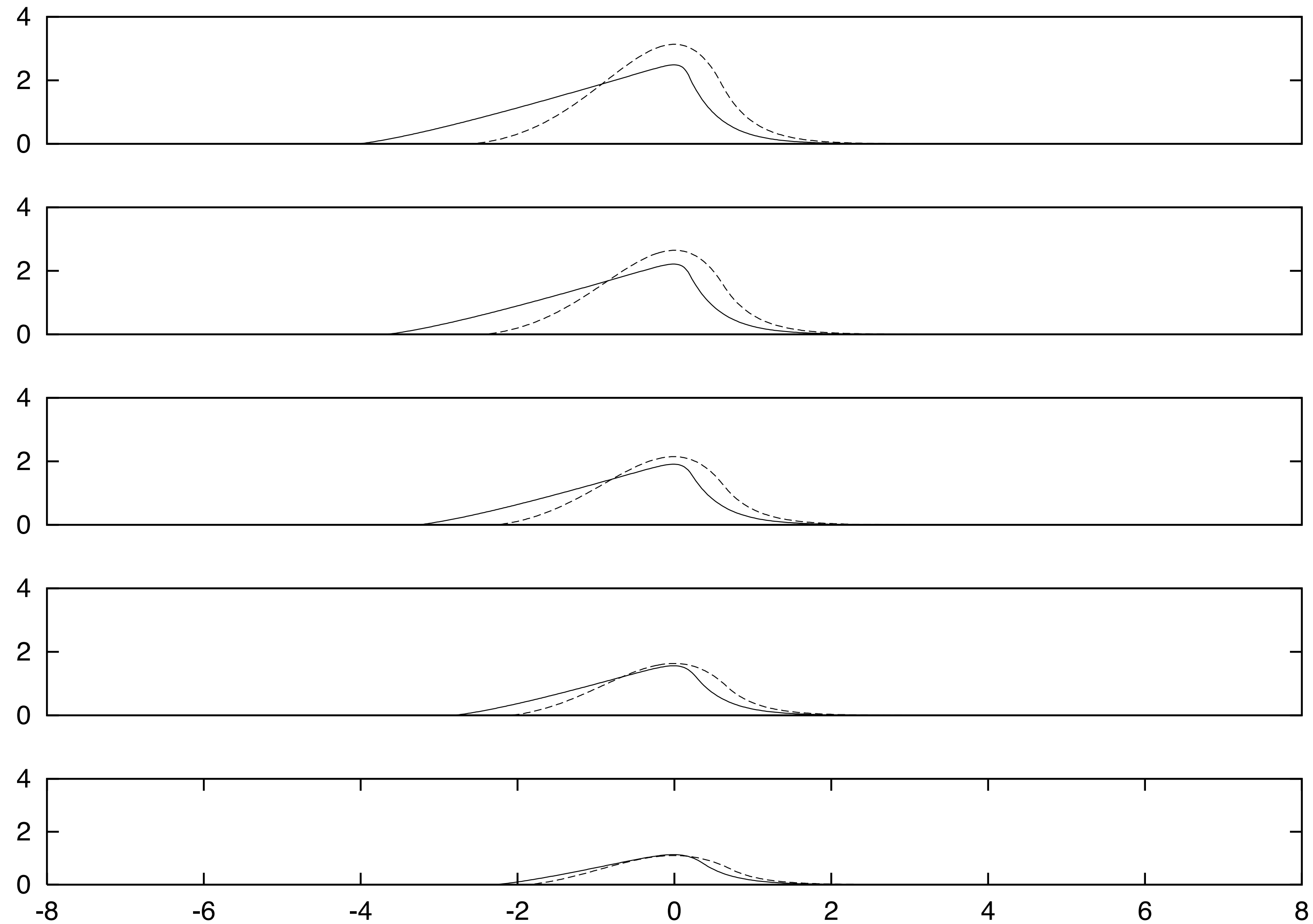

Fig. 5. The non-linear final moving "dune" solution $f_{fin}(x-ct)$ is represented with solid lines, the linear solution is represented with dashed lines, and $\tau_s = 0.9$, $1/l_s = 2.5$, $m = 2, 3, 4, 5$ (bottom curve to top curve).

$cm^{1/4}$

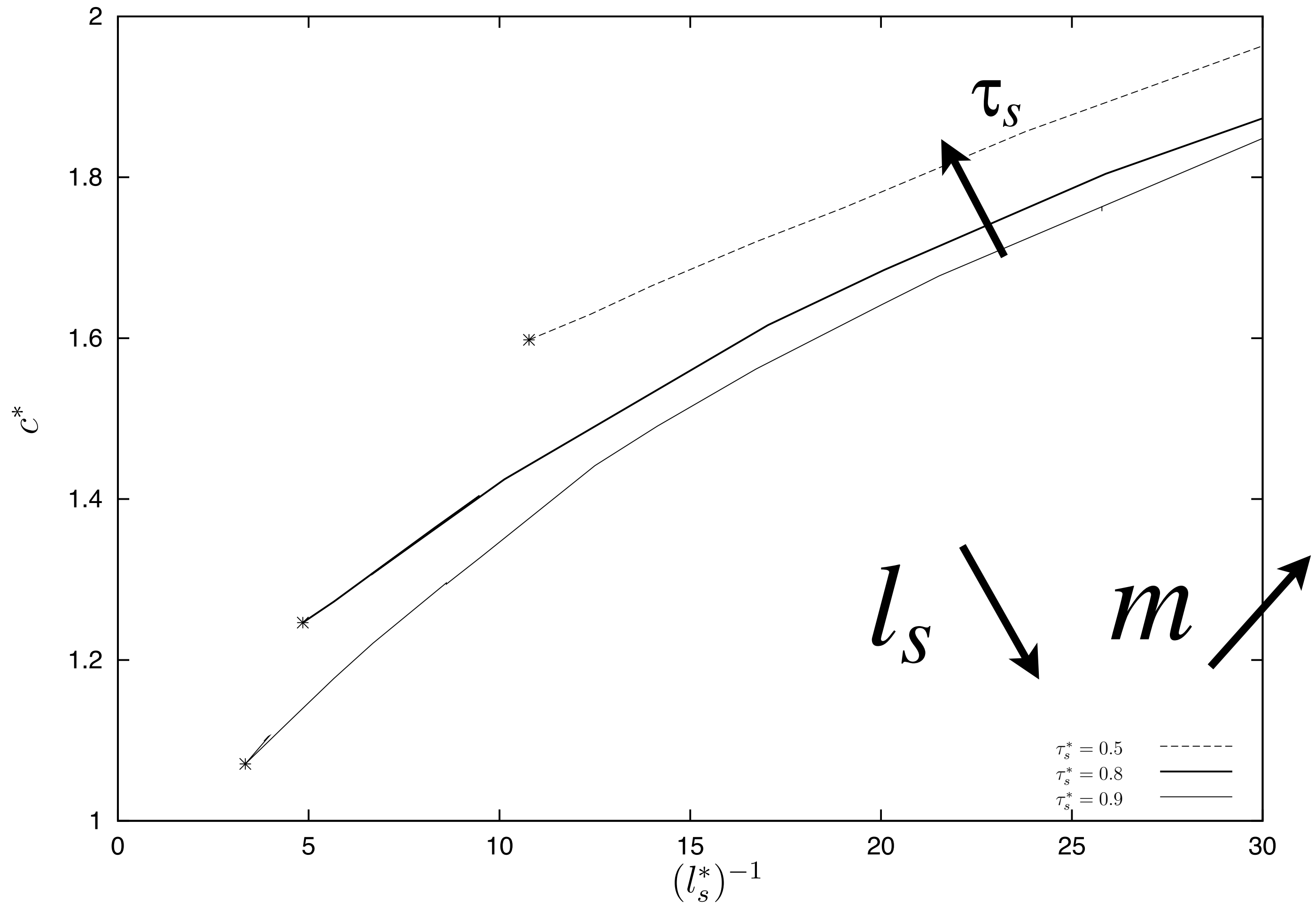

$l_s^{-1} m^{3/4}$

velocity in $m^{-1/4}$

there is a minimal size

Bilan V

- Ripple instabilities needs a good description of shear
- try Navier Stokes now....

back to the experimental setup of IPGP

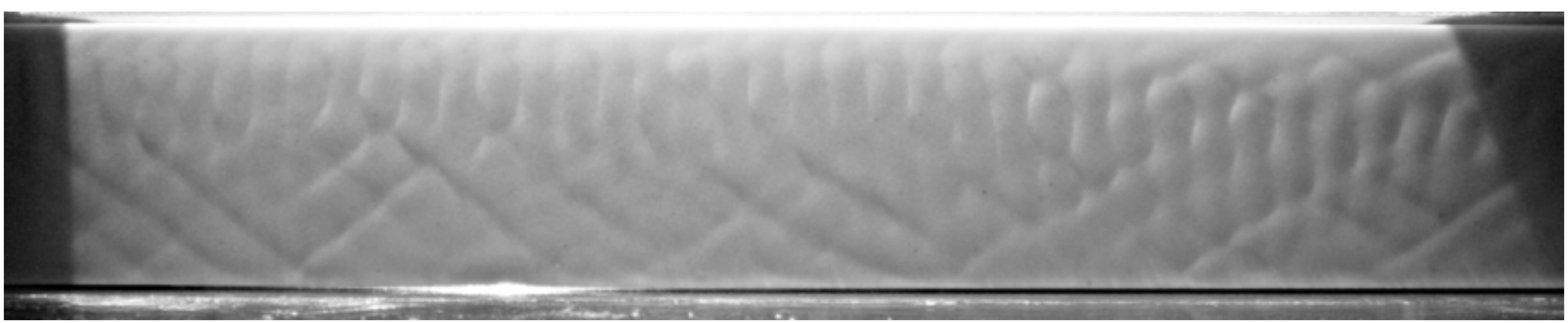

Saint-Venant

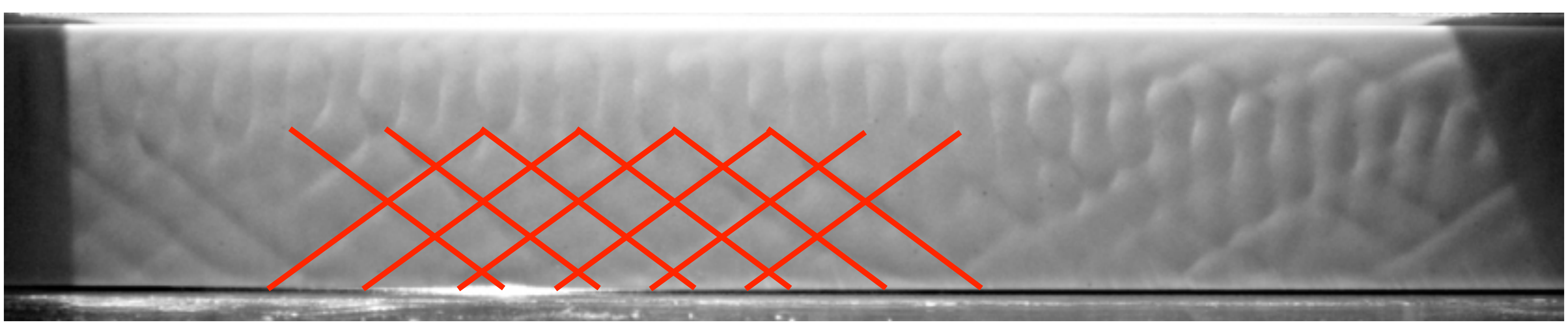

Saint-Venant asymptotic

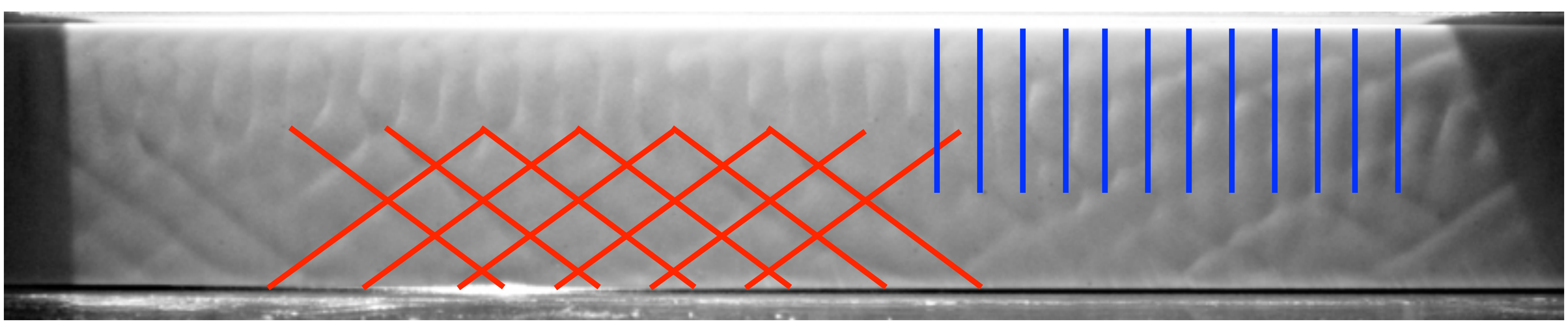

Saint-Venant asymptotic

complete 3D linear stability approach

> Steady Orr Sommerfeld

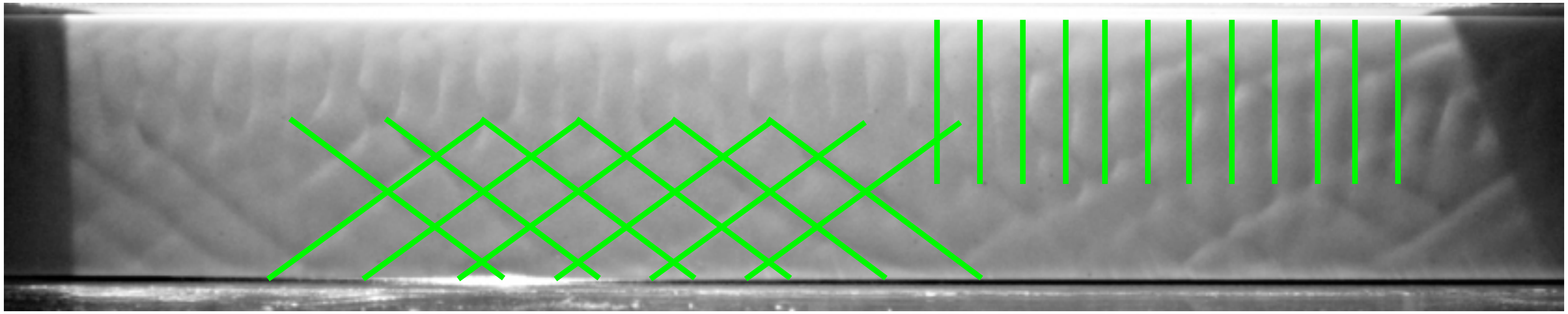

But maybe the best model to evaluate the skin friction near the wall is NAVIER STOKES ;-)

linear perturbation of a quasisteady flow with a given wavy bed

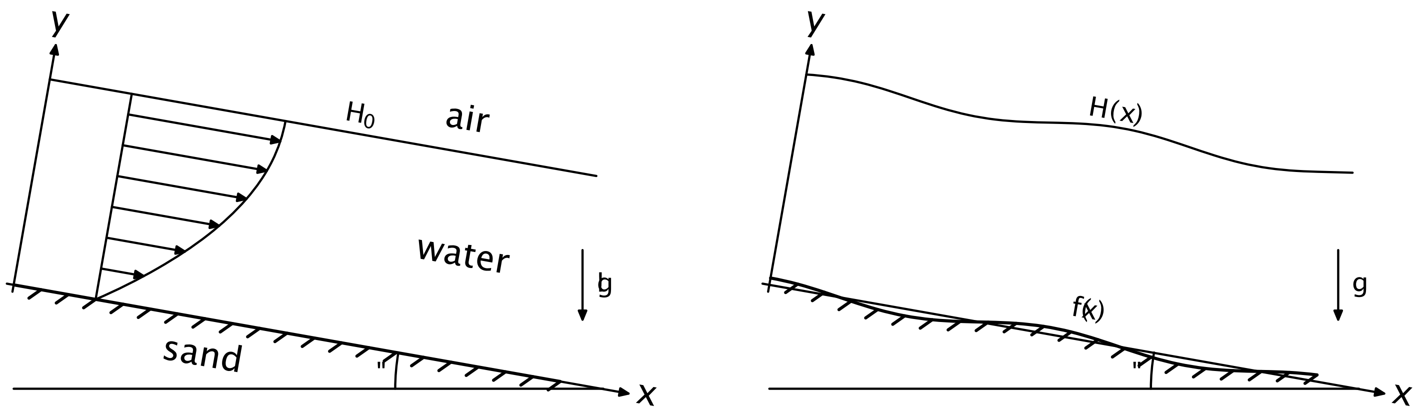

basic flow is Nuβelt (half Poiseuille)

linear perturbation of a quasisteady flow with a given wavy bed

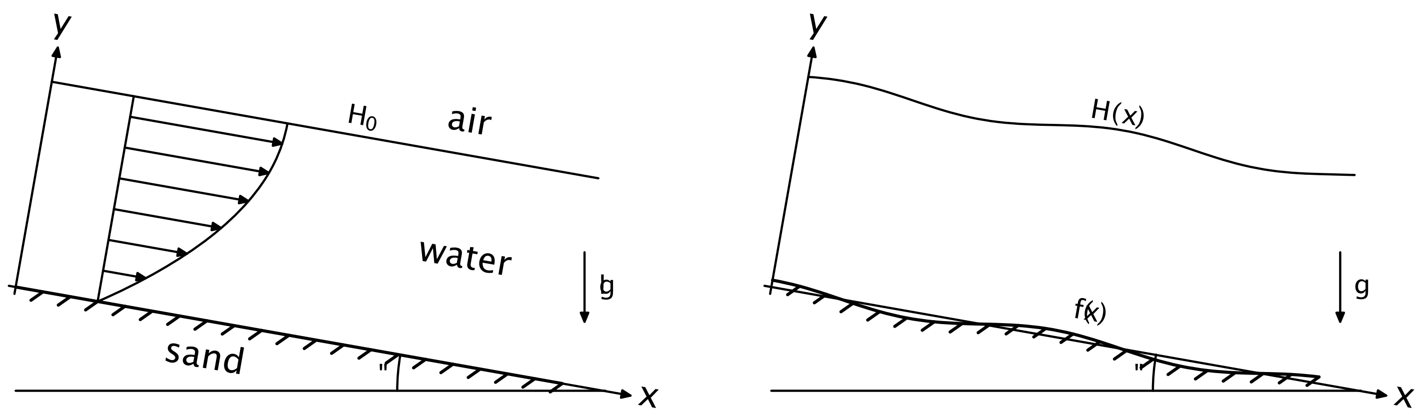

basic flow is Nuβelt (half Poiseuille)

+ linear perturbation

$$u = U_0 + \varepsilon\psi'(y)e^{ikx} \quad v = -\varepsilon ik\psi(y)e^{ikx}$$

$$\psi'''' - 2k^2\psi'' + k^4\psi = ikRe\{U_0(\psi'' - k^2\psi) - U_0''\psi\}$$

linear perturbation of a quasisteady flow with a given wavy bed

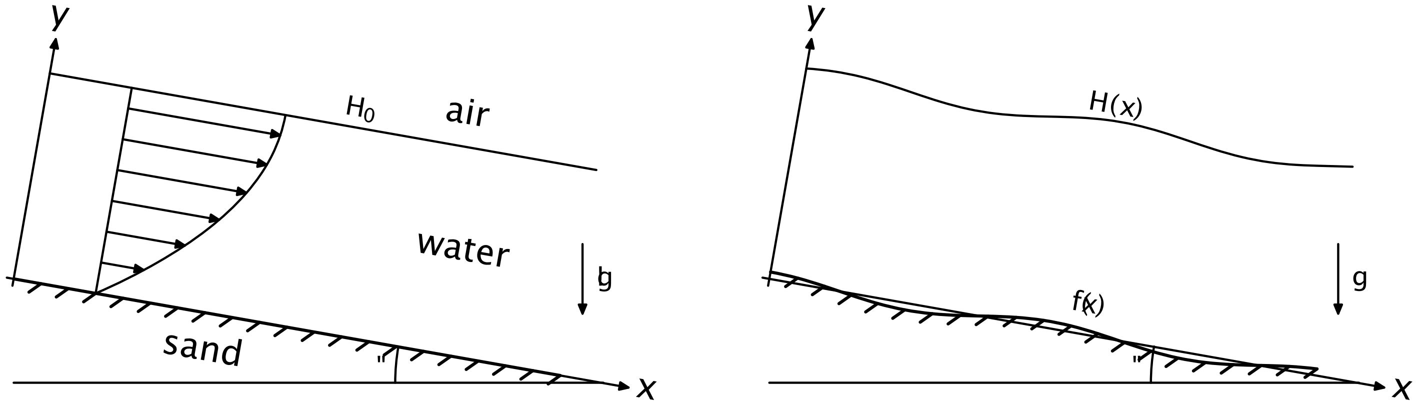

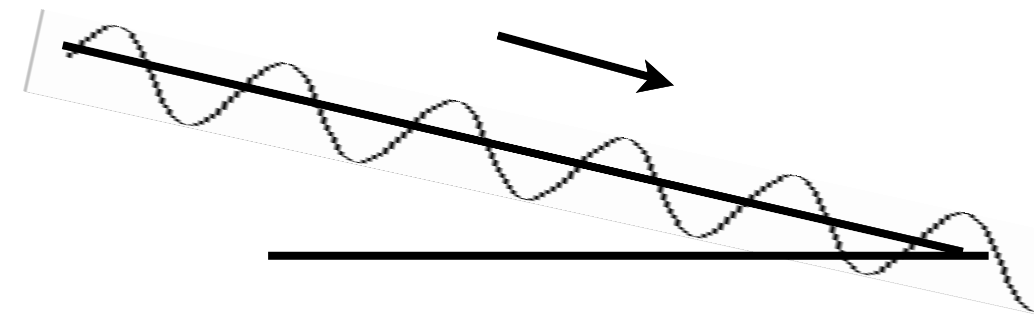

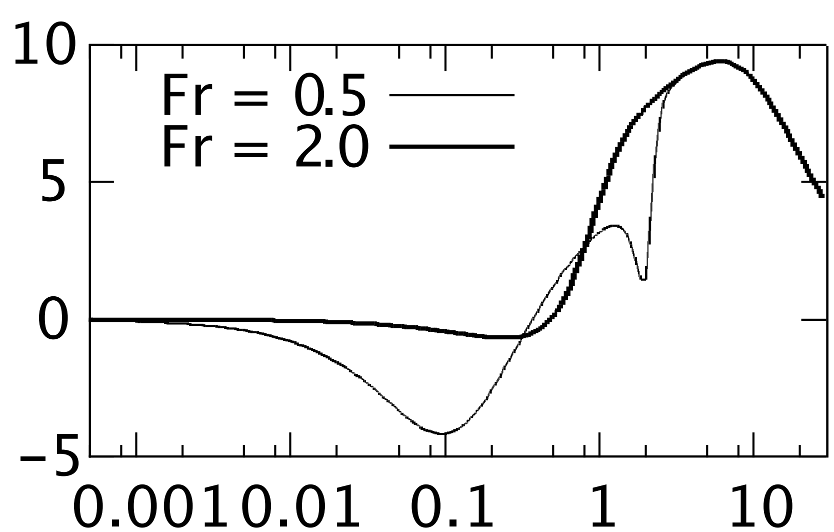

Re=50

skin friction response

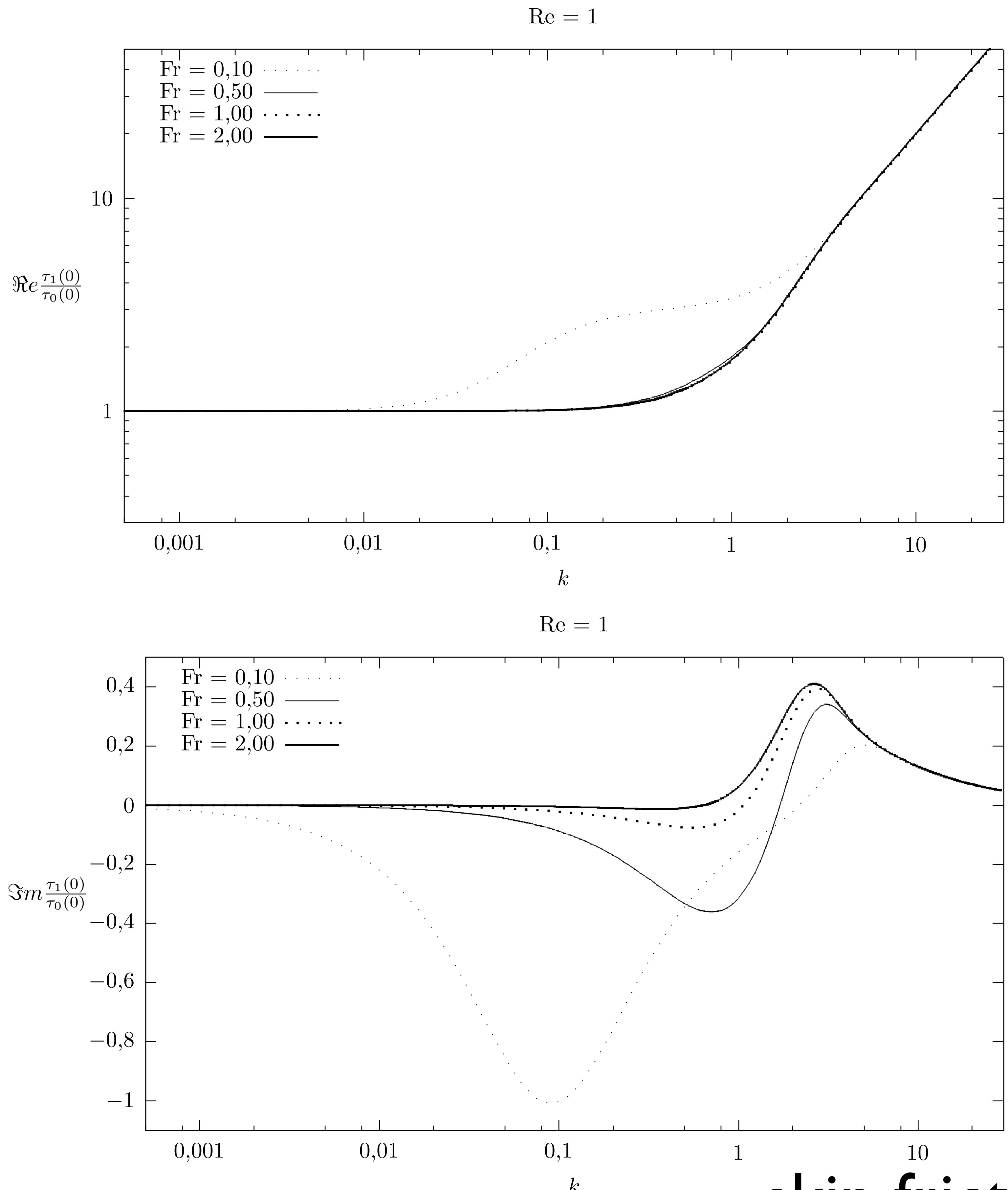

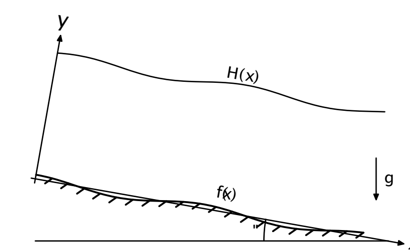

skin friction response

FIG. 2.3 – *Parties réelles (en haut) et parties imaginaires (en bas) de la perturbation du cisaillement au fond renormalisée, pour $Re = 1$ et différentes valeurs de Fr.*

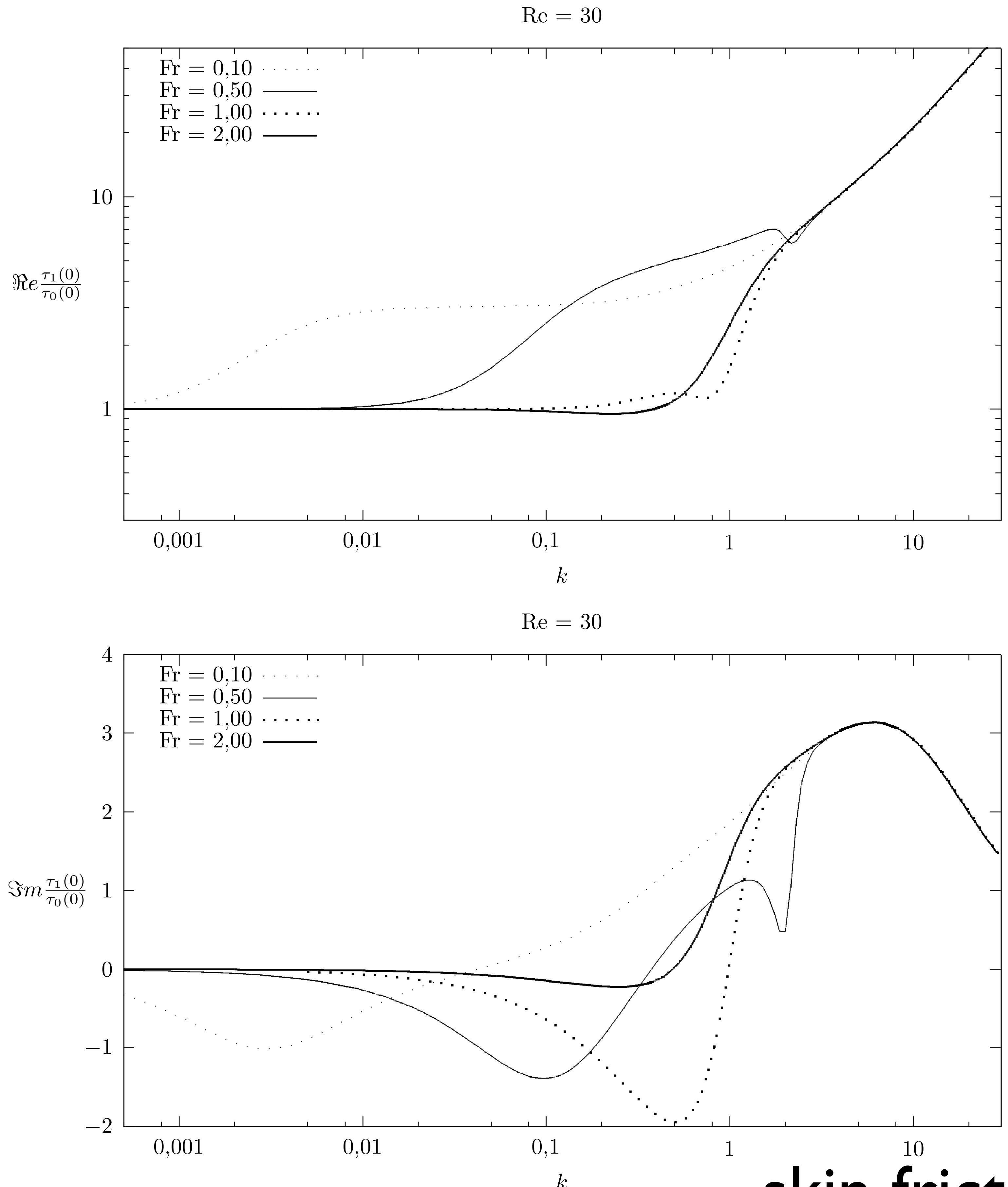

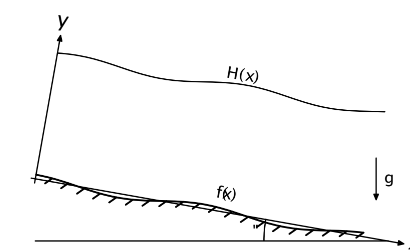

skin friction response

FIG. 2.4 – *Parties réelles (en haut) et parties imaginaires (en bas) de la perturbation du cisaillement au fond renormalisée, pour $Re = 30$ et différentes valeurs de Fr.*

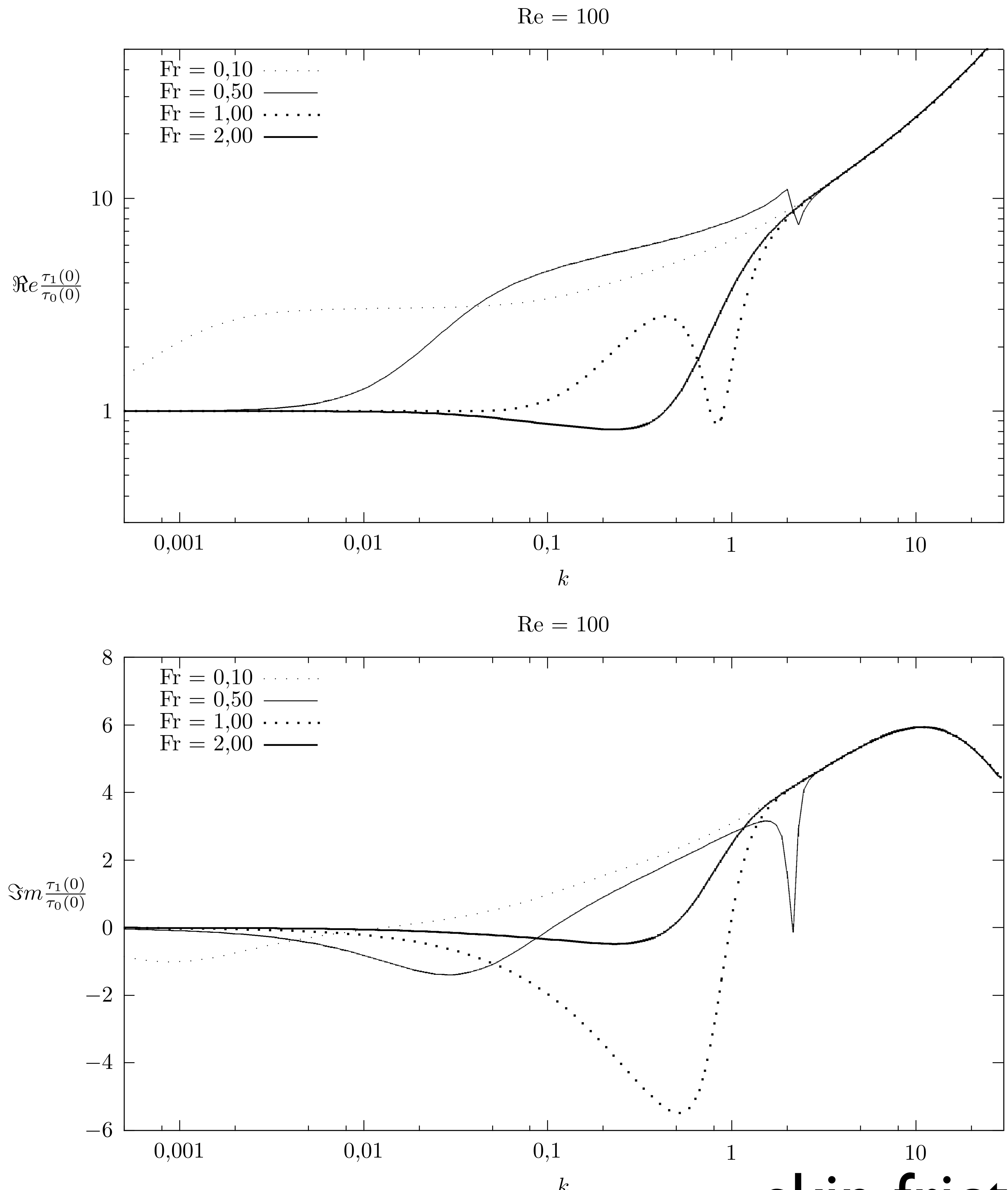

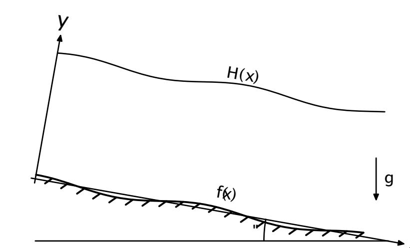

skin friction response

Fig. 2.5 – *Parties réelles (en haut) et parties imaginaires (en bas) de la perturbation du cisaillement au fond renormalisée, pour $Re = 100$ et différentes valeurs de Fr.*

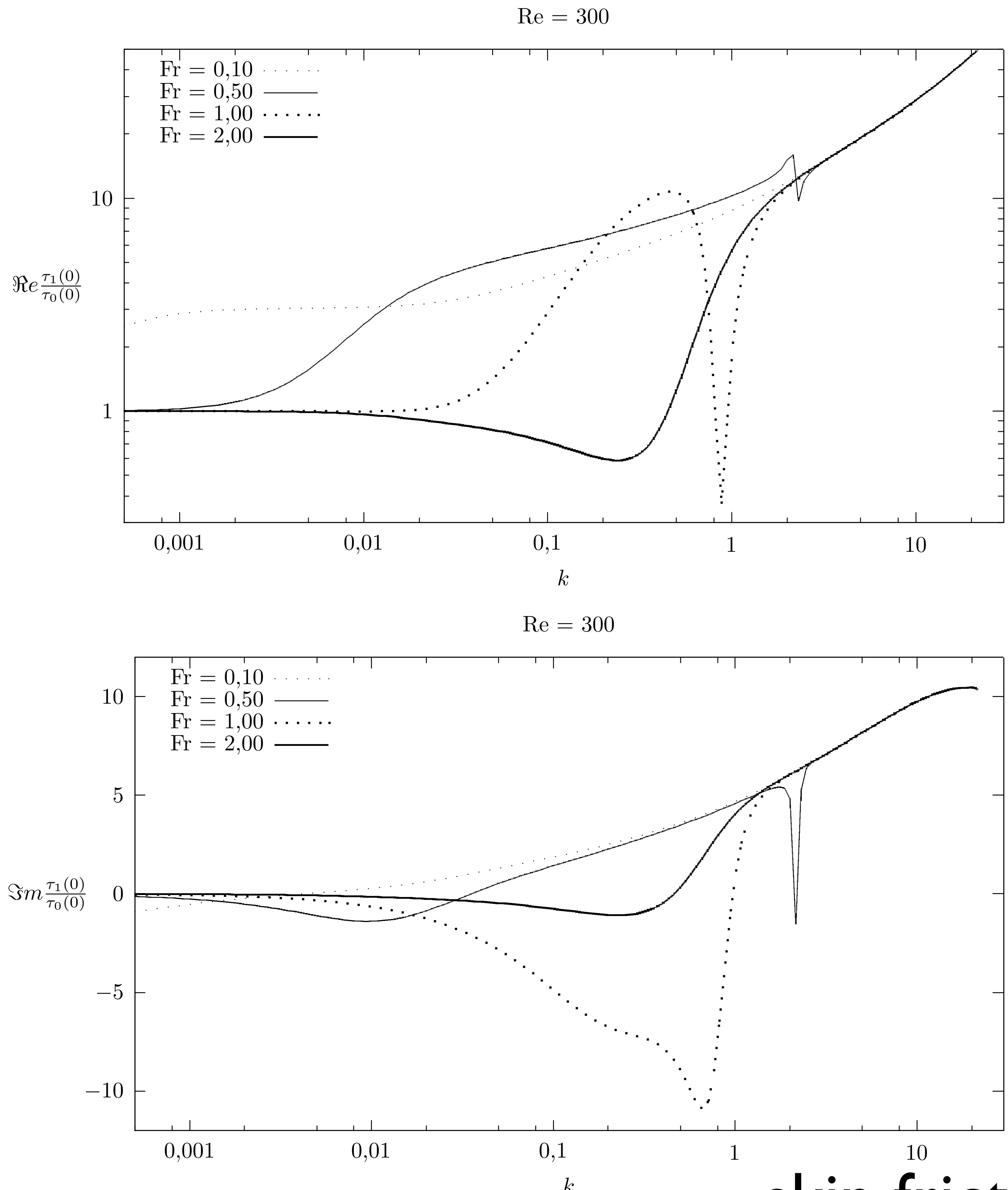

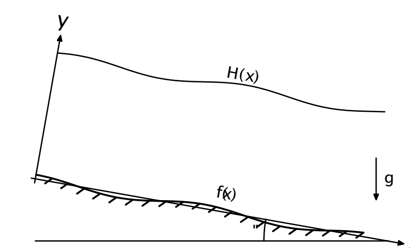

skin friction response

FIG. 2.6 – *Parties réelles (en haut) et parties imaginaires (en bas) de la perturbation du cisaillement au fond renormalisée, pour $Re = 300$ et différentes valeurs de Fr.*

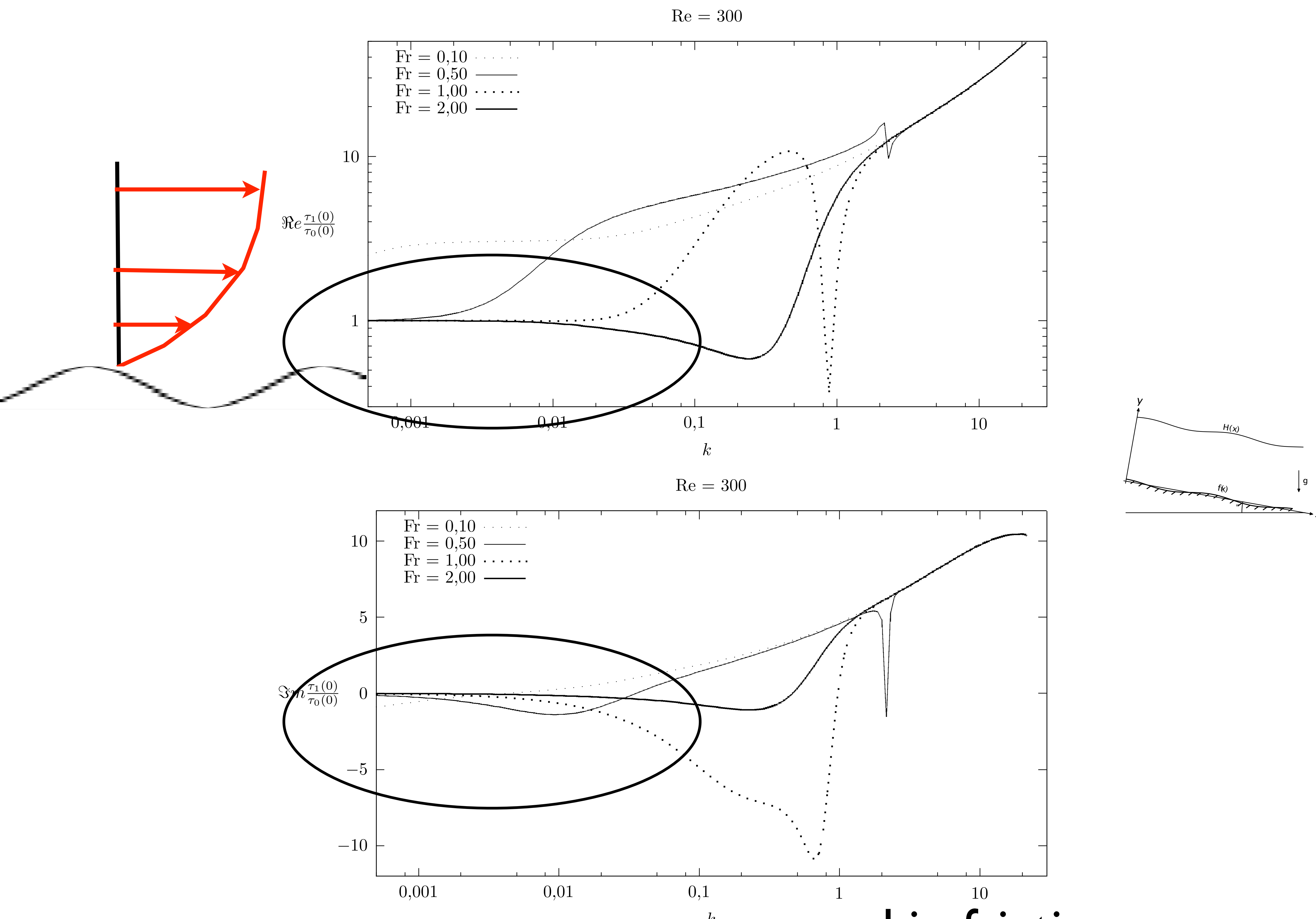

skin friction response

Fig. 2.6 – *Parties réelles (en haut) et parties imaginaires (en bas) de la perturbation du cisaillement au fond renormalisée, pour Re = 300 et différentes valeurs de Fr.*

Saint Venant/ Orr Sommerfeld Stationnaire 2D

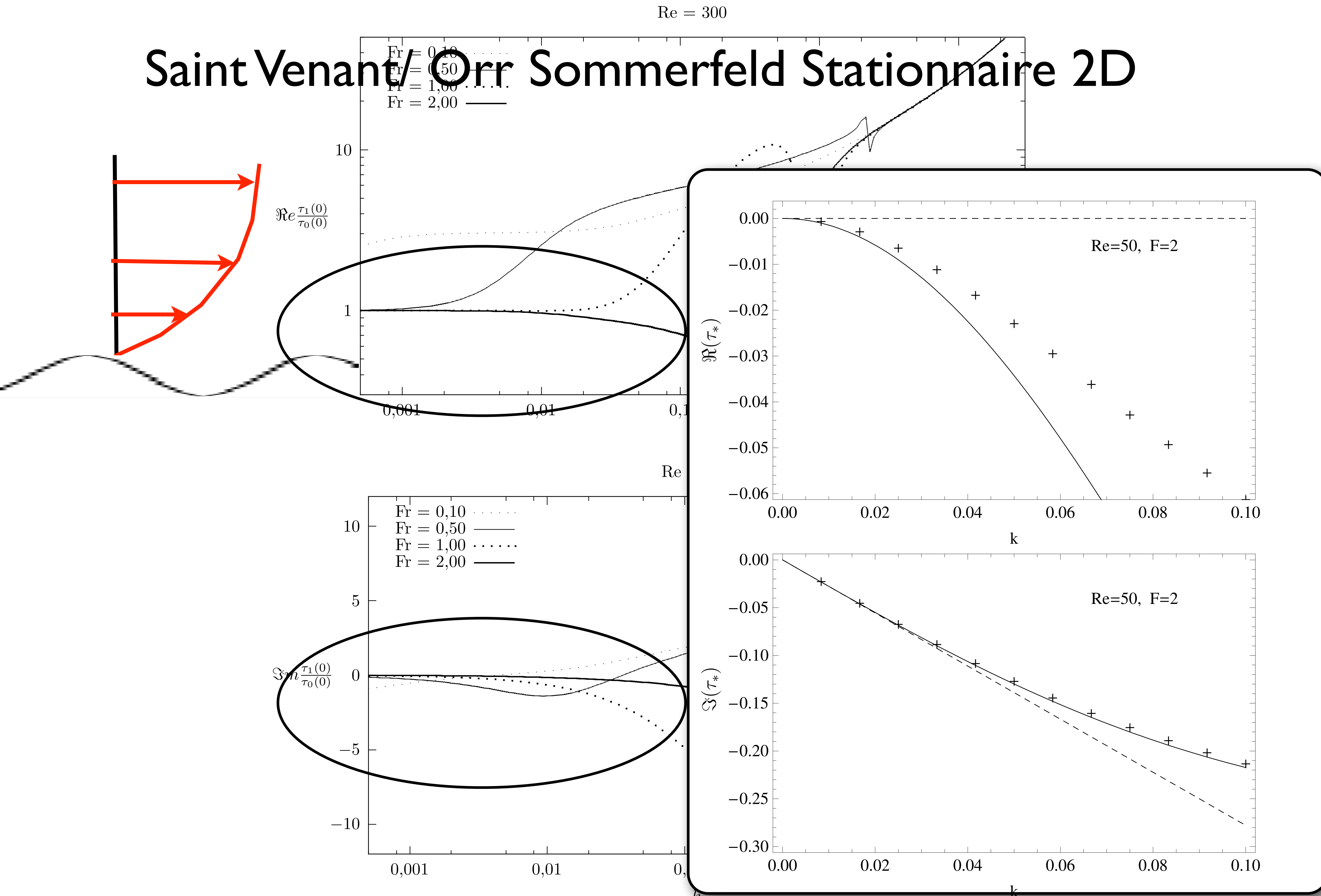

always stable

FIG. 2.6 – *Parties réelles (en haut) et parties imaginaires (en bas) de la perturbation du cisaillement au fond renormalisée, pour $Re = 300$ et différentes valeurs de Fr.*

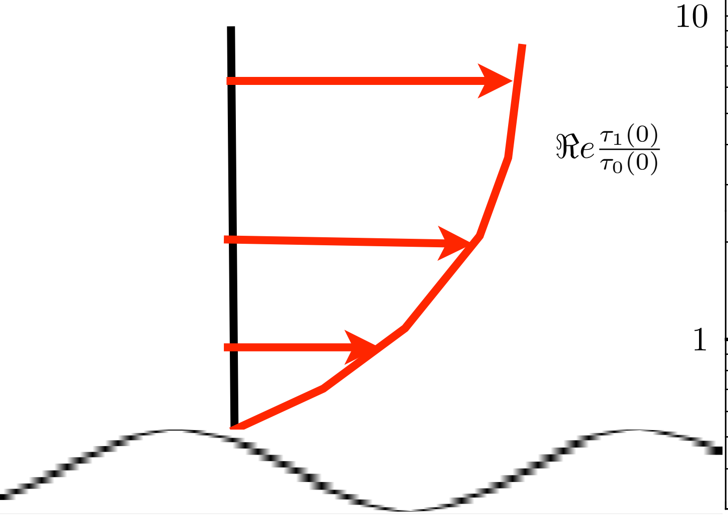

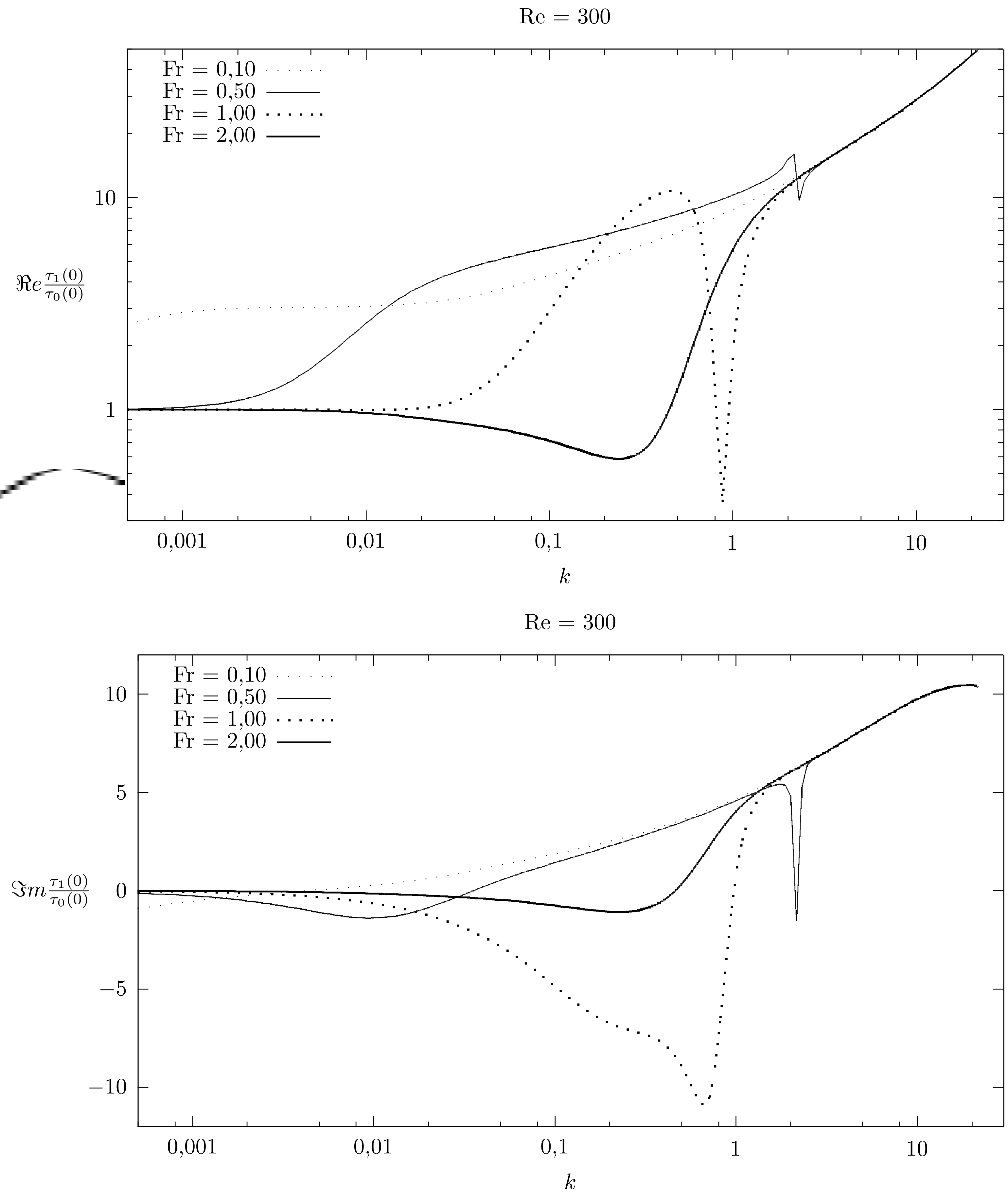

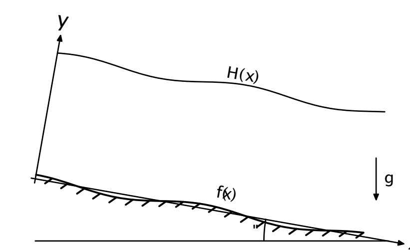

FIG. 2.6 – *Parties réelles (en haut) et parties imaginaires (en bas) de la perturbation du cisaillement au fond renormalisée, pour* $Re = 300$ *et différentes valeurs de Fr.*

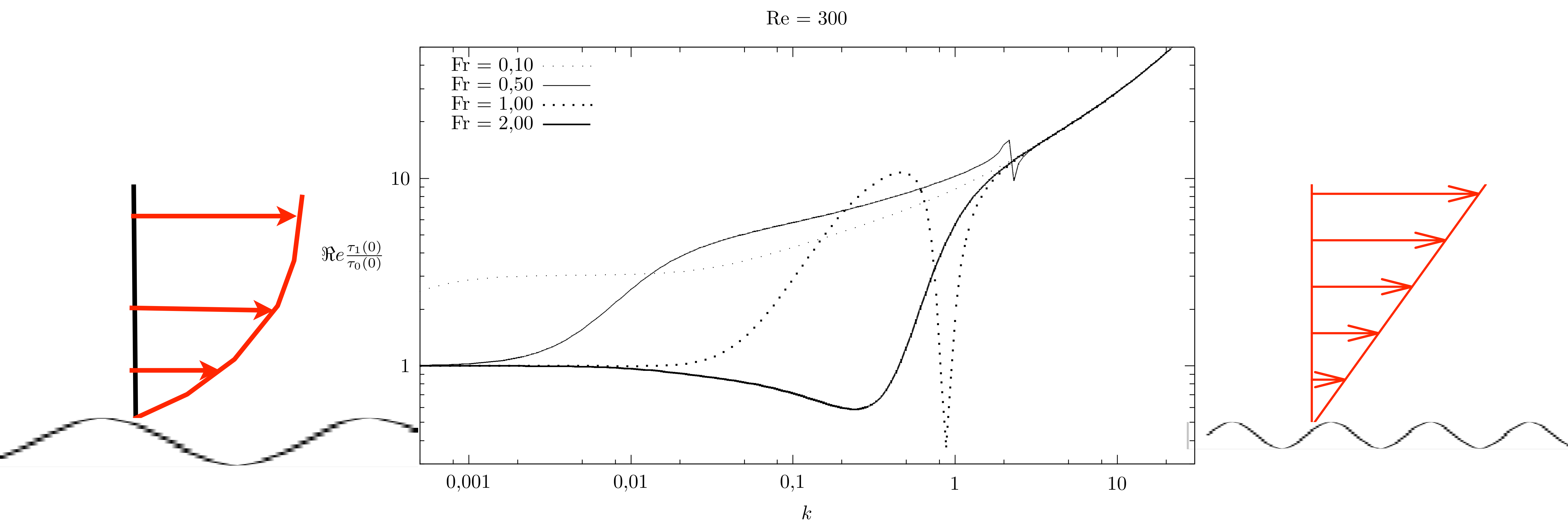

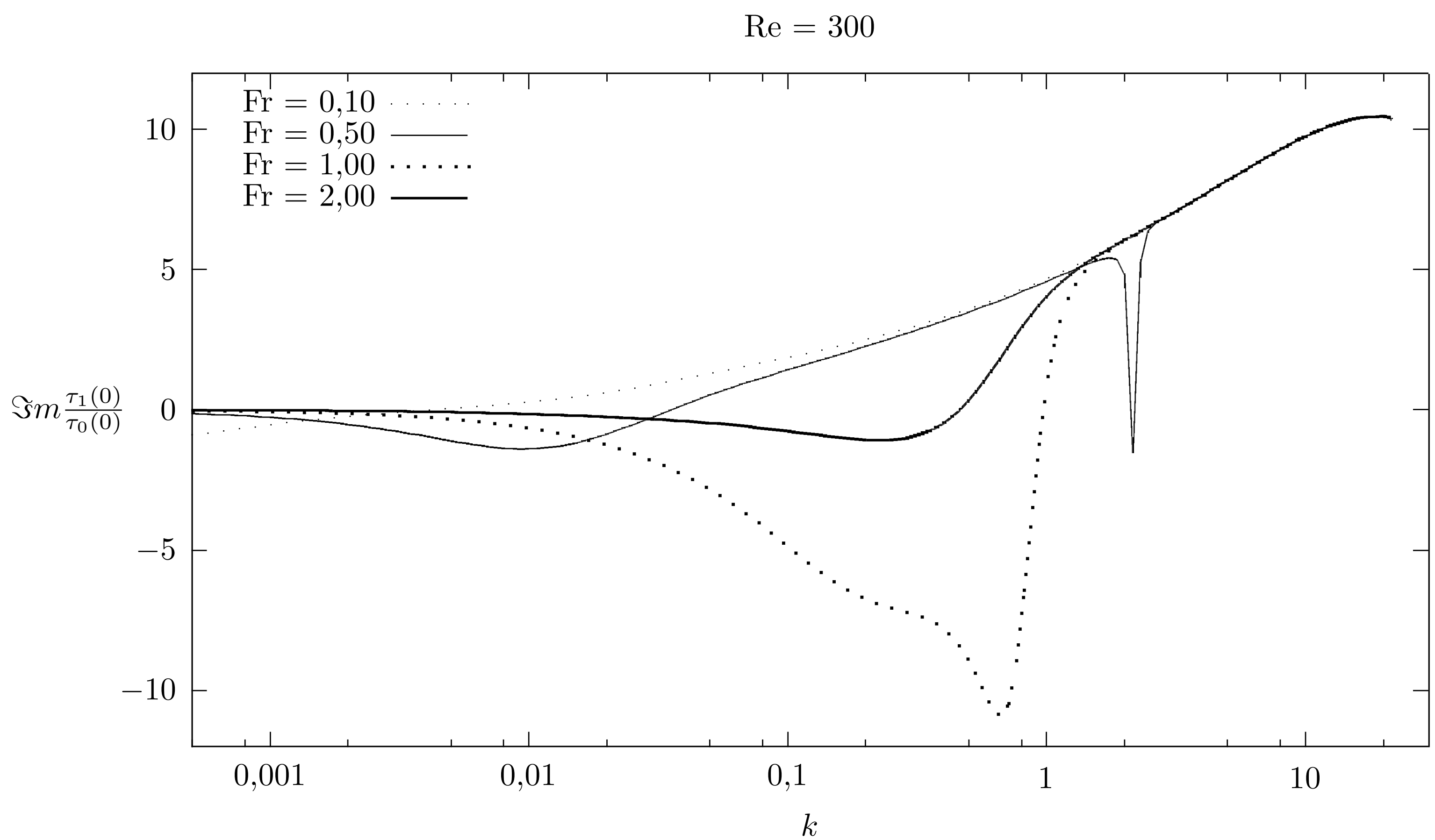

$k^{1/3}$

FIG. 2.6 – *Parties réelles (en haut) et parties imaginaires (en bas) de la perturbation du cisaillement au fond renormalisée, pour Re = 300 et différentes valeurs de Fr.*

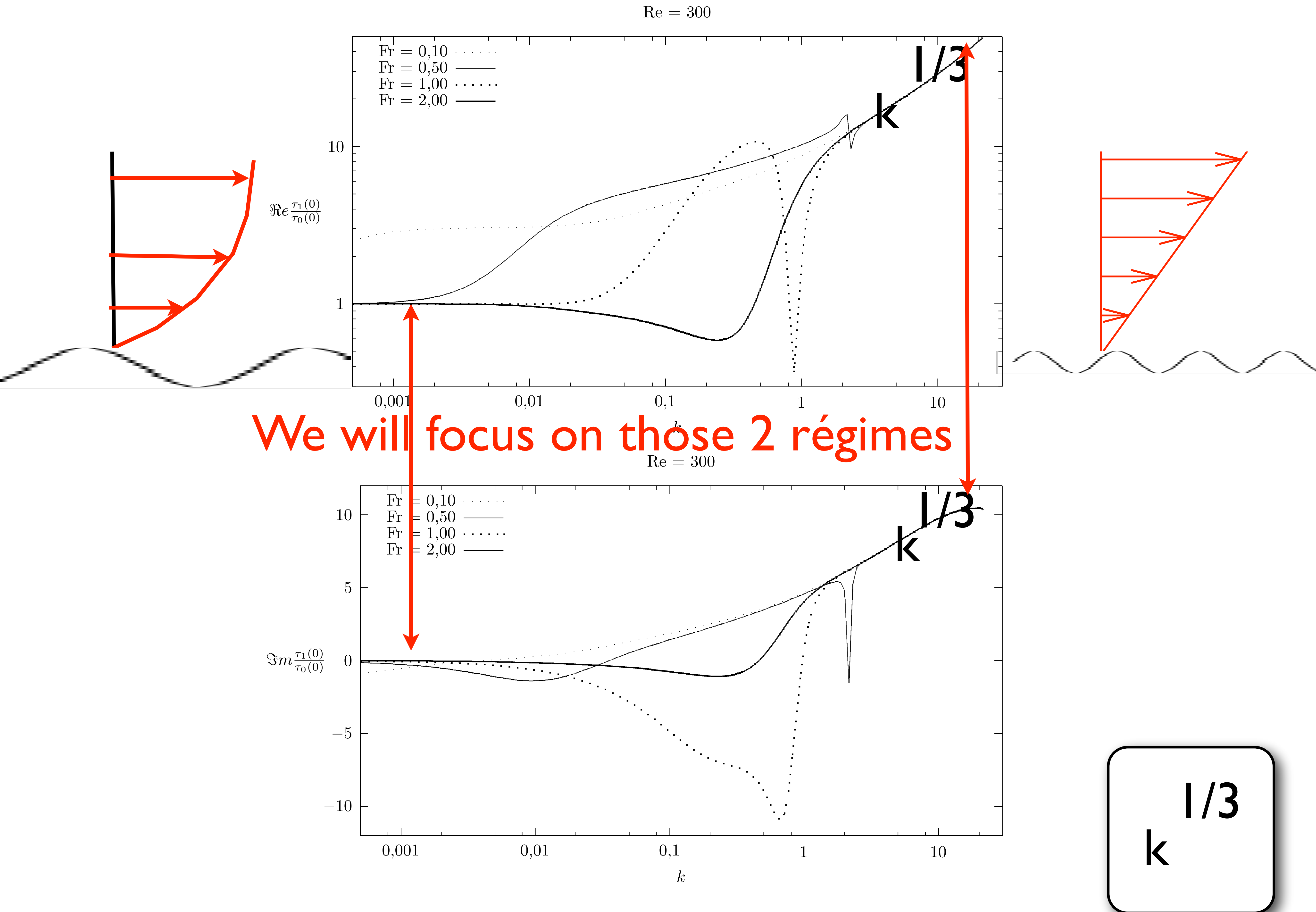

FIG. 2.6 – *Parties réelles (en haut) et parties imaginaires (en bas) de la perturbation du cisaillement au fond renormalisée, pour Re = 300 et différentes valeurs de Fr.*

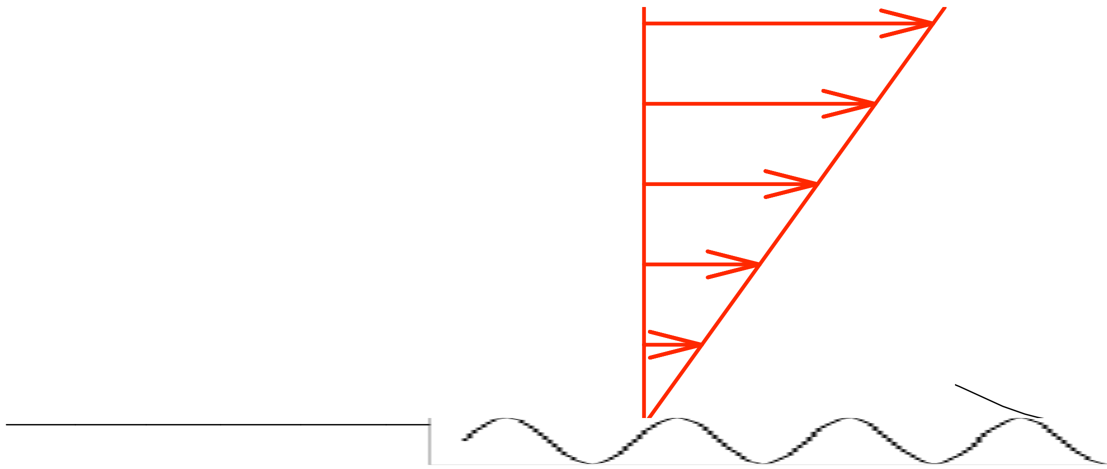

$\boxed{k^{1/3}}$

Viscous effects are important near the wall

Perturbation of a shear flow Non linear resolution (with flow separation) possible

But first we linearise

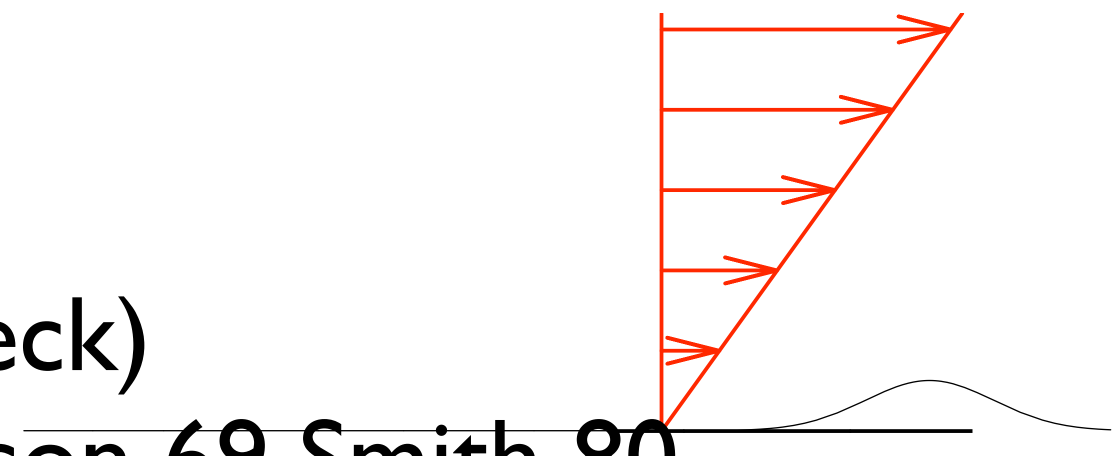

It is called Double Deck (Triple Deck)

Introduced by Neiland 69 Stewartson 69 Smith 80...

linear solution

$$\begin{cases} -ik\hat{u}_1 + \dfrac{\partial \hat{v}_1}{\partial y} = 0, \\ -iky\hat{u}_1 + \hat{v}_1 = ik\hat{p}_1 \quad + \dfrac{\partial^2 \hat{u}_1}{\partial y^2}, \end{cases}$$

$$\downarrow$$

$$-iky\hat{\tau}_1 = \frac{\partial^2 \hat{\tau}_1}{\partial y^2} \longrightarrow Ai((-ik)^{1/3} y)$$

$$\boxed{k^{1/3}}$$

Viscous effects are important near the wall

Perturbation of a shear flow Non linear resolution (with flow separation) possible

But first we linearise

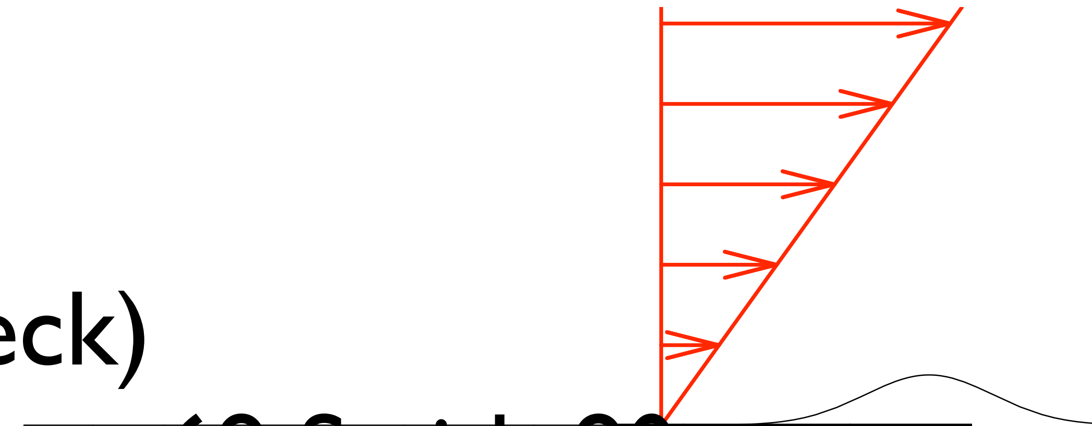

It is called Double Deck (Triple Deck)

Introduced by Neiland 69 Stewartson 69 Smith 80...

$k^{1/3}$

$$\tau = \mu U_0'(\bar{U}_S'(1+(\frac{U_0'}{\nu\lambda})^{1/3}H\tilde{c})), \text{with } \tilde{c} = FT^{-1}[FT[\tilde{f}]3Ai(0)(-(i2\pi\tilde{k})\bar{U}_S')^{1/3}]$$

complete 3D linear stability approach

> Steady Orr Sommerfeld

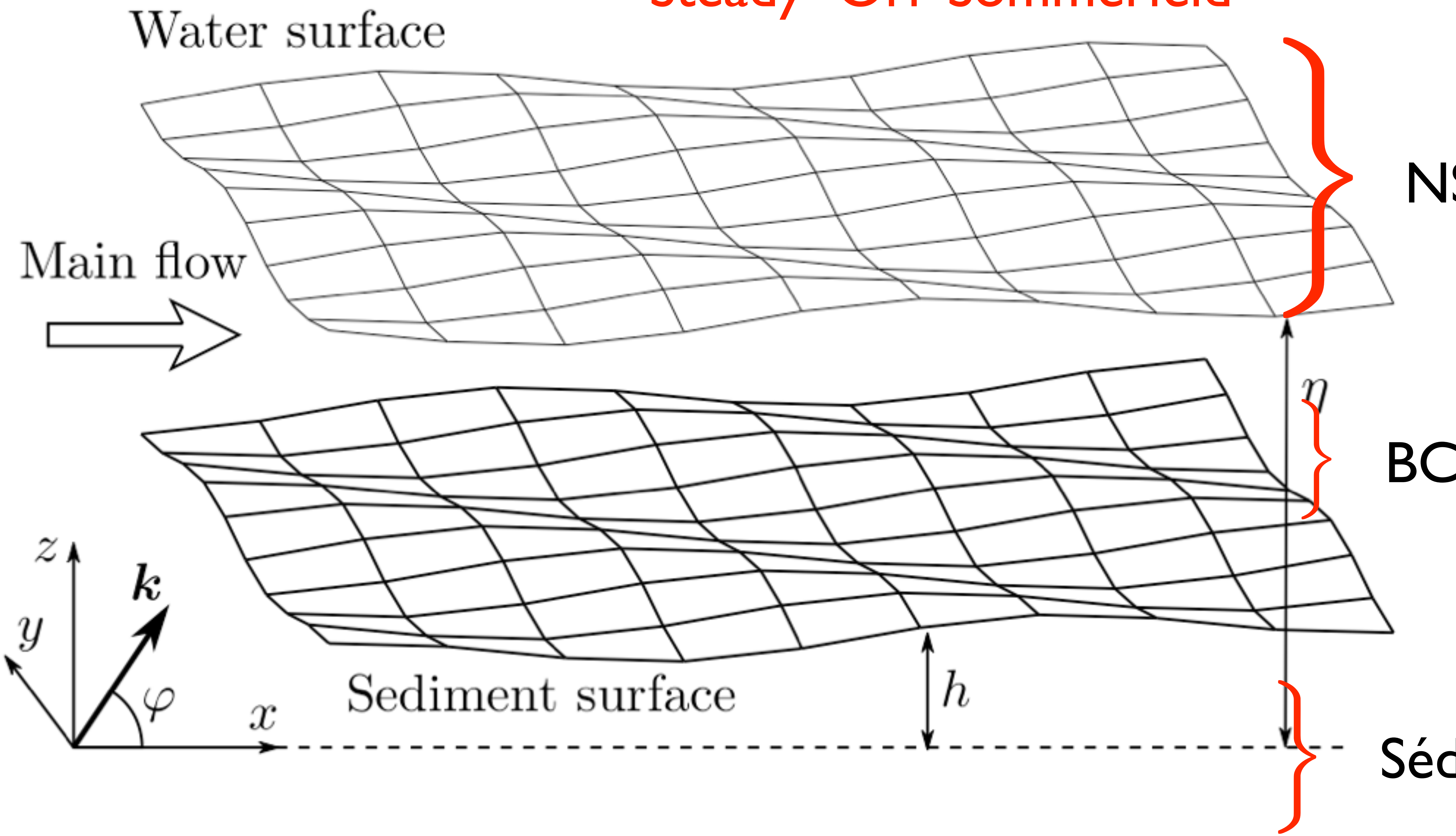

complete 3D linear stability approach

> Steady Orr Sommerfeld

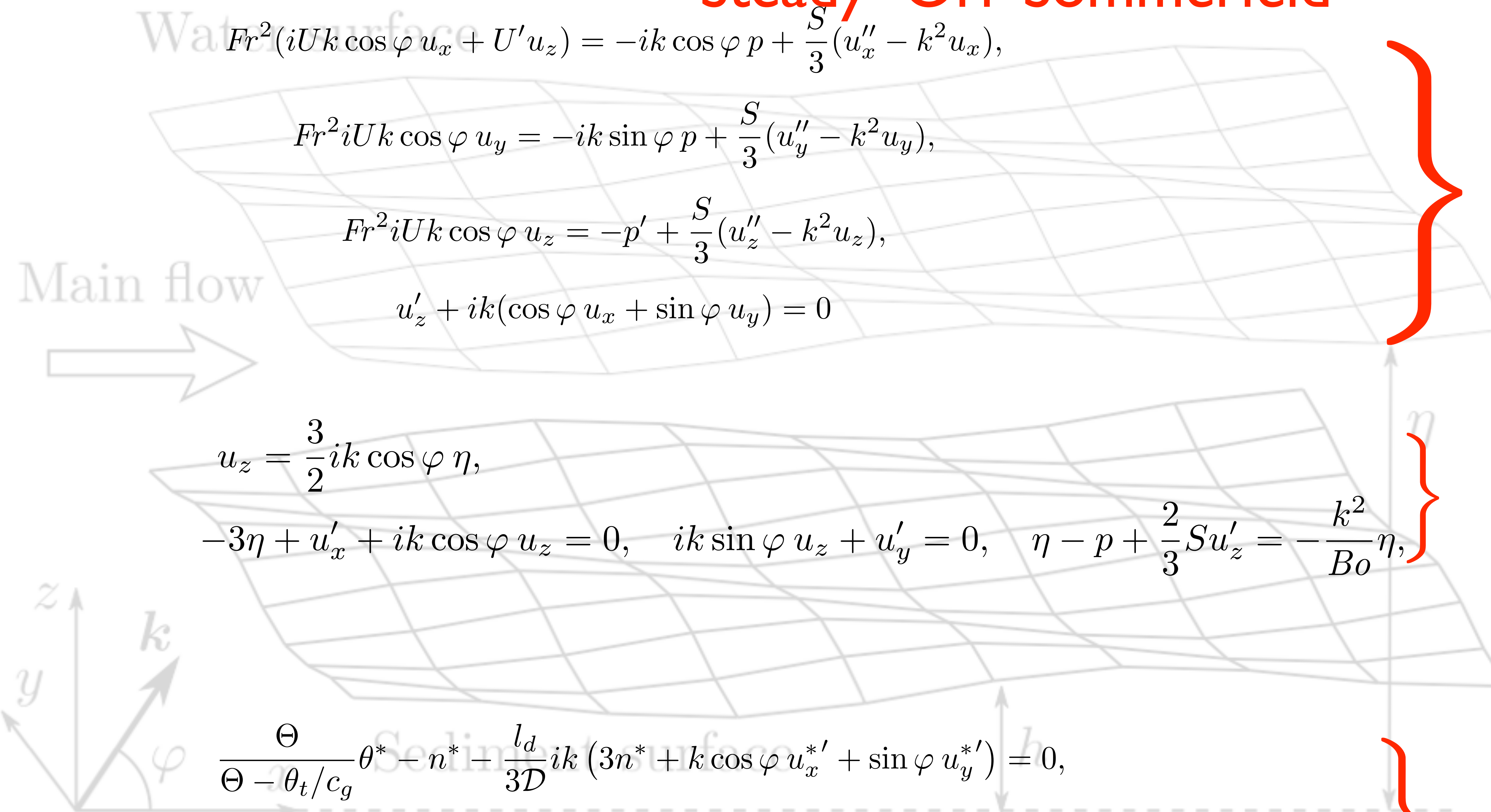

$$Fr^2(iUk\cos\varphi\, u_x + U' u_z) = -ik\cos\varphi\, p + \frac{S}{3}(u_x'' - k^2 u_x),$$

$$Fr^2 iUk\cos\varphi\, u_y = -ik\sin\varphi\, p + \frac{S}{3}(u_y'' - k^2 u_y),$$

$$Fr^2 iUk\cos\varphi\, u_z = -p' + \frac{S}{3}(u_z'' - k^2 u_z),$$

$$u_z' + ik(\cos\varphi\, u_x + \sin\varphi\, u_y) = 0$$

NS

$$u_z = \frac{3}{2} ik\cos\varphi\, \eta,$$

$$-3\eta + u_x' + ik\cos\varphi\, u_z = 0, \quad ik\sin\varphi\, u_z + u_y' = 0, \quad \eta - p + \frac{2}{3} S u_z' = -\frac{k^2}{Bo}\eta,$$

BC

$$\frac{\Theta}{\Theta - \theta_t/c_g}\theta^* - n^* - \frac{l_d}{3\mathcal{D}} ik\left(3n^* + k\cos\varphi\, u_x^{*\prime} + \sin\varphi\, u_y^{*\prime}\right) = 0,$$

$$\theta^* = \frac{1}{3}\Big(2\tilde{\theta}^2\left(u_z^{*\prime} - 3ih^* k\cos\varphi\right) - 3ih^* k\cos\varphi\, \left(1 + S^2\right) + \frac{Sh}{c_q}\left(u_x^{*\prime} + 2S u_z^{*\prime} - 3h^*(1 + 3ik\cos\varphi\, S)\right)\Big).$$

Séd

complete 3D linear stability approach

> Steady Orr Sommerfeld

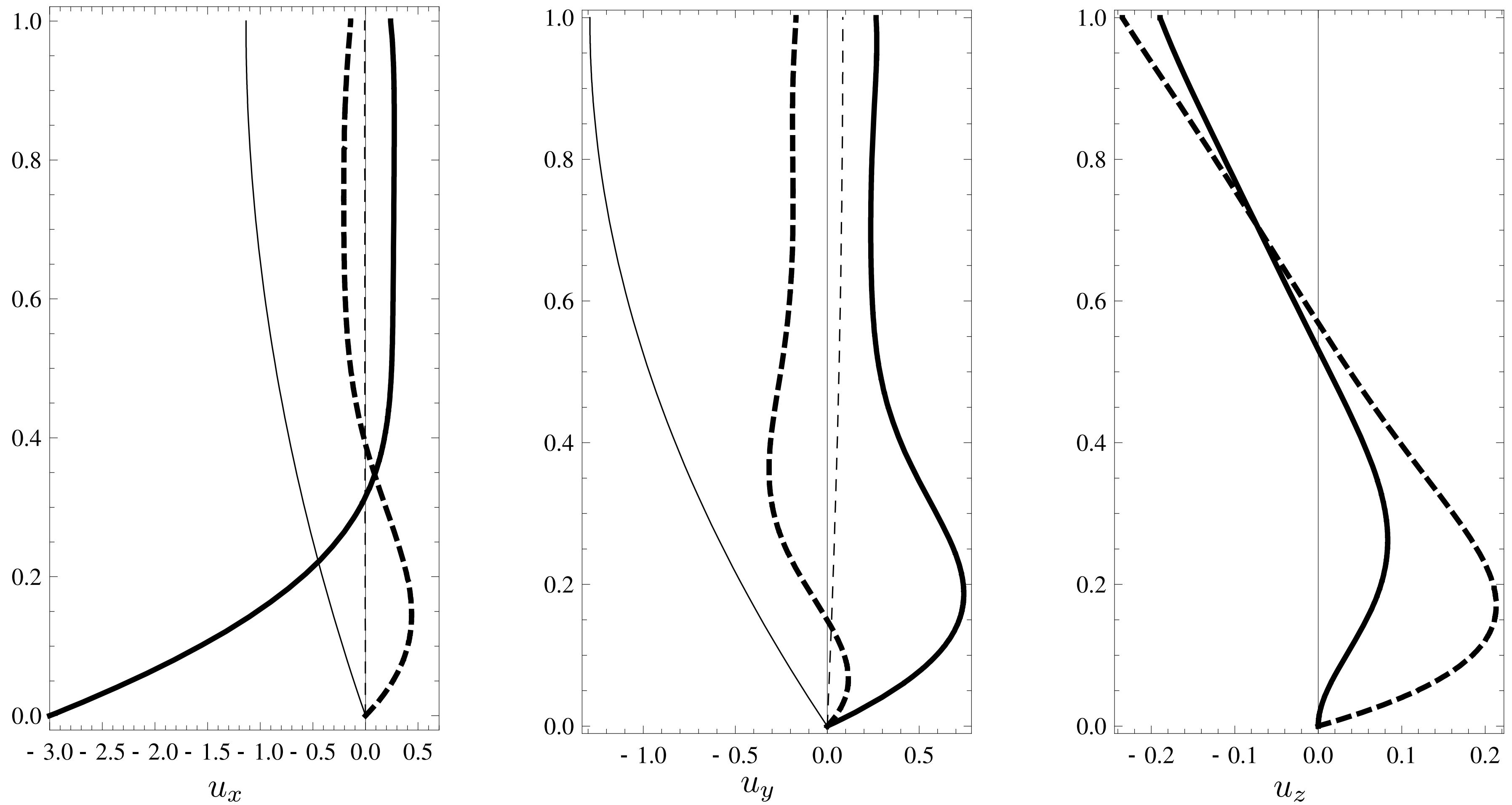

complete 3D linear stability approach

> Steady Orr Sommerfeld

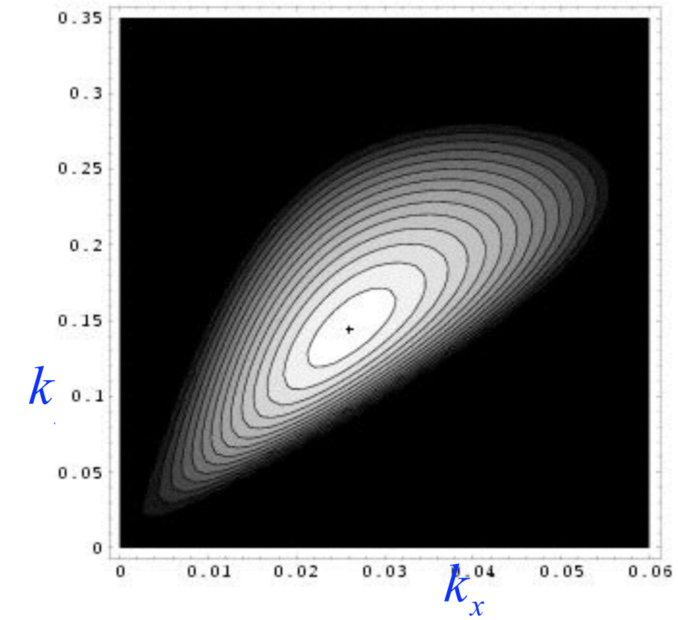

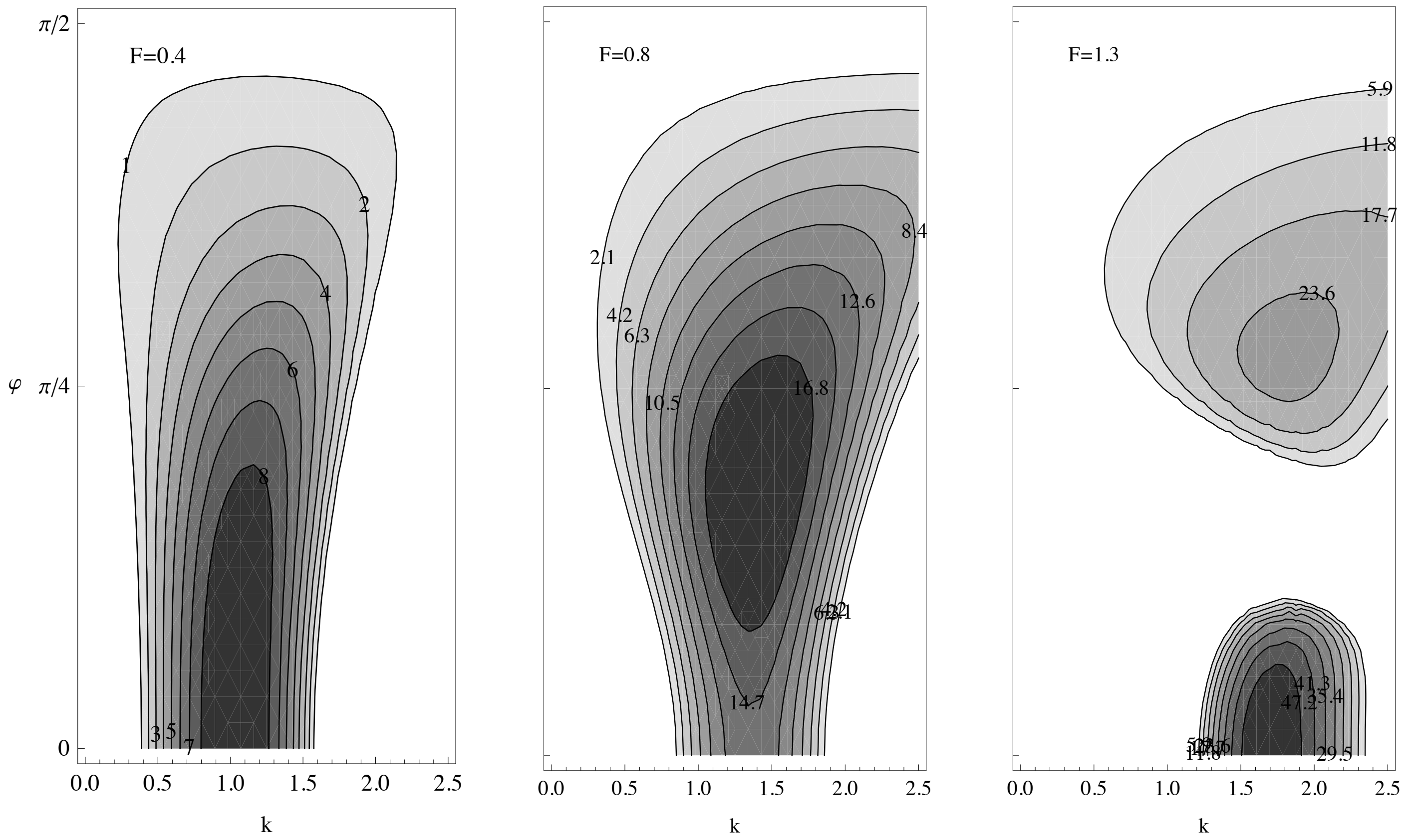

Mussel curve

+

Ripple

complete 3D linear stability approach

> Steady Orr Sommerfeld

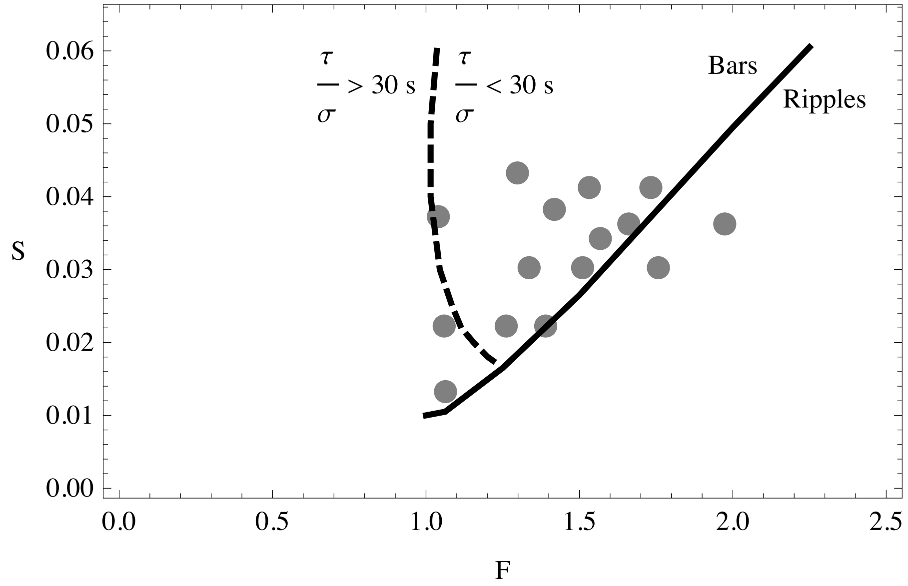

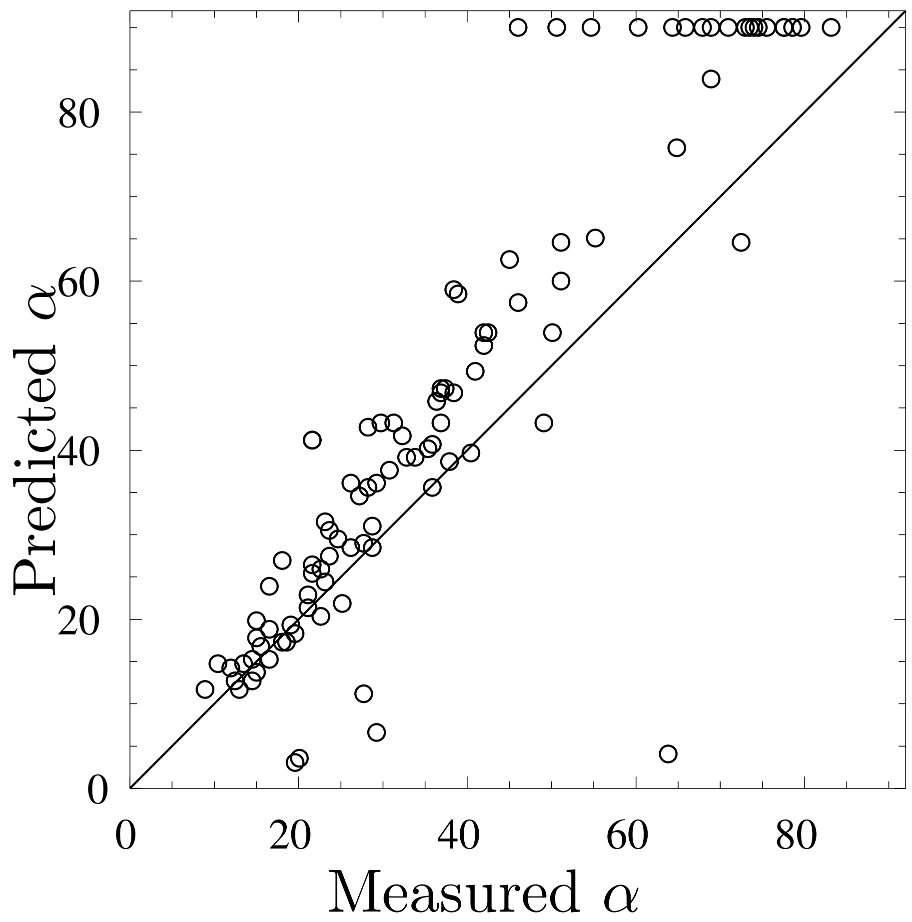

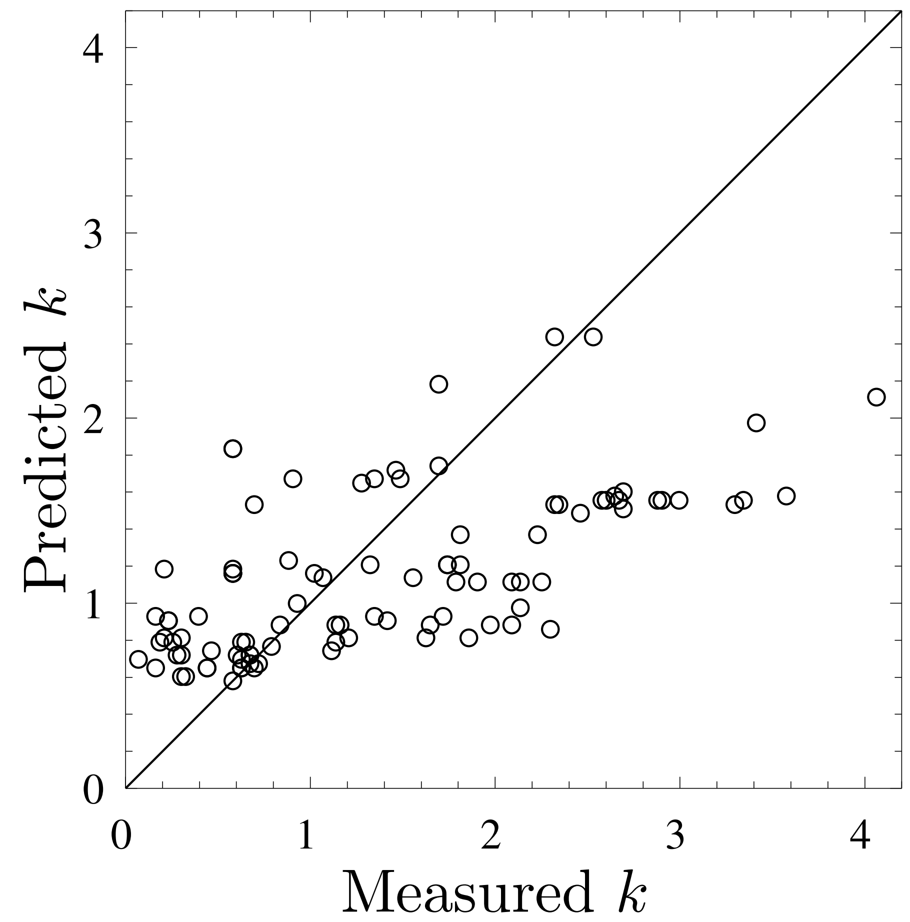

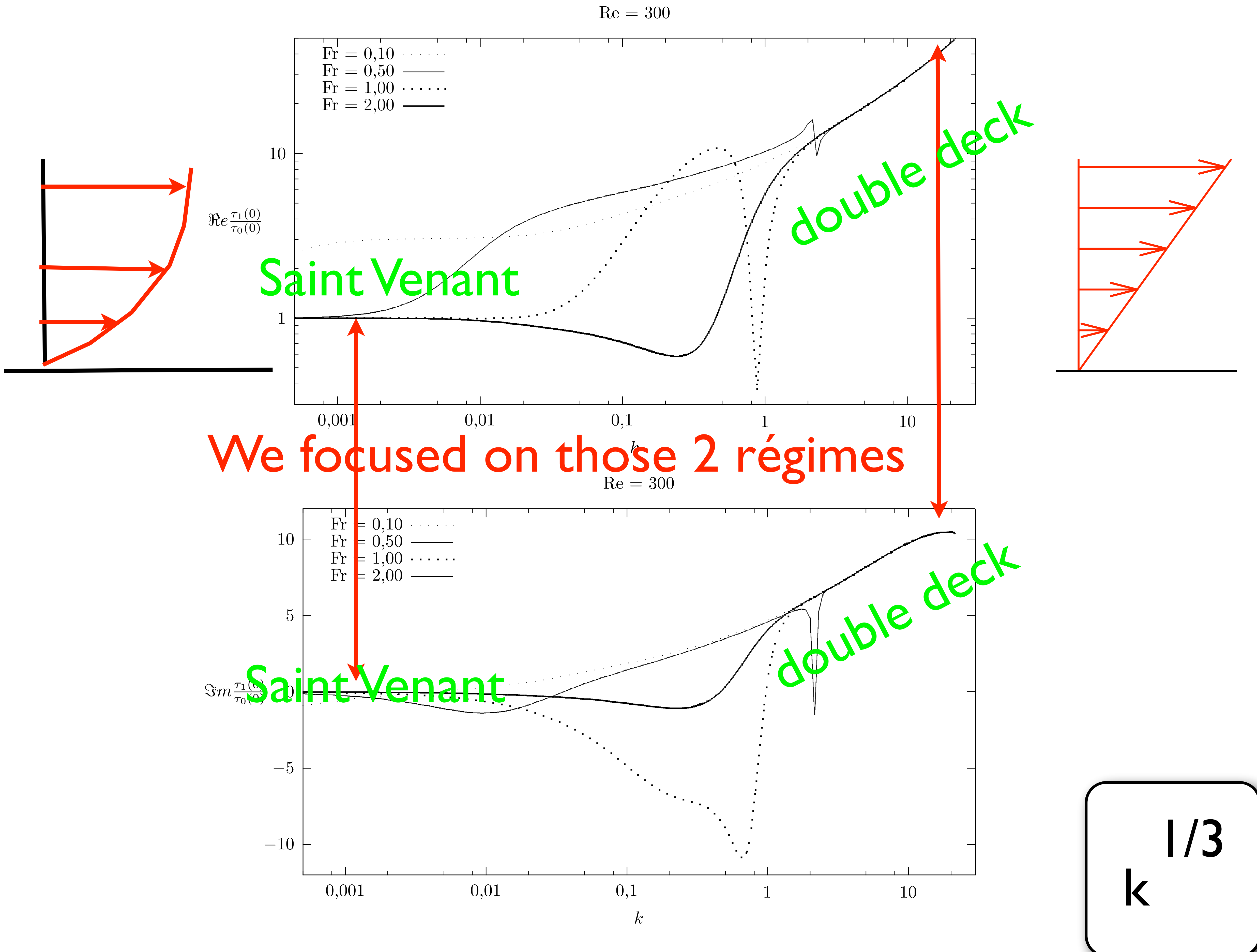

FIG. 2.6 – *Parties réelles (en haut) et parties imaginaires (en bas) de la perturbation du cisaillement au fond renormalisée, pour Re = 300 et différentes valeurs de Fr.*

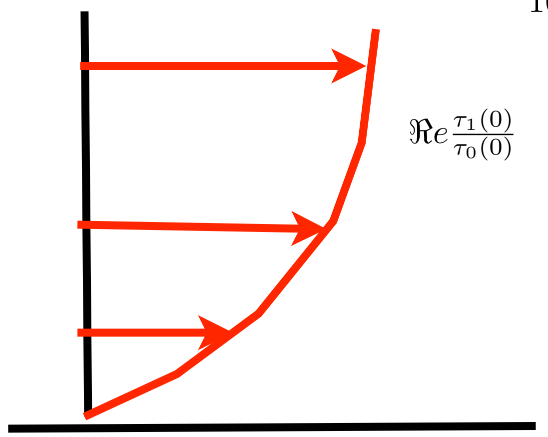

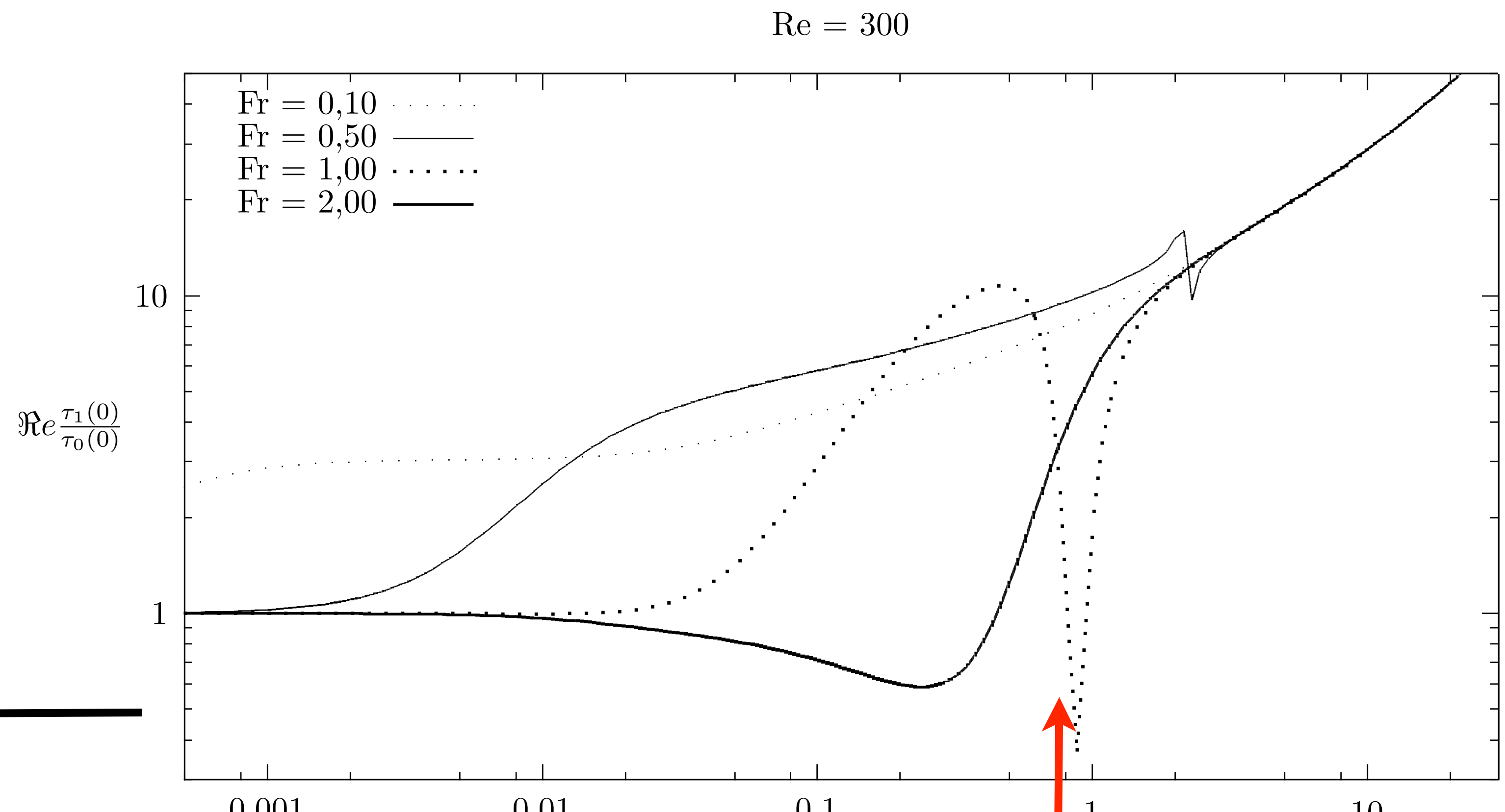

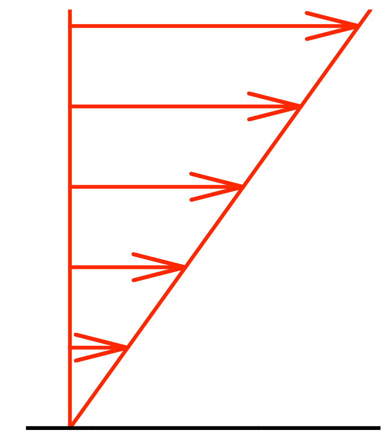

coarsening of ripples

maximum size of dunes?

conclusion

linearized Fluid BUT not Saint Venantized

Flux $$l_s \frac{\partial q}{\partial x} + q = E(\tau - \tau_s - \Lambda \frac{\partial f}{\partial x})_+$$

Exner $$\frac{\partial f}{\partial t} = -\frac{\partial q}{\partial x}$$

PATTERNS

Alternate bars

Rhomboid paterns
Lingoid bars

Ripples

Dunes

conclusion

-Saint Venant is a poor model
-need all the terms of Navier Stokes
-need a not to crude granular description

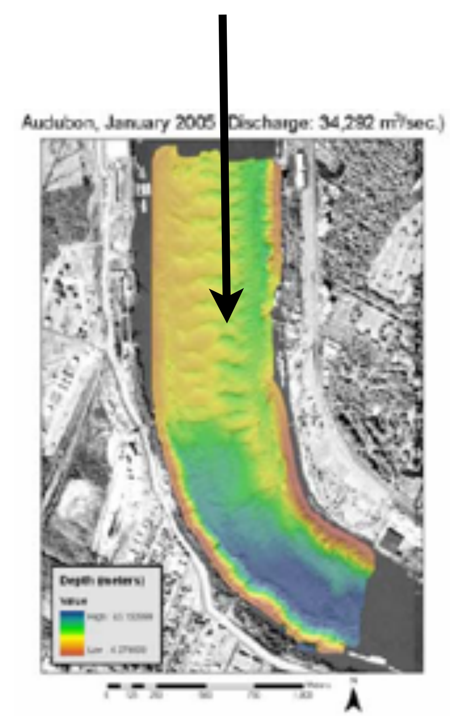

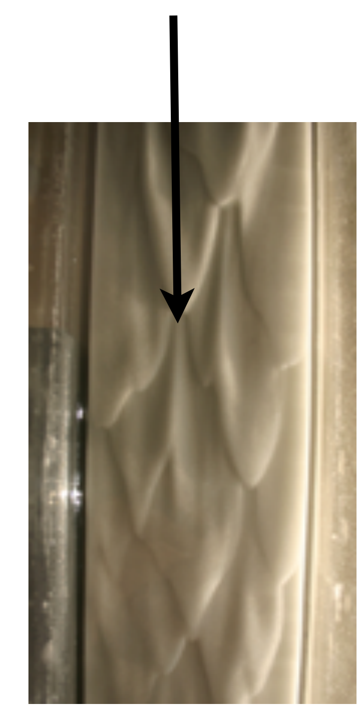

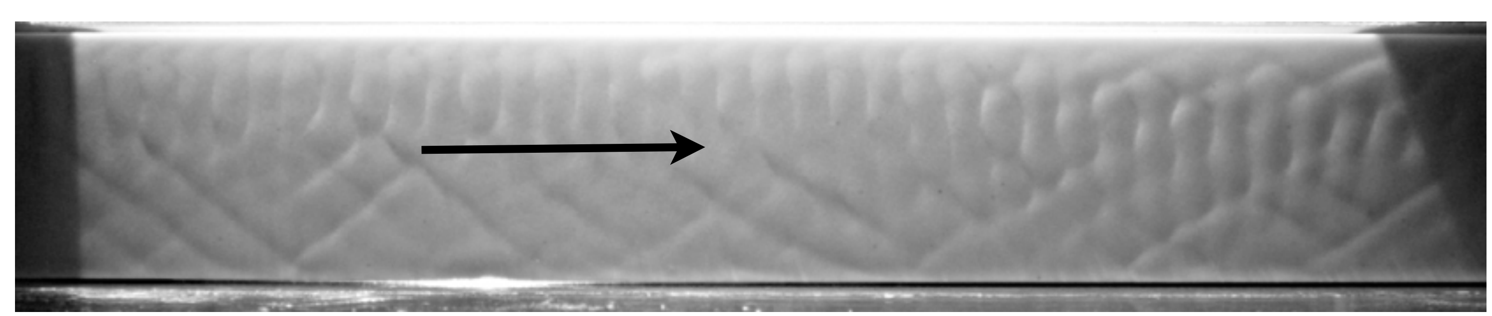

conclusion

to do

- non linear evolution of the rhomboid patterns
- Saint Venant with Boundary Layer (Mathilde)
- Boundary Layer- pre Saint Venant
- full asymptotic description of the wavy bed
- other flows: sloping beach?
- applications to practical configurations
- coupling with «gerris flow solver»

Publications

-O. Devauchelle, L. Malverti, É. La Jeunesse, C. Josserand, P.-Y. Lagrée, & F. Métivier (2010)
"Rhomboid Beach Pattern: a Benchmark for Shallow water Geomorphology"
J. Geophys. Res., 115, F02017, doi:10.1029/2009JF001471, 2010

- O. Devauchelle, L. Malverti, É. La Jeunesse, P.-Y. Lagrée, C. Josserand & K.-D. Nguyen Thu-Lam (2010)
Stability of bedforms in laminar flows with free-surface: from bars to ripples
Journal of Fluid Mechanics, vol 642 p 329-348

O. Devauchelle, C. Josserand, P.-Y. Lagrée and S. Zaleski (2008):
"Mobile Bank Conditions for Laminar Micro-Rivers"
C. R. Geoscience (2008), doi:10.1016/j.crte.2008.07.010

O. Devauchelle, C. Josserand, P.-Y. Lagrée, and S. Zaleski (2007):
"Morphodynamic modeling of erodible laminar channels"
Phys. Rev. E 76, 056318

P.-Y. Lagrée (2007):
"Interactive Boundary Layer in a Hele Shaw cell".
Z. Angew. Math. Mech. 87, No. 7, pp. 486-498

K.K.J. Kouakou & P.-Y. Lagrée (2006):
"Evolution of a model dune in a shear flow".
European Journal of Mechanics B/ Fluids Vol 25 (2006) pp 348-359.

C. Josserand, P.-Y. Lagrée, D. Lhuillier (2006):
" Granular pressure and the thickness of a layer jamming on a rough incline"
Europhys. Lett., 73 (3), pp. 363–369 (2006)

K.K.J. Kouakou & P.-Y. Lagrée (2005):
"Stability of an erodible bed in various shear flow".
European Physical Journal B - Condensed Matter, Volume 47, Issue 1, Sep 2005, Pages 115 - 125

P.-Y. Lagrée, K.K.J. Kouakou & E. Danho (2003):
"Effet dispersif de la loi d'Exner menant à l'équation de Benjamin-Ono: formation de rides sur un sol meuble",
C. R. Acad. Sci. Paris, vol 331/3 pp 231 - 235

P.-Y. Lagrée (2003):
"A Triple Deck model of ripple formation and evolution",
Physics of Fluids, Vol 15 n 8, pp. 2355-2368.

Lagrée P.-Y. (2000):
" Erosion and sedimentation of a bump in fluvial flow",
C. R. Acad. Sci. Paris, t328, Série II b, p869-874, 2000

http://www.lmm.jussieu.fr/~lagree/TEXTES/pub.html